UNIVERSITY OF SOUTHAMPTON

FACULTY OF LIFE SCIENCES

School of Biological Sciences

Modelling Climate Change Impacts on the Productivity of Short Rotation Coppice

by

Matthew John Aylott

Thesis for the degree of Doctor of Philosophy

April , 2010

UNIVERSITY OF SOUTHAMPTON

ABSTRACT

Climate Change Impacts on the Availability of Short Rotation Coppice

Matthew John Aylott

Fast growing hybrids of *Salix* and *Populus* can be grown in a short rotation coppice (SRC) system to produce renewable energy. This PhD investigates the interactions between the environment and productivity, with a view to finding the key limiting factors to yield and the potential of these crops to fulfil UK renewable energy obligations, now and in the future.

An empirical modelling technique, using partial least squares regression was developed to extrapolate actual field observations to a national scale. Genotype x age x environment interactions were studied to examine the key limiting factors to productivity. Modelled yields differed between genotypes, with mean annual above-ground biomass ranging from 4.9 to 10.7 oven dry tonnes (odt) per hectare for *Populus trichocarpa x P. deltoides* genotype 'Beaupré' and *Salix triandra* x *S. viminalis* genotype 'Q83', respectively. Variation in yield was primarily described by spring and summer precipitation, suggesting water availability is the key limiting factor to yield.

Output from the model was up-scaled across the UK using a geographic information system (GIS), and scenarios were developed to better understand the role and impact of land use management and policy development on potential crop distribution. For example, to meet UK biomass and biofuel targets without compromising food security or ecosystem services, would require 5 % of grade 3 land, 56 % grade 4 land and 47 % of grade 5 land. This quantity of biomass would produce 7.5 M tonnes of biomass per annum and would theoretically generate 15.5 TWh yr^{-1} of electrical energy, displacing 3.3 M tonnes of oil – approximately 4% of current UK electricity demand. The South West and North West alone producing over a third of this figure (5.2 TWh yr^{-1}). These results suggest that SRC has the potential to become a significant component of a mixed portfolio of renewables.

Furthermore, climate change is predicted to have far reaching consequences on crop growth. Process-based models can help quantify these interactions and predict future productivity. Here we use ForestGrowth-SRC, a process-based model originally designed for high-forest species and parameterised for a coppice system. Climate change scenarios (UK Climate Projections) were run with the model to assess the impact of a changing climate on the growth and spatial distribution of SRC poplar. Results suggest ForestGrowth-SRC is capable of accurately simulating growth over a large spatial and temporal scale. However, pests and disease were found to significantly affect yield. In the absence of pests and disease, productivity could increase by 20 % nationwide by 2080 (under a medium emissions scenario), suggesting we will see a future increase in the value and production of these crops as feedstocks for heat, power and liquid transportation fuels.

CONTENTS

LIST OF FIGURES

LIST OF TABLES

ACKNOWLEDGEMENTS

This research was funded by the NERC through a PhD studentship to Matthew Aylott (NER/S/J/2005/13986), linked to the Towards a Sustainable Energy Economy (TSEC)-BIOSYS project (www.tsec-biosys.ac.uk).

Forest Research is also acknowledged for provision of the site-genotype yield data and for assistance in developing the modelling approach. Particularly I would like to thank my colleagues in the biometrics department: Ian Tubby (Director of the Biomass Energy Centre, for information on the field trials network), Tim Randle (Modeller, for his help identifying problems with the process model) and Paul Henshall (Programmer, for his help developing the code).

I must also thank the kind support of my supervisors Prof Gail Taylor, Prof Pete Smith and particularly Dr Eric Casella. I also thank my colleagues at the University of Southampton for their input, in particular Dr Nathaniel Street, Dr Mat Tallis, Miss Rebecca Rowe and Miss Suzanne Milner. Also to Miss Jenny Bagot who taught me to never give up. I owe them all drink. And to my parents, thank you, I couldn't and wouldn't have done it without you.

LIST OF ABBREVIATIONS

£	British pound sterling
$	US dollars
°	degree
°C	degrees celsius
%	percent
ARBRE	Arable Biomass Renewable Energy
BERR	Department of Business, Enterprise and Regulatory Reform
BSi	British Standards Institute
C	carbon
CEC	closed environment chamber
CHP	combined heat and power
CO_2	carbon dioxide
DECC	Department of Energy and Climate Change
Defra	Department of Environment, Fisheries and Rural Affairs
DTI	Department of Transport and Industry
DW	dry weight
ECS	Energy Crops Scheme
EEA	European Environment Agency
e.g.	*exempli gratia* (Latin), translated as 'for the sake of example'
et al.	*et alia* (Latin), translated as 'and others'
EU	European Union
EU27	27 Member States of the European Union (as of January 2007)

FACE	free air enrichment
GJ	giga joules
GW	giga watt (10^9 W)
GIS	Geographical Information System/Science
GPP	gross primary productivity
H_2O	water
h	hour
ha	hectare
i.e.	*id est* (Latin), translated as 'it is'
IEA	International Energy Agency
IMF	International Monetary Fund
kg	kilogram
km	kilometre or kilometre squared (km^2)
LAD	leaf area density
LAI	leaf area index
LAL	leaf area lost
LCM	land cover map
m	metre or metre squared (m^2)
M	millions
MAFF	Ministry of Agriculture, Forestry and Fisheries
mm	millimetres
mph	miles per hour
MW	mega watt (10^6 W)
N	Nitrogen

n	number
NNFCC	National Non-Food Crops Centre
NOAA	National Oceanic and Atmospheric Administration
NPP	net primary productivity
O_3	ozone
odt	oven dried tonne
Ofgem	Office of Gas and Electricity Markets
OPEC	Organization of the Petroleum Exporting Countries
OPSI	Office of Public Sector Information
OTC	open top chamber
PAR	photosynthetically active radiation
PCA	principle component analysis
***p*LAI**	potential leaf area index
PLS	partial least squared
ppm	parts per million
ppt	precipitation
PW	peta watt hour (10^{15} W)
QTL	quantitative trait loci
RFA	Renewable Fuels Agency
SD	standard deviation
SRC	short rotation coppice
t	tonne
toe	tonnes of oil equivalent
TW	tera watt (10^{12} W)

RO	Renewables Obligation
RuBP	ribulose 1,5-bisphosphate
UK	United Kingdom
UKCIP	United Kingdom Climate Impact Programme
UKERC	United Kingdom Energy Research Centre
UN	United Nations
UNFCC	United Nations Framework Convention on Climate Change
US	United States
VIP	variable importance plot
$\bar{x}$	mean
yr	year

Chapter 1 . General Introduction

1.1 Project Overview

Atmospheric carbon dioxide (CO_2) has reached the highest level in human history, 385 parts per million (ppm), and is continuing to rise by 1-2 ppm each year (NOAA, 2009). Continued increases in atmospheric CO_2 are predicted to have far reaching consequences to human development (Root *et al.*, 2003; Thomas *et al.*, 2004; Stern, 2006). Consequently, nearly 95 % of the world's nations have signed the Kyoto Protocol (UNFCC, 2009). The Protocol is a legally binding agreement, requiring all developed nations reduce emissions from greenhouse gases (GHG), of which CO_2 is the most prevalent, to at least 5.2 % below 1990 concentrations by 2012. The EU agreed to reduce its emissions to 8 % below 1990 levels, with the most heavily polluting member countries assuming the greatest responsibility for this reduction. Hence, as the second highest producer of CO_2 in Europe (UN, 2006), the UK is committed to a 12.5 % decrease (below 1990 levels) in GHG emissions by 2012 (Defra, 2004). An important component of this commitment is securing more energy from local renewable sources. The UK is currently a net importer of fossil fuels (DECC, 2009a) and the trend of increasing crude oil prices – reaching a peak in July 2008 at $130 per barrel (OPEC, 2010) – has led to alternatives, such as energy from biomass (bioenergy), becoming more economically feasible.

This project investigates the spatial variability in above-ground biomass production of two such bioenergy crops – poplar (*Populus*) and willow (*Salix*) – grown using a short rotation coppice (SRC) system. Both species have a wide provenance, are fast growing and have considerable potential to reduce our dependence on non-renewable sources of

electricity, heat and liquid transportation fuel. However, it is the economic viability of these crops and how they use the finite land resources available, which will determine their success in competing in a rapidly expanding renewables market. The most obvious way to help meet these challenges is to increase productivity.

Trialling and breeding high-yielding species and good agronomic practices will help maximise productivity. However, they do not expand our understanding of the physiological basis of yield. Plant models offer a more cost and time efficient alternative to large scale field trials, enabling both micro (e.g. field) and macro (e.g. national) estimates of productivity to be made. Two modelling approaches were used in this thesis. Firstly, an empirical model was developed to identify principal factors limiting growth, using data gathered from the UK SRC field trials network. Results from this model were then spatially extrapolated to a national scale using a geographic information system (GIS). This allowed us to describe potential productivity of SRC poplar and willow across England and estimate the area required to meet energy crop targets, without compromising sustainability. Secondly, a robust process-based model was developed to investigate the possible future impacts of climate change on SRC poplar productivity. UK Climate Projections ('baseline': 1991-2000, '2020s': 2010-2039, '2050s': 2040-2069 and '2080s': 2070-2099) were used to quantify the temporal effects of climate change on yield. Again a GIS was used to extrapolate values to a national scale and make further assessment of crop potential.

The first chapter of this thesis considers the context and rationale for this work, reviewing the current state of the biomass market, future targets, sustainability and the

physiological basis of yield. In addition, we evaluate current modelling approaches and identify where improvements in our understanding are needed.

1.2 Energy from biomass

Biomass describes all organic plant and animal products used to produce energy (Table 1.1). SRC refers to any woody plant species managed in a coppice system, such as poplar or willow. These crops are typically grown for 2-5 years, harvested, then re-grown from the stool, with stools remaining viable for up to 30 years (Defra, 2004).
In a coppice system, natural growth patterns are artificially controlled to maximise competition between stems, which results in rapid canopy closure. Consequently, coppiced crops exhibit high above-ground biomass growth, making such systems well suited for energy production.

Using plants for fuel is not a new concept and has been practised since the beginning of human history. Traditionally, plants were used for heating and cooking because they were widely accessible, inexpensive and easily converted to energy. However, the large-scale deployment of dedicated crops for energy is a more recent concept, driven by the demand for reductions in GHG emissions and the maintenance of a secure and sustainable energy supply (Berndes *et al.*, 2003; European Commission, 2005; UKERC, 2006; IEA, 2007; Scottish Executive, 2007).

Table 1.1. Biomass energy sources, characteristics, common conversion routes and end uses. Latin species names of plants in parenthesis.

Source	Characteristics	Conversion Routes	Uses
Bamboo (*Phyllostachys*) Eucalyptus (*Eucalyptus*) Poplar (*Populus*) Willow (*Salix*)	Woody perennial plants (C_3 photosynthesis); typically highly suited to coppicing, high water use	Direct combustion, second-generation technologies (pyrolysis, gasification, enzyme-activated hydrolysis)	Solid fuel biomass, bioethanol (second-generation)
Forest residues	Waste from clear-felling & thinning		
Elephant Grass, EG (*Miscanthus*) Reed Canary Grass, RCG (*Phalaris arundinacea*) Switchgrass, S (*Panicum virgatum*)	Coarse perennial grasses (C_4); juvenile EG is susceptible to winter frosts, RCG has high tolerance to waterlogging & drought, S highly tolerant of poor soils, flooding & drought	Direct combustion, fermentation	Solid fuel biomass, bioethanol
Wheat (*Triticum*) Sugar Beet (*Beta vulgaris*) Sugar Cane (*Saccharum*)	Annual arable crops (C_4); long history of breeding for high yield across a variety of sites	Fermentation	Bioethanol
Rapeseed (*Brassica napus*) oil Soybean (*Glycine max*) oil		Solvent-based extraction	Biodiesel
Algae	Produce up to 60% of their biomass in the form of oil (biodiesel), naturally produce ethanol and butanol	Solvent-based extraction (biodiesel), fermentation (bioethanol/biobutanol)	Biodiesel, bioethanol, biobutanol,
Livestock slurry & manure	Widely available and easily converted, can contain trace toxins such as Hydrogen Sulphide	Anaerobic digestion/ combustion	Biogas
Landfill & sewage gas		Direct combustion	Biogas

Plants produce biomass by converting solar energy, water and carbon dioxide to complex molecules – such as glucose – through the process of photosynthesis. Globally, approximately 100-120 billion tonnes of carbon are fixed by photosynthesis each year (Post *et al.*, 1990). We can utilise this biomass to produce energy by a variety of means. Energy crops can be combusted directly to generate electrical power and heat, which is low risk but has low conversion efficiency. The energy efficiency of direct combustion of energy crops to electricity is typically between 20 and 40 % (Gigler *et al.*, 2001; McKendry, 2002b), increasing to 70 % when used to produce heat and electricity (Cannell, 2003). Alternatively, biomass can be converted to liquid transportation fuel.

Conventional or first-generation biofuels are made from plant oils such as soy or rapeseed (biodiesel) or produced by fermenting plant sugars from crops like sugar cane, sugar beet or wheat (bioethanol). Advanced or second-generation biofuels can be made from a wider range of feedstocks, like poplar and willow, which require more advanced technologies to convert biomass into fuel.

These feedstocks are converted to advanced or second-generation biofuels in one of two ways – biochemical or thermochemical. Biochemical processes typically employ pre-treatment to accelerate the hydrolysis process, which separates out the cellulose, hemicellulose and lignin. Once these constituents are separated, the cellulosic fractions can be fermented into alcohols, and the lignin can be combusted.

Alternatively, biofuel can be made by gasification; a thermochemical conversion process which reacts carbon-based materials at high temperatures (800-1200°C) with a

limited amount of oxygen, air and/or steam. The reaction yields a combustible gas, mainly comprising of carbon monoxide and hydrogen. This gas can be fermented (in the same way as first-generation biofuels) or chemically synthesised into a range of fuels, including ethanol, synthetic diesel or jet fuel. Pyrolysis is a similar thermal process where carbon-based materials are heated at 400-1000°C, in the absence of oxygen or air. The pyrolysis process yields three products; a combustible gas, a condensable vapour and a solid char. The condensed vapour can subsequently be upgraded into transport fuels.

These technologies are typically characterised by high conversion efficiencies and high risks (e.g. high start up costs). For example, gasification has conversion efficiencies of 40-50 % (Gigler *et al.*, 2001; McKendry, 2002b), but start-up costs are much higher than for first generation biofuels and the technology is less mature.

1.2.1 Targets for biomass production

The EU Biomass Action Plan (European Commission, 2005), estimated that biomass could contribute around 150 M toe to EU energy needs by 2010. Furthermore, a European Environment Agency sustainability report (2006) concluded that 190 M toe could be grown by 2010 without harming the environment, rising to around 295 M toe by 2030 (15–16 % of projected primary energy demand). If 295 M toe were grown, at least 10 M ha of agricultural land across Europe would need to be placed under energy crop production (not considering biomass imported from outside the EU). In line with these recommendations, the European Commission detailed its strategy for renewables in the Renewable Energy Road Map (2007), which resulted in the Renewable Energy

Directive (2009). The directive is a legally binding requisite for EU member states to meet 20 % of energy consumption using renewable sources and 10 % of transport fuels from biofuel by 2020. Each member state is required to meet a share of these figures, based on per capita gross domestic product (GDP). In fulfilment of its obligation the UK must deliver 15 % of its energy from renewable sources. The Renewable Energy Strategy (DECC, 2009b) outlines the UK governments response to that commitment. Its key proposals are to meet 30 % of electricity supply, 12 % of heat supply and 10 % of transport fuel using renewables by 2020. These targets comply with current policy objectives to meet 10 % of UK energy from renewables sources by 2010 (BERR, 2007) and 5 % (by volume) of all transport fuel from biofuel by 2014 (RFA, 2008).

To encourage the use of renewables, the UK government introduced the Renewables Obligation Order (OPSI, 2002). The order ensures electricity supply companies provide a set amount of their electricity from eligible renewable sources or pay a financial penalty. Suppliers meet their obligations by presenting Renewables Obligation Certificates (ROCs). Following reform (OPSI, 2009), ROCs are issued on a per MWh basis and banded according to the technology used (Table 1.2). This allows 'grandfathering' of less established technologies that are perceived to be higher risk, by increasing the number of ROCs granted to those technologies. According to Ofgem (2010), 42 ROC accredited generating stations were co-firing biomass by April 2009 – including Drax, the UK's largest power station – compared to 38 stations using dedicated biomass. Similar policy governs the use of biofuels. The Renewable Transport Fuels Obligation (RTFO) came into force in April 2009 and required oil companies to replace a certain percentage of their fossil fuels with biofuels. The

2008/09 target was 2.5%, rising to 5% by the end of 2014.

Current targets present considerable challenges to the UK energy industry and require a substantial increase in renewable energy production. The contribution of biomass is predicted to be high and estimated annual demand for electricity from dedicated energy crops could reach 3.5 M odt[†] (oven dried tonnes) by 2020 (DTI and Defra, 2007). Furthermore, the annual demand for bioethanol from wheat could reach 4.0 M odt[††] by 2014 (NNFCC, 2009). Based on current yields[†] and assuming like for like energy conversion ratios per tonne, using SRC for both electricity generation and transportation fuel would require 0.75 M ha (or 4.1 % of the UK's 18.5 M ha of agricultural land). However, the UK Biomass Strategy Report (DTI and Defra, 2007) suggests as much as half of this biomass may be imported.

Table 1.2. Eligibility for Renewable Obligation Certificates (ROC) and value of each ROC per MWh produced by a given technology (OPSI, 2009)

Renewable technology	**ROC/MWh**
Landfill gas	0.25
Sewage gas; co-fired standard biomass	0.5
Onshore wind; hydroelectric; geo-pressure; co-fired energy crop biomass; co-fired standard biomass with CHP; waste with CHP; standard gasification; standard pyrolysis	1.0
Offshore wind; dedicated standard biomass; co-fired energy crop biomass with CHP	1.5
Wave; tidal; photovoltaic; geothermal; dedicated energy crop biomass; dedicated energy crop biomass with CHP; dedicated standard biomass with CHP; anaerobic digestion; advanced gasification; advanced pyrolysis	2.0

[†] based on average yield of 10 odt ha^{-1} for SRC.
[††] based on average yield of 8 odt ha^{-1} for wheat.

EU reform to the Common Agricultural Policy has made more land available for alternative uses (Natural England, 2008). Reform has led to the withdrawal of set-aside payments – which paid farmers to leave land fallow – subsequently making 0.6 M ha (2005) of UK fallow land available for other purposes (Defra, 2006). This may prove to be an effective short-term strategy to make more land available to energy crops. However, if we are to meet longer-term targets (2014 and beyond) more action is urgently required. It is likely areas currently under arable production will in future need to be used for energy crops. The Biomass Task Force (2005) concluded that by 2020, up to 1 M ha of agricultural land could realistically be available to energy crops. However, Cannell (2003) suggests an achievable potential of just 0.6 M ha.

1.2.2 Current biomass production

Globally, biomass is the most widely used renewable energy resource. An estimated 10.8 % of the total energy consumed in the world each year is derived from biomass, corresponding to 1080 million tonnes of oil equivalent (M toe). In some developing countries this figure increases to as much as 80 % (El Bassam, 1998). As of 2006 biomass was supplying 4.8 % of the total energy consumed within the EU27 (European Union 27 member states), representing 88 M toe. In general, the UK is a less prolific user of biomass, where it accounts for 2.9 % of total energy consumption or 4.8 M toe (DECC, 2009a). Nonetheless biomass remains the largest source of renewable energy in the UK, contributing 81 % to the total renewables market (Figure 1.1). However, more than two thirds of this biomass is derived from landfill gas, sewage gas, municipal waste or forest residues, rather than dedicated energy crops (DECC, 2009a). The two

primary energy uses of biomass in the UK are in the production of electricity and liquid transportation fuels. Biomass is currently responsible for 2.4 % (9.3 GWh) of the total electricity generated in the UK (389.6 GWh) (DECC, 2009a). Biomass also accounts for 2.6 % of all road fuels (RFA, 2008), but most is derived from imported plant oils with no second-generation biofuels.

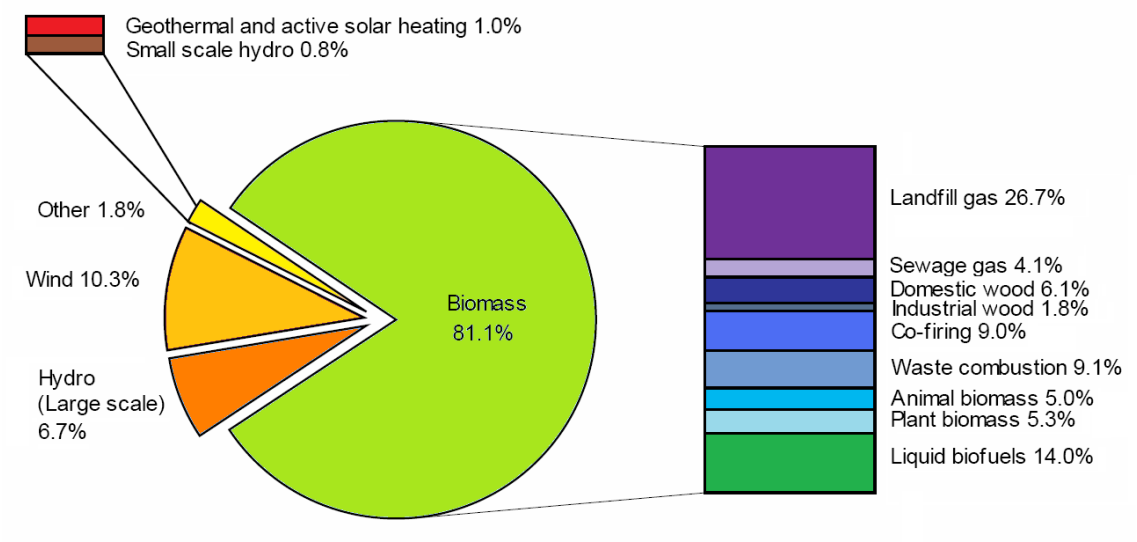

Figure 1.1. UK renewable energy utilisation in 2008. Adapted from DECC (2009a)**.**

The most common use of biomass in the UK is in the co-firing market (DECC, 2009a), where solid biomass is mixed with a fossil fuel and combusted, typically in a coal-fired power station. Co-firing is attractive as it requires little new infrastructure, uses a mature technology and is eligible under the ROC scheme. Alternatively, electricity can be made from 100 % biomass (i.e. dedicated biomass) or converted to both electricity and heat (i.e. combined heat and power, CHP). Decentralised CHP production is becoming popular in rural areas, as it offers localised electricity without the losses associated with transmission networks and a reliable low-cost heat source for industrial or commercial uses (e.g. small communities or hospitals).

Between 2000 and 2007 only 0.006 M ha (million hectares) of SRC poplar and willow and 0.01 M ha of *Miscanthus* were planted for energy use (NNFCC, 2009); a small area compared to the 4.60 M ha under arable crop production (Defra, 2006). By multiplying production by a simple energy conversion ratio (Cannell, 2003), we calculate dedicated energy crops are currently responsible for less than 0.1 % of the UK energy and electricity markets. There clearly remains a large deficit between meeting targets for biomass use and current production (summarised on an area basis in Figure 1.2). However, agricultural land use has a history of responding quickly to market forces (Kilpatrick, 2008). In future, we can envisage a rapid expansion of land under energy crop production. This rapid expansion is dependent on the right economic environment and the sustainable growth of the industry.

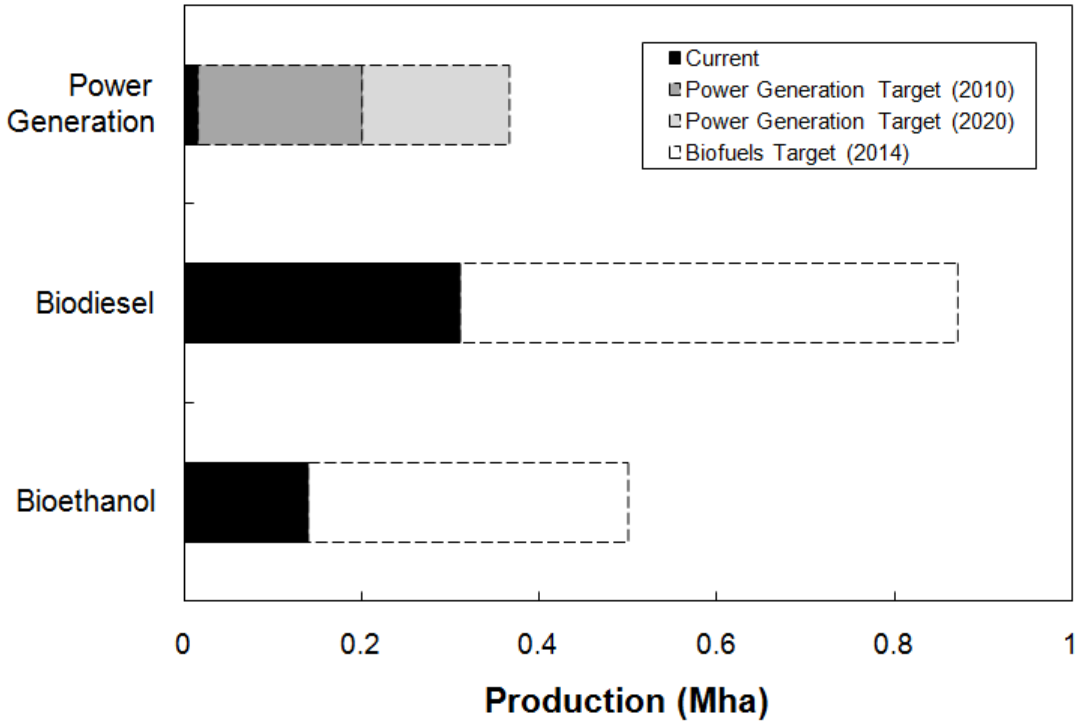

Figure 1.2. Current and future production targets (M ha) for biomass in the UK. Power generation current production: NNFCC (2009). Power generation target 2010: DTI (2003b). Power generation target 2020: DTI & Carbon Trust (2004). Biofuels current production and future targets: NNFCC (2009), assuming 50:50 split of future targets between bioethanol to biodiesel.

1.2.3 Barriers and benefits

Biomass has significant potential to reduce our dependence on non-renewable sources of energy. However, governments face difficult choices between meeting climate change priorities and addressing the concerns raised by the potentially rapid expansion of land under energy crop production. Consequently, all planting of energy crops should adhere to strict rules of sustainability. This has significant implications for predicting the potential availability of energy crops. The issues raised by the growth of the biomass market broadly fall into three categories: economic, social and environmental. However, the challenges are complex and often inter-related.

1.2.3.1 Economic Sustainability

Market security

A study by DEFRA and the DTI (2006), suggested uptake of energy crops in the UK was initially slow because growers were cautious to invest in an unfamiliar agricultural system, supported by a immature and uncertain market. The market's vulnerable nature was emphasised in 2001, when the UK's flagship £30M gasification plant (ARBRE, Arable Biomass Renewable Energy) closed after only eight days of operation due to technical problems and management issues (Piterou *et al.*, 2008). As a consequence of the plant closure its owners went into liquidation and 47 local farmers were left without a market to sell their crop, having planted 1500 ha of SRC (Strawson, 2003). Sherrington *et al.* (2008) described farmer attitudes to energy crops and found the majority of farmers were uncertain over their costs and potential returns. There was also widespread belief that co-firing was the only viable market and that without

competition, power stations would dictate prices.

Economic feasibility

Provided local markets exist, energy crops can offer growers the chance to make a profit and diversify into non-food crops. Furthermore, energy crops suffer little intermittency of supply as they can be stored for use during periods when other renewable energy sources (such as wind and tidal) may have reduced output. This also allows farmers to receive a sustained income after their other crops have been harvested (poplar and willow are typically harvested in November). However, the costs involved in establishing and maintaining biomass energy crops can be high. According to Jones (2007) establishment costs in the UK (including cutting or seedling purchase, feedstock transport and storage, herbicide and fertiliser) are on average £1,638 ha^{-1} for SRC poplar and willow, £1,792 ha^{-1} for *Miscanthus* and £2,464 ha^{-1} for SRC ash, birch, sycamore and sweet chestnut (Figure 1.3). These figures suggest poplar and willow are the cheapest crops to establish, giving them an initial capital benefit over other energy crops. However, coppice crops provide no supplemental annual income (i.e. returns are seen after harvest, every 2-5 years) and cannot be used for other purposes (i.e. *Miscanthus* can be used for animal bedding).

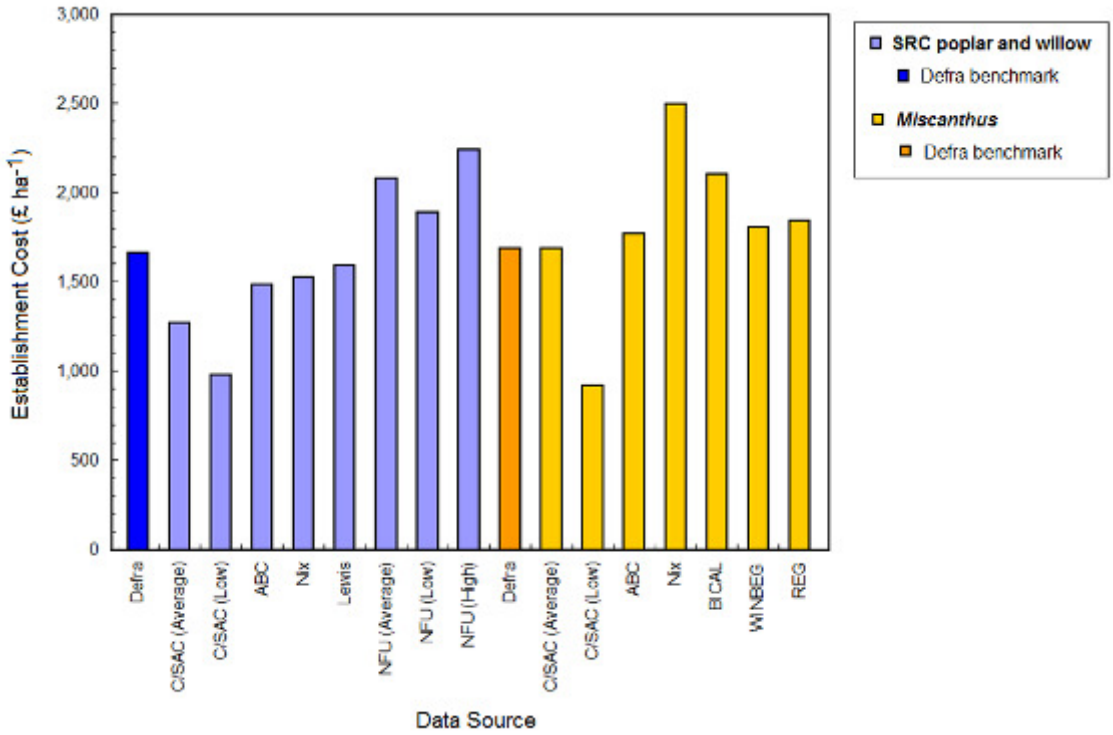

Figure 1.3. Review of establishment costs of SRC poplar and willow (blue) and *Miscanthus* (yellow). Adapted from Jones (2007).

The large establishment costs highlight the necessity of government subsidisation. One mechanism designed to stimulate the market for biomass is the England Rural Development Programme's Energy Crops Scheme (ECS). The ECS provides a one-off grant to support the use of approved energy crops by providing 50% of the actual costs associated with land preparation, planting and establishment, up to £1000 ha^{-1}. To qualify, growers must plant at least 3 ha of energy crop on land compliant with environmental standards and the crop must be grown for a minimum of 5 years (Natural England, 2008). Until reform of the scheme in 2008, each crop also had to be planted within 10 miles of small power installations (>4 MW) or within 25 miles of larger installations, but is now evaluated case-by-case.

The competitiveness of energy crops with other arable systems is important to farmers

(Sherrington *et al.*, 2008). SWS Forestry Services (2006) calculate annual net returns[†] from SRC are between £95 and £145 ha^{-1}. This is dependent on biomass market prices. Current prices range from £40-60 t^{-1} for SRC and £50-60 t^{-1} for *Miscanthus* (DTI, 2007). However, with future wheat prices predicted to increase to over £138 t^{-1} by May 2011 (Farming Online Ltd., 2009), farmers are apprehensive about committing land to energy crops and particularly perennial energy crops. Conversely, as oil prices rise so does the demand for biofuels, resulting in higher prices for energy crops (currently only refers to first-generation energy crops).

Biomass also has wider economic implications, for example in job creation, particularly in rural areas. In India, biomass is the largest energy sector source of jobs, employing an estimated 3-4 million people and in Brazil, the world's second largest producer of bioethanol, the biomass industry employs an estimated 700,000 people (Domac *et al.*, 2005). The European Commission (2005) estimated that by 2010 employment in the EU biomass sector could reach between 84,000[††] and 270,000[†††]. While an ECOTEC study (1999) concluded that up to 840,000 jobs could be created in the EU by 2020. In the UK, the DTI (2004) estimated that each MW of electrical capacity from biomass would create up to 6.5 jobs and Turley *et al.* (2002) estimated each tonne of biodiesel (from rapeseed) would create between 0.65 and 1.15 jobs.

1.2.3.2 Social Sustainability

Food security

If the fuel value of a crop exceeds its food value, it is likely to be used as fuel rather

than food – this is the central tenet of the food vs. fuel argument. Consequently, as oil prices rise and biofuels continue to receive subsidies, they become more economically competitive with food crops. As this happens more agricultural land is used to produce crops intended for the biofuels market and conversely the amount of land available for food decreases. This has raised concerns that food prices will rise and those worst affected may be the poor.

The International Monetary Fund's index of internationally traded food commodity prices recorded an increase of 130 % between January 2002 and June 2008, with a 56 % increase in the 18 months prior to June 2008 alone (IMF, 2010). Many studies attributed the increasing price of food to the growth in biofuels (Elobeid and Hart, 2007; Naylor *et al.*, 2007; Gallagher, 2008; Mitchell, 2008). Although food prices have since stabilised, the possibility of further fluctuations remain and some even predict they will become more frequent in the future (Inderwildi and King, 2009).

Other studies (Headey and Fan, 2008; Urbanchuk, 2008) downplay the role of biofuels in inflating food prices, instead attributing higher than expected costs to a combination of poor food crop yields, increasing demand from China for livestock feed, increasing cost of agricultural inputs and the decline in the value of the dollar, in addition to biofuel growth.

---

† based on then current chip prices and energy crop payments
†† based on business as usual model
††† based on biomass action plan recommendations model

Schmidhuber (2006) suggests that increasing food prices may in fact benefit many rural households, by raising revenues and creating new, better paid employment opportunities. There also remains a large area of available land for biofuels that does not compromise food security; an outlook published in 2009 by the Organisation for Economic Co-operation and Development and the United Nations Food and Agriculture Organisation (OECD and UN Food and Agriculture Organisation, 2009) suggests that current cropland could be more than doubled by adding 1.6 billion hectares – mostly from Latin America and Africa – without impinging on land needed for forests, protected areas or urbanisation.

In the future, the issue of food security may be marginalised further with the development of second-generation biofuel technologies. These technologies produce fuel from the residual parts of current crops, such as stems, leaves and husks that are left behind once the food part of the crop has been extracted. Second-generation technologies also allow non-food crops – such as SRC poplar and willow – to be used in the manufacture of biofuel. Furthermore, by using idle and marginal lands for energy crops we can mitigate the conflict with areas of food production.

Visual impact

Energy crops, such as SRC poplar and willow, can grow to 6 metres (m) and obscure landscape features and views. A UK study (DTI, 2000) of 13 SRC plantations found that four sites (31 %) resulted in adverse effects on the quality of the visual landscape. However, the same study suggested that in certain landscapes SRC and *Miscanthus* could increase visual interest. In addition, the Forestry Commission has published

guidelines for sympathetic planting (Bell and McIntosh, 2001) and all new plantations under the Energy Crop Scheme must be accompanied by an Environmental Impact Assessment.

1.2.3.3 Environmental Sustainability

Soil water and nutrients

During summer in the UK, water use from mature SRC exceeds that of all other vegetation and on an annual basis is second only to coniferous forest (Hall, 2003b). This is due to high transpiration rates and interception losses, as a result of large leaf areas (Souch and Stephens, 1998; Wikberg and Ogren, 2004). In addition, C_3 photosynthesising crops (e.g. poplar and willow) use water less efficiently than C_4 species (e.g. *Miscanthus* and switchgrass). For example, Hall (2003a) found annual water use in *Miscanthus* was 40-100 mm less, on a per unit area basis, than that of SRC. However, these crops are not currently planted on a large enough scale to severely affect water tables or catchments. However, there is also a perception amongst farmers that the deep, coarse roots typical of these species can affect drainage ditches and be difficult and expensive to remove from the field (Sherrington *et al.*, 2008).

Poplar and willow have also been identified as having significant potential in phytoremediation (Aronsson and Perttu, 2001; Pulford *et al.*, 2002; Vandenhove *et al.*, 2004). Phytoremediation is the process by which plants take up contaminants from the soil; highly applicable to scenarios such as waste water treatment and remediation of contaminated land. Poplar and willow are highly suited to this purpose as a consequence

of their fast growth, deep rooting systems and high transpiration rates, which rapidly draws water and nutrients from the soil. Moreover, they can take up and degrade high amounts of organic contaminants and certain heavy metals without serious ill effect to the plant.

Greenhouse gas and waste emissions

Energy crops are generally perceived to have a positive impact on reducing GHG emissions. However, studies show that the species grown, its energy conversion route and the land use it displaces, play important roles in determining the speed at which GHG savings are seen (relative to fossil fuels). St. Clair *et al.* (2008) found that SRC and *Miscanthus* grown for power and electricity abated more GHG emissions than either grasslands or traditional crop systems, as a consequence of decreased fossil fuel inputs and increased carbon sequestration. However, the converse was true when these crops were compared to broadleaf woodland.

Overall, the ratio of energy input to output for the direct combustion of SRC is 1:13-1:30 (Matthews, 2001; Manzone *et al.*, 2009) and for *Miscanthus* is 1:7-1:36 (Lewandowski *et al.*, 1995; Bullard and Metcalfe, 2001; Acaroglu and Semi Aksoy, 2005). Less favourable energy balances are generally realised when energy crops are used to produce liquid transportation fuels, particularly when using first-generation biofuel crops (i.e. cellulosic rapeseed and maize). The energy input to output ratio for liquid biofuel production from rapeseed is as low as 1:1.4-1:2.2 (Venturi and Venturi, 2003) and 1:1.2-1:4 for Maize (Lorenz and Morris, 1995; USDA, 2002; Hill *et al.*, 2006).

St. Clair *et al.* (2008) found that rapeseed biodiesel production offered little or no GHG emissions benefit over traditional crop systems. Furthermore, Searchinger *et al.* (2008) and Fargione *et al.* (2008) found that displacing existing agricultural systems or grasslands with bioethanol production from maize significantly increased emissions, leading to long GHG 'pay-back' periods. For example, Fargione *et al.* concludes that it would take 93 years before a net GHG emission saving relative to fossil fuel production (i.e. pay-back) was seen from maize displacing grassland, consequently rendering this form of biofuel counter-productive in contributing to GHG savings. However, the authors offer conservative estimates of GHG savings from bioethanol production, without taking account of increased future crop productivity or technological improvements. In future, second-generation technology will allow lignocellulosic biomass (i.e. *Miscanthus* and SRC) to be used in the production of biofuel.

Second-generation biofuels offer several benefits over their first-generation alternatives. For example, second-generation crops require lower inputs than more traditional arable energy cropping systems, such as maize. Maize is among the most fertiliser-intensive crops in the world (Hill *et al.*, 2006) and nitrogen-based fertilisers generate nitrogen oxides, which are important greenhouse gases. Moreover, these fertilisers have potentially damaging consequences on animal life – remnants of the fertilisers used with maize in the US are swept into the Gulf of Mexico, creating 'dead zones', devoid of sea life (Rabalais *et al.*, 2002). Furthermore, first-generation biofuel crops also tend to be annuals, which sequester less carbon because they are generally lower yielding and have no annual accumulation of root biomass. They also carry the carbon costs associated

with annual harvesting. Using second-generation crops to produce bioethanol releases approximately 10 % of the CO_2 emissions associated with fossil petroleum, compared to 30-80 % for first-generation biofuel crops (Edwards *et al.*, 2008). In addition, direct combustion of biomass produces 20-25 % less sulphur than low sulphur coal (Demirbaş, 2004). However, lignocellulosic biomass combustion produces problems of slagging, fouling and corrosion associated with the mineral composition of ash waste (Narodoslawsky and Obernberger, 1996; Kaufmann *et al.*, 2000; Nielsen *et al.*, 2000; Llorente and Cuadrado, 2007). This is particularly true with biomass that has a high alkaline compound content, such as *Miscanthus*. Potassium compounds are also abundant in many second-generation biofuel crops (Kumar *et al.*, 2008).

Rainforest deforestation

As oil prices have increased it has become profitable to plant energy crops in place of less economically productive land uses. For example, in Malaysia palm trees are grown for their oil, which can then be blended into diesel fuel. While the carbon footprint of palm oil may be lower than that of fossil fuels, many new palm tree plantations are created by deforestation of rainforest. Malaysia is now the world's second highest producer of palm oil and an estimated 4.3 M ha of primary rainforest have been deforested and the land converted to palm oil production (Malaysian Palm Oil Council, 2008). This land-use change creates a so-called 'carbon debt', which has to be paid back by the biofuel; in the case of palm oil this would take an estimated 423 years (Fargione *et al.*, 2008). Deforestation not only threatens carbon sinks but also biodiversity. News headlines such as 'Biodiesel enthusiasts accidentally invent the most carbon-intensive fuel on earth' and 'Choose the right biofuel or the Orang-utan gets it!' highlight the

perceived risk of deforestation caused by biofuel development. However, it is estimated that only 1 % of palm oil in Malaysia is currently used to produce biodiesel; most is used to manufacture margarine, cooking oil or healthcare products (Malaysian Palm Oil Council, 2008).

Ecosystem services

The protection of ecosystem services is an important constituent of the environmental agendas of both national (Natural England, 2008) and international (European Commission, 2008) government. The Millennium Ecosystem Assessment defines ecosystem services as the benefits people obtain from ecosystems (Millennium Ecosystem Assessment, 2005). These include provisioning services such as food, water, timber, and fiber; regulating services that affect climate, floods, disease, wastes, and water quality; cultural services that provide recreational, aesthetic, and spiritual benefits; and supporting services such as soil formation, photosynthesis, and nutrient cycling.

While short rotation coppice poplar and willow energy crops are in themselves ecosystem services – supporting wildlife, providing wood fuel and helping to regulate the climate – careful planting is required to reduce their conflict with other ecosystem services. In the UK, the Energy Crop Scheme specifies areas which cannot be planted with energy crops, either because of mechanical constraints (i.e. topography) or where land is protected by UK and EU legislation as environmentally, geographically or historically important (Defra, 2004; Wildlife and Countryside Link *et al.*, 2007). However, energy crops also offer potential benefits to biodiversity conservation. When

planted in place of conventional arable agriculture, energy crops can enhance biological diversity (Rowe *et al.*, 2009), although biodiversity may decrease if energy crops are used to replace grasslands or woodlands.

1.3 Biomass Yield

Humans can manipulate the productivity of plants by changing water and nutrient availability and managing the way in which they intercept light. However, yield is ultimately governed by the complex interactions between plant genetics and the physical environment. A review of 1180 yield field trials[†], suggests a large variability in the productivity of energy crops. Mean species yields ranged from to 1.2 odt ha^{-1} yr^{-1} for maple ($n = 1$) to 20.6 odt ha^{-1} yr^{-1} for Acacia ($n =1$) (Figure 1.4). The review also highlights the high within-species variability in yield. Annual poplar yields varied from 0.2 to 35.2 odt ha^{-1} yr^{-1} ($\bar{x} = 6.6$, $n = 384$), whilst willow yields ranged from 0.3 to 30.9 odt ha^{-1} yr^{-1} ($\bar{x} = 10.7$, $n = 344$). This large variation in productivity suggests there is significant opportunity to make step-scale improvements in the future yields of these largely undomesticated crops.

[†] identified by searching the Web of Science and Google Scholar (between 8th June and 17th July 2009) for the key words 'biomass yield', 'bioenergy yield' and 'energy crop yield'. The first 100 responses to each search were read and if their results met the qualification criteria they were recorded. The criteria for inclusion were as follows: (1) trial must be recent (1980-present), (2) trial (or trial plot) must be separated from another by species, crop age, planting density, geographic location, water or nutrient treatment, (3) trial must be grown under scientific conditions, (4) non-food crop and (5) yields from establishment years were excluded.

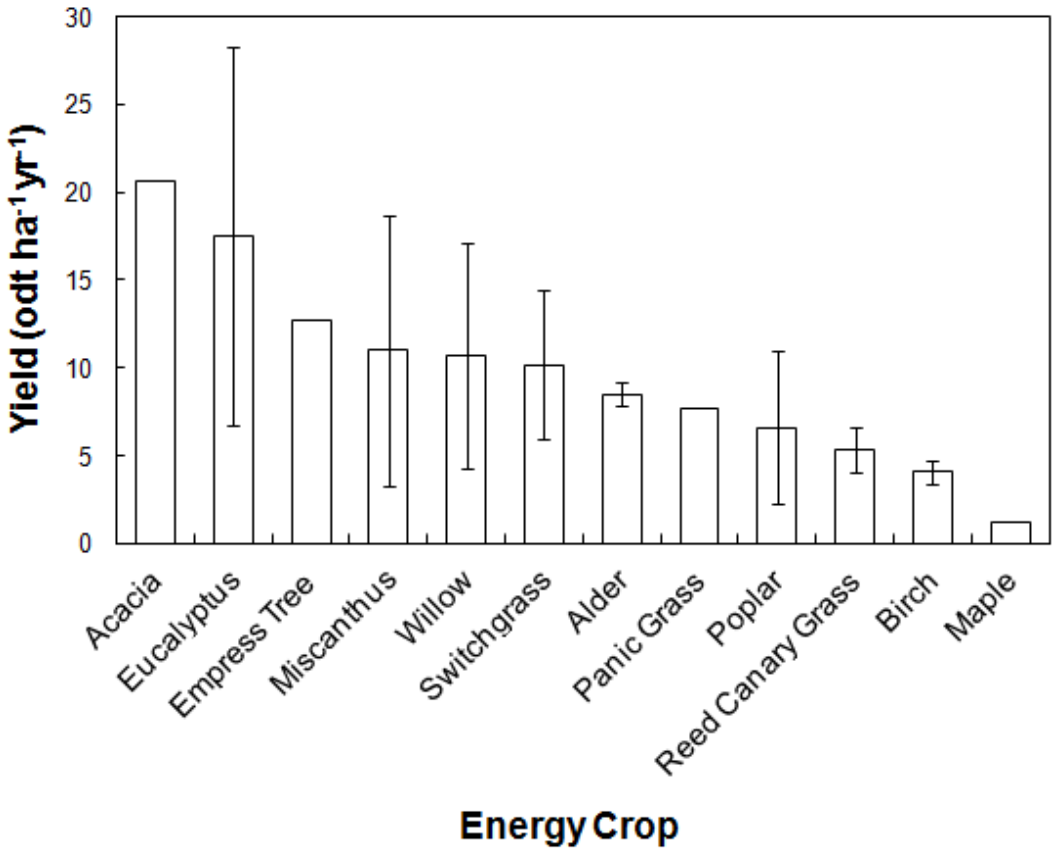

Figure 1.4. Mean annual yields (odt ha^{-1}) of dedicated energy crops, from field trials conducted after 1980 (n = 1180, error bars denote 2 standard deviations)

Where known, the climatic and agronomic conditions of each field trial were recorded and their statistical relationships to yield were modelled, using partial-least squares regression (Simca-P version 11.5, Umetrics, Sweden). Crop age, planting density, annual rainfall and volume of irrigation (in decreasing order of significance) were found to have the strongest impact on yield ($p<0.05$). This approach is useful in identifying principal factors determining yield, but the inconsistency between trial methodologies (e.g. differences in recording climatic variables, number of replicates, small trials with greater edge effects) makes it difficult to reliably quantify these interactions. While statistical assessment of yield may highlight trends in data, it also important to understand the physiological basis to productivity. Consequently, this can help improve

our understanding of the processes involved in plant growth, anticipate future changes in productivity and aid in the interpretation of model results.

1.3.1 Water

Water is used in many biochemical processes within the leaf, most notably in photosynthesis, whereby it reacts with carbon dioxide in the presence of sunlight to produce carbon (and oxygen). Water also acts as a medium for the flow of nutrients from the soil and keeps the plant upright by turgor pressure. A plant's main source of water is the soil. The amount of water held in the soil, is primarily controlled by the rate of incoming water (i.e. precipitation) and the water holding capacity of the soil structure. Rates of precipitation will also indirectly influence humidity levels and general cloudiness (altering evaporation and surface rates of photosynthetically active radiation). Water is primarily lost from the plant system by evapotranspiration through leaf stomata.

Poplar and willow are riparian species and are generally characterised by high water use (Hall, 2003b). Guidelines suggest SRC crops should only be planted where annual precipitation rates are in excess of 400 mm yr^{-1} (Tuck *et al.*, 2006; Agriculture and Agri-Food Canada, 2009), unless given supplemental irrigation or where tree roots are able to access the water table. Future predictions for lowland England suggest decreased precipitation (Figure 1.5) and increased soil moisture deficit is likely during summer months (Hulme *et al.*, 2002), which may lead to dehydration and increased plant water stress. In winter months the opposite may be true, leading to an increased risk of

flooding, which could damage roots reducing their effectiveness and ability to cope with summer droughts (Redfern and Hendry, 2002).

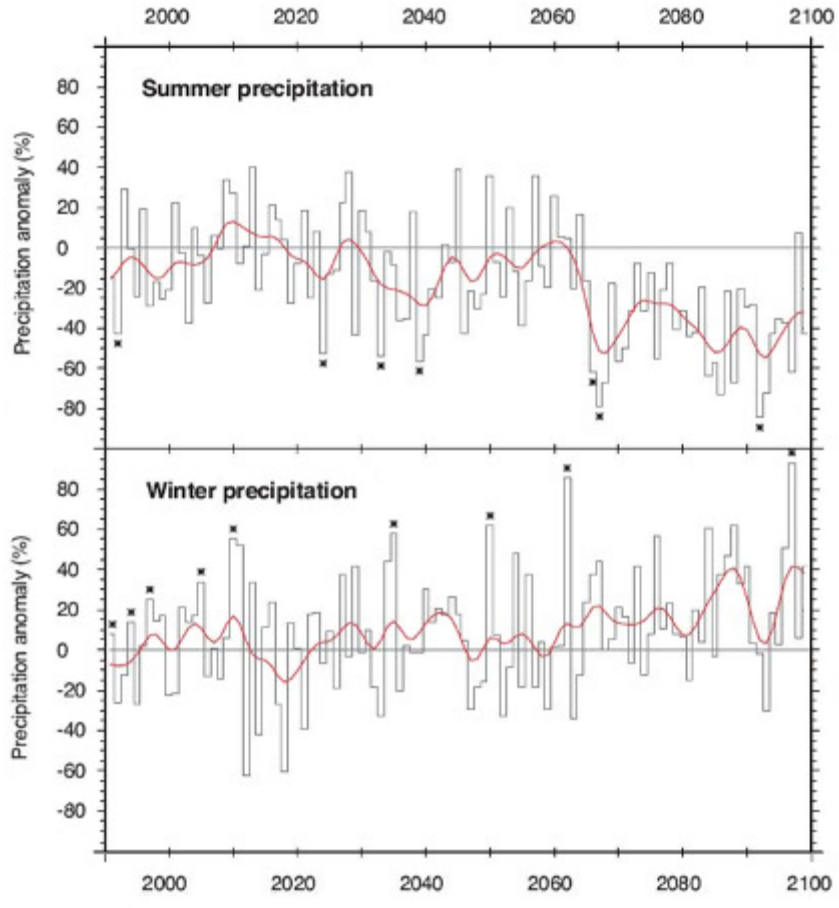

Figure 1.5. Mean summer (top) and winter (bottom) precipitation rates, based on UKCIP02 medium emission scenarios from 1990-2100. Adapted from Hulme *et al.* (2002).

Souch & Stephens (1998) showed that poplar genotypes in severe drought conditions produced 60-75 % less dry matter than those in the well-watered conditions. Concomitantly, Mahoney & Rood (1991) recorded similar reductions to above-ground biomass production under drought conditions, but also found an increased root to shoot ratio as roots lengthened under stress to find new sources of water.

One important consequence of reduced water availability in vascular plants is xylem cavitation. Cavitation occurs when the water tension in the xylem becomes so great that dissolved air expands to fill the vessel, preventing functionality. Xylem vulnerability to cavitation has been identified as a promising criterion for identifying more drought resistant poplar varieties (Sparks and Black, 1999; Pockman and Sperry, 2000; Cochard *et al.*, 2007). Although, Harvey and van der Driessche (1997) found phosphorus fertilisation helped reduce susceptibility of poplar to cavitation.

In response to drought stress plants have developed varied adaptive responses. In general, both poplar and willow are able to cope with short periods of drought by improving water use efficiency (Linderson *et al.*, 2007; Guo *et al.*, 2010). Some poplar genotypes close their stomata during water stress events (in response to abscisic acid translocation to leaves) to reduce transpiration losses (Sparks and Black, 1999; Wikberg and Ogren, 2004). Conversely, the stomata of other genotypes appear unresponsive to drought (Ridolfi *et al.*, 1996). Stomata are also responsive to flooding, Liu & Dickmann (1996) found that the onset of flooding resulted in partial stomatal closure in poplar. However, net photosynthesis significantly declined after prolonged exposure to flood conditions. Emergence of adventitious roots on the submerged portions of stems in both clones seemingly helped photosynthesis recovery. Identifying genotypic sensitivity to water stress can help us identify the genetic traits associated with drought resistance (e.g. stomatal closure), which can then be bred into future crops.

1.3.2 Temperature

Temperature has a direct impact on the rates of plant photosynthesis and respiration.

Photosynthesis is typically geared towards an optimal species-specific temperature and is less efficient above or below this value (Berry and Bjorkman, 1980). Shifts in temperature affect the affinity of rubisco for CO_2, the capacity of rubisco activase to maintain rubisco in an activated state and rates of electron transport (Yamori *et al.*, 2005). In contrast, dark respiration steadily increases (exponentially) with temperature, until the rate rapidly decreases near the lethal heat limit (Morison and Morecroft, 2006). Poplar and willow species are characterised by a wide provenance and in general, are suitable for climates with a temperature range from 3-38 $^{\circ}C$ and 1-38 $^{\circ}C$, respectively (Tuck *et al.*, 2006). Optimal growth temperatures vary between genotypes and change rapidly over the growing season but can be considered to be between 15-25 $^{\circ}C$ (Medlyn *et al.*, 2002; Ow *et al.*, 2008).

Current environmental conditions appear more favourable for photosynthesis rather than respiration. However, temperatures are likely to rise in the future, with summer temperatures increasing at a greater rate than those in winter. In the UKCIP low emissions scenario for 2050 (Figure 1.6) mean summer temperature is predicted to increase by up to 2.5 $^{\circ}C$ (Hulme *et al.*, 2002). If temperatures exceed specific plant threshold levels (at critical stages of plant development) for even a few hours crop damage may be irreversible (Wheeler *et al.*, 2000).

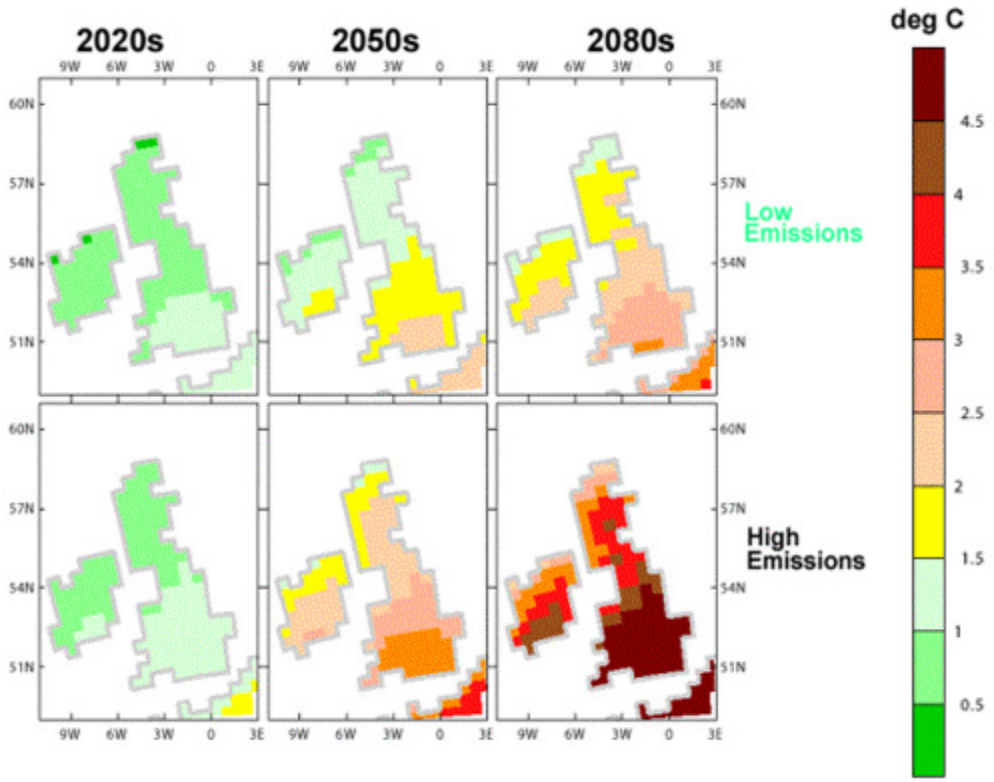

Figure 1.6. Mean summer temperature change, based on the UKCIP02 low (top) and high (bottom) emission scenarios; given for the 2020s (left), 2050s (middle) and 2080s (right). Adapted from Hulme *et al.* (2002).

In the short-term, an increase in temperature will result in an immediate alteration in the rate of respiration, determined by the respiratory Q_{10} (a measure of the rate of change of a biological system as a consequence of increasing the temperature by 10 ^{o}C). However, long-term exposure to a change in temperature is likely to result in partial or full acclimation of respiration (Atkin *et al.*, 2000; Loveys *et al.*, 2003; Armstrong *et al.*, 2006). Furthermore, photosynthetic acclimation to long-term changes in temperature may result in a new thermal optimum (Berry and Bjorkman, 1980; Turnbull *et al.*, 2002; Sage and Kubien, 2007). Turnbull *et al.* (2002) found that *P. deltoides* exposed to daytime warming, fully acclimated photosynthesis to a 6 ^{o}C range of temperature. While we can potentially foresee short-term reduced rates of productivity in response to

warming, the converse may be true in cooler areas where photosynthesis is currently limited (Lawlor, 1987). Furthermore, we can expect warming to bring forward bud burst (Peñuelas and Filella, 2001; Parmesan and Yohe, 2003; Root *et al.*, 2003; Menzel *et al.*, 2006) and increased deposition of anthropogenic nitrogen as ammonium or nitrate, which acts as a plant fertiliser (Nadelhoffer *et al.*, 1999; Quinn Thomas *et al.*, 2010). Conversely, elevated temperatures may also increase transpiration and respiration rates, and autumnal frost damage (Redfern and Hendry, 2002). Temperatures may also have an effect on the ratio of above- to below-ground biomass storage (Constable and Retzlaff, 2000), potentially having serious implications for coppiced crops. Landhausser (2003) found cuttings of poplar exposed to a soil temperature of 5, 15 and 25 $^{\circ C}$ had the highest above to below-ground biomass ratio at 25 $^{\circ C}$.

1.3.3 Carbon dioxide

Carbon dioxide is the primary component of photosynthesis, the mechanism by which plants create carbon (sugar). This carbon makes up nearly 50 % of the mass of each poplar and willow tree (Wullschleger *et al.*, 1997; Luo *et al.*, 2006). Predictions suggest atmospheric CO_2 could increase to between 525-810 ppm by the middle of the 21st century (Hulme *et al.*, 2002). Rising CO_2 is predicted to have a fertilisation effect on plant growth by increasing the rate of photosynthesis, resulting in more carbon storage (Norby *et al.*, 1999). Conversely, rising CO_2 will decrease stomatal conductance, generally resulting in an increase to the water use efficiency of the crop (Beadle *et al.*, 1993).

To quantify our understanding of the role of CO_2 in the plant, many gas exchange

experiments have been established. However, varied and inconclusive results arose due to trials being conducted in closed environment (CEC) and open top chambers (OTC), which have problems of microclimatic variation and limited size. The development of Free Air Carbon Enrichment (FACE) systems has gone some way to eliminating these problems (Ainsworth and Long, 2005). Furthermore, improved analytical tools have helped scientists better understand the physiological responses associated with CO_2 gas exchange.

Poplar has been widely used in CO_2 experiments, as a consequence of its fast response mechanism to changing environmental conditions (Gielen and Ceulemans, 2001). Experimental data for poplar suggests biomass production could be over 31 % higher under CO_2 concentrations between 500-700 ppm (compared to ambient, 350-370 ppm) (Table 1.3). This fertilisation effect is related to photosynthetic stimulation and evidence suggests no long-term loss in sensitivity (Norby *et al.*, 1999; Liberloo *et al.*, 2007), although other studies dispute this (Kalina and Ceulemans, 1997; Taylor *et al.*, 2001b).

Table 1.3. Above-ground biomass (AGB) growth responses to elevated CO_2 from poplar field trials.

Species	Genotype	Location	Trial type	Age	Soil	CO_2 (ppm)	AGB change (%)	Reference
P. tremuloides	-	Wisconsin, US	CEC (pots)[†]	<1 yr	Forest topsoil	650	+ 53	Kinney & Lindroth (1997)
P. deltoides x P. nigra	Eugenei	Minnesota, US	OTC[$]	<1 yr	Low fertility dry sand	707	+ 25 (LN); + 49 (HN)	Lussenhop *et al.* (1998)
P. deltoides x P. nigra	DN-33	Minnesota, US	OTC (pots)*[$]	<1 yr	Peat: sand: vermiculite (2:1:1)	500	- 16	Dickson *et al.* (1998)
	DN-34						+ 29	
	DN-70						+ 34	
	DN-74						+ 34	
P. nigra x P. maximowiczii	NM-6						+ 36	
P. tremuloides	-	Minnesota, US	CEC (pots)[†$]	<1 yr	Pure silica sand: loam, peat, sand mix (4: 1)	580	+ 90	Tjoelker *et al.* (1998)
P. tremuloides	Six genotypes	Minnesota, US	OTC[$]	3 yrs	Low fertility dry sand	707	+ 16 (LN); + 38 (HN)	Zak *et al.* (2000)
P. tremula x P. tremuloides	-	Nancy, France	FRCEC (pots)	<1 yr	–	700	+ 34	Loewe *et al.* (2000)
P. trichocarpa	Idunn	Idunn, Iceland	CTC[$]	3 yrs	Silt loam	700	- 8 (LN); + 44 (HN)	Sigurdsson *et al.* (2001)
P. trichocarpa x P. deltoides	Boelare	Hampshire, UK	OTC (pots)	<1 yr	Compost: vermiculite (1:1)	-	+ 38	Taylor *et al.* (2001b)
P. alba	2AS11	Tuscany, Italy	FACE*	3 yrs	Silt loam	550	+ 27	Calfapietra *et al.* (2003)
P. x euramericana	I-214						+ 27	
P. nigra	Jean Pourtet						+ 15	

[†] irrigated, * O_3 treatment, [$] = fertilised, LN = low nitrogen, HN = high nitrogen

1.3.4 Ozone

Any future yield increase, which may occur as a result of increased atmospheric CO_2, may be partially or fully offset by rising tropospheric ozone (O_3) in the lower atmosphere (Isebrands *et al.*, 2001). Unlike stratospheric ozone which is being depleted, tropospheric ozone – a key component of photochemical smog – is predicted to triple from concentrations of 5 ppm (2000) up to 15 ppm (2100) across Europe (Felzer *et al.*, 2004); this particularly effects urban areas but is now also affecting rural areas. O_3 possesses powerful oxidising properties and many fast growing plants, including poplar and willow, show a hypersensitive response to increasing concentrations (Kline *et al.*, 2008). In native and managed poplar populations, elevated O_3 has been shown to negatively affect yields and carbon sequestration (Dickson *et al.*, 2000). Coleman *et al.* (1995a; 1995b) also report accelerated leaf senescence and changes to the allocation of carbon (resulting in reduced winter storage). On a leaf level, O_3 inhibits stomatal opening by directly affecting the guard cells that control the stomata, reducing photosynthetic rates and gas exchange functionality (Riehl Koch *et al.*, 1998; Bortier *et al.*, 2000). However, responses to elevated O_3 have a strongly genetic component, and some poplar genotypes exhibit tolerance to small increases in O_3 (Ceulemans and Isebrands, 1996; Ryan *et al.*, 2009).

1.3.5 Soils

Soils play an important role in determining yield. High yields tend to be found on sites with loamy, podzolic or alluvial soils whilst heavy clay and saline soils will

significantly reduce yield (Mitchell *et al.*, 1999; van der Perk *et al.*, 2004; Andersen *et al.*, 2005). Heavier textured soils require less precipitation than light textured sandy soils to maintain optimum soil water and consequently growth (Agriculture and Agri-Food Canada, 2009). An unimpeded soil depth of at least 1 m is recommended, to allow roots to find water and nutrients (Ledin and Willebrand, 1995; Agriculture and Agri-Food Canada, 2009).

Soil pH also has a direct effect on the ability of plant root cells to absorb both nutrients and water from the soil. For example, when pH falls below 6.5, phosphorus begins to become unusable by plant roots and below 6.0 nitrogen, potassium, calcium and magnesium will also decline in their effectiveness (Kilmer and Hanson, 1982). Above 6.5, iron and manganese begin to become locked up and unavailable; above 7.0 boron, copper and zinc begin their decline (Kilmer and Hanson, 1982). Although iron is an abundant trace element in the soil, poplars can have difficulty in absorbing sufficient quantities especially in high pH, calcareous soils (Agriculture and Agri-Food Canada, 2009). Guidelines recommend willow be grown on soils with a pH between 5.5-7 (Defra, 2004) and poplar on soils between 5.5-8 (Jobling, 1990; Shock *et al.*, 2005). This is supported by Mitchell *et al.* (1999) who suggest the optimal soil pH for SRC to grow is between 6-7. Mitchell *et al.* also suggest very wet sites restrict herbicide use and timing, which can allow pest and disease damage, however, they go on to say soils should be kept moist throughout growing season.

1.3.6 Topography

Temperature, humidity, atmospheric pressure, radiation and carbon dioxide concentrations change with elevation, potentially limiting yield. Tuck *et al.* (2006) recommends a minimum elevation of 0 m and a maximum of 1100 m, although no justification for this is given. Shaw *et al.* (2001) did find a significant negative correlation between yield and elevation in Alaska, linked to soil quality. Whilst, Armstrong (2003) suggested farmers would be more likely to grow SRC at lower elevations and therefore advised a maximum elevation of 250 m for growing SRC in the UK. Flat (<12 ^{O}) and well-drained soils are also recommended (Mitchell *et al.*, 1999; Andersen *et al.*, 2005), in order to allow access for machinery to cultivate and harvest the crop and to prevent soil waterlogging.

1.3.7 Pests and disease

Vulnerability to pests and disease is genetic and varies considerably between species and even within species. While not all pests and diseases are damaging to SRC crops – most insects are largely benign and for example, may help increase biodiversity by supporting bird populations – there are those that can seriously affect yield by damaging photosynthetic cells, obstructing plant water functionality, disrupting chemical signals and weakening stem structure.

In high yielding species such as poplar and willow, where leaf size is closely linked to productivity, damage to leaf functionality can be particularly problematic. However, a

relatively high level of leaf damage can be tolerated with little adverse effect to yield (Tubby and Armstrong, 2002). For example, the removal of 90 % of a willow crops leaves results in a yield loss of less than 40 % (Pei *et al.*, 2002). However, the timing and duration of attack is important and can potentially lead to premature plant death. Considering the significant potential for pests and disease to adversely affect yield, it is not only important to understand the affects they have on the crop, but also their cause, development and spatio-temporal distribution.

Leaf rust

Leaf rusts (*Melampsora* spp.) are often cited as the most significant threat to poplar and willow species in the UK (Parker *et al.*, 1993; Pei *et al.*, 1998; Lonsdale and Tabbush, 2002; McCracken and Dawson, 2003; Tubby, 2005). Of the thirty *Melampsora* species worldwide, three are found on UK willow: *M. epitea* and *M. capraearum* being the most common, followed by *M. ribesii-viminalis* (Pei *et al.*, 1998). The variety of rusts afflicting poplar is more expansive (e.g. *M. larici-populina* and *M. allii-populina*) and as such poplars have a high vulnerability to rust attack (Tubby, 2005). Rust commonly overwinters on fallen leaves and during spring will establish itself in pustule colonies on leaves and shoots (spread by wind and rain splash), affecting stool growth and restricting leaf photosynthesis causing premature leaf fall (Pei *et al.*, 1998). SRC is particularly susceptible to fungal pathogens due to the trees close proximity, large surface area and high rust pathogenicity. Taking provisional data from the national SRC field trials (Armstrong *et al.*, 1998), we can identify spatio-temporal interactions between yield and rust (Figure 1.7). Severity was generally higher in successive rotations, which supports results from other trials (McCracken and Dawson, 2003).

Between 4.7 and 30.2 % (variable by species) of the 51 sites recorded >20 % leaf-area-lost (LAL) for poplar and 6.3-21.9 % for willow (Evans *et al.*, 2002).

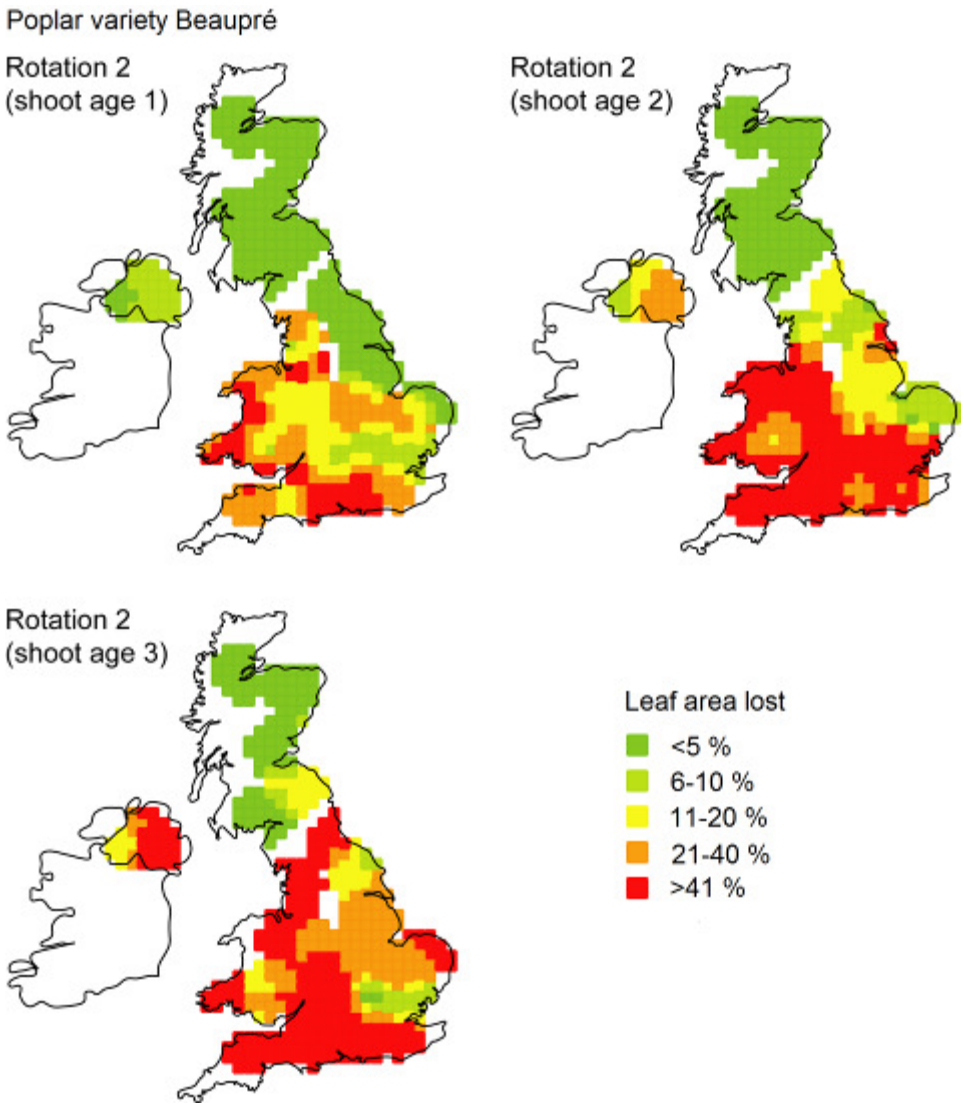

Figure 1.7. Incidence maps of *Melampsora* rust infection in *Populus trichocarpa* x *P. deltoides* genotype Beaupré. Measurements taken during the second rotation (stem ages 1-3) and scored on a leaf area lost basis. Adapted from Forest Research (2003).

Careful planting can reduce the impact of leaf rust. Tabbush & Parfitt (1999) recommend planting varietal mixtures of between 5 and 20 genotypes. Planting mixtures of genetically diverse, rust tolerant varieties can help improve long-term crop yield (McCracken and Dawson, 1997). However, the pathogenicity and specificity of

rust can change over time. Rust 'tolerance' (causing only superficial damage) as opposed to rust 'resistance' is recommended, as 'tolerance' is often controlled by single genes making them vulnerable to rust adaptation (Tabbush and Parfitt, 1999). A further strategy for controlling rust is to introduce virulent strains of hyper-parasites (e.g. *Sphaerellopsis filum*) into plantations (Whelan *et al.*, 1997). It is also important to avoid planting poplar close to European larch (*Larix decidua*), as this species acts as a secondary host for *M. larici-populina*; and Tubby (2005) suggests that no poplar should be planted within 2 km of any larch.

Other diseases

Other diseases (e.g. *Marssonina* leaf spot, poplar mosaic virus, willow scab and black canker) accounted for a high percentage of leaf damage in the national field trials network. By the end of the first rotation 17 % of poplar and 12 % of willow plots showed 20 % LAL from such damage (Evans *et al.*, 2002). Some poplar plots recorded up to 83 % LAL, resulting in almost complete crop loss; poplar variety Ghoy was the worst affected (20 of 51 sites). Disease is also seasonally variable; pathogens typically develop more rapidly later in the growing season and at temperatures between 16-28 ^{o}C, which favour germination (Sinclair *et al.*, 1987). Primary infections can also leave trees vulnerable to secondary infections, which exploit already stressed trees (Sinclair *et al.*, 1987).

Other pests

Defoliating insects (particularly those of the order *Lepidoptera*) caused a 9-12 % LAL in both poplar and willow species, with their greatest prevalence in July and September.

Stem infestation and sap suction by aphids (e.g. giant willow aphid *Tuberolachnus salignus* and black willow aphid *Pterocomma salicis*) can cause serious problems for willow. Aphid species can also act as hosts for numerous viruses. Though not identified as a threat from the field trials network, Tucker and Sage (1999) identified willow beetles of the order *Chrysomelidae* (e.g. brassy beetle *Phratora vitellinae* and blue beetle *P. vulgatissima*) as the most damaging insect species to SRC willow, with young shoots being particularly palatable. It is suggested that populations of mature *Chrysomelidae* at densities greater than 10 per m^2 within plantations should be controlled by pesticide (Tucker and Sage, 1998). Other problem species identified by literature include the winter moth larvae (*Operophtera brumata*) in Ireland (Neenan, 1990), and the white satin moth (*Leucoma salicis*), puss moth (*Cerura*) and willow web moth larvae (*Halias chlorana*) in Denmark (Sage, 1994). Browsing mammals also sporadically cause damage; deer can rub the bark off the trees, and squirrels and voles can damage juvenile crops, therefore it is essential to provide and maintain suitable fencing (Tubby and Armstrong, 2002).

1.3.8 Agronomical practices

Management strategies should also be considered important tools for improving productivity. For example, increasing the plant spacing within rows of coppice crops, such as poplar, is likely to increase their light interception efficiency (Kopp *et al.*, 1997; Casella and Sinoquet, 2007; Fang *et al.*, 2007). Concomitantly, increasing planting densities should benefit less productive varieties because of their weak potential in canopy closure dynamic. Planting genotypes with narrow leaves and small petioles may similarly increase productivity of high-density coppice poplar crop systems by

improving light interception (Casella and Sinoquet, 2007).

1.3.9 Technology

In the future, breeding programmes and genomic tools could enable the rapid deployment of plants with improved productivity, that remain free from pests and disease, tolerant to drought and adaptive to rising CO_2 (Taylor *et al.*, 2001a; Sims *et al.*, 2006; Street *et al.*, 2006). Rook (1991) suggested improved breeding could theoretically produce yields of up to 30 odt ha^{-1} yr^{-1} in SRC crops. Production physiology has identified architectural traits associated with high poplar and willow biomass growth, including the production of leaves with many small cells, late season branching and the production of large leaves (Rae *et al.*, 2004; Robinson *et al.*, 2004; Marron and Ceulemans, 2006). The availability of the full poplar DNA sequence should enable the identification of underlying genes that control these traits. Areas of the poplar genome determining yield have already been identified (Wullschleger *et al.*, 2005; Rae *et al.*, 2008), suggesting large-step improvements in yield are likely in the future.

1.4 Productivity Modelling

Trialling and breeding high-yielding species and good agronomic practices help maximise productivity. However, such exercises do not expand our understanding of the physiological basis of yield. Plant models offer a more cost and time efficient alternative to large scale field trials, enabling both micro (e.g. field) and macro (e.g. national) predictions of productivity to be made. To identify where improvements can

be made in our understanding, it is important to compare and contrast the methodologies behind productivity models.

1.4.1 Empirical models

Empirical models are simple statistical tools used to predict trends in observed data. In biology, they are useful because they require no biological knowledge of system processes and have wide applications, including in yield modelling. Empirical models using simple regression techniques (e.g. general linear modelling) can predict linear relationships between predictors and multiple variables, for example yield and climatic observations (Bateman and Lovett, 1998; Landau *et al.*, 2000; Price *et al.*, 2004). However, many plant interactions with the physical environment are non-linear. Consequently, this has led to the development of non-linear models (Hansen and Indeje, 2004; Prasad *et al.*, 2006; Richter *et al.*, 2008).

Providing an empirical model is robust (i.e. the predictions are statistically close to the observations) and the necessary data exists for upscaling, results from empirical models can be extrapolated to larger scales. This makes empirical models particularly useful in estimating yield potentials across a wide geographic area. However, caution is necessary when extrapolating outside the range of the original model inputs as they may be unrepresentative. Furthermore, using empirical models can lead to over-fitting observations and giving a false sense of meaning (Moore, 1971; Beatty, 1980), therefore careful interpretation of results is necessary. To make biologically meaningful predictions of how yield changes with time and under variable conditions a process-

based model is necessary.

1.4.2 Process models

Process-based models use empirical observations and 'first principle' assumptions to represent the interactions between multiple data themes. They require expert knowledge to parameterise and validate. In biology, process-based models can be used to simulate the complex interaction between plant growth mechanisms and the physical environment. Estimation of whole plant dynamics are made by combining (or coding) smaller models that simulate specific plant processes (e.g. photosynthesis). Process-based models for forest species are less developed that those for traditional crops, because for trees and forests, flux dynamics can change over time in relation to stages of development, resource availability and varying climate (Gower *et al.*, 1996). Recent advances in mechanistic modeling approaches for forests (Table 1.4) have closed much of the gap in our understanding. However, SRC crops (i.e. poplar and willow) differ significantly from other forest species, as a result of their unique management and physiological responses. In SRC, natural growth patterns are controlled to drive competition between stems and produce high above-ground biomass growth. This presents considerable modelling challenges.

Table 1.4. Summary of key process-based forest models.

Model	Species	Scale		Inputs	Primary Processes	Outputs	Reference
Sievanen	SRC willow	Stand (big-leaf, homogen. canopy)	Daily	T (air), incoming radiation	P, C partitioning based on empirical function, no water or nutrient stress and no senescence	GPP & harvest index	Sievanen (1983)
ECOPHYS	Poplar	Plant (stem no branching)	Daily	T (air), incoming radiation, genotype-specific phenology, leaf shapes and orientation	P, light interception, mortality & nutrient uptake	Height, leaf morphology	Rauscher *et al.* (1990)
SOILN-FOREST	Multiple	Stand (big-leaf)	Daily	T (air and soil), sunshine hours, water and nutrient availability	P, C partitioning as a function of leaf nitrogen and water, R	GPP	Eckersten (1991)
VIMO	Grapevine	Stand (big-leaf, big-root)	Daily	T (air), incoming radiation, growing days degrees	P, C partitioning based on empirical function, N assimilation, R, senescence (function of min. T)	GPP	Wermelinger *et al.* (1991)
BIOMASS	Pine	Plant (equal sized crowns)	Hourly	Incoming radiation, moisture availability	P, C allocation based on empirical function, R	GPP	McMurtie *et al.* (1992)
PnET-CN	Boreal forest	Plant	Monthly	T (air), incoming radiation, soil water holding capacity, nitrogen availability	P, C allocation based on empirical function, R, water and nutrient uptake, evapo-transpiration	GPP	Aber & Federer (1992)
SECRETS	Multiple	Plant	Daily	Climatic, photosynthetic, soil, C:N leaf ratio, LAI	P, C allocation based on C:N ratio and nutrient uptake, R	GPP, soil water	Deckymn *et al.* (2004)
ForestETP	Multiple	Plant (variable leaf canopy)	Daily	Climatic, photosynthetic, soil, LAI, CO_2 and water vapour exchanges	P, C allocation based on LAI, water and nutrient uptake, R, evapo-transpiration	GPP, wood quality, soil water	Evans *et al.* (2004)
ANAFORE	Multiple	Plant (variable leaf canopy)	Daily	Climatic, photosynthetic, soil, CO_2 and water vapour exchanges	P, C allocation based on refined pipe theory, water and nutrient uptake, R, evapo-transpiration	GPP, soil water, LAI	Deckymn *et al.* (2006)

T is temperature, P is photosynthesis, R is respiration, LAI is leaf area index, C is carbon, N is nitrogen, GPP is gross primary productivity

Simple forest models parameterised for poplar and willow, such as ECOPHYS and SOILN-FOREST, use the big-leaf model principle (i.e. a single leaf without a canopy structure) and are driven by simple climatic interactions. For example, ECOPHYS is primarily driven by the inputs of solar radiation and air temperature, and in the case of SOILN-FOREST also by soil temperature and nitrogen-water-plant dynamics. These models have proved to be useful tools in investigating general environmental interactions but are poor simulators of plant level growth (Philippot, 1996).

Using a small number of determinants for plant growth can only be used reliably when that particular factor overwhelmingly controls productivity. In general, plant mechanisms do not change in isolation and yield is controlled by complex interactions and feedback processes between many variables (Johnsen *et al.*, 2001). This is particularly true for poplar and willow (see chapter 1.3). Until recently, physiological processes, such as water balance or nutrient cycling, received less attention in the modelling context (Mäkelä *et al.*, 2000). However, these processes are highly significant for understanding the controls on photosynthesis and the effects of climate change on tree growth. More contemporary models look at whole system processes. For example, SECRETS is a widely-used, soil-vegetation-atmosphere transfer model adapted to simulate forest management practices, such as thinning and coppicing (Deckmyn *et al.*, 2004). It simulates many of the above- and below-ground processes associated with plant-carbon and plant-water fluxes to accurately predict poplar growth.

However, there is an optimum structure and level of complexity for any model, which is based on the resolution and level of accuracy required by the user (Battaglia and Sands,

1998). Every variable, input or process added to a model increases the uncertainty in its estimates, as each variable has its own degree of associated uncertainty. Therefore, there is a balance between an increase in explanatory power and the generality required from a model. For example, process-based forest models are seldom used as practical tools in forest management, because they are considered too complex, with too many uncertainties and poorly fitted parameters (Mohren and Burkhart, 1994; Johnsen *et al.*, 2001). However, process-based models have high importance in climate change modeling (Battaglia and Sands, 1998).

Chapter 2．Yield and spatial supply of bioenergy poplar and willow short rotation coppice in the UK

The findings of this chapter have been published in two papers. These can be found in Appendix F.

(1) Modelling supply: *New Phytologist* (2008, Vol. 178: 358-370)
(2) Modelling demand: *Bioresource Technology* (2010, Vol. 101 (21): 8132-8143)

2.1 Introduction

Using biomass to produce energy has been identified as having significant potential to contribute to reductions in greenhouse gas emissions and to the maintenance of a secure and sustainable energy supply, within the UK (UKERC, 2006; Scottish Executive, 2007), Europe (European Commission, 2005) and more widely (Berndes *et al.*, 2003; IEA, 2007). Dedicated SRC energy crops, such as poplar and willow, are grown commercially for heat and electricity generation as a consequence of their rapid growth rate and favourable energy ratio. In the future, SRC crops may also be grown as feedstock for second-generation liquid biofuels (Houghton, 2006). Rather than simply extracting sugars by fermentation (i.e. first generation), second-generation technology breaks down plant lignin and cellulose. This allows biofuel to be produced from any plant material, therefore reducing the conflict between food and fuel.

Biomass in the UK currently accounts for 81 % of renewable energy consumption or 2.9 % (4.8 Mtoe) of total energy consumption (DECC, 2009a). However, more than two thirds of this biomass is derived from waste or forest residues, rather than dedicated energy crops (DECC, 2009a). The two primary energy uses of biomass in the UK are in the production of electricity and liquid transportation fuels. Biomass is currently

responsible for 2.4 % (9.3 GWh) of the total electricity generated in the UK (DECC, 2009a). Biomass also accounts for 2.6% of all road fuels (RFA, 2008), but most is derived from oilseed rape with no second-generation biofuels.

Between 2000 and 2007 only 5,700 ha of poplar and willow and 9,800 ha of *Miscanthus* were established (NNFCC, 2009). To meet the Renewables Obligation, it is anticipated that up to 125,000 ha of dedicated energy crops may be required (Britt *et al.*, 2002). In addition, meeting the Renewable Transport Fuel Obligation would be require 870,000 ha of oilseed rape (biodiesel) and 500,000 ha of wheat (bioethanol) (NNFCC, 2009). To meet these targets, up to 8.1 % of the UK's 18.5 M ha of agricultural land would need to be committed to energy crops. However, these estimates are based on average species yields and do not account for spatial variation. Improving yield estimates will help give a better understanding of the likely land use change in the future. Furthermore, careful consideration of site suitability for planting will be beneficial in minimising the conflict between energy crops and food, population growth and the natural environment.

Here, an empirical model was developed to find linear relationships between environmental variables and crop yield, using observed data gathered by Forest Research from the UK SRC field trials network (Armstrong, 1997). To take into account the closely correlated variables and contextually small number of sites compared to the number of independent variables, a partial least squared (PLS) regression was used. The resultant weightings of variable influence (coefficients) were then used to produce a series of high resolution gridded productivity maps, based on topography, climate and soil using a GIS.

This project fits into the mosaic of existing work and should offer various novel approaches to mapping and modelling SRC distribution. In a larger context results derived from this thesis may be useful for growers of biomass energy crops and policy planners in assessing crop suitability and national capacity.

2.2 Material and Methods

2.2.1 Field trials network

The SRC field trials network was established in 1995. The trials were the largest of their kind and designed to provide an extensive and unique database for measuring productivity of SRC poplar and willow. Each trial was grown for two rotations, each of three years, concluding in 2002. Sixteen genotypes of each species (Appendix A), from contrasting parentages, were selected by Forest Research to assess genetic diversity in relation to yield. These represented commercially important and inter-specific hybrids, which were high yielding and tolerant to pests and disease. New genotypes that were not commercially available at the time of planting were also included to measure future yield potential.

Sites were selected based on ecological land classification studies (Pyatt and Suarez, 1997) and distributed across a physically diverse range of climatic zones and soil types (Table 2.1), to assess environmental yield limitations. Land above 250 m was rejected, on the understanding that farmers would be most attracted to growing the crop in lowland areas. The sites had formerly been uniform arable or improved grassland.

Table 2.1. Environmental ranges; SRC field trials network measurements, taken in-situ between 1995-2002 vs. UK-wide measurements, taken from widely available GIS datasets and measured between 1991-2000 (Perry & Hollis (2005), unless stated)

Variable	Field trials			UK	
	Minimum	Maximum		Minimum	Maximum
Annual rainfall (mm)	487	**1702**	vs	762	**5211**
Mean monthly maximum temperature (°C)	14.4	**21.2**		9.3	**20.6**
Growing day degrees	777	**1982**		488	**2445**
Frost days	0.8	**22.4**		4.4	**84.8**
Sunshine hours	3.7	**5.5**		1.7	**6.1**
Cloud cover (%)	59.4	**73.4**		44.9	**76.2**
Wind speed (mph)	5.3	**12.5**		1.7	**21.1**
Relative humidity (%)	79.5	**86.2**		80.5	**89.6**
Elevation (m)†	0	**185**		-5	**1057**
Slope (°)†	0	**11**		0	**39**
Soil water content (mm)*	48	**494**		40	**400**
Soil pH*	5.0	**7.9**		3.3	**8.8**
Soil organic carbon (%)*	0.1	**15.0**		0.1	**50.0**
Soil sand (%)*	1.7	**85.0**		10.0	**97.0**
Soil silt (%)*	9.5	**83.7**		10.0	**84.0**
Soil clay (%)*	5.1	**68.4**		8.0	**69.0**

† Land-Form Panorama DTM (Ordnance Survey)
* NATMAP vector (Cranfield University)

Forty-nine sites (Figure 2.1) were planted with the six most promising, high yielding and widely grown genotypes ('intensive' trials) – three of each species. Of these sites seven were also planted with an additional 13 poplar and 13 willow genotypes ('extensive' trials). Sites were cleared using a glyphosate herbicide spray at 5 litres ha^{-1} and the soil was broken up to reduce plough pan and compaction. Weeds were further controlled by residual herbicide application as necessary. Three further sites were established for physiological studies for use in the process-based model ForestGrowth (discussed in Chapter 4).

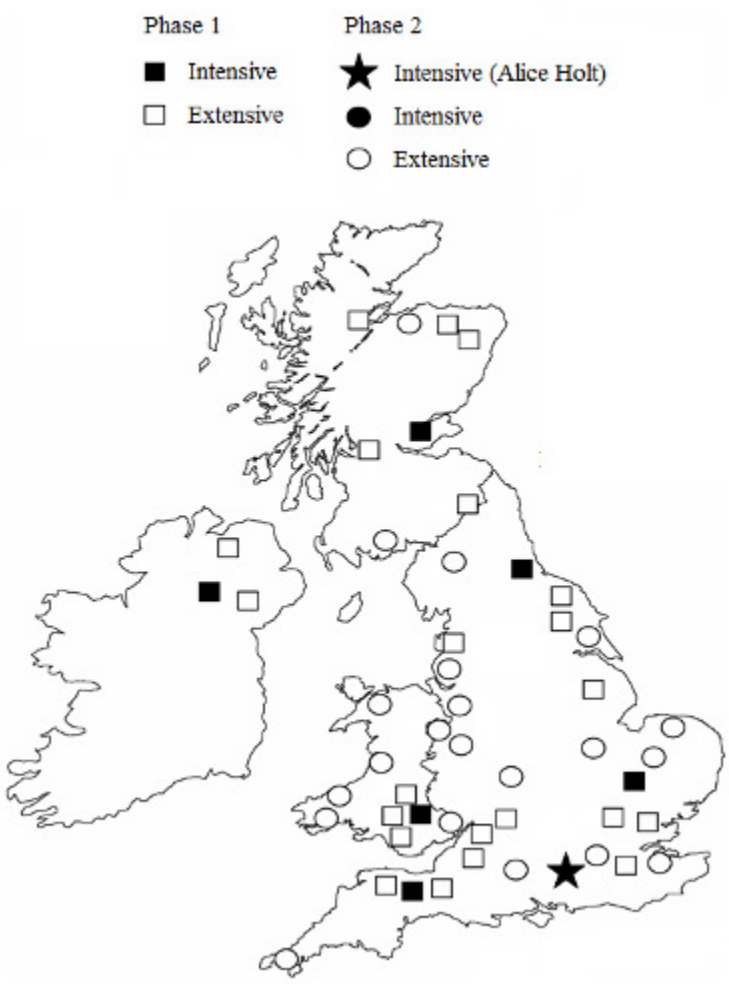

Figure 2.1. Location of UK SRC field trial sites. Adapted from Armstrong (1997).

Hardwood cuttings with a length of 0.25 m were planted in April 1995 (phase 1) and April 1996 (phase 2) in a 'double row' system as used in commercial SRC plantations, essential for mechanical harvesting. Alternating inter-row distances were 0.75 m and 1.5 m, with a within row spacing of 0.9 m, to yield a planting density of 10,000 cuttings ha^{-1}. A randomised block design with 16 genotypes x 3 replicated plots was used according to protocols suggested by the British Forestry Commission (Armstrong, 1997). Individual monoclonal plots were 9 x 11.5 m in size, containing 10 north-south oriented rows of 10 cuttings each. Fencing was also constructed around the sites to protect shoots from predation by deer and rabbits. All plants were cut back the year after planting to a

height of 0.05 m to create a coppice system. Measurements were taken on the 36 plants (i.e. 6 x 6) in the centre of each plot and for each genotype. No nutrients were added to the soil during the course of the trial.

Nested Design

Nested design is an experimental design in which the variables have an implicit hierarchy or levels, for example in certain multifactor experiments – such as this one – where the levels of one factor (site) are similar but not identical for different levels of another factor (replicate) we get nesting (Montgomery, 2008). Nested factors are an unavoidable feature of any study in which treatments are applied across one organisational scale and responses are measured at a finer scale (Doncaster and Davey, 2007). Here we have a balanced three-level nested design with plots/replicates nested within sites and observations measured at each site.

With a nested design one factor is nested within another when each of its levels belongs to only one level of the other. For example, Doncaster and Davey (2007) explain that a response measured per leaf for a treatment factor applied across replicate bushes must declare the bushes as a random factor nested in the treatment levels. The sampling unit of Leaf, L, is then correctly nested in Bush, B, nested in Treatment, T. The model is: $Y = B(T) + \varepsilon$, where the residual error term ε refers to L(B(T)). This model can be called in a statistics package by requesting the terms: T + B(T) and declaring B as a random factor.

Using a nested design structure in statistics will lead to reduced degrees of freedom,

which means that we have lost power to detect a treatment effect, explain Doncaster and Davey (2007). However, this cost has been traded against the benefit of sampling from across a wider region in order to obtain a more robust prediction. The analysis also has the possibility of post hoc pooling in the event that sub plots (replicates) within each site differ little from each other, which would reinstate the error degrees of freedom.

Doncaster and Davey (2007) go on to explain that if a study is planned with the correct analysis in mind, the distribution of sampling effort could be targeted to give a more powerful test. For example, a better design could have been to pool the data, because replication at the lowest organisational level is informative only about the variation among leaves on that bush. At lower levels of nested designs, power is much less an issue, as degrees of freedom generally increase from top to bottom of hierarchical designs (Quinn and Keough, 2002). Increases in replication at higher levels of the hierarchy will have cascading effects on power at lower levels (Quinn and Keough, 2002). We can use replication to increase our confidence that differences seen when comparing treatments are real and not just random chance or the effects of some other factor (Morrison *et al.*, 2008).

The only difference in the analysis of variance of a nested design from the one-factor analysis of variance is that total variation is identified as variation amongst sample replicates, variation among units within plots and within replicates (Morrison *et al.*, 2008). However, if such sources of variation are not well addressed, it can make it impossible to guarantee a high level of precision. For example, ignoring this nesting effect or non-independence could incorrectly reduce the standard error, artificially

increasing the confidence in our estimates or associations with the outcome, and, thus, increasing the possibility of rejecting the null hypothesis when we should have failed to reject it (O'Connell and McCoach, 2008).

Researchers have been able to address these conceptual and statistical issues using multilevel modelling, also commonly referred to as hierarchical linear modelling (Raudenbush and Bryk, 2002), and Li *et al.* (2005) have proposed a nested algorithm to this effect for partial least squares analysis. Alternatively, Nash *et al.* (2005) – who uses partial least squares to assess the association of landscape metrics to surface water chemical and biological properties – simply pools data to eliminate nested structure and remove confounding effects linked to existing data collinearity.

In this study, analysis could have been improved by using a hierarchical modelling structure that would account for site and plot variation as well as allowing for correlations inherent in repeated observational measurements. The use of a hierarchical error structure would allow the correct balance of between and within site variation to be examined. In a statistics package this would mean specifying site (S) as a random effect and plot/replicate (P) as a fixed effect: P + S(P).

Measurements

A detailed soil survey consisting of between 6 and 30 auger borings and at least one soil pit, sunk to a depth of 0.8-1.2 m (according to the soil texture), was undertaken across each site. Differences in the number of measurements related to the soil variability and

size of the site. Soil series (Avery, 1980) were recorded in-field, with samples further analysed in the laboratory for texture (Gee and Bauder, 1986) and pH (BSI, 1995). From this, available water content of the soil was derived, based on soil texture (Hall *et al.*, 1977). Measurements of slope and elevation were recorded using a clinometer (Suunto PM-5, Suunto Oy, Finland). Climatic variables (e.g. rainfall and dry bulb air temperature) were measured using (a) basic weather sensors (Holtech Associates, UK) and (b) more comprehensive automatic weather stations (ELE International Ltd, Hemel Hempstead, UK), at the extensive and intensive trial sites respectively. Measurements for each variable were recorded at one minute intervals to provide hourly means. For standing biomass estimation, the diameter at 1 m above the ground was measured using digital callipers (Masser, Savcor Group Limited Oy, Finland) on all live shoots per plant at the end of each growing season from 1996 to 2002 (with a total aboveground harvest every three years). Concomitantly, three shoots per plot were harvested from the assessment plot, spanning a representative range of the diameter distribution, to obtain a minimum of 54 shoots per genotype and per site over the six years of the trials. Harvested shoots (including branches) were oven dried at 95 ^{o}C and site specific allometric relationships between shoot diameter and shoot dry mass were computed for each genotype to estimate standing biomass at plot level, using methodology as described by Matthews *et al.* (2003). A cube root transformation was then applied to the data to create a linear relationship. Subsequently, a potential yield (odt ha^{-1} yr^{-1}) for each genotype was up-scaled and computed over all plots and assessed years. This approach gave residual mean square errors of 0.030 (x 0.258, cube root transformation) for willow and 0.052 (x 0.032, cube root transformation) for poplar.

The incidence of rust (*Melampsora* spp.) on the leaf was also recorded (Appendix A) by selecting one branch from each plant within the three central rows of the assessment plot. Three leaves were randomly selected from the top, middle and bottom third of the branch. This gave a total of 54 leaves per genotype for each plot and for each year of the trials. Each leaf was then visually assessed using a 0-5 scoring system (class 0 = no rust incidence (<5 % LAL), class 1 = very light (6-10 % LAL), class 2 = light (10-20 % LAL), class 3 = moderate (20-40 % LAL), class 4 = severe (40-65 % LAL), class 5 = very severe (>65 % LAL)).

2.2.2 Linear regression

An empirical model uses observed values to predict trends in data. Here we use climatic, topographical, soil and yield measurements from the SRC field trials network to predict yield outside the observed range. Only data from the intensively grown genotypes was used (n = 147), as insufficient data existed for the extensively grown genotypes. Annual yields were grouped together (by first and second rotation) to better understand cumulative trends in biomass development over time.

Criteria for the selection of variables used in the model, were based on literature and understanding of plant physiology. In addition, only variables which could be up-scaled using high resolution UK-wide GIS datasets were taken into consideration. The variables considered for the model were as follows:

- *Climate*: seasonal mean precipitation (mm, May-Aug for poplar and May-Sep for willow), monthly precipitation (mm), annual maximum and monthly mean dry-bulb temperatures (ºC), summer growing day degrees (ºC) and days of ground frost
- *Topography*: elevation (m) and slope (º).
- *Soil*: available water content (mm), pH (H_20), organic matter content (%),clay, silt and sand content (%) and soil quality index (Avery classification; expanded into sets of 'dummy' boolean values (i.e. 1/0) to overcome non-linear distribution).

To test the hypothesis of null effect on yield from pests and disease, we also included a value of LAL as an independent variable. However, this was removed before upscaling because the effect cannot be replicated at a national scale (i.e. no spatially referenced data exists for the distribution and prevalence of rust on SRC energy crops).

The data was input into Minitab (Minitab 15.1, Minitab, US) and a fitted line plot was used to test the assumptions of linearity and residuals of each variable against yield (Table 2.2). If the assumptions were not met the variable was log, square or square root transformed. A best subsets regression was then used to eliminate those variables not having a significant contribution to yield. Mallows' Cp was used as the criterion for selecting the number of variables used in best subsets (Mallows, 1973). The model with the lowest Mallows' Cp was selected and only statistically significant variables were included ($p<0.05$).

Table 2.2. Assumptions of multivariate linear regression

Factor	Assumption
Linearity	Relationship between variables and predictors is linear
Non-stochastic	Errors are uncorrelated to individual predictors

Zero mean	Mean of residuals is zero
Constant variance	Variance of residuals is zero
Non-autoregression	Residuals are random and uncorrelated in time
Normality	Error term is normally distributed

Simple linear regression was then performed on the best subset variables. In its simplest form, a linear model specifies the (linear) relationship between a dependent variable, Y (in this case yield), and a set of predictor variables, X_i (in this case environmental constraints), so that:

$$Y = b_0 + b_1X_1 + b_2X_2 + ... + b_pX_p$$

In this equation, b_0 is the regression coefficient for the intercept and the b_i values are the regression coefficients for variables 1 through p. Outliers were identified from residual analysis (±2) and removed. Errors were attributed to differences in management practices, inaccurate measurements and variable pests and disease damage. Results from the linear regression are presented in Appendix B. However, these models described only a small proportion of the variation in yield (r^2 = 0.37-0.52). There is also an inherent danger with this approach of overfitting the data and multicollinearity. Multicollinearity is where variance in correlated variables affects the relationship with the response variable. Additionally as a rule of thumb, for normal linear regression to be valid $n \geq 104 + m$ (where n is the number of dependant data points and m is the number of independent variables) (Tabachnick and Fidell, 2007).

2.2.3 Partial least squares regression

To account for multicollinearity and the limited number of data points, we used partial

least squares (PLS) regression (Simca-P version 11.5, Umetrics, Sweden). PLS is specifically designed to deal with small datasets with many related variables (Abdi, 2003). It is an extension of multiple linear regression that has a similar statistical structure to Principal Component Analysis (PCA), but additionally allows the user to define a response variable (i.e. yield). The same basic assumptions of normal linear regression also apply to PLS regression (Table 2.2). PLS has been widely applied to analytical chemistry but is also relevant to ecological yield modelling (Magnusson, 2002; Pettersson *et al.*, 2006; Williams *et al.*, 2008).

Here, plot data for each genotype was modelled probabilistically using PLS regression. All environmental variables (from Chapter 2.2.2) were considered when predicting yield. Only statistically significant principal components ($p<0.05$) contributing to a net increase in the predictive ability of the model were used (cumulative $Q^2 > 0.4$ and $r^2 = Q^2 \pm 0.2$). The relative importance of a variable to yield was given by a variable importance plot (VIP) and the positive or negative correlation of that variable to yield was described by a coefficient loading score. Outliers derived from normal probability analysis of component residuals were removed (if outlier $p>0.05$), but accounted for >2 % of sites. The predictive ability of each model (genotype/rotation) was assessed using an r^2 score, which compares the observed and predicted yield scores. r^2 scores lower than 0.5 (50 %) often indicate a large amount of 'noise' in the data (i.e. unwanted and uncorrelated variables) and suggests the model has a poor correlation with the observed values (Umetrics, 2002). The errors associated with the modelled estimates of yield are given by the root-mean-square error (RMSE).

2.2.4 Visualisation

GIS software (ArcMap version 9.2, ESRI, UK) was used to up-scale modelled PLS coefficients and visualise their outputs across England and Wales (Figure 2.2). Scotland and Northern Ireland were excluded from this element of the study, as the necessary soils GIS data was unavailable.

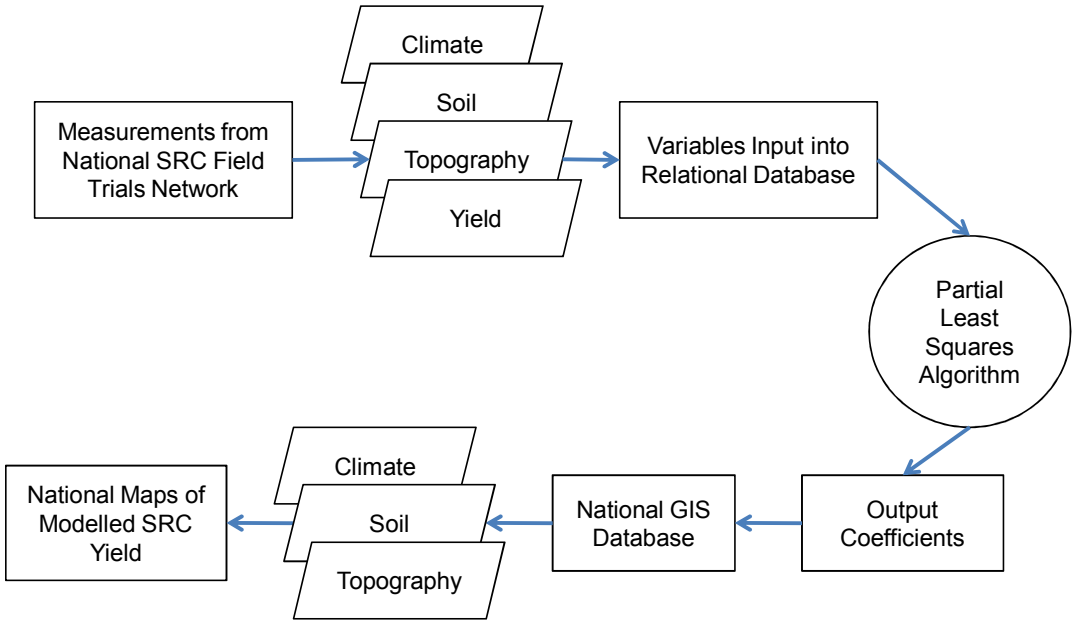

Figure 2.2. Flow chart diagram of basic empirical study methodology.

The GIS datasets used for up-scaling and further analyses were as follows:

1. 5 km^2 resolution climatic data averaged from 1991 to 2000 (Perry and Hollis, 2005): mean monthly temperature and precipitation, seasonal precipitation, summer mean daily maximum temperature, summer growing day degrees and days of ground frost. Seasonal trends used summed data.
2. 1:50,000 scale digital terrain model (Land-Form Panorama DTM, Ordnance Survey, UK): elevation. Slope was extrapolated using ArcMap slope tool.

3. 1:250,000 scale map of soil series (NATMAPvector, Cranfield University, UK): soil texture, water content and pH for each series. England and Wales only.
4. 1:200,000 scale vector boundary data maps (Great Britain boundary data, Collins Bartholomew, UK): urban areas and water features.
5. 25 m^2 resolution land classification map (LCM2000, Centre of Ecology and Hydrology, UK).

All GIS datasets were rasterised and converted to 100 x 100 m (1 hectare), 32 bit floating pixels (to account for decimals). This allowed ArcMap to run the PLS regression equation for each genotype/rotation using the map algebra tool and assign a yield value to each 100 x 100 m cell. To show a clear diverging pattern of yield a diverging Green-Yellow-Brown colour scheme was used, as these colours are less emotive than blue or red and give clear and easily distinguishable differences in values (Brewer, 1994). A mask was applied to all maps, outputting land above 250m (where the model reached its extrapolative limit), urban areas and inland water.

Land classification

The UK land classification map (LCM2000) was used to present modelled yield potentials under different land use scenarios. These scenarios were intended to present maximum displacement opportunities for SRC production under five different land uses (based on land use in the year 2000). The five broad displacement scenarios considered were: 100 % conversion of land used for (1) cereals, (2) horticulture/non-cereal/unknown agriculture, (3) non-annual crops, (4) improved grasslands and (5) set-aside grasslands. This was achieved by selecting LCM2000 features by class and creating a layer for each of the five scenarios, yields were then converted to vector data

and clipped to each scenario layer.

Case study: Co-firing at Drax power station

Spatially up-scaling modelled yield data allows potential supply to be analysed at a regional scale. By taking a regional approach we can assess practical deployment opportunities and limitations for SRC energy crops. Here we predict the available supply of biomass from SRC poplar and willow to Drax power station. Drax is the UK's largest power station and began co-firing biomass with coal in 2004. By mid 2010, its owners hope 12.5 % of the stations electricity will be generated from biomass (Drax Power Limited, 2008), making it an ideal benchmark case. One stipulation of the Energy Crop Scheme is that no feedstock should be sourced more than 25km from the power station it supplies (Natural England, 2008). Therefore, using Drax as the centre, a 25 km radius 'buffer' can be drawn and only yields falling within this buffer may be considered as potential supply. Merged yield map of the two most productive SRC crops were clipped to the buffer and then further clipped to each scenario layer.

Hot spot analysis

An alternative approach to looking at supplying existing infrastructure is to analyse future expansion opportunities for energy crops. To meet future targets it is likely additional dedicated biomass power stations will be built to meet UK energy demand. Therefore it is important to identify where opportunities exist. From a merged yield map of the two most productive genotypes, we can also analyse hot spots to identify the most suitable locations for the deployment of new bioenergy power stations (based only on yield potential). Hot spot analysis, using Getis-Ord Gi* statistical rendering was

performed on the data in ArcMap and took points within 25 km radius around each grid square. Getis-Ord Gi* statistic identifies those clusters of points with values higher in magnitude than you might expect to find by random chance; z scores show the magnitude of the hot spot ($p<0.05$).

2.3 Results

2.3.1 Observed yields

Field trial results show that observed SRC yield varied significantly between genotype and rotation (Appendix A). The highest yields were recorded in willow over the two rotations, with the 16 genotypes averaging 9.0 odt ha^{-1} yr^{-1} compared with 6.3 odt ha^{-1} yr^{-1} for the poplar genotypes. The highest-yielding parental line was the Swedish *S. vimanlis* × *S. schwerinii*, which displayed consistently high yields over both rotations and a high resistance to rust. This parent line included the highest-yielding single genotype, Tora, with an average yield across both rotations of 11.3 odt ha^{-1} yr^{-1}. The lowest-yielding parental line was *P. deltoides* × *P. trichocarpa*, which also contained the lowest-yielding single genotype 71009/1, producing just 2.5 odt ha^{-1} yr^{-1} over the two rotations of the study (reaching 2.0 odt ha^{-1} yr^{-1} in its second rotation, the lowest of any in the field trials). Root system maturation in the developing plant may be expected to give rise to increasing yields in successive rotations, which was the case with willow but not with the poplar genotypes grown in these trials. All but two of the poplar genotypes had reduced yields in the second rotation; conversely, all but one of the willow genotypes had improved measured yields in the second rotation. It is important to note that yields would likely decline if these genotypes were grown at true commercial scale as a result of less stringent and scientific management methods (Hansen, 1991). The incidence of infection by rust (*Melampsora* spp.) varied between genotypes and rotation (Appendix A). Heavy rust infection preceded crop death on several plots, including plots of previously resistant genotypes Hoogvorst and

Hazendans. In the trials, 5–30% of the poplar genotypes (variable between sites) recorded > 20% leaf area lost, and 6–22% of willow genotypes, as a direct result of rust. Rust prevalence was generally highest in southern England.

2.3.2 Predicted yield: model limitations and uncertainty

For complete outputs from PLS regression see Appendix C. Henceforth, all figures concern the three highest yielding genotypes (Jorunn, Q83 and Trichobel) only. PLS regression results show that each model was able to account for between 51 and 75 % of the total variation in yield (Figure 2.3). The error (RMSE) associated with modelled predictions were 1.37-2.37 odt, reflecting the large difference in yields within and between sites.

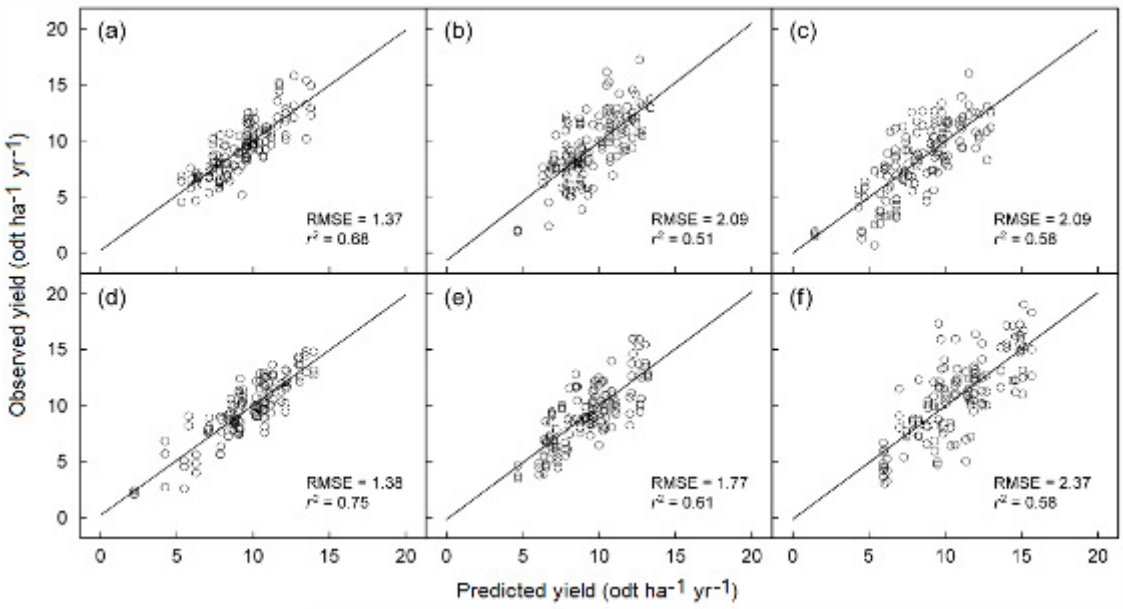

Figure 2.3. Relationship between observed and predicted yield values (odt ha^{-1} yr^{-1}) at plot level for poplar genotype Trichobel (a, d) and willow genotypes Jorunn (b, e) and Q83 (c, f). (a–c) first rotation, (d–f) second rotation ($P < 0.05$). RMSE, root-mean-square error (odt).

Residuals and Spatial Autocorrelation

A residual is a like-for-like comparison between measured and modelled data; it quantifies the error associated with a prediction. By mapping these residuals in space (Appendix C) we can assess if there is spatial autocorrelation in the underlying data. Spatial autocorrelation is a measure of the degree to which a set of spatial features and their associated data values tend to be clustered together in space (positive spatial autocorrelation) or dispersed (negative spatial autocorrelation) (Goodchild, 1986).

Moran's I is a parametric test that can check for autocorrelation in spatial data. Results from this study using poplar Trichobel, second rotation as an example, suggest the data has high spatial autocorrelation; Moran's I index = 0.40 ($p = 0.01$, SD = 3.81). Moran I scores close to 1 indicate clustering and scores close to -1 indicate dispersion. This suggests that there is less than a 1% likelihood that the clustered pattern we identify in this study could be the result of random chance, indicating that the assumption of independent errors was violated. This is a possible weakness of the PLS regression method.

Spatial autocorrelation comes either from the physical forcing of environmental variables or from community processes, and presents a problem for statistical testing because autocorrelated data violates the assumption of independence of most standard statistical procedures (Legendre, 1993). If spatial autocorrelation is ignored, then analyses of ecological patterns in terms of environmental factors can produce misleading results (Lennon, 2000), for example spatial autocorrelation may alter the parameter estimates and error probabilities of linear models (Kühn, 2007) such as the

partial least squares model we use in this study. Lennon (2000) suggests that simple, non-spatial correlations and regressions should be the beginning of an analysis (the exploratory data analysis stage) rather than reported as results.

In Dormann (2007) – where the author compares spatial and non-spatial models in ecological studies – it was found that coefficient estimates for environmental correlates of species distributions were affected by spatial autocorrelation, leading to an average predictor misestimation of 25%. Model fit was improved by incorporating spatial autocorrelation. Dormann suggests that exogenous factors, such as climate, soil type, stochastic disturbances or even solar activity, may lead to a similar occurrence probability in neighbouring sites, simply because the external factors show a specific autocorrelation pattern. These exogenous factors could be included into the statistical model as environmental covariates, reducing and even removing the residual spatial autocorrelation. If omitted, residuals are likely to display spatial autocorrelation.

Kühn (2007) assessed the relationship between plant species richness and environmental variables by different non-spatial and spatial methods. The author demonstrated how an error-based simultaneous autoregressive (ESAR) model, which assumes autocorrelation of the residuals, could produce different results to an ordinary least square (OLS) model, which is a non-spatial model similar to partial least square (PLS) as used in this thesis. It was found that the r^2 score increased from 0.35 to 0.66 when using the ESAR model. In addition the spatial ESAR model estimated a negative relationship between plant species richness and altitude (and a positive relationship between plant species richness and temperature), which is more consistent with

ecological theories and/or previous observations, whereas the OLS model suggested the opposite. The results clearly show that ignoring spatial autocorrelation can produce contrasting results.

Legendre (1993) suggests that when spatial autocorrelation is present in data several solutions are open to ecologists. First, the user can attempt to remove the spatial dependency among observations so that the usual statistical tests can be used either by removing samples until spatial independence has been attained (a solution that is not recommended because it entails a net loss of expensive information) or by filtering out the spatial structure using trend surface analysis. The alternative is to modify the statistical method in order to take spatial autocorrelation into account. This approach is to be preferred, Legendre suggests, when such a method is available, especially in cases where spatial structuring is seen as a part of the ecological process under study rather than a nuisance.

Lennon (2000) outlines two relatively straightforward ways that ecologists can make an immediate improvement over classical correlation. One way is to apply the spatially explicit correlation test of Clifford *et al.* (1989). Lennon also outlines another more flexible approach based on the surface randomisation methodology. Other proposed methods to account for spatial autocorrelation include modified correlograms that test for significant autocorrelation between sites located within any given range of distances apart (Koenig and Knops, 1998; Legendre *et al.*, 2002). However, correlograms assume second-order stationarity, an assumption which is violated, for instance, by the presence of a big patch in the centre of the field (Legendre *et al.*, 2002). Keitt *et al.* (2002)

proposes three autoregressive models – the standard autoregressive model (AR), conditional autoregressive model (CAR) or spatial autoregressive model (SAR) – which include an additional term to the standard linear model that accounts for patterns in abundance that are not predicted by local habitat variables, but are instead related to abundance in neighbouring locations. Griffith and Layne (1999) suggest when spatial autocorrelation is due to unobserved and unmodelled environmental variables, a SAR or CAR model may be the more appropriate choice of model. In such models, the value at a location depends on the residuals at nearby locations. A spatial generalized least-squares (GLS) approach may also be useful in particular circumstances (Ver Hoef *et al.*, 2001). However, Diniz-Filho *et al.* (2003) explain that this method de-emphasises predictors with strong autocorrelation, such as long distance clines and so, ecologically, it tends to give more importance to mechanisms acting at local geographical scales.

Keitt *et al.* (2002) and Kühn (2007) further highlight the importance of scale, remarking that shorter and shallower gradients in both response and predictor variables are seen at local scale. In such cases, fit is often worse and autocorrelation structure is often more patchy (Dormann, 2007) and important (spatially autocorrelated) variables may be missed more easily. This is because the scale of analysis is too small to reflect steep and long trends that are visible at global or continental levels, yet too large to reflect small-scale processes such as dispersal or competition. Therefore, the incorporation of a spatially autocorrelated component into the model will catch some of this misspecification.

Furthermore, Lennon (2000) and Diniz-Filho *et al.* (2003) argue that if the response

variable largely reflects the autocorrelation structure (lag-distance and autocorrelation coefficient) of a predictor, then it is possible that residual autocorrelation will be removed using a non-spatial model. However, this is much more likely to happen at large spatial scales (global or continental) where steep (autocorrelated) gradients (e.g. in temperature and water availability) account for most of the variance in the observed (autocorrelated) variable (e.g. species richness).

Diniz-Filho *et al.* (2003) raise the important point that spatial autocorrelation should be investigated, but it does not necessarily generate bias. Rather, it can be a useful tool to investigate mechanisms operating on richness at different spatial scales. Diniz-Filho *et al.* suggest claims that analyses that do not take into account spatial autocorrelation are flawed are without foundation, and autocorrelation is really a question of deciding at which spatial scale one is interested in explaining diversity or variance.

2.3.3 Predicted yield: factors affecting yield

Results show that the dominant factors affecting yield were seasonal precipitation patterns. PCA scatter plots identify the high association between yield and water availability, particularly spring and summer precipitation rates (Appendix C). To quantify this affect we can look at PLS regression VIP scores. Results show that over 40 % of the most important factors determining yield (VIP scores >1) were related to precipitation, while these factors accounted for less than one third of the total variables used in the regression analysis. Jorunn was the least water dependent genotype (32 % of VIP scores >1) and Trichobel the most water dependent genotype (44 %). Yield

correlation with precipitation was also strongly related to crop age, with precipitation being 50 % more likely to be a highly important factor determining yield (VIP scores >1) in the second rotation compared to the first. PLS plots also showed a high correlation between yield and winter temperatures, particularly for poplar (Appendix C). Furthermore, the direction of the correlation between each variable and yield tells us how variables influence crop growth (described by the coefficient loading score). The greatest positive influence on yields were summer precipitation, available water content, slope and frost days for willow genotypes, and summer precipitation, summer temperature and frost days for poplar. Winter temperatures showed negative correlation in all but one genotype; therefore in areas of high winter temperatures the model predicts you will find low yields. By contrast, all genotypes showed a strong negative correlation between yield and elevation.

Pest and disease were found to have a significant effect on yield. Models using pests and disease data were found to more accurately predict yield – r^2 scores increased by 3-12 %. This suggests pests and disease are amongst the most significant limiting factors to the growth of SRC species, particularly Trichobel, second rotation: $r^2 = 0.75$ (no pests and disease data) vs. 0.87 (with pests and disease data).

2.3.4 Predicted yield: spatial analysis

Mean species yields† (6 yr mean) across England and Wales ranged from between 9.3(Jorunn) to 9.5 odt ha^{-1} yr^{-1} (Q83). This equates to a maximum supply of biomass of between 111.4 and 113.9 M odt yr^{-1} (6 yr mean). Each genotype showed a large spatial variation in yield; yields were generally highest in the North West and lowest in the South East of England, although some variation is lost as a result of up-scaling (Figure 2.4).

Results show SRC can be planted on a wide range of soils, from heavy clay to sand, but yields were generally higher on loamy and clayey soils with naturally high water tables and lowest on pelosols and shallow lime-rich soils over chalk or limestone.

The combined yield of the three genotypes ranged from 4.7 to 15.8 odt ha^{-1} yr^{-1} across England and Wales. Yields were up to 0.5 odt ha^{-1} yr^{-1} lower on land under cereal production and up to 0.4 odt ha^{-1} yr^{-1} higher than average on improved grasslands and set-aside; although, there was no significant difference ($p>0.05$, t-test). Replacing 10 % of arable land (scenarios a–c in Table 2.3), 20 % of improved grassland (scenario d) and 100 % of set-aside grassland (scenario e) in England and Wales with these genotypes would yield 12.6 M odt yr^{-1} of biomass and require 1.3 M ha of land.

† on all available land which is not classified as urban, water or above 250 m.

Development under such a scenario could produce 25.8 TWh of electricity, equivalent to 6.7 % of UK electricity production (BERR, 2008) and displace 5.5 Mtoe (Cannell, 2003). Alternatively, if this biomass was used for CHP, these genotypes could produce 45.3 TWh of energy, equivalent to 48.3 % of UK CHP production (BERR, 2008). In order to broaden the picture of biomass potential in the UK, it is important to consider Scotland in any calculations. By aggregating potential yields from the maps for England and Wales with the potential in Scotland[†], we conclude the UK has the potential to supply 28.1 TWh of electricity (7.3 % of electricity production) or 49.3 TWh of energy from CHP (52.6 % of CHP production).

Case study: Co-firing at Drax power station

Applying the same land conversion as above to an area within 25 km of Drax, would provide 0.7 M odt yr-1 of biomass. This value would produce nearly 1.4 TWh of electricity, which is approximately 6 % of the station's electrical production. Therefore, if Drax is to meet its biomass co-firing target (12.5 % of electrical production by mid 2010), more than twice as much land may be required than is realistically available locally.

Hot spot analysis

Getis-Ord Gi* hot spot analysis found the most suitable locations were predominantly in southern Wales and north western England (Figure 2.5). Spatial analysis does not take into account reduced yields at commercial scale or wider socio-economic barriers and opportunities to uptake, but instead demonstrates that a variety of locations may be suitable for new bioenergy infrastructure.

[†] assuming 5 % uptake on the most suitable land, 0.7 M odt yr^{-1} (Andersen *et al.*, 2005)

Figure 2.4. Spatial productivity maps (2.5 x 2.5km) for poplar genotype Trichobel (a, d) willow genotype Jorunn (b, e) and willow genotype Q83 (c, f) in the first (a, b, c) and second rotation (d, e, f).

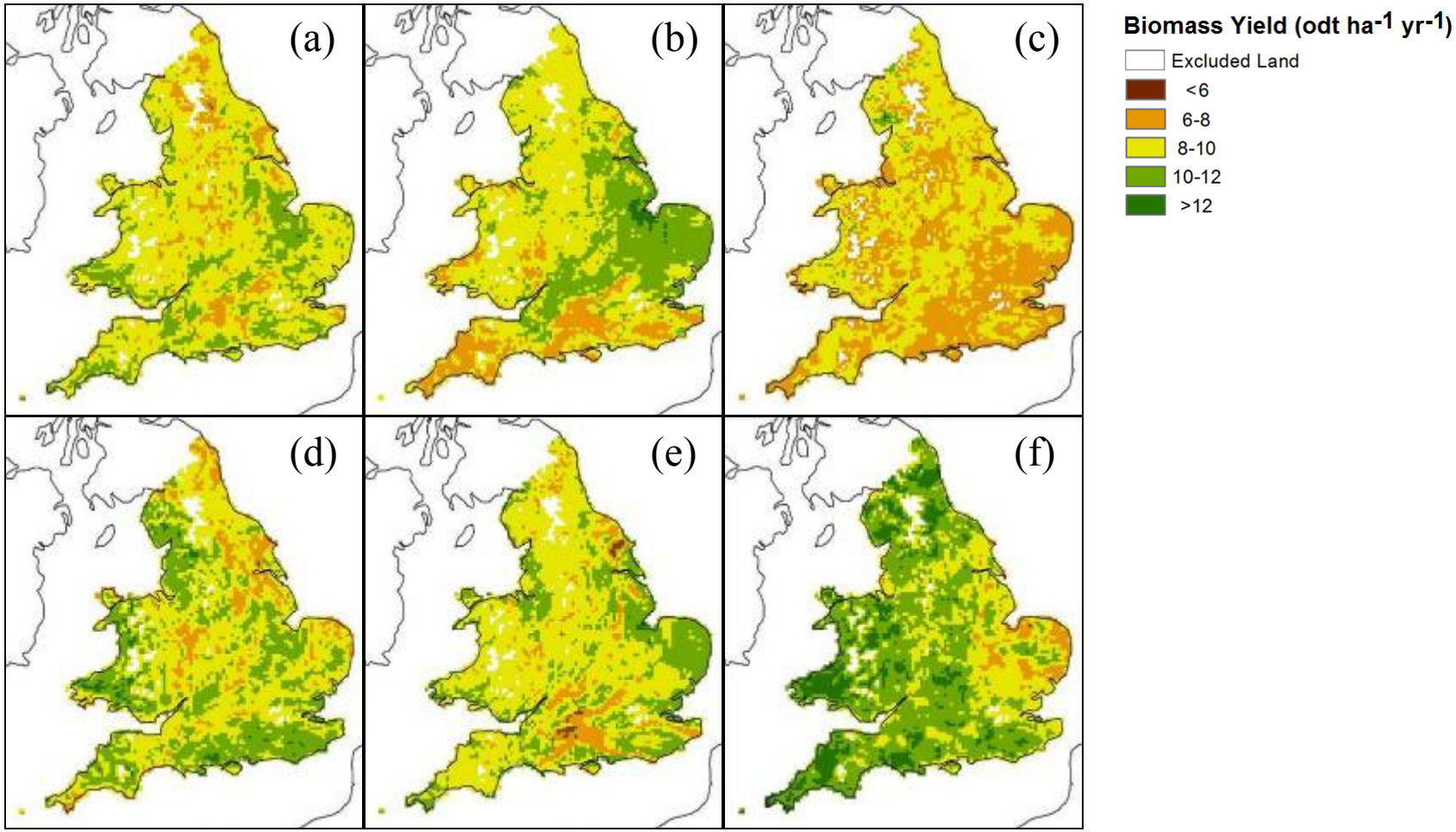

Table 2.3. Total computed yields (M odt yr^{-1}), mean yield (odt ha^{-1} yr^{-1}) and energy value (TWh) from 100 % conversion of five contrasting land uses to energy crop production. Values given for each genotype (willow genotypes Jorunn and Q83, and poplar genotype Trichobel).

Genotype	*Salix*		*Populus*
	Jorunn	**Q83**	**Trichobel**
a. Total yield from 100 % conversion of *Cereals (2.1 M ha)*	18.6	17.9	18.3
Mean yield	9.5	9.4	9.1
Energy value (electricity)	38.2	37.6	36.8
Energy value (combined heat and power)	67.2	66.1	64.6
b. Total yield from 100 % conversion of *Horticulture/non-cereal/unknown agriculture (3.0 M ha)*	26.3	25.2	25.7
Mean yield	9.4	9.2	9.1
Energy value (electricity)	54.1	52.8	51.8
Energy value (combined heat and power)	95.0	92.8	91.0
c. Total yield from 100 % conversion of *Non annual crops (0.1 M ha)*	0.6	0.6	0.6
Mean yield	9.4	9.6	9.2
Energy value (electricity)	1.2	1.2	1.1
Energy value (combined heat and power)	2.2	2.2	2.1
d. Total yield from 100 % conversion of *Improved grasslands (4.2 M ha)*	31.2	34.1	32.8
Mean yield	9.0	9.5	9.9
Energy value (electricity)	64.1	67.4	70.1
Energy value (combined heat and power)	112.7	118.4	123.1
e. Total yield from 100 % conversion of *Set-aside grasslands (0.2 M ha)*	1.6	1.5	1.6
Mean yield	9.6	9.4	8.9
Energy value (electricity)	3.3	3.2	3.1
Energy value (combined heat and power)	5.8	5.7	5.4

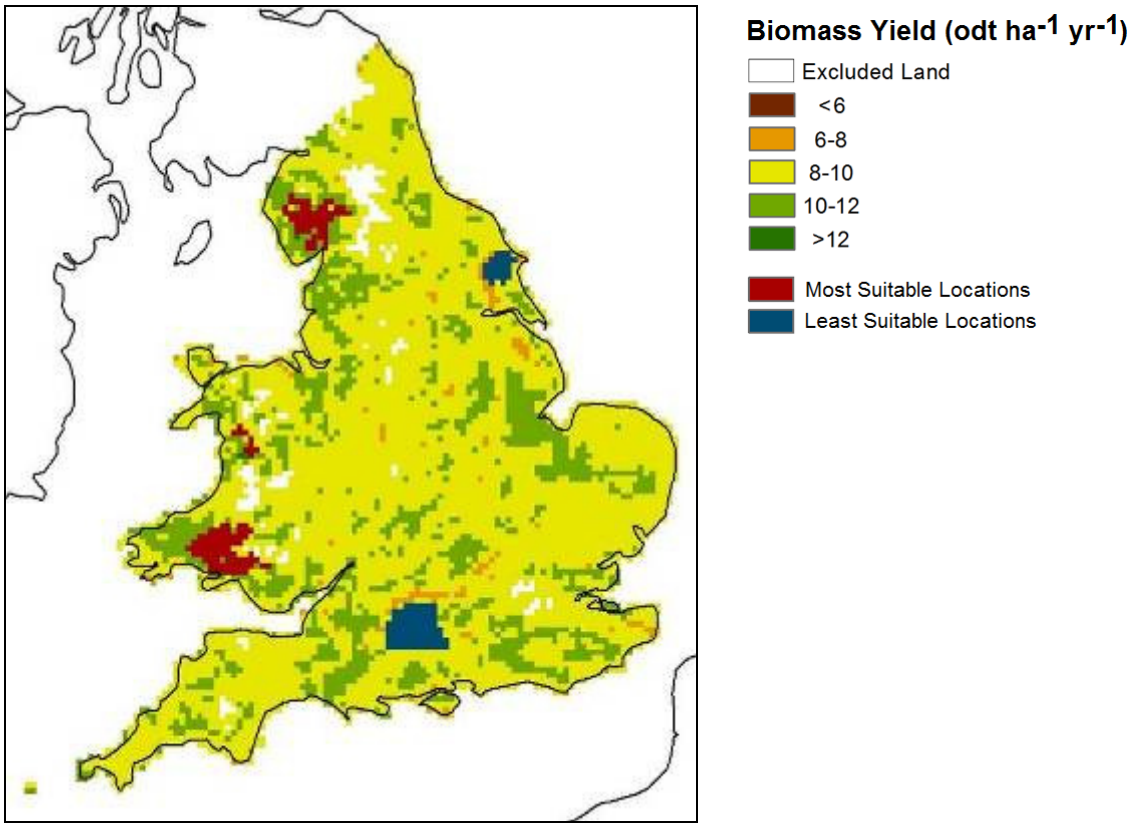

Figure 2.5. Spatial productivity map (2.5 x 2.5 km) combining the three highest yielding modelled genotypes (6 yr mean). Most suitable 2% (red) and least suitable 2% (blue) of sites for new dedicated biomass power stations (based on Getis-Ord Gi* hot spot analysis of crop yields).

2.4 Discussion

2.4.1 Predicted yield: model limitations and uncertainty

Not all of the variation in SRC yield could be accounted for by the variables used in the model (r^2 = 0.51-0.75). Therefore, results suggest yield is governed by complex interactions between a large number of site variables that cannot be fully quantified using this approach. The field trials network covers a contextually small number of sites and a large number of associated variables – leading to confounding relationships between correlated variables. Model outputs should be considered a guide for up-scaling

rather than a rule, as multicollinearity can and does show incongruous results (e.g. if increasing rainfall is strongly correlated to rising yield, then decreasing temperature may also be linked to increasing yields as areas of high rainfall and low temperature in the UK can occupy the same area). Models could be improved by the provision of more site data across a wider geographic range.

It should also be noted that the results provided have a static temporal context. The genotypes used in the trials are no longer extensively utilised on a commercial scale, planting densities have increased by 50 % and SRC is now planted in mixtures of genotypes to improve disease resistance. Despite these limitations, the models developed in this study represent the best predictive tools for measuring UK SRC productivity currently available to growers and planners. It is likely that the spatial context of the outputs will remain valid for genotypes from similar genetic backgrounds and serve as a useful predictor for geographic suitability of SRC bioenergy crops.

2.4.2 Predicted yield: factors affecting yield

Results indicate a strong correlation between water availability and SRC yield (Appendix C). This confirms the findings of other studies, which have found water use during summer months by mature poplar and willow exceeds most other vegetation (Hall and Allen, 1997; Lindroth and Båth, 1999). In addition, these fast-growing species tend to show poor resistance to drought stress (Lindroth and Båth, 1999; Wikberg and Ogren, 2004; Cochard *et al.*, 2007). However, Linderson *et al.* (2007) and Guo *et al.* (2010) suggest that some species of willow and poplar are able to cope with short-term

reduced water availability by improving water-use efficiency, but stem growth is still reduced. Despite drought not being a significant issue during the SRC field trials, future predictions for lowland England suggest increased soil moisture deficit, leading to water stress, is likely during summer months (Hulme *et al.*, 2002) and will remain an issue of critical future concern.

Appendix C also showed that hydrology affected species differently. VIP scores for the intensively grown genotypes identified willow as being more dependent on precipitation for growth than poplar. This is in accordance with the findings of Cochard *et al.* (2007), who established a strong correlation between high biomass in four willow genotypes and xylem vulnerability, when compared with five poplar genotypes. Other studies have found that differences in water use between poplar and willow are negligible (Hall *et al.*, 1998). Thus caution is necessary in generalisation on how these two species cope with drought. The dependence of poplar yield on water was variable amongst genotypes, with small-leaved Ghoy being less vulnerable to reduced water availability than large-leaved Trichobel. This result is in accordance with the findings of Souch and Stephens (1998) and may be attributed to increased surface area for evapotranspiration in larger leaves and the inability of *P. trichocarpa* species to close their stomata during periods of drought. The genes determining drought tolerance in poplar have recently been identified using a transcriptomics approach (Street *et al.*, 2006) and it is likely that in future such information will be used to develop genotypes with improved water-use efficiency within poplar and willow breeding programmes.

2.4.3 Predicted yield: accounting for variation

Results show that SRC is generally suitable for growth across a range of environments, including marginal and set-aside land (Table 2.3). This may be because of the tolerance of poplar and willow species to high soil toxicity and waterlogging (Robinson *et al.*, 2000; Nixon *et al.*, 2001). However, field measured yield was variable between species and genotypes, with willow yields generally higher than poplar, particularly in the second rotation. For example, Trichobel yields were generally higher on the north and west of England (Figure 2.4). If we compare this to the trees native distribution in North America we find that the tree family (*Populus trichocarpa*) similarly favours coastal areas and its range extends into Alaska (Figure 2.6), suggesting it can grow well in cooler climates such as north western England.

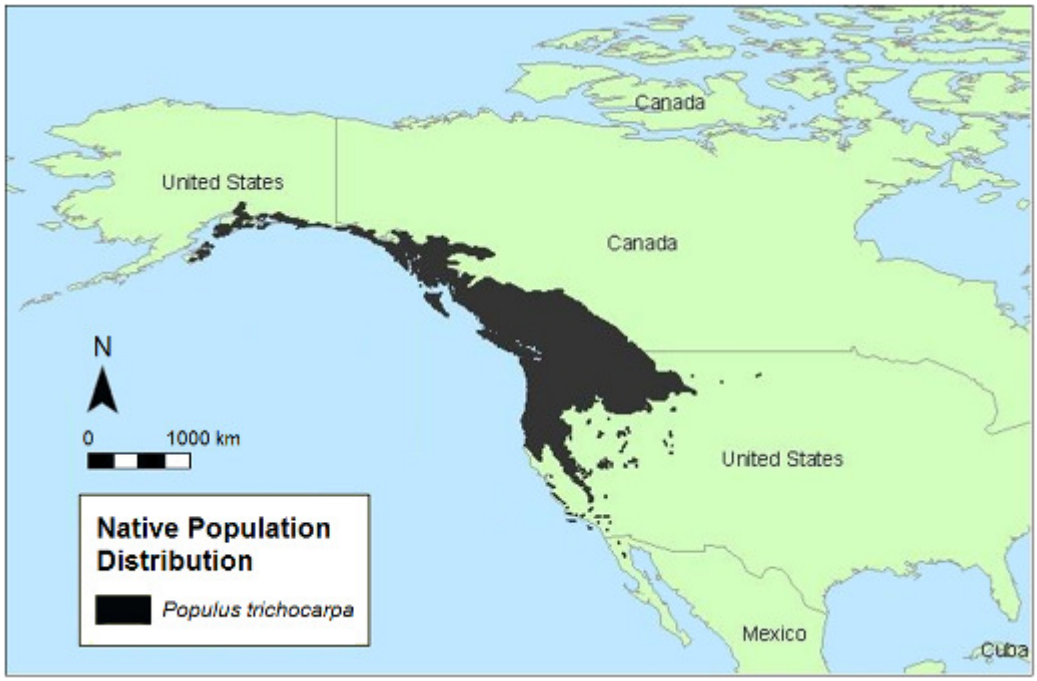

Figure 2.6. Map of native *Populus trichocarpa* distribution. Adapted from Little (1971).

Poplar and willow are largely undomesticated, and improvement with breeding is limited to the development of F_1 hybrids. Rae *et al.* (2004) recorded productivities of an F_2 progeny of SRC poplar with highly differentiated stem and canopy architectures – yields ranged between 0.04 and 23.7 odt ha^{-1} yr^{-1}, suggesting that considerable genetic variation exists on which to improve this genus for future use. In particular, poplar breeding programmes to date have focused on selecting plants for single straight stems with high apical dominance, including the genotypes used in this study. However, lower second-rotation yields for poplar suggest that this tendency for single stems may detrimentally affect yield. Growing poplar and willow with multiple stems speeds up canopy closure and weed suppression. Concomitantly, coppicing is believed to increase final biomass production and is an inexpensive alternative to replanting (Sennerby-Forsse *et al.*, 1992; Liberloo *et al.*, 2009). In contrast, Proe *et al.* (2002) found a reduction in biomass compared to single stem systems.

Variation in rotational yield may also be attributed to differences in climatic conditions. For example, during the first rotation (1995–1999) rainfall was 3 % above the 1961–1990 baseline, while during the second rotation (1998–2002) rainfall was 19 % higher than the baseline (Perry and Hollis, 2005). The spatial pattern of climatic variability was also variable between rotations and could explain changes in the geographic spread of yield over time. Alternatively, changes in temporal geographic distribution may be attributed to root system maturation, resulting in roots being able to take water and nutrients from greater depths.

Results also suggest variation in rotational yield is closely linked to leaf rust (Appendix

A). It is known that infections causing leaf blemishes, such as rust, may be correlated with decreased photosynthetic activity and yield (Erickson *et al.*, 2004). Infection also decreases the energy available for processes involving the development of frost hardiness and influencing the successive year's growth (Christersson, 2006). Rust scores were generally higher in the second rotation, suggesting a breakdown in resistance. This may be attributed to the rust pathogen remaining in leaf litter, on the stool or in a secondary host (i.e. larch) between rotations.

A parallel study conducted in Belgium, showed similar trends in genotypic mean annual yields, ranging from 2.0 odt ha^{-1} $yr^{-1}$for poplar genotype Gibecq to 10.4 odt ha^{-1} $yr^{-1}$for poplar genotype Hazendans (Laureysens *et al.*, 2004). Genotypes with the highest first rotation yields again typically performed poorly in the second, a finding was generally attributed to poor rooting capacity and rust. Other European trials from similar climates have shown yields comparable to those achieved in the field trials network. For example, Nordh and Verwijst (2004) grew twelve genotypes of willow in southern Sweden (4 yr rotation, 20 000 plants ha^{-1}), and recorded yields between 6.2 and 9.5 odt ha^{-1} yr^{-1}. A single-site trial in Washington state (US) recorded poplar yields of 14–35 odt ha^{-1} yr^{-1} (4 yr rotation, 10 000 cuttings ha^{-1}) (Scarasscia-Mugnozza *et al.*, 1997). High productivity was attributed to rich alluvial soils and length of the frost-free period. More recently Labrecque and Teodorescu (2005) showed poplar genotypes grown in southern Quebec (Canada) could yield between 16.6 and 18.1 odt ha^{-1} yr^{-1}without the application of fertiliser (4 yr rotation, 18 000 cuttings ha^{-1}). Willow biomass productivity from the same trial was between 9.0 and 16.9 odt ha^{-1} yr^{-1}. It was hypothesised that the high yields found in these trials could be the result of high soil

quality, good drainage conditions and a lack of disease infestation.

2.5 Conclusions

Both poplar and willow may be suitable for biomass production across a wide range of sites in the UK, with observed yields varying between 1.97 and 13.34 odt ha^{-1} yr^{-1}. Using PLS regression modelling to upscale these yields across England and Wales (three highest-yielding extensively grown genotypes), showed that the UK has the potential to exceed its short and long term energy crop targets to plant 125 000 ha (Britt *et al.*, 2002) and 1 M ha (UK Biomass Task Force, 2005), respectively. If these genotypes (or similar) were grown across the UK on the land proposed by this thesis, 1.3 M ha could be grown to produce 12.6 M odt yr^{-1}.

The UK has a largely rain-fed agricultural system and its is unsurprising that low precipitation was identified as the principal limiting factor to crop yield and should be taken into account during site selection and for future breeding and improvement programmes. Developing consistently high yielding energy crops will help reassure farmers of the sustainability of such crops and their economic feasibility. However, observed and predicted yields were highly variable and in general less than 50 % of potential yields, suggesting step-change improvements are likely over the coming decades in these largely undomesticated plants. In the future temperate landscape, it is likely we will see an increase in value and production of these crops as feedstocks for heat, power and liquid transportation fuels.

Chapter 3 . Social, economic and environmental impacts on the supply of biomass from short rotation coppice in England

The findings of this chapter have been published in two papers. A copy of these can be found in Appendix F.

(1) Land use challenges: *Biofuels* (2010, Vol. 1 (5): 719-727)
(2) GHG emissions: *Global Change Biology Bioenergy* (2009, Vol. 1 (4): 267-281)

3.1 Introduction

Climate change and concerns over fuel security have led to a growth in demand for locally-sourced renewable energy. Provided local markets exist, SRC energy crops offer growers the chance to diversify into non-food crops and when planted in place of conventional arable agriculture can reduce GHG emissions (Edwards *et al.*, 2008; St. Clair *et al.*, 2008), enhance biological diversity (Tucker and Sage, 1998; Cunningham *et al.*, 2004) and stimulate the rural economy (Turley *et al.*, 2002; Sims, 2003; Walsh *et al.*, 2003; Parcell and Westhoff, 2006).

However, growing energy crops presents challenges as well as opportunities. Current production of first-generation biofuels has been attributed to the rising cost of food (Gallagher, 2008; Mitchell, 2008). These first-generation 'cellulosic' crops are currently the only viable options for producing biofuels and are typically derived from food crops (e.g. wheat and maize). Concomitantly, when the fuel value for a crop exceeds its food value, it is more likely to be used for fuel, leading to higher food prices. Furthermore, displacing existing land uses with first-generation biofuels can lead to long GHG emission 'pay-back' periods (Fargione *et al.*, 2008; Searchinger *et al.*, 2008; St. Clair *et*

al., 2008), consequently rendering this form of biofuel counter-productive in contributing towards GHG savings. However, in the future second-generation technology will allow biofuels to be made from 'lignocellulosic' crops (i.e. dedicated energy crops, such as SRC). Second-generation crops can be dual purpose, with lignin being burned for heat and electricity and cellulose used for fuel. This allows more efficient land use and partially negates the conflict with food and other land uses. In addition, the use of second-generation biofuels offers more immediate GHG savings (DTI, 2003a). For example, second-generation biofuel crops reduce emissions of CO_2 by up to 90 % (relative to fossil petroleum), compared to only 20-70 % for first-generation biofuel crops (Edwards *et al.*, 2008). However, to meet present biomass and biofuel targets with second-generation crops will still require a large expansion of land under energy crop production. The predicted growth in energy crop production has raised concerns over their competition with other land uses.

The protection of ecosystem services is an important constituent of the current environmental agendas of both UK (Defra, 2007b; 2007a) and European government (European Commission, 2000; 2008). Ecosystem services are defined as the benefits people obtain from ecosystems (Millennium Ecosystem Assessment, 2005). These include provisioning services such as food, water, timber, and fibre; regulating services that affect climate, floods, disease, wastes, and water quality; cultural services that provide recreational, aesthetic, and spiritual benefits; and supporting services such as soil formation, photosynthesis, and nutrient cycling. Many of these ecosystem services are protected by law from energy crop planting or are ineligible under the Energy Crop Scheme (Natural England, 2008), which subsidises the establishment costs associated

with planting SRC and *Miscanthus*. Therefore, these factors should be taken into consideration when making estimates of energy crop potential. This will provide a more holistic framework for analysing the implications of changing land use under future biomass development.

Here we provide regional estimates of biomass supply from short rotation coppice poplar and willow in England, taking into account economic, social and environmental constraints. We also provide estimates of greenhouse gas emissions for poplar genotype Trichobel when displacing three alternative land uses. Potential biomass supply scenarios were developed on the broad assumptions that energy crops should only be planted where they (1) return a profit, (2) do not conflict with food production, (3) do not impact on ecosystem services and (4) do not displace alternative land uses which offer greater greenhouse gas savings. This information should be useful to breeders, farmers, landscape managers and policy makers.

3.2 Materials and Methods

3.2.1 Biomass estimation

Multiple linear [partial least squares] regression (Simca-P version 11.5, Umetrics, Umeå, Sweden) was used to determine the yields of coppiced poplar, by creating coefficients that predict yield from observed data. The dataset and approach is outlined in Aylott *et al.* (2008) – chapter 2 – but the model is improved to eliminate errors in precipitation and soil profile measurements. In the Aylott *et al.* model measured

precipitation was found to be underestimated in some areas by up to 30 %. This was as a result of general logger errors and particularly the outbreak of foot and mouth disease in 2001, whereby the batteries of the climate data loggers were not changed and data was lost. Consequently, measured precipitation values were substituted by widely available precipitation data from the UK Met Office, specific to the time period of each rotation (Perry and Hollis, 2005). Avery soil classification was also removed from the model (as it was considered to have minimal biological meaning) and soil profiles were aggregated to a depth of 1m profile rather than using 25cm layers to account for more general yield trends. Organic soil matter and seasonal precipitation variables were also added. Only those models remaining that predicted more than 50 % of the variation in yield were retained for subsequent analysis: poplar Trichobel (*Populus trichocarpa* Torr. & A. Gray) in the first and second rotations (mean $r^2 = 0.6$, mean RMSE = 1.7 odt ha^{-1}) – henceforth referred to generically as SRC poplar. See Appendix C for regression equations.

3.2.2 Land availability analysis

Coefficients from the PLS regression model were upscaled using Map Algebra in Geographic Information Systems (GIS) software (ArcMap version 9.2, ESRI, Aylesbury, UK). Yield was divided into NUTS 1 regions (EU units for terrestrial statistics) to enable regional assessment of productivity. Scenarios were developed on this basis. Restricted and semi-restricted land [for planting SRC] (Figure 3.1) was excluded from analysis - in total 46 land designations were used (Table 3.1). Designations were based on official Energy Crop Scheme guidelines (Natural England,

2008), wider literature (DEFRA, 2008b; Lovett *et al.*, 2009) and general assumptions of physical constraints (e.g. urban areas). In addition, spatially referenced Agricultural Land Classification (ALC) grades (MAGIC, 2008) were used to assess different scenarios of energy crop uptake, helping account for land used in food production. Grades range from one to five (one being the highest and five being the poorest quality) and are based on a number of criteria, including climate (temperature, rainfall, aspect, exposure, frost risk), site (gradient, micro-relief, flood risk) and soil (depth, structure, texture, chemicals, stoniness) (MAFF, 1988). ALC data was only accessible for England, consequently Wales is removed from the study area.

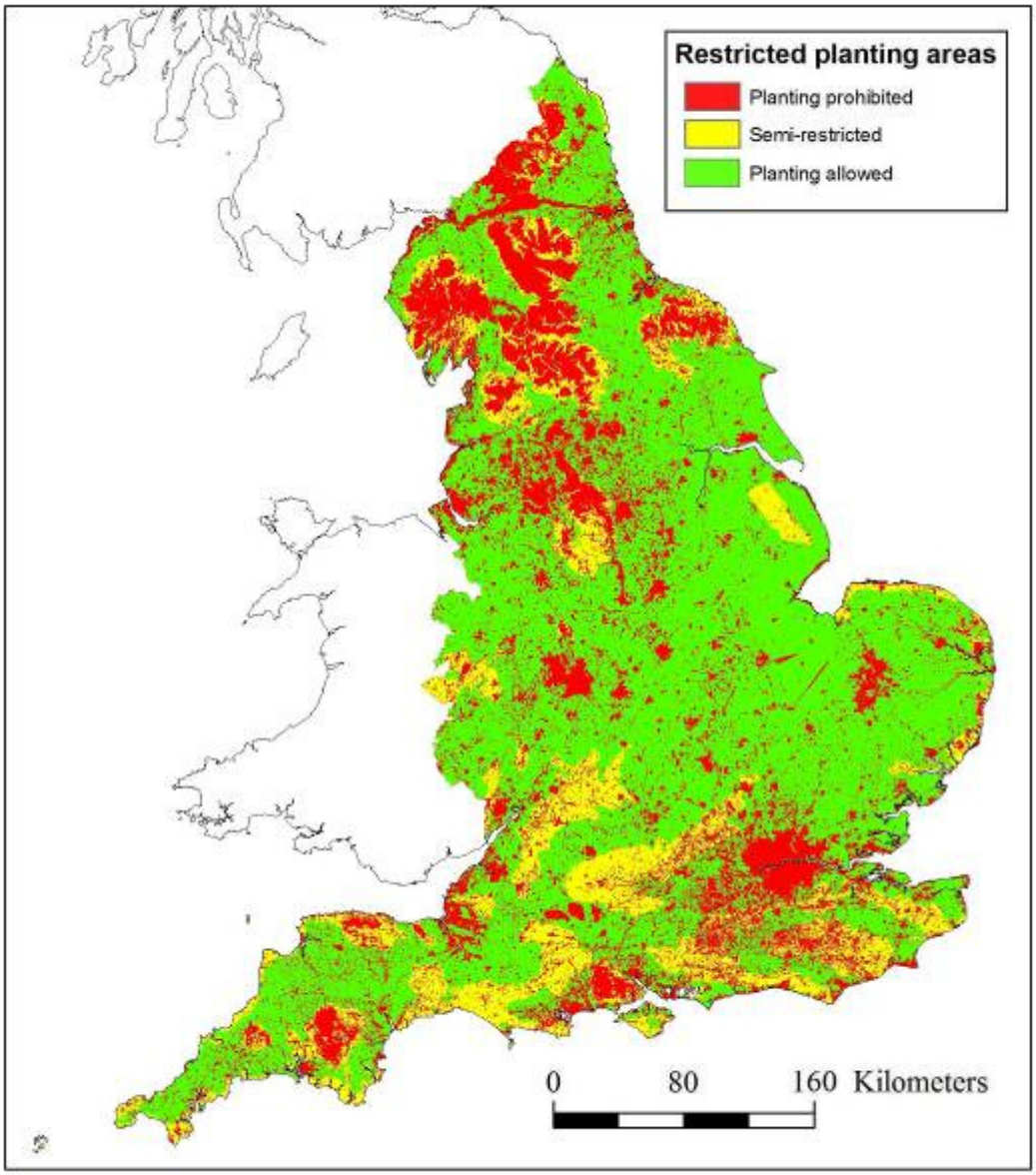

Figure 3.1. Map of restricted planting areas for energy crops in England (areas shaded green can be planted with energy crops without restriction, areas shaded yellow are semi-restricted and areas shaded red cannot be planted with energy crops).

Table 3.1. Areas restricted or unsuitable for growing energy crops in England.

Restriction	Land Use	Designation	GIS Data Source
Fully Restricted	Water	(1) Rivers, (2) Ponds and Lakes	Collins Bartholomew
	Urban	(3) Urban areas	
	Topography	(4) Elevation above 250m, (5) Slope above 15%	Land-Form Panorama DTM, Ordnance Survey
	Designated Areas	(6) Public Rights of Way (PRoW) and land within 3m (*Miscanthus*) and 5m (SRC) of PRoWs, (7) Local Nature Reserves, (8) National Nature Reserves, (9) Ramsar Sites, (10) Sites of Special Scientific Interest, (11) Special Protected Areas, (12) Special Areas of Conservation, (13) National Forest, (14) Community Forests, (15) Environmentally Sensitive Areas, (16) Forest Parks, (17) Country Parks, (18) Millennium Greens, (19) Doorstep Greens, (20) National Character Areas, (21) National Trust Areas, (22) Heritage Coasts, (23) Woodland Trust Sites, (24) National Bird Areas, (25) RSPB Reserves, (26) Quarries, (27) Registered Common Land	Natural England; Forestry Commission; RSPB
	Cultural Heritage	(28) World Heritage Sites, (29) Scheduled Monuments, (30) Registered Battlefields, (31) Listed Buildings, (32) Registered Parks and Gardens	English Heritage; Natural England
	Natural Habitats	(33) Blanket Bog, (34) Fen, (35) Mire Network, (36) Wet Woodlands, (37) Heath Network, (38) Floodplains, (39) Mudflats, (40) Deciduous Woodland Network, (41) Reedbeds, (42) Ancient Woodland, (43) Coastal Sand Dunes, (44) Maritime cliff and slope	Natural England
Semi Restricted	Designated Areas	(45) Area of Outstanding Natural Beauty, (46) National Parks	Natural England

3.2.3 Greenhouse gas emissions

The soil C turnover model RothC was used to simulate carbon emissions from SRC production. RothC requires information regarding C inputs to the soil from the plant (including those from leaf litter and from the root system). We characterise C input as a function of yield, as employed in SUNDIAL (Bradbury *et al.*, 1993; Smith *et al.*, 1996; Smith *et al.*, 2005):

$$C_{input}\ (t\ ha^{-1}\ yr^{-1}) = C_1(C_2 + C_3(1e^{C_4 \cdot Yield(t\ ha\text{-}1)}))$$

As yield increases, C_{input} increases monotonically up to an asymptotic value of $C_1(C_2 + C_3)$, at a rate determined by the shape factor C_4. For SRC, we assume that the variation in yield accounted for half of the variation in C inputs, therefore setting $C_2 = C_3 = 0.5$. The shape factor C_4 was assumed to be the average of those for winter wheat and rapeseed oil (Smith *et al.*, 2005). The parameter C_1 was determined via calibration of RothC on the data of Gielen *et al.* (2005) and Hoosbeek *et al.* (2004): where the topsoil (25cm) had an initial soil C of 30.2 t ha^{-1}, an average soil clay content of 14.6 %, an average annual sequestration rate of 0.73 t ha^{-1}, for an average yield of 10.1 t ha^{-1}. This gave the following parameterisation for SRC:

$$C_{input} = 8.01(0.5 + 0.5(1 - e^{-0.23 \cdot Yield})) \quad (1)$$

Annual C input was calculated using equation (1) and the spatial yield estimates of SRC poplar genotype Trichobel. Only second rotation yields were considered to reflect the C

inputs of an established crop. Subsequently, annual C input, climatic data, soil clay percentage, soil organic carbon and the previous land use were used to initialise RothC.

Soil carbon emissions calculated by RothC (20 yr mean) were then included in a wider GHG emissions life cycle analysis (LCA). Farm gate GHG balance was estimated by considering annual emissions associated with the management of SRC poplar and those offset by the management of the land under its previous use. Management emissions for SRC poplar were estimated at 40 kg carbon equivalent ha^{-1} yr^{-1} (Matthews, 2001). Management of arable, grassland and natural/forest land were estimated according to St Clair *et al.* (2008). To complete the LCA we estimated emissions from combustion of poplar (co-firing) compared to those associated with obtaining the equivalent amount of energy from fossil fuel (coal). The energy density of poplar[†] was estimated at 12.1 GJ t^{-1} (Phyllis, 2003), compared to 30.5 GJ t^{-1} for coal (Defra, 2008a). CO_2 emissions from biomass combustion are considered 'carbon neutral'. However, CH_4 (0.002 kg GJ^{-1}) and N_20 (0.05 kg GJ^{-1}) emissions are accounted for (DTI, 2003a).

[†] assuming 30 % moisture content

3.3 Results

3.3.1 Area of restricted planting

The total land area in England is 13.3 M ha (Defra, 2006). Of this figure over 36% cannot be planted with energy crops due to agronomic or legislative constraints. A further 10% was excluded when removing semi-restricted Areas of Outstanding Natural Beauty (AONB) and National Parks. Excluding all semi- and fully-restricted land left 6.9 M ha available for planting energy crops in England.

3.3.2 Regional yield (odt ha^{-1} yr^{-1})

The mean yield of SRC poplar across England (excluding semi- and fully-restricted areas) was 9.7 odt ha^{-1} yr^{-1}; ranging from 3.5 to 15.4 odt ha^{-1} yr^{-1} (Figure 3.2a). On agricultural land only (ALC grades 1-5), the highest yields were found in the North West (10.9 odt ha^{-1} yr^{-1}), East (10.6) and London (10.5) regions (Table 3.2). Conversely, the South West (8.2 odt ha^{-1} yr^{-1}) and North East (8.8) were identified as the least productive regions of England for SRC poplar. Yields on ALC 1 [best quality] land were significantly higher than on ALC 5 [worst quality] land (t-test, $p<0.01$); 10.8 and 8.2 odt ha^{-1} yr^{-1} respectively. However, this general trend was not true in all regions, where differences between grades were not always present or significant. For example, in the North West yields on grades 1-4 were not statistically different (t-test, $p<0.01$) from one another.

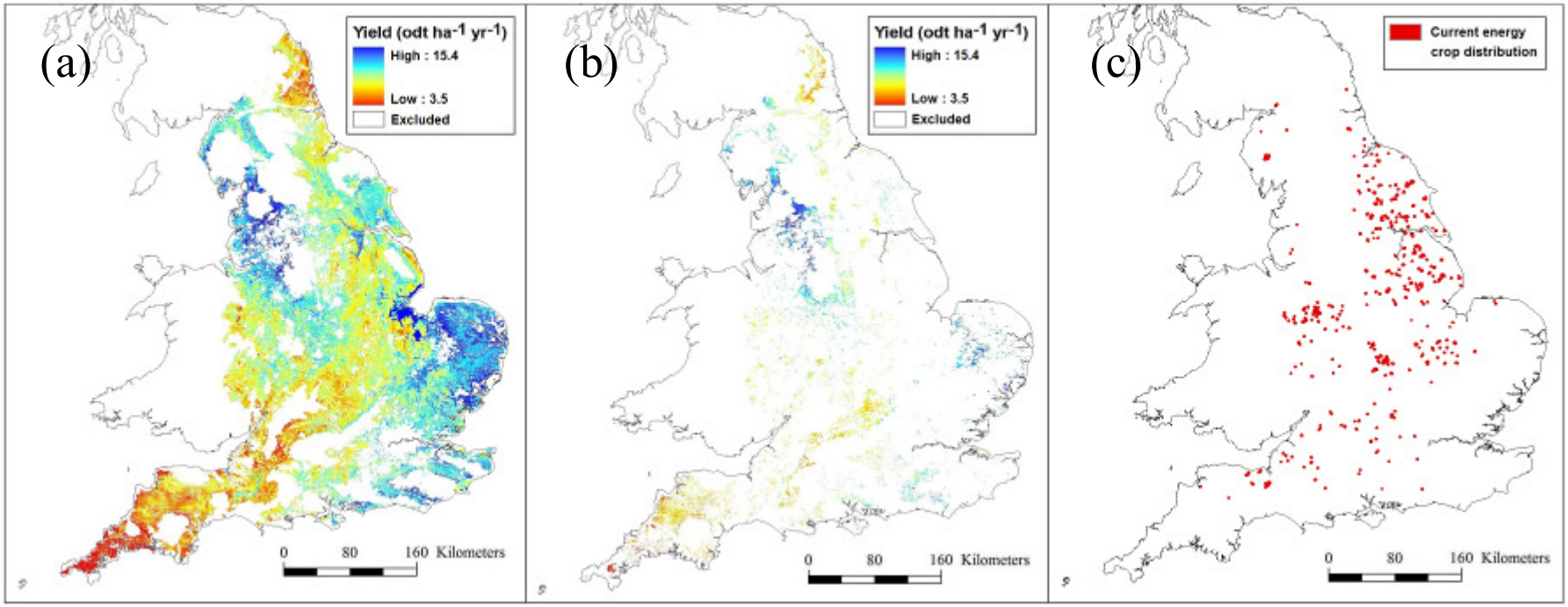

Figure 3.2. (a) estimated yields of SRC poplar (odt ha^{-1} yr^{-1}) when displacing all available land, (b) estimated yields of SRC poplar when displacing ALC 5 and the most productive 97 % of ALC 4 and (c) current energy crop distribution, based on Energy Crop Scheme Agreements prior to March 2009 (Natural England, UK). Estimated yields exclude land semi- or fully-restricted land for planting energy crops (shaded white).

Table 3.2. Maximum potential biomass supply (M odt yr^{-1}) and mean 6 yr annual yield of SRC poplar (odt ha^{-1} yr^{-1}), shown for each NUTS1 region (excluding semi- and fully-restricted land) and on five different ALC grades: 1 being the best, 5 the worst. The difference in total mean yield for each land class is shown statistically (numbers with the same letter are not significantly different, t-test, $p<0.01$). Standard deviations are shown in parenthesis.

Region		ALC 1	ALC 2	ALC 3	ALC 4	ALC 5	ALC 1-5
North West	**Maximum supply**	**0.2**	**0.6**	**3.8**	**1.2**	**0.1**	**5.9**
	Mean yield	11.3 (0.8)	10.8 (0.8)	10.8 (1.0)	11.3 (1.0)	10.5 (1.0)	10.9 (1.0)
East England	**Maximum supply**	**0.8**	**2.4**	**7.5**	**0.6**	**0.003**	**10.9**
	Mean yield	10.3 (1.6)	10.4 (1.0)	10.8 (1.0)	11.3 (0.9)	10.9 (0.7)	10.6 (1.1)
London	**Maximum supply**	**0.02**	**0.01**	**0.1**	**0.006**	**-**	**0.1**
	Mean yield	11.0 (0.5)	11.3 (0.5)	10.4 (0.6)	10.2 (0.4)	-	10.5 (0.7)
Yorks & Humber	**Maximum supply**	**0.2**	**2.6**	**4.3**	**0.8**	**0.04**	**7.9**
	Mean yield	10.8 (0.8)	10.0 (0.8)	9.8 (0.8)	10.3 (1.2)	9.8 (1.2)	9.9 (0.8)
South East	**Maximum supply**	**0.4**	**1.2**	**4.5**	**1.2**	**0.006**	**7.3**
	Mean yield	10.6 (0.8)	10.2 (1.0)	9.8 (1.1)	9.4 (1.0)	9.4 (0.8)	9.8 (1.1)
East Midlands	**Maximum supply**	**1.1**	**5.2**	**7.6**	**0.7**	**0.004**	**14.6**
	Mean yield	11.7 (1.4)	9.6 (0.9)	9.4 (0.7)	9.9 (0.8)	10.3 (1.1)	9.6 (1.0)
West Midlands	**Maximum supply**	**0.1**	**1.9**	**5.1**	**0.8**	**0.006**	**8.0**
	Mean yield	9.4 (0.9)	9.5 (0.8)	9.4 (0.8)	9.5 (1.0)	9.3 (1.4)	9.4 (0.8)
North East	**Maximum supply**	**-**	**0.2**	**2.3**	**0.5**	**0.1**	**3.1**
	Mean yield	-	9.1 (0.8)	8.8 (0.8)	8.7 (0.8)	8.2 (0.8)	8.8 (0.8)
South West	**Maximum supply**	**0.2**	**0.8**	**6.0**	**1.4**	**0.05**	**8.6**
	Mean yield	9.0 (0.8)	8.4 (1.1)	8.1 (1.0)	8.1 (0.9)	8.0 (1.4)	8.2 (1.0)
England (total)	**Maximum supply**	**3.1**	**15.0**	**40.8**	**7.3**	**0.4**	**66.4**
	Mean yield	10.8^{a} (1.5)	9.3^{b} (1.1)	8.9^{c} (1.2)	8.8^{c} (1.4)	8.2^{d} (1.5)	9.0 (1.2)

3.3.3 Regional biomass resource (M odt yr^{-1})

The theoretical maximum biomass supply for each NUTS1 region was determined by multiplying the mean yield by the number of available hectares (excluding all semi- and fully-restricted land). In England up to 69.2 M odt of biomass was estimated to be available annually, with the East of England (15.2 M odt yr^{-1}), East Midlands (11.2 M odt yr^{-1}) and South West (8.9 M odt yr^{-1}) having the largest regional resources (Figure 3.3). The East Midlands and South West had large biomass resources despite showing low mean yields, as a result of their large areas of available land. In total, ALC grade 3 had the largest resource (62%), followed by ALC 2 (22%), ALC 4 (11%), ALC 1 (5%) and ALC 5 (0.6%). Comparatively, 48% of the total land area of England is graded as ALC 3, 14% is ALC 2, 14% is ALC 4, 3% is ALC 1 and 8% is ALC 5.

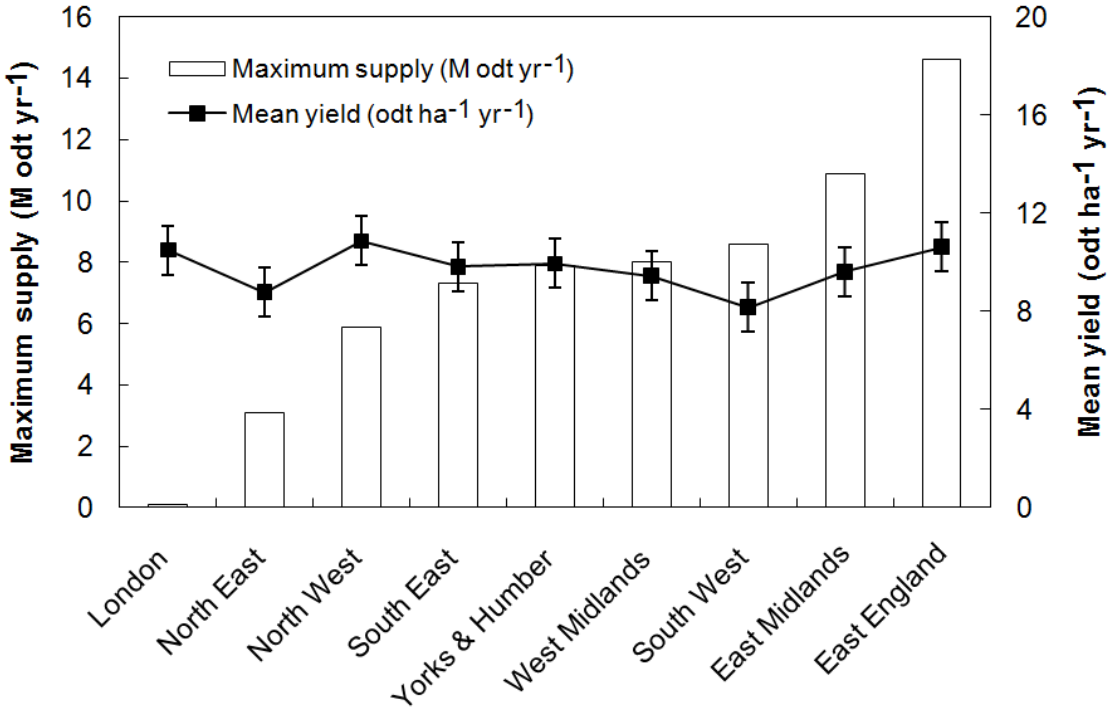

Figure 3.3. Regional distribution of SRC poplar biomass availability (excluding semi- and fully-restricted land): maximum supply (M odt yr^{-1}) given by the bars and mean yield (odt ha^{-1} yr^{-1}) given by the line. Error bars show 2 standard deviations.

3.3.4 Greenhouse gas emissions (t CE ha^{-1} yr^{-1})

SRC poplar generally reduced soil carbon emissions ($\bar{x}$ = -0.24 t CE ha^{-1} yr^{-1}) across England and Wales, particularly when compared to rapeseed (biodiesel) and winter wheat (bioethanol) (Figure 3.4). Emissions were comparable to those of *Miscanthus*.

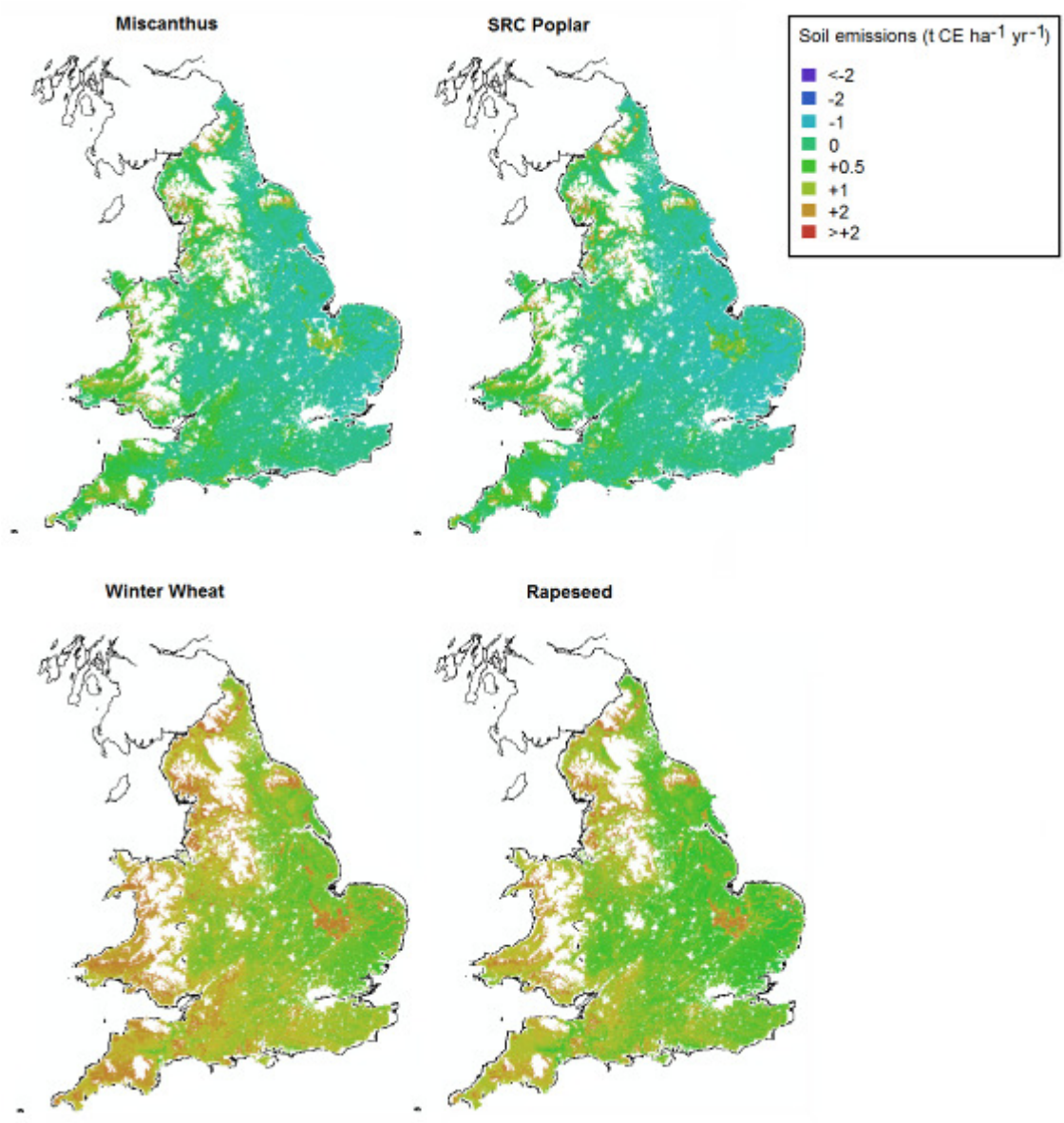

Figure 3.4. Predicted soil emissions (t CE ha^{-1} yr^{-1}) for *Miscanthus*, SRC poplar, winter wheat and rapeseed: annualised 20 yr averages from RothC.

In respect to the complete life cycle, SRC poplar showed a GHG saving when displacing arable and grasslands (Figure 3.5). However, the converse was true when SRC was used to displace forest/semi-natural land. The estimated break-even yield before a net GHG saving from SRC poplar was -5.8 odt ha^{-1} yr^{-1} when displacing arable land, -2.5 when displacing grassland and +12.0 when displacing forest/semi-natural land.

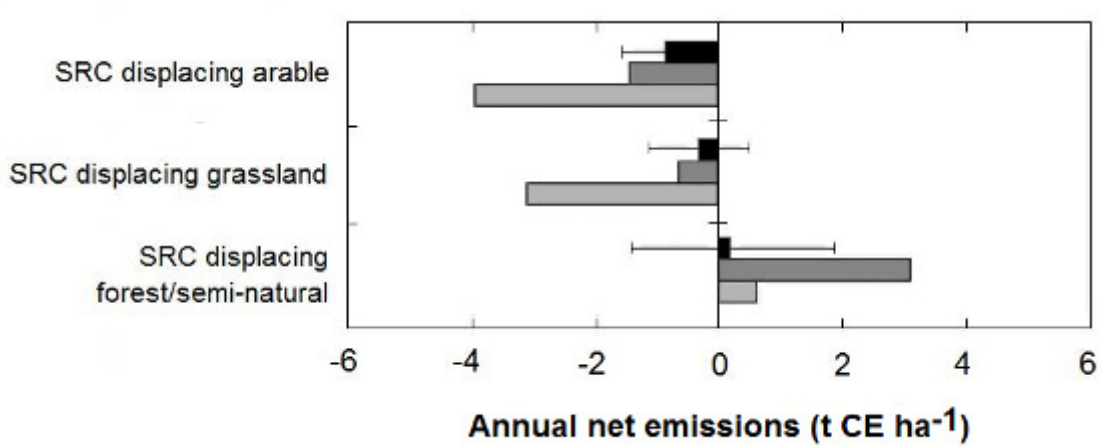

Figure 3.5. Net annual greenhouse gas balance (t CE ha^{-1}) for growing SRC poplar, when displacing arable, grassland or forest/semi natural land; soil emissions (black bars, error bars represent 2 standard deviations), emissions after incorporating management (dark grey bars) and emissions incorporating fossil fuel displaced (light grey bars).

3.4 Discussion

3.4.1 Energy crop competition with food production

Results presented here suggest when we exclude land which is semi- or fully restricted, up to 6.9 M ha (from a total of 13.3 M ha) remains available for growing SRC in England. However, much of this land is and will continue to be used for food

production. For example, between 2001 and 2009 the land area under arable crop production in the UK remained generally constant at an average of 4.5 M ha (± 5 %) or 19 % of total land area (Defra, 2005; 2009). The growing demand for energy crops could potentially reduce the area and production of food crops. The Gallagher Review (2008) highlights the conflict between energy and food, suggesting more marginal and abandoned land should be used for energy crops. Gallagher defines marginal land as land unsuited for food production (e.g. with poor soils or harsh weather) and areas that have been degraded (e.g. through deforestation). Therefore, scenarios were developed on the assumption that higher grade land (ALC grades 1, 2 and 3) was already in use for food production and unavailable for planting energy crops.

Estimates suggest that SRC poplar could meet present electricity and biofuel targets (7.5 M odt) without using any grade 1-3 land. Instead, meeting targets would require all grade 5 and the highest yielding 97% of grade 4 land (Figure 3.2b). This equates to a total land area of nearly 0.8 M ha. Under this scenario, the South West would have the largest capacity of any region, with 19% of the total available resource (1.4 M odt yr^{-1}), followed by the North West with 17% (1.3 M odt yr^{-1}) owing to their large areas of poor grade land.

3.4.2 Economic considerations

Nearly 44% of the land required to meet biomass targets (described above) would fail to meet the assumed economic profitability threshold of 9.2 odt ha^{-1} yr^{-1} at a fuel price of £40 odt^{-1} (Rosenqvist and Dawson, 2005) – although this value is dependent on

fluctuations in the market value of the feedstock, harvesting costs and subsidies. Using only land yielding over 9.2 odt ha^{-1} yr^{-1} to meet biomass targets would require 47% of available Grade 5 land (0.02 M ha), 56% of available Grade 4 land (0.4 M ha) and 5% of available Grade 3 land (0.3 M ha). However, in the future step-change improvements in productivity are likely in these largely undomesticated plants, making SRC more economically viable. It is also likely that new technologies (Rook, 1991; Calfapietra *et al.*, 2003; Taylor, 2008) and the predicted changes in temperature and atmospheric CO_2, will lead to improved yields in these crops – at least for the UK and northern Europe (Oliver *et al.*, 2009) – reducing the possible conflicts with food production.

3.4.3 Greenhouse gas emissions from SRC

Soil emissions from SRC are comparable to *Miscanthus* and compare favourably to those of winter wheat (bioethanol) and rapeseed (biodiesel) (Figure 3.4). In the future, second-generation technology will allow lignocellulosic biomass (i.e. *Miscanthus* and SRC) to be used in the production of biofuel. However, results presented here are only for the conversion of SRC to electrical energy. Converting SRC to bioethanol is an energy intensive process; however, we can anticipate GHG savings when SRC is used to produce bioethanol compared to winter wheat. Winter wheat requires annual harvesting (with associated fossil fuel costs) and has high fertiliser requirements. For example, using first-generation crops (e.g. winter wheat) to produce bioethanol releases approximately 30-80 % of the CO_2 emissions associated with fossil petroleum, compared to just 10 % from second-generation biofuel crops (e.g. winter wheat straw) (Edwards *et al.*, 2008).

Results suggest that converting SRC crops to electrical energy is largely beneficial in reducing GHG emissions, relative to fossil fuel. However, SRC crops should generally not displace forest/semi-natural land (Figure 3.5). Scenarios developed here only consider displacing agricultural land. When SRC crops displace arable or grassland (i.e. agricultural land) net GHG emission savings are predicted above yields of -5.8 and -2.0 odt ha^{-1} yr^{-1} respectively (i.e. all yields). GHG emissions are abated as a consequence of decreased fossil fuel inputs and increased carbon sequestration. Therefore, displacing agricultural land with energy crops can contribute to GHG savings and help meet Kyoto Protocol requirements. However, since the cultivation of grassland and forest/semi-natural land results in an initial soil disturbance, there is a potentially significant early soil C loss (Guo and Gifford, 2002), which we have not explicitly explored here.

3.4.4 Future implications for SRC

Scenarios presented here suggest meeting present UK targets (7.5 M odt yr^{-1}) without compromising food production or other ecosystem services, is achievable. Such a resource could be grown across 0.8 M ha and use 5 % of grade 3 land, 56 % grade 4 land and 47% of grade 5 land. This is within the theoretical maximum land area available to perennial energy crops suggested by literature – 0.9 M ha[†] (Andersen *et al.*, 2005; BERR, 2007), 1 M ha (UK Biomass Task Force, 2005) and 3.1 M ha (Haughton *et al.*, 2009).

[†] assuming UK could use just 5% of its agricultural land to grow energy crops.

Producing 7.5 M tonnes of biomass per annum would theoretically generate 15.5 TWh yr^{-1} of electrical energy and displace 3.3 M tonnes of oil (Cannell, 2003) – approximately 4% of current UK electricity demand (DECC, 2009a). The South West and North West alone producing over a third of this figure (5.2 TWh yr^{-1}).

Results suggest that SRC crops are most productive on higher grade land but may also be suitable across a wide range of sites, including poor grade land. Poor grade land may have low nutrient availability or be prone to waterlogging. However, over 20 % of applications to the Energy Crop Scheme (the UK's main subsidisation mechanism for supporting the planting of the dedicated energy crops, *Miscanthus* and SRC) were on the highest quality agricultural land: Agricultural Land Classification (ALC) grades 1 and 2 (Natural England, UK) (Figure 3.2c). This suggests that farmers are displacing high quality agricultural land that would otherwise be used for food production, with energy crops. Changes to agricultural land use will be required in the future to negate the conflict with food production.

In the future, we can anticipate greater expansion of energy crops on marginal lands. Results show high yields for SRC can be achieved on ALC grades 4 and 5, particularly in areas with high rainfall (i.e. North West England) and/or high soil water availability (i.e. East England). Therefore, if energy crops were optimally planted based on yield, we could see a shift from current energy crop distribution to more marginal lands in the North West and East of England. Given that both poplar and willow are riparian species, physiological adaptations to high water tables (Cochard *et al.*, 2007; Gong *et al.*, 2007; Kreuzwieser *et al.*, 2009) and variable nutrient availability (Pulford *et al.*,

2002; Vandenhove *et al.*, 2004) are typical – making them useful for planting on floodplains and in phytoremediation. In contrast, Richter *et al.* (Richter *et al.*, 2008) and Lovett *et al.* (2009) found the yield of *Miscanthus x Giganteus* across England was strongly correlated to land quality, making planting on ALC grade 5 unfeasible. Therefore, while yields in England are in general higher for *Miscanthus* (Price *et al.*, 2004; Richter *et al.*, 2008), SRC may have potential to expand energy crops to more marginal lands. This is in line with the recommendations of the Gallagher review and unlikely to be achieved from a C_4 tropical grass grown in a temperate environment (i.e. *Miscanthus*). We can consequently envisage a future landscape where SRC may be widely planted with *Miscanthus*, as a niche crop in areas of poor land quality.

3.5 Conclusions

In conclusion, we find that bioenergy has the potential to meet current UK renewable energy targets, without appreciably compromising food production or our protected areas. We have identified the South West and North West as two areas with the potential to supply over a third of this biomass requirement.

The GIS-based approach outlined here is an important tool for making the informed decisions needed regarding the placement of energy crops. If bioenergy is to remain a viable and sustainable renewable energy option, careful consideration must be made to ensure energy crops are both economically competitive and complimentary to other land use resources.

Chapter 4 . ForestGrowth-SRC: A process-based model to simulate the growth and yield of short rotation coppice poplar

4.1 Introduction

Climate change and increasing demand for renewable energy has led to considerable interest in developing dedicated energy crops as a source of biomass. Poplar, coppiced and grown under a short rotation, is considered among the most suitable energy crops in temperate climates (McKendry, 2002a; Scholz and Ellerbrock, 2002). Selection and breeding have in the past, led to the development of highly productive genotypes of poplar. However, for poplar to become economically sustainable as a source of energy, yields need to be increased further and maintained at a consistently high level (Scholes, 1998). Identifying the attributes which affect crop productivity will help develop higher yielding genotypes. Furthermore, making reliable predictions on current energy crop yields will help determine land use requirements in current and future climates.

The productivity of poplar has been intensively studied in field trials (Scarasscia-Mugnozza *et al.*, 1997; Laureysens *et al.*, 2004; Fang *et al.*, 2007; Aylott *et al.*, 2008). Consequently, empirical models have been used to determine the statistical relationships between measured yield and abiotic factors. These relationships can then be used to predict productivity across a wider range of sites (Lobell and Field, 2007; Aylott *et al.*, 2008; Richter *et al.*, 2008; Wagner *et al.*, 2009). However, empirical models are not intuitive and are unlikely to improve our understanding of the complex mechanisms underlying plant growth. Furthermore, extending empirical predictions beyond the range of the original trials should be performed with caution, as many factors are responsible for controlling yield and responses to specific factors are difficult to quantify under natural conditions (i.e. impact of extreme weather or pests and disease).

Process-based models use our best understanding of the physiological basis to growth and development, in order to predict productivity. Such models are versatile; allowing each variable to be controlled and cumulative responses to be assessed. Many process-based forest models exist, but those specifically designed to simulate a coppice system are less common. SRC crops differ significantly from other forest species, as a result of their unique management and physiological responses. In a coppice system, natural growth patterns are artificially controlled to stimulate competition between shoots and rapidly close the canopy. The result of which is high above-ground biomass growth. Therefore explicit modelling of labile C pools (i.e. storage) is of great importance, as these pools carry over effects between one growing season or rotation and the next. Many current models are deficient in this respect, using simple growth curves and empirical allometric relationships.

The purpose of this study was to develop a robust process-based model (ForestGrowth-SRC), which could accurately simulate the productivity of short rotation coppice poplar under variable climatic conditions and over multiple coppice rotations. To assess the predictive capability of the model, simulations were conducted across seven sites and validated against existing field data.

4.2 Materials and Methods

4.2.1 Model overview

ForestGrowth-SRC is a modular, fully coupled, daily timestep soil–vegetation–atmosphere transfer (SVAT) model. The core structure of the model was originally

parameterised for ash, scots pine, beech and sitka spruce but has significant implications for short rotation coppice modelling. The model links several well known models together and uses a series of morphological, physiological, soil and meteorological inputs to drive the primary processes of plant development (Figure 4.1). The modular approach minimises the risk of failure associated with development of a single and unified modelling system, as it allows full assessment of the predictive capabilities of each module, independently of interactions with other model components.

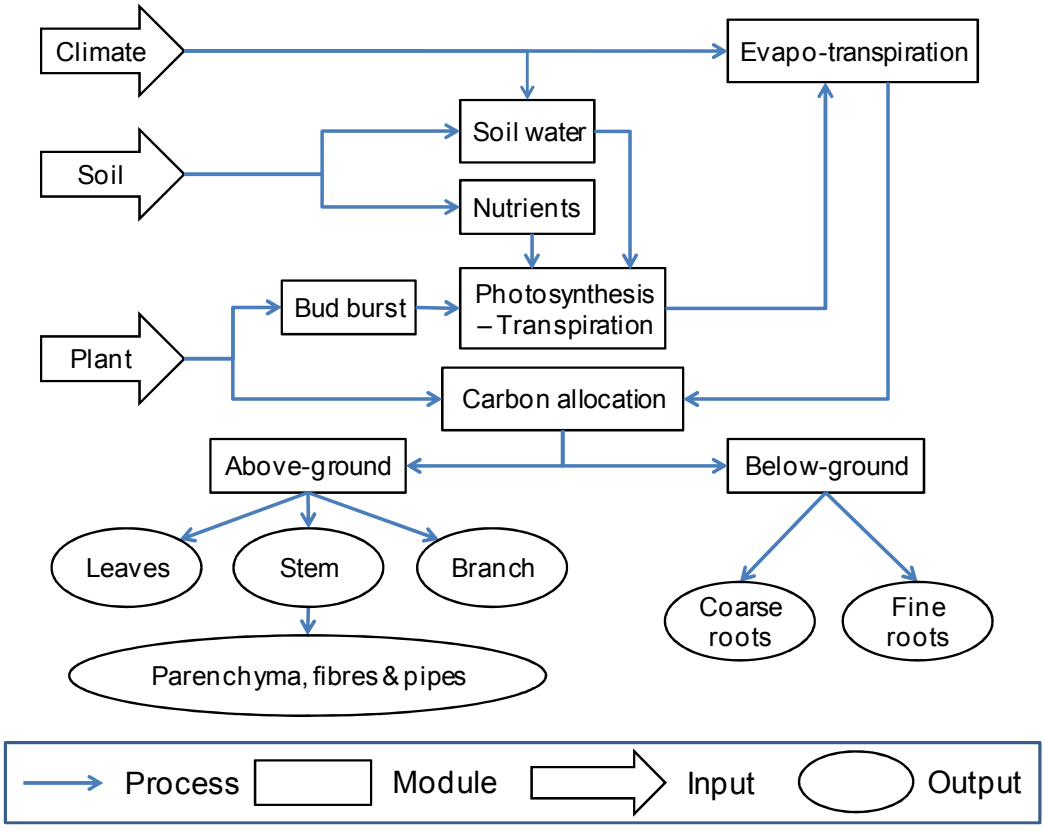

Figure 4.1. Overview of ForestGrowth-SRC structure.

Arguably the two most important processes are the vertical and lateral movements of water through the soil–vegetation–atmosphere continuum and the manufacture of carbon via photosynthesis. The allocation of available C depends on species-specific allocation

patterns and the growing phase of the tree, of which there are four phenological phases (Table 4.1). Input parameters for the model (Appendix D) were based on available literature, where possible specific to the poplar genotypes used in validation.

Table 4.1. Growth phases of ForestGrowth-SRC.

Phase	Overview
Phase 1. Budburst	Budburst begins when a specific number of chilling days and warming days are met. Initially, the canopy is replenished with leaves using stored C; 1/25th is used each day for 20 days. If the canopy is filled before that time, the tree will go into phase 2 and no longer use stored C.
Phase 2. Stem and leaf growth	If there is insufficient light in the canopy, height growth occurs. For each new layer, leaves, stems and branches are added with their associated parenchyma, fibres, pipes and roots. If the available C is negative (respiration is higher than photosynthesis), this is subtracted from the C storage pool – if the stored C >0 then the shoot dies.
Phase 3. Leaf fall	Leaves fall from the start of phase 3 onwards. This is determined by a species-specific fixed date. Leaves are removed from the bottom to the top. In phase 3 available C is used to replace lost pipes. The remaining C is allocated to storage. Stem width will only increase because of pipe replacement or if all storage space is filled.
Phase 4. Dormancy	Phase 4 begins when there are no remaining leaves. Since there will be no C assimilation, there is no allocation. However, available C will be negative because of respiration and this will be subtracted from stored C.

4.2.2 Photosynthesis module

Following budburst the developing leaves subsequently absorb carbon from the atmosphere, according to the widely used photosynthesis model developed by Farquhar *et al.* (1980) and von Caemmerer and Farquhar (1981), with modifications by Long (1991), McMurtrie and Wang (1993) and Friend (1995). Rates of photosynthesis change in response to physiological variables (which in turn are governed by abiotic factors, such as photosynthetically active radiation and temperature) as follows:

$$A_i = \left(1 - \frac{\Gamma *}{c_i}\right) \min\{w_c, w_j\} - R_d \quad (1)$$

Where A_i is gross rate of photosynthesis (assimilation), Γ* is the compensation point in the absence of daylight respiration, c_i is the inter-cellular concentration of CO_2 at the site of reaction, w_c is the ribulose biphosphate [RuBP] carboxylase-oxygenase (Rubisco) activity (μmol mol^{-1} s^{-1}), w_i is the rate of RuBP regeneration through electron transport (μmol mol^{-1} s^{-1}) and R_d is the mitochondrial (dark) respiration (μmol mol^{-1} s^{-1}).

RubP limited photosynthesis is defined as:

$$\frac{4}{g_c} A_{j,n}{}^2 + \left(\frac{(4 * R_d - J)}{g_c} - 8\Gamma^* - 4C_a\right) A_{j,n} + \left[J(C_a - \Gamma^*) - 4R_d(C_a + 2\Gamma^*)\right] = 0 \quad (2)$$

$A_{j,n}$ is the RubP limited value of net photosynthesis (μmol mol^{-1} s^{-1}), J is the rate of electron transport rate per unit leaf area (μmol m^{-2} s^{-1}), g_c is the stomatal conductance for CO_2 (mol m^{-2} s^{-1}), Γ* is the CO_2 compensation point in the absence of respiration (μmol mol^{-1}), C_a is the atmospheric carbon concentration (μmol mol^{-1})

Rubisco limited photosynthesis is defined as:

$$\frac{1}{g_c} A_{c,n}{}^2 + \left(\frac{R_d - V_{cmax}}{g_c} - C_a - k_m\right) A_{c,n} + \left[V_{cmax}(C_a - \Gamma^*) - R_d(C_a + k_m)\right] = 0 \quad (3)$$

$A_{c,n}$ is the Rubisco limited value of net photosynthesis (μmol mol^{-1} s^{-1}), V_{cmax} is the

maximum rate of carboxylation by Rubisco (μmol m^{-2} s^{-1}) and k_m is the effective Michaelis-Menten constant (mol m^{-2} s^{-1}).

Stomatal behaviour is defined by the Ball-Berry model of stomatal conductance (Ball *et al.*, 1987), this allows explicit responses to environmental variables to be modelled (i.e. atmospheric CO_2 concentrations). After Ball *et al.* (1987), internal leaf CO_2 pressure (*C*i) is determined within the leaf as a function of the interactions between CO_2 assimilation and stomatal conductance to CO_2, regulated by the leaf boundary layer and mesophyll cell surface resistances to CO_2 transfer.

After Farquhar *et al.* (1980) and Friend (1995), leaf nitrogen content (linearly) influences two of the rate-limiting photosynthetic processes, namely the potential maximum velocity of fully activated Rubisco that is inhibitor free (V_{cmax}) and the maximum potential rate of electron transport (J_{max}) according to the equations:

$$e_t = \frac{8 * 6.25 * 0.22 N_{leaf}}{550} * 10^6 \quad (4)$$

and

$$V_{cmax,25} = 1.584 e_t \quad (5)$$

and

$$J_{max,25} = 2.1 \cdot V_{cmax,25} \quad (6)$$

where e_i is the leaf Rubisco catalytic site content (μmol m^{-2} s^{-1}), N_{leaf} is the leaf nitrogen content (kg m^{-2}), $V_{cmax,25}$ is the maximum rate of carboxylation by Rubisco at 25 °C

(μmol m^{-2} s^{-1}) and $J_{max,25}$ is the maximum rate of electron transport rate at 25 °C (μmol m^{-2} s^{-1}).

Canopy leaf nitrogen, per m^2 leaf is fitted to the canopy profile as defined by the equation:

$$N_c = (N_0 - N_b)\frac{(1 - e^{-k_n})}{k_n} + N_b \quad (7)$$

where N_c is the canopy nitrogen content per m^2 leaf area (mmol m^{-2}), N_0 is the leaf nitrogen content at the top of the canopy (mmol m^{-2}), N_b is the leaf nitrogen content not associated with photosynthesis (mmol m^{-2}), k_n is the leaf nitrogen allocation coefficient.

Photosynthesis is also directly affected by the role of pests and disease. Pests and disease are known to have a significant impact on the yield of crops such as SRC poplar. ForestGrowth-SRC does not explicitly model the affect of disease on chemical processes with the plant or any reaction of the plant to combating the disease/infection. Instead a simple surrogate of defoliation has been included in the model, which is set to remove a specific fraction of leaves on a daily basis in accordance with an input value. This value defines a daily defoliation term for a specific period of time (e.g. 1% removal of leaves per day for 90 days, beginning on day 180).

Concomitantly, photosynthesis is in flux with the rate of mitochondrial respiration (R_d) and unlike photosynthesis is a constantly active part of the model. R_d is subtracted from GPP as follows:

$$R_d = A_i * R_g * Q_{10}^{\left(T_{day} - T_{Q10}/10\right)} + \left(C_{pool} * R_m * Q_{10}^{\left(T_{day} - T_{Q10}/10\right)}\right) \quad (8)$$

Where R_g is the growth respiration at a reference temperature of 15^{oC} (expressed as a fraction of gross photosynthesis lost per unit new growth), C_{pool} is the remaining available carbon, R_m is the maintenance respiration at $15\ ^{oC}$ (per unit area), Q_{10} is the temperature coefficient for each compartment and T_{day} is the average daily temperature.

4.2.3 Light interception module

Early attempts within the model to simulate inter-shoot competition were abandoned in favour of a more simplistic single stem design. Simulating multiple stems to account for inter-shoot competition leads to unnecessary complexity and stem class mortality (i.e. stems of a particular class either live or die; there is no gradual loss of shoots). In addition, it is difficult to parameterise the model with meaningful empirical data (i.e. height, diameter and number of stems per class). Therefore, we assume a single straight stem with whorls and branches, driven primarily by light interception and a height area growth ratio.

The canopy radiative transfer module considers the heterogeneity of radiation in the canopy, as the necessary precursor to approximating the non-linear response of photosynthesis to irradiance. The model employs a radiative transfer scheme that approximates the transmittance, reflectance and absorption of direct and diffuse photosynthetically active radiation (PAR) by canopy layers, where canopy interactions

are determined by the area and distribution of foliage.

After Norman (1980) and de Pury and Farquhar (1997) the module separates penetration of direct and diffuse radiation (net of albedo) through a canopy in which two classes of leaves (sunlit and shaded) are distributed in a multi-layer canopy model. This approach allows the explicit description of within-canopy profiles (on a per layer basis) of both environmental (e.g. wind profile, vapour pressure deficit) and physiological (e.g. leaf temperature) variables in response to radiation attenuation. It does so through a canopy with uniform leaf distribution (spherical) as prescribed by Beer's law (Monsi and Saeki, 1953) for each leaf class. In each layer, sunlit leaves are assumed to receive both direct and diffuse radiation and shaded leaves receive diffuse light only, assuming no radiative energy transmittance through leaves.

Direct beam irradiance absorbed by sunlit leaves is described by the equation:

$$I_{clbSun} = I_b(0)\,(1-\sigma)\,(1-e^{-k_b L_c}) \quad (9)$$

where I_{clbSun} is the direct beam irradiance absorbed by sunlit leaves (μmol m^{-2} s^{-1}), $I_b(0)$ is the beam PAR per unit ground area at top of canopy (μmol m^{-2} s^{-1}), σ is the leaf scattering coefficient of PAR, k_b is the radiation extinction coefficient of canopy for beam irradiance, L_c is the canopy leaf area index (m^2 m^{-2}).

Similarly, diffuse irradiance absorbed by sunlit leaves is described by the equation:

$$I_{cldSun} = \frac{I_d(0) * (1 - \rho_{cd}) * (1 - e^{-(k_d' + k_b) * L_c}) * k_d'}{(k_d' + k_b)} \quad (10)$$

where I_{cldSun} is the diffuse irradiance absorbed by sunlit leaves (μmol m^{-2} s^{-1}), ρ_{cd} is the canopy reflection coefficient for diffuse radiation(dimensionless), k_d' is the radiation extinction coefficient of canopy for diffuse irradiance, adjusted for scatter (dimensionless).

The diffuse and scatter irradiance absorbed by shaded leaves is described as follows:

$$I_{lSh} = I_{ld}(L_c) + I_{bs}(L_c) \quad (11)$$

and

$$I_{lbs} = \frac{I_b(0)(1 - \rho_{cb})(1 - e^{-(k_b' + k_b) * L_c}) * k_b'}{(k_b' + k_b)} - \frac{(1 - \sigma)(1 - e^{-2k_b L_c})}{2} \quad (12)$$

and

$$\sigma = \rho + \tau \quad (13)$$

where I_{lSh} is the irradiance PAR absorbed by shaded leaves (μmol m^{-2} s^{-1}), I_{ld} is the diffuse irradiance PAR per unit ground area (μmol m^{-2} s^{-1}), L_c is the canopy leaf area index (m^2 m^{-2}), I_{lbs} is the scattered beam irradiance (PAR) per unit ground area - scattered beam (μmol m^{-2} s^{-1}), $I_b(0)$ is the beam PAR per unit ground area at top of canopy (μmol m^{-2} s^{-1}), ρ_{cb} is the canopy reflection coefficient for beam radiation, k_b' is the radiation extinction coefficient of canopy for beam irradiance, adjusted for scatter (dimensionless), k_b is the radiation extinction coefficient of canopy for beam irradiance, σ is the leaf

scattering coefficient of PAR, ρ is the leaf reflection coefficient for PAR, τ is the leaf transmissivity to PAR.

The within-canopy profiles of leaf nitrogen follow the predicted distribution of absorbed irradiance through each canopy layer, separately for sunlit and shaded leaves. Seasonal variation of nitrogen content in foliage can also be represented with suitable input. Given the separate descriptions of sun and shade leaves and within-canopy variation of photosynthesis, the module allows non-uniform vertical profiles of photosynthetic capacity to be developed.

4.2.4 Allocation module

Following the initial transfer of carbon from storage to the canopy, new leaf layers are subsequently added when there is insufficient light reaching the existing canopy. This is modified according to the maximal leaf area density (LAD) or as dictated by the light interception coefficient for direct and diffuse radiation. Species-specific allocation patterns then distribute the available carbon (net of photosynthesis minus respiration) to the different compartments (stem, branch, leaf, storage, coarse and fine root) and types of stem tissue (parenchyma, fibres and vessels). New leaf growth ends at a species-specific date, after which point all subsequent carbon produced by photosynthesis is added to storage. Leaves are removed at a constant linear rate, relative to a fixed period of time specified in the input file (leaf fall duration). Once all leaves have fallen dormancy begins.

The allocation module uses the assumptions of refined pipe theory (Deckmyn *et al.*, 2006), which state that there must be a balance between the leaf area and the pipes through which the water flows to the leaves. ForestGrowth-SRC directly relates leaf area to the actual number and size of the pipes.

$$\frac{C_l}{C_p} = \frac{\pi(\psi_r - \psi_l - \rho g h) r_i^4 P_e L_{wr}}{8\eta h^2 E_{\max} P_c} \tag{14}$$

Where C_l is the leaf mass (kgC), C_p is the pipe mass (kgC), ψ_r is the root water potential (Pa or kg m^{-1} s^{-2}), ψ_l is the leaf water potential (Pa or kg m^{-1} s^{-2}), ρ is the water density (10^3 kg m^{-3}), g is the acceleration due to gravity (9.8 m s^{-2}), h being the stem height (m), r_i is the pipe radius (m), P_e describes the conductive efficiency of a pipe (0 or 1), L_{wr} is the ratio of leaf mass to leaf area (kgC m^{-2}), η is the viscosity of water (0.001 kg m^{-1} s^{-1}), E_{max} is the maximum transpiration per unit leaf area at steady state (m^3H_2O m^{-2} s^{-1}), P_c is the carbon required to build a unit length of pipe (kgC m^{-1}).

Some pipes loose functionality during the course of the year and must be replaced or the associated leaves will lose functionality also. The fraction of pipes embolised during winter is defined by the parameter Emb_{win}, and those losing functionality each day during the growing season is defined by the parameter Emb_{sum}.

By coppicing, root biomass becomes relatively high compared to above-ground biomass. Therefore a maximum coarse root to stem ratio ($Root:Stem_{max}$) is used, which is variable throughout each rotation. In addition, fine roots (those not removed by the process of

turnover) may also remain over winter to facilitate the faster assimilation of soil water needed to drive rapid above-ground biomass growth post coppicing.

4.2.5 Water balance module

Water is important in many biochemical processes within the plant system, and is primarily absorbed through fine roots and transported to other plant compartments through the xylem (vessels) by stemflow. The rate of uptake is governed by the size of the plant, volume of water present in the soil and proximity of roots to the transient perched water table according to the SWBCM soil water balance capacity model (Evans *et al.*, 1999). The soil water pool is replenished by precipitation (minus interception) and filled up to a maximal soil water capacity value, specific to each soil type (NATMAP, Cranfield, UK). The tree canopy partitions gross rainfall into three downward water fluxes (free throughfall precipitation, canopy drip and stemflow) and an upward gaseous flux, resulting from evaporation of the intercepted rainfall (Rutter *et al.*, 1975; Gash *et al.*, 1995; Valente *et al.*, 1997). The Gash interception model (Gash *et al.*, 1995), originally developed for the description of interception in conifers stands, was modified to deal with broadleaf deciduous stands. This was achieved by introducing a direct dependence between interception and the temporal evolution of the canopy:

$$S_c = S_{c0} * LAI \tag{15}$$

and

$$c = 1 - \exp(-k * LAI) \tag{16}$$

where Sc is the canopy storage capacity (mm per unit canopy cover), c is the canopy fractal cover (van Dijk and Bruijnzeel, 2001), LAI is the leaf area index (m^2 m^{-2}) and k is a constant.

4.2.6 Evapotranspiration module

Concomitantly to interception, water is lost via run-off (Evans *et al.*, 1999) and evapotranspiration, based on the Penman-Monteith equation (Monteith, 1965). ForestGrowth-SRC computes evaporation from soils and plants separately, as described by Ritchie (1972). The equation is disaggregated to approximate daily leaf and canopy level evapotranspiration, bare and shaded soil evaporation and wet canopy evaporation, separately for wet and dry days as determined by the climatic inputs. In ForestGrowth-SRC total evapotranspiration is calculated as:

$$E_{total} = (1 - p_{dry}) * E_{wet} * p_{\cov} + p_{dry} * E_{trans} * p_{\cov} + E_{shade} * p_{\cov} + E_{bare} * (1 - p_{\cov}) \qquad (17)$$

where E_{tot} is the total evapotranspiration, p_{dry} is the proportion of the daylight time that is dry (dimensionless), E_{wet} is the evaporation from a wet canopy (mm day^{-1}), p_{cover} is the projected canopy cover (dimensionless), E_{trans} is the transpiration from a dry canopy (mm day^{-1}), E_{shade} is the evaporation from soil shaded by the canopy (mm day^{-1}), E_{bare} is the evaporation from the bare soil (mm day^{-1}). Evaporation from a wet canopy is defined by the equation:

$$E_{wet} = 3600 D_{hr} \frac{\Delta V \left(\frac{R_n}{3600 D_{hr}} - \frac{G}{3600 D_{hr}} \right) * f_{abs} + \rho_a c_p \left(\frac{e_s - e_a}{r_a} \right)}{\lambda \times 10^3 (\Delta V + \gamma_p)} \quad (18)$$

and

$$G = 0.033 * R_n \quad (19)$$

and

$$\lambda = 2500.78 - 2.3601 * T \quad (20)$$

and

$$\Delta V = \frac{4098.25 e_s}{(\overline{T} + 237.3)^2} \quad (21)$$

where D_{hr} is the daylit time for the day (h), ΔV is the rate of change of saturated vapour pressure with temperature (mbar K^{-1}), R_n is the net daily radiation (J m^{-2} day^{-1}), G is the ground heat-sink (J m^{-2} day^{-1}), f_{abs} is the fraction of incoming radiation absorbed by the canopy (dimensionless), ρ_a is the air density (kg m^{-3}), c_p is the specific heat capacity of air (J kg^{-1} K^{-1}, assumed to be 1005.01), e_s is the saturated vapour pressure (mbar), e_a is the actual vapour pressure (mbar), r_a is the aerodynamic (boundary layer) resistance of the canopy to water diffusion (s m^{-1}), λ is the latent heat of vapourisation (kJ kg^{-1}), γ_p is the psychometric constant (mbar K^{-1}).

Canopy aerodynamic resistance follows the equation:

$$r_a = \frac{\ln\left(\frac{z_m - d}{z_{om}} \right) \ln\left(\frac{z_h - d}{z_{oh}} \right)}{k^2 u_z} \quad (22)$$

where r_a is the aerodynamic resistance (s m^{-1}), z_m is the height of wind measurements (m), z_h is the height of humidity measurements (m, assume z_m), d is the zero plane displacement height (m, assume 0.75), h is the crop height (m), z_{om} is the roughness length governing momentum transfer (m, assume 0.123), z_{oh} is the roughness length governing transfer of heat and vapour (m, assume 0.1), k is the Von Karman's constant (dimensionless, assume 0.41), u_z is the windspeed at height z_m (m s^{-1}).

4.2.7 Validation

The model was validated for two contrasting species of poplar: large leaf 'Trichobel' (*Populus trichocarpa* Torr. & A. Gray) and small leaf 'Ghoy' (*P. deltoides* Bartr. x *P. nigra* L.). Biomass allocation (stem, branch, leaf), leaf area index (LAI) and canopy profiles were validated against a physiological trial at Alice Holt, Farnham (Casella and Sinoquet, 2003; Casella and Sinoquet, 2007), planted at a density of 10,000 stools ha^{-1} and measured between May and September 2001 (two-year old shoots, six-year old stools). Alice Holt has a productive clay loam soil with an available soil water capacity (0.137 cm^3 water per cm^3 soil) close to the UK average (0.139).

Total above-ground biomass was validated against the recorded yield data from seven national SRC field trial sites, all with contrasting soil and climatic characteristics (Aylott *et al.*, 2008). Data from the national field trials network is effective for validation as it uses the same genotypes, establishment and management protocols as the model but is independent (i.e. data not used in the model parameterisation). A sensitivity analysis was performed by simulating a ± 10 % change in key inputs. This helps indicate the

robustness of the model and its sensitivity to specific parameters.

4.3 Results

4.3.1 Alice Holt validation

Above-ground woody biomass

Plant above-ground biomass pools are allocated carbon according to species-specific functions. They are also described by the phenological phase of the tree. To account for variation in yield attributed to pests and disease we include a defoiliation term. Trichobel was largely unaffected by pests and disease. However, for genotype Ghoy we include a daily defoiliation term of 1.5 % leaf removal from day 180 (each year) for 60 days. Results presented here show a close fit between measured and simulated stem biomass data for genotypes Trichobel ($r^2 = 0.87$) and Ghoy ($r^2 = 0.80$) (Figure 4.2). Branching is similarly well described, $r^2 = 0.80$ and $r^2 = 0.86$ for Trichobel and Ghoy respectively. For Trichobel, total above-ground woody biomass production measured 17.21 odt ha^{-1} yr^{-1} vs. a simulated yield of 16.68 odt ha^{-1} yr^{-1}. Ghoy is a lower yielding genotype producing 5.19 odt ha^{-1} yr^{-1} vs. a simulated yield of 5.26 (with pests and disease).

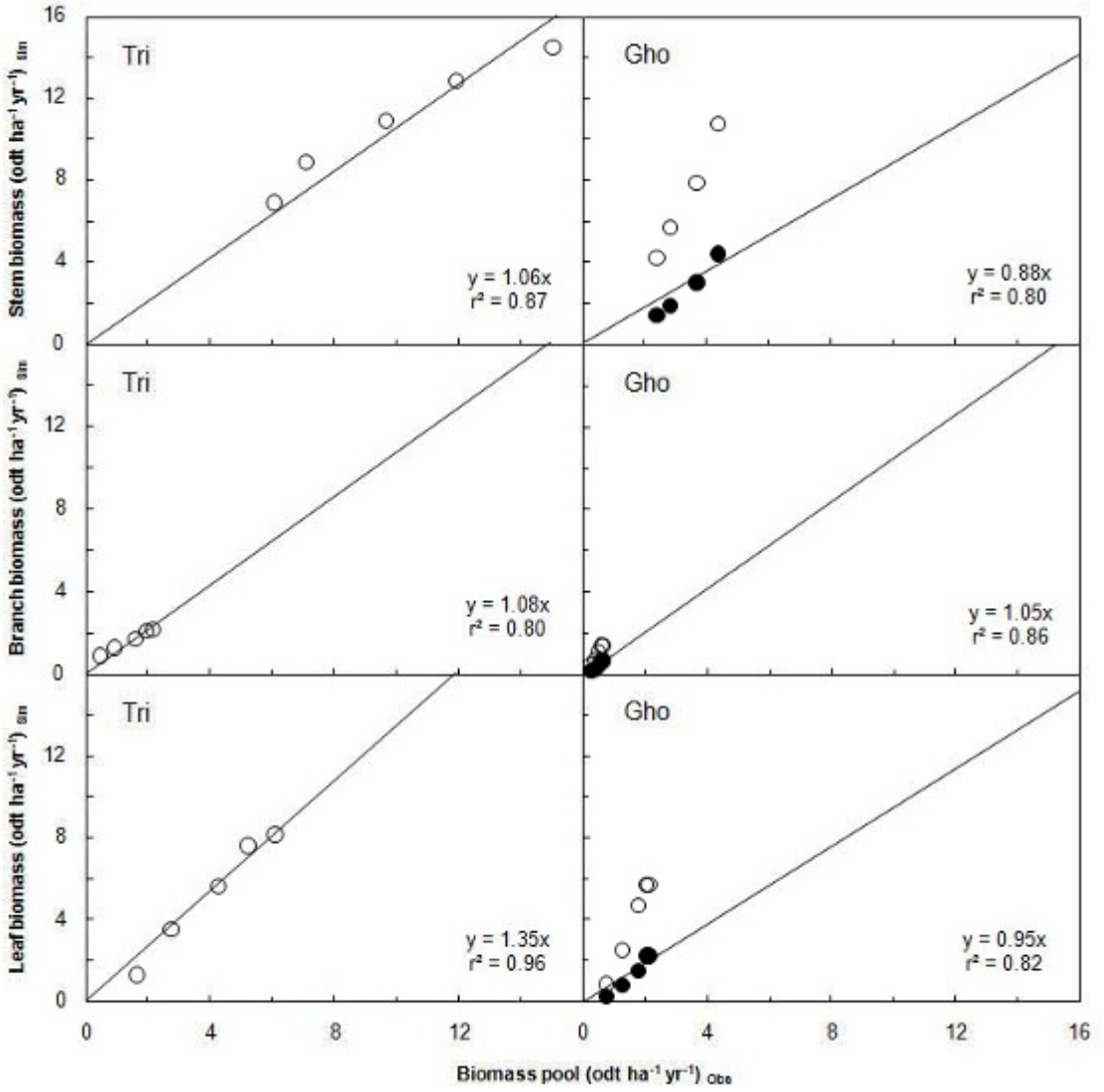

Figure 4.2. Measured vs. simulated biomass pools (odt ha^{-1}) for poplar genotypes Trichobel (Tri, left) and Ghoy (Gho, right) at Alice Holt. Open circles (○) are for biomass without pests and disease. Closed circles (●) are for biomass with pests and disease.

Foliage biomass

Leaf biomass was well described by ForestGrowth-SRC, $r^2 = 0.96$ and $r^2 = 0.82$ for Trichobel and Ghoy respectively (Figure 4.2). However, there tended to be an under-simulation of leaf biomass in spring and an over-simulation towards the end of the growing season. Linked to leaf biomass is leaf area. The model simulates potential leaf area index (pLAI), where no abscission occurs during the growing season. For Trichobel,

*p*LAI is accurately simulated by the model ($r^2 = 0.92$) but is less accurately simulated for Ghoy ($r^2 = 0.66$) (Figure 4.3).

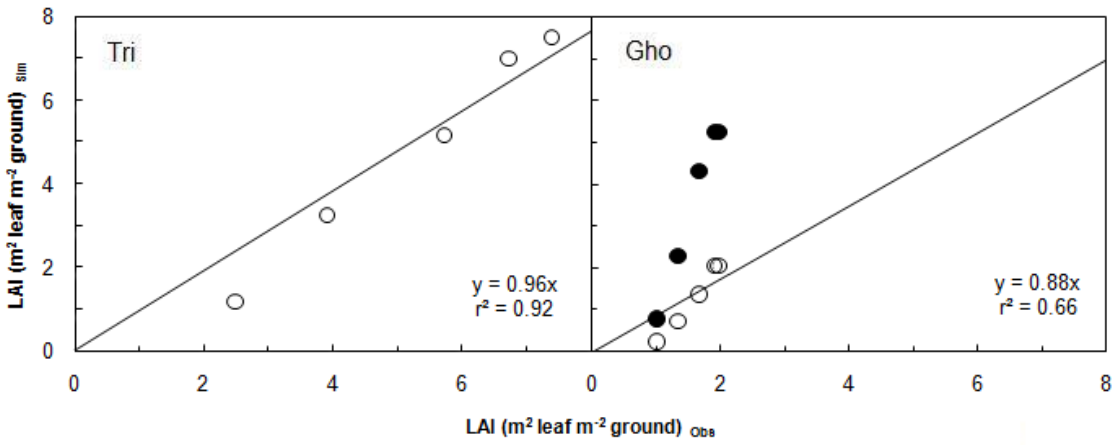

Figure 4.3. Measured vs. simulated *p*LAI (m^2 leaf m^{-2} ground) for poplar genotypes Trichobel (Tri, left) and Ghoy (Gho, right) at Alice Holt. Open circles (○) are for biomass without pests and disease. Closed circles (●) are for biomass with pests and disease.

The physical structure of the canopy is important in light interception, which is a primary mechanism in photosynthesis according to the Farquhar equation. Canopy profiles are also well described by the model, reaching a height of 4.75 and 2.75m for Trichobel and Ghoy respectively (Figure 4.4). LAD is accurately fitted to these profiles according the maximal leaf area density per 25cm layer function, canopy light extinction coefficient and light interception dynamics (as described in the methodology).

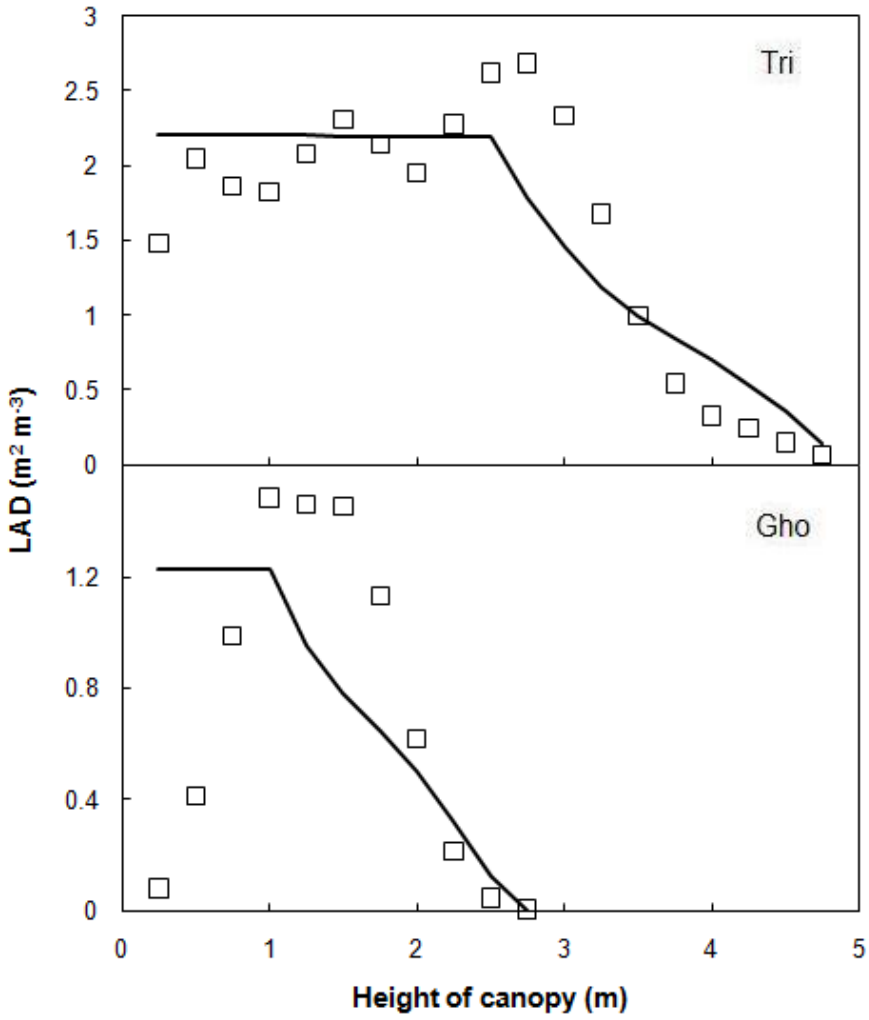

Figure 4.4. Measured vs. simulated LAD (m^2 leaf m^{-3} ground) for poplar genotypes Trichobel (Tri, top) and Ghoy (Gho, bottom) at Alice Holt, inclusive of pests and disease. Black line represents simulated canopy profile and squares (□) represent measured data.

4.3.2 UK validation

Above-ground woody biomass

The average measured yield across two rotations and all seven validation sites was 8.59 and 5.26 odt ha^{-1} yr^{-1} for Trichobel and Ghoy respectively. In general, above-ground woody biomass production [across the seven validation sites] was lowest on silt soils and highest on clay soils (Table 4.2).

Table 4.2. Measured vs. simulated biomass (odt ha^{-1}) at seven contrasting sites, for two contrasting poplar genotypes (*Populus trichocarpa* genotype Trichobel and *P. deltoides* x *P. nigra* genotype Ghoy).

Site	Date	Trichobel		Ghoy	
		Measured	Simulated	Measured	Simulated
Alice Holt (clay loam)	1997	2.75	2.83	1.53†	1.61
	1998	10.57††*	15.71	3.80†††*	11.02
	1999	19.53†**	30.07	6.07†††***	24.07
	2000	3.55†**	7.71	1.09†††*	4.74
	2001	14.18†	19.90	3.81†**	15.86
	2002	29.05†††**	30.53	7.32†††*	25.21
Balbirnie (fine sand)	1996	5.46	5.45	3.38	3.41
	1997	23.05	18.94	14.15	13.12
	1998	37.08	37.87	24.19*	30.18
	1999	3.04*	5.11	2.29*	3.16
	2000	14.84	16.63	15.13	11.11
	2001	32.66	31.10	29.36	23.77
Loughall (fine sand)	1996	4.53	4.56	5.70	5.66
	1997	12.47†	17.10	14.31	17.14
	1998	17.72†*	31.97	17.53†††*	31.02
	1999	5.01*	5.64	3.17†**	4.79
	2000	4.52*	19.97	2.76†††*	16.83
	2001	6.63†**	35.69	3.27†††*	31.02
Loyton Bampton (clay)	1996	4.39†	4.48	2.50††††*	2.59
	1997	14.49†*	16.28	5.63†††*	10.16
	1998	24.19†*	26.81	6.60†††**	19.52
	1999	5.80	4.01	0.96†**	2.14
	2000	8.58†††***	15.03	1.00†††*****	9.26
	2001	26.70†††***	29.50	2.03†††***	21.44
Thorpe Thewles (medium sand)	1996	3.15*	3.21	2.89	2.91
	1997	9.39*	11.78	7.50	10.08
	1998	24.76**	23.76	20.45†*	20.57
	1999	8.13	3.97	8.45	2.88
	2000	11.21†**	16.19	10.85†**	13.03
	2001	28.74***	31.50	23.19†††**	27.04
Trefeinon (silt)	1996	3.02	3.02	3.01	3.07
	1997	13.35	13.16	13.59	11.55
	1998	26.35	27.06	20.53†	24.27
	1999	7.07	3.02	5.66†††**	2.20
	2000	15.24*	13.10	9.29†**	9.65
	2001	28.81*	26.93	14.18†**	22.30
Trumpington (silt clay)	1996	-	3.78	-	5.38
	1997	14.97†	15.04	16.06†	16.21
	1998	27.53†	25.99	27.74††	25.48
	1999	4.03	4.02	1.72†††	3.48
	2000	10.23	13.37	6.24††	11.32
	2001	31.20*	27.59	18.61†††***	24.92

Daggers denote sites affected by rust: † = 5-10 % leaf area lost (LAL), †† = 10-20 % LAL, ††† = 20-40 % LAL. Asterisks denote leaf chewers, skeletonising *Phyllodecta* spp or other photosynthesis limiting disease spots and blotches: * = 5-10 % LAL, ** = 10-20 % LAL, *** = 20-40 % LAL, **** = 40-65 % LAL, ***** = >65 % LAL.

In the absence of compensation for leaf loss as a result of pests and disease damage, simulated yield accuracy was variable. There was a close fit between observed and simulated yields (± 10 %) on sites where pest and disease were not prevalent (i.e. Trichobel plots at Balbirnie, Trefeinon and Trumpington).

Pests and disease

Pests and disease evidently play a significant role in yield. Rust, leaf chewers and skeletonising *Phyllodecta* severely damaged both genotypes of poplar and all three genotypes of willow during the field trials and were negatively correlated to their yield in each case (linear regression, $p>0.01$). Fitting a defoliation term is a simple but effective method for accounting for this effect (Figure 4.2 and 4.3).

4.4 Discussion

4.4.1 Simulated growth and yield

Genotypic variation

Of the genotypes considered, the model predicts Trichobel will have a higher leaf area and be more productive than Ghoy across all the seven sites used for model validation (Table 4.2). This clearly shows the difference in productivity between the large (Trichobel) and small (Ghoy) leaf genotypes, but it also demonstrates a successful implementation of the way the model differentiates between varieties. Differences in genotypic yield are defined by three key inputs: (1) initial C storage, (2) maximum closed canopy LAD (per 25cm layer) and (3) date/duration of leaf fall. To ensure wider

applicability to a range of genotypes, it is important that clonal differences are defined by simple and easy to parameterise inputs. However, it should also be considered that this simplistic method of differentiating genotypes does not account for clonal differences in C allocation, susceptibility to environmental conditions (e.g. drought) or morphological leaf traits (e.g. SLA).

Although developed for poplar, owing to the large volume of validation data available, ForestGrowth-SRC may also be applied to other coppiced species belonging to the *Salicaceae* family (e.g. willow). Species of the *Salicaceae* family bear many similar traits and characteristics, being fast growing, riparian species utilising C_3 photosynthetic pathways. SRC poplar and willow both produced similar canopy profiles with comparable leaf morphologies and light interception (Ceulemans *et al.*, 1996). However, Cannell *et al.* (1988) suggests poplar partitions more dry matter to roots (and correspondingly less to stems) and intercepted less light over the growing season. Poplar also has a greater tendency for single stem apical dominance (Aylott *et al.*, 2008).

In season variation

High growth rates in poplar are explained by the high allocation of carbon to leaves, resulting in rapid leaf development in spring, fast canopy closure and high rates of photosynthesis (Barigah *et al.*, 1994). In general, ForestGrowth-SRC was able to accurately model the productivity and genotypic differences in short rotation coppice poplar (Table 4.2). However, variation existed between simulated and measured data. The model tended to under-simulate the growth rate of leaves in spring and over-simulate later in the growing season. This highlights the inherent danger interpreting models where

constants are fitted to non-linear biological functions, either because of insufficient data for validation or simplification. In poplar allocation patterns change over the growing season, whereby more carbon is allocated to leaves in spring and roots in autumn (Nguyen *et al.*, 1990; Stettler, 1996; Scarasscia-Mugnozza *et al.*, 1997).

In order to take the seasonal variation of the carbon partitioning into account, Zhang *et al.* (1994) interpolate allocation coefficients at different times of the year. However, this is not a quantitative function and does not account for external factors. Mäkelä and Hari (1986) account for variability in allocation patterns as functions of the light environment. This should be considered in future parameterisation of ForestGrowth-SRC.

Between rotations

In most cases [measured and simulated] yields were lower in the first rotation because the root and stool had yet to fully develop. However, genotypes that performed well in the field trials during the first rotation did not always do so in the second rotation (Table 4.2). ForestGrowth-SRC similarly simulated a decrease in annual growth at Balbirnie, Trefeinon and Trumpington (Ghoy plot). This effect may be attributed to climatic factors, crop age effects and the increased cost of maintaining the existing roots (i.e. respiration). Conversely, respiration costs decline with tissue age as wood structure changes through time (i.e. thickening).

In general, ForestGrowth-SRC marginally underestimated second rotation yields compared to the first. After coppicing, the model uses a specific fraction of the coarse roots as storage carbon, subsequently all available carbon is used in the construction of

above-ground biomass (defined by a maximum root to stem ratio). However, measured yields (Table 4.2) highlight the complex nature of the underlying mechanisms of re-growth after coppicing. Higher fractions of below-ground carbon were used to re-grow stems at some sites (e.g. Thorpe Thewles) than at others (e.g. Balbirnie).

4.4.2 Pests and disease

ForestGrowth-SRC accurately simulates biomass allocation and photosynthetic processes for poplar genotypes Trichobel and Ghoy on sites with limited or no pests and disease. However, on sites with pests and disease (e.g. Loyton Bampton) the model is less robust. Rust, leaf chewers and skeletonising *Phyllodecta* severely damaged both genotypes of poplar across the seven validation sites, up to 80 % LAL. Leaf area is a key determinant of yield (Rae *et al.*, 2004) and by removing leaf biomass the photosynthetic capacity of the plant is reduced, consequently reducing biomass (Reichenbacker *et al.*, 1996).

The model does not explicitly simulate the dynamics and environmental factors determining pest and disease prevalence. Instead ForestGrowth-SRC uses a surrogate value for leaf defoliation set to a specific date and for a specific duration. This establishes a clearly defined relationship between yield and pest and disease damage. However, this does not simulate the pathogenicity and specificity of pests and disease, which change over time and have wider implications on plant health (Newcombe *et al.*, 2001; Lonsdale and Tabbush, 2002; Pei *et al.*, 2004). Furthermore, there is no modelled resistance or response to attack which might be seen in a real world environment (McNaughton, 1981; Williams and Whitham, 1986; Major and Constabel, 2007). Using a defoliation term

expressed as a percentage removal of leaf area is also not ideal as this is not easily parameterised. Results highlight the necessity for further work on pests and disease modelling in poplar. Therefore it is important to model and account for plant damage as a result of pests and disease.

4.4.3 Sensitivity analysis

The model has a large number of parameters, many of which in normal usage are 'stable' (i.e. the model is not sensitive to a 10% change in the value). However, if conditions change, then the model may become more sensitive to previously stable parameters. Model input values were often highly variable in published literature and as such the sensitivity of the model to accurately describe their functions was important to quantify. A sensitivity analysis was undertaken by simulating a ± 10 % change in key inputs (Table 4.3). In general, no input parameters exhibited extreme sensitivity to change. However, above:below-ground carbon allocation, growth respiration and specific leaf area were among the most sensitive key parameters relating to above-ground biomass accumulation.

Table 4.3. Sensitivity analyses of key input parameters for the ForestGrowth-SRC model and their effect on total above-ground biomass (3 yr and 6 yr old stems), for two contrasting poplar genotypes (*Populus trichocarpa* genotype Trichobel and *P. deltoides* x *P. nigra* genotype Ghoy).

	Alice Holt yr 3 yield (odt ha^{-1})		Alice Holt yr 6 yield (odt ha^{-1})	
	Tri	Gho	Tri	Gho
Initial C storage				
+10 %	31.02 (+3.2 %)	24.95 (+3.7 %)	30.90 (+1.2 %)	25.33 (+0.5 %)
- 10 %	30.21 (+0.5 %)	23.56 (-2.2 %)	30.55 (0 %)	25.07 (-0.6 %)
Above:below ratio				
+ 10 %	29.80 (-0.9 %)	24.02 (-0.2 %)	29.74 (-2.6 %)	24.02 (-4.8 %)
- 10 %	30.32 (+0.8 %)	24.35 (+1.2 %)	31.50 (+3.2 %)	26.11 (+3.6 %)
Coarse root storage				
+ 10 %	-	-	31.75 (+4.0 %)	26.49 (+5.1 %)
- 10 %	-	-	29.18 (-4.4 %)	23.59 (-6.4 %)
Days storage used				
+ 10 %	29.77 (-1.0 %)	23.85 (-0.9 %)	30.18 (-1.0 %)	24.92 (-0.9 %)
- 10 %	30.71 (+2.1 %)	24.71 (+2.7 %)	31.28 (+2.1 %)	25.75 (+2.7 %)
Fine root turnover				
+ 10 %	30.22 (+0.5 %)	24.27 (+0.8 %)	31.61 (+3.5 %)	26.01 (+3.2 %)
- 10 %	29.88 (-0.6 %)	24.10 (+0.1 %)	29.64 (-0.3 %)	23.85 (-5.4 %)
Height area increase ratio				
+ 10 %	30.24 (+0.7 %)	24.20 (+0.5 %)	30.48 (-0.4 %)	25.31 (+0.4 %)
- 10 %	30.24 (+0.7 %)	24.36 (+1.2 %)	30.67 (+0.5 %)	25.47 (+1.0 %)
Respiration				
+ 10 %	29.66 (-1.4 %)	23.73 (-1.4 %)	29.54 (-3.3 %)	23.73 (-5.8 %)
- 10 %	30.83 (+2.5 %)	24.83 (+3.2 %)	31.91 (+4.5 %)	26.48 (+5.0 %)
SLA				
+ 10 %	34.00 (+13.1 %)	25.66 (+6.6 %)	33.63 (+10.2 %)	28.81 (-4.8 %)
- 10 %	25.83 (-14.1 %)	19.62 (-22.7 %)	25.78 (-15.6 %)	19.16 (+3.6 %)
Maximum LAD				
+ 10 %	29.84 (-0.8 %)	23.86 (-0.9 %)	30.64 (+0.1 %)	24.91 (-1.2 %)
- 10 %	30.54 (+1.6 %)	24.79 (+3.0 %)	30.81 (+0.1 %)	25.46 (+1.0 %)

4.5 Conclusions

Process-based plant productivity models are an important tool for assessing the influence of climatic conditions on yield and predicting plant stress responses. They also have wider implications for modelling plant responses to future climates. Here, we show ForestGrowth-SRC can effectively account for interactions between the environment and

the growth of two contrasting poplar genotypes. Across the seven validation sites simulated poplar yields (with no pest and disease damage) ranged from 6.5-10.3 odt ha^{-1} yr^{-1} for genotype Ghoy and 7.9-12.6 odt ha^{-1} yr^{-1} for genotype Trichobel. This is in keeping with measured yields and simulated yields from other process-based models for SRC (Deckmyn *et al.*, 2004). ForestGrowth-SRC also demonstrates an ability to accurately simulate leaf dynamics and allocation of C to different biomass pools. However, modelling the impacts of pests and disease on plant growth is less developed and should be an area for future research. Sensitivity analysis also highlights the importance on good parameterisation, particularly considering the high variability in input parameter values seen in literature. It would be beneficial to replace some of these simple inputs with processes or empirical functions, e.g. within season variation in carbon allocation, respiration relationships with tissue age and pest and disease dynamics. In general, modelled yields demonstrate that SRC poplar could be useful in meeting our renewable energy targets, particularly if pest and disease issues can be overcome through breeding more rust tolerant species. Future climates are likely to expand this potential further.

Chapter 5 . Predicting future climate impacts on yields of short rotation coppice poplar

5.1 Introduction

Climate change and the increasing demand for renewable energy have led to the rapid growth in demand for energy crops. Short Rotation Coppice (SRC) poplar is considered among the most suitable energy crops under current UK climatic conditions. However, climate change could have a profound impact on the distribution and productivity of the world's crops, including those grown for energy (Gielen *et al.*, 2005; Tuck *et al.*, 2006).

Predictions suggest carbon dioxide (CO_2) could increase to between 525-810 ppm by the middle of the 21st century (Hulme *et al.*, 2002). In general, studies forecast plant yields will increase under elevated CO_2 (for a review see Norby *et al.*, 2005). Experimental data for poplar suggests biomass production could be between 15-27 % higher under elevated CO_2 concentrations (350 vs. 550 ppm) (Calfapietra *et al.*, 2003). Norby *et al.* (2005) showed that in forests with a low LAI, the increased net primary productivity (NPP) in elevated CO_2 resulted mainly from increased light absorption through enhanced LAI, whereas in high-LAI forests NPP was enhanced through increased light use efficiency. Furthermore, McCarthy *et al.* (2006) suggested that enhanced above-ground carbon storage may only occur when resource availability supports increased LAI. Evidence suggests no long-term loss in sensitivity to CO_2 fertilisation (Norby *et al.*, 1999; Liberloo *et al.*, 2007), although other studies dispute this (Kalina and Ceulemans, 1997; Taylor *et al.*, 2001b).

As CO_2 rises temperatures are also likely to rise (due to the greenhouse gas effect), with summer temperatures increasing at a greater rate than those in winter. By 2050 mean

summer temperature is predicted to increase by between 2.5 (low emissions scenario) and 3.5 $^{\circ C}$ (high emissions scenario) in parts of southern England (Hulme *et al.*, 2002). Higher temperatures are expected to bring forward budburst but are also expected to increase transpiration and respiration rates (defined in the short-term by the Q_{10} function). Earlier budburst and later senescence may also consequently increase frost damage (Redfern and Hendry, 2002). Furthermore, chemicals and gases tend to become more readily available at higher temperatures, with intercellular oxygen becoming more concentrated (von Caemmerer *et al.*, 1994).

Future predictions for lowland England suggest decreased precipitation and increased soil moisture deficit is likely during summer months (Hulme *et al.*, 2002), which may lead to increased plant water stress. In winter months the opposite may be true, leading to an increased risk of flooding, which could damage roots reducing their effectiveness and ability to cope with summer droughts (Redfern and Hendry, 2002). SRC is a high water demanding crop and is vulnerable to low water availability during the growing season (Finch *et al.*, 2004). Souch & Stephens (1998) showed that poplar genotypes in severe drought conditions produced 60-75 % less dry matter than those in the well-watered conditions. Moisture deficits in excess of 220–240 mm can cause moisture stress and stem crack (Ray, 2007). Water acts as a solvent for biochemical reactions and helps transport mineral nutrients through the plant. Water stress will cause wilting and a decrease in photosynthetic activity.

Making valid predictions on current and future growth of these crops is important to the development of these crops as sources of energy. To achieve this, a sound

understanding of the physiological basis to plant growth and development is required. This knowledge can then be applied to process-based models of crop growth.

The process-based model ForestGrowth-SRC was developed to simulate the physiological responses of poplar to coppicing and investigate the interactions between productivity and climatic conditions. Our objectives here were to accurately simulate and visualise the impacts of a changing climate on the productivity of short rotation coppice poplar. We use ForestGrowth-SRC and the UK Climate Projections for the 2020s, 2050s and 2080s, to demonstrate the potential impacts that future climates may have on SRC poplar.

5.2 Materials and Methods

5.2.1 ForestGrowth-SRC

ForestGrowth-SRC is a modular, fully coupled, daily timestep soil–vegetation–atmosphere transfer (SVAT) model designed to simulate the productivity of SRC poplar. The model was tested and validated against seven yield trials sites from the UK SRC national field trials network. Once a robust structure had been established the model was run for all 49 sites of the field trial network, using *Populus trichocarpa* genotype Trichobel as a test species. Trichobel was chosen as it is a typically high yielding variety, robust to pest and disease and supported by a significant amount of measured field data.

5.2.2 UK Climate Projections

To assess the impact of a changing climate on the growth of SRC poplar, ForestGrowth-SRC utilises the UK Climate Projections (Murphy *et al.*, 2009). These projections predict future climates under different emission scenarios, using the Met Office climate model.

Here we use the 'UK probabilistic projections of climate change over land' medium emissions scenario ("very rapid economic growth, low population growth and rapid introduction of new and more efficient technology" [SRES A1B]), absolute values (50 % probability). The temporal effect on growth is assessed over four time periods – the baseline period from 1991-2000 (the period of the field trials network), 2020s, 2050s and 2080s. The raw climatic data is available in monthly time-steps. However, this must be downscaled for use in ForestGrowth-SRC as the model uses daily time-step weather data to drive the physiological processes associated with growth. To downscale the more widely available monthly data to a daily time-step, ForestGrowth-SRC uses a weather generator (Evans *et al.*, 2004).

Instrumental monthly rainfall totals and wet day frequencies are input into a first-order two-state Markov chain (Richardson, 1981; Ross, 1983) to generate daily estimates of precipitation on a given rain day. The standard deviation around the observed mean, coupled to an auto-correlation intensity factor, is used to generate daily scale estimates of mean, maximum and minimum temperature, wind speed and relative humidity (Hutchinson, 1991). In the absence of values of standard deviation for the UK Climate

Projections we use the standard deviation from the baseline scenarios. Total, direct and diffuse solar radiation is approximated using spherical geometry, corrected for latitude, slope and aspect (Lui and Jordan, 1960; Klein, 1977). Inter-dependence between variables is outlined to adjust terrestrial solar radiation for cloudiness (Nikolov and Zeller, 1992); terrestrial radiation is used to develop temperature amplitude and solar beam atmospheric attenuation is approximated using a set of atmospheric turbidity factors (Iqbal, 1983).

Carbon dioxide is an important input for ForestGrowth-SRC as it drives the rate of RuBP and Rubisco limited photosynthesis and stomatal conductance. For the baseline scenario (1991-2000) the concentration of atmospheric carbon dioxide (CO_2) was assumed to be 363 parts per million (ppm). Atmospheric CO_2 under future climatic conditions (SRES A1B scenario) were predicted by the ISAM (Jain *et al.*, 1994) and BERN (Joos *et al.*, 1996) carbon cycle models – 419ppm (2020s), 527ppm (2050s) and 644ppm (2080s).

5.2.3 GIS scaling to UK scale

Above-ground biomass (odt ha^{-1} yr^{-1}) simulated by ForestGrowth-SRC was attributed to the co-ordinate data for each field trial site. Inverse distance weighting was then used on the 49 data points using Geographic Information Systems (GIS) software (ArcMap version 9.2, ESRI, Aylesbury, UK). This provided a simple spatially referenced map of UK poplar yield under baseline (1991-2000), 2020s, 2050s and 2080s climate scenarios.

5.3 Results

5.3.1 Elevated temperature

Each key climatic parameter was tested individually against yield for poplar genotypes Ghoy and Trichobel, using values from the 2050 medium emissions scenario (Alice Holt site). By changing one variable at a time and using baseline values for the other variables, we can assess individual parameters impact on model functions. Under elevated temperatures (2050 medium emissions scenario, all other variables remain unchanged) yields decreased at the Alice Holt site. Above-ground biomass production decreased by 19 % for genotype Ghoy (4.58 vs. 5.62 odt ha^{-1} yr^{-1}) and 17 % for Trichobel (6.85 vs. 8.29 odt ha^{-1} yr^{-1}) by year six (Figure 5.2). Elevated temperatures increase respiration (defined by the Q_{10} temperature coefficient).

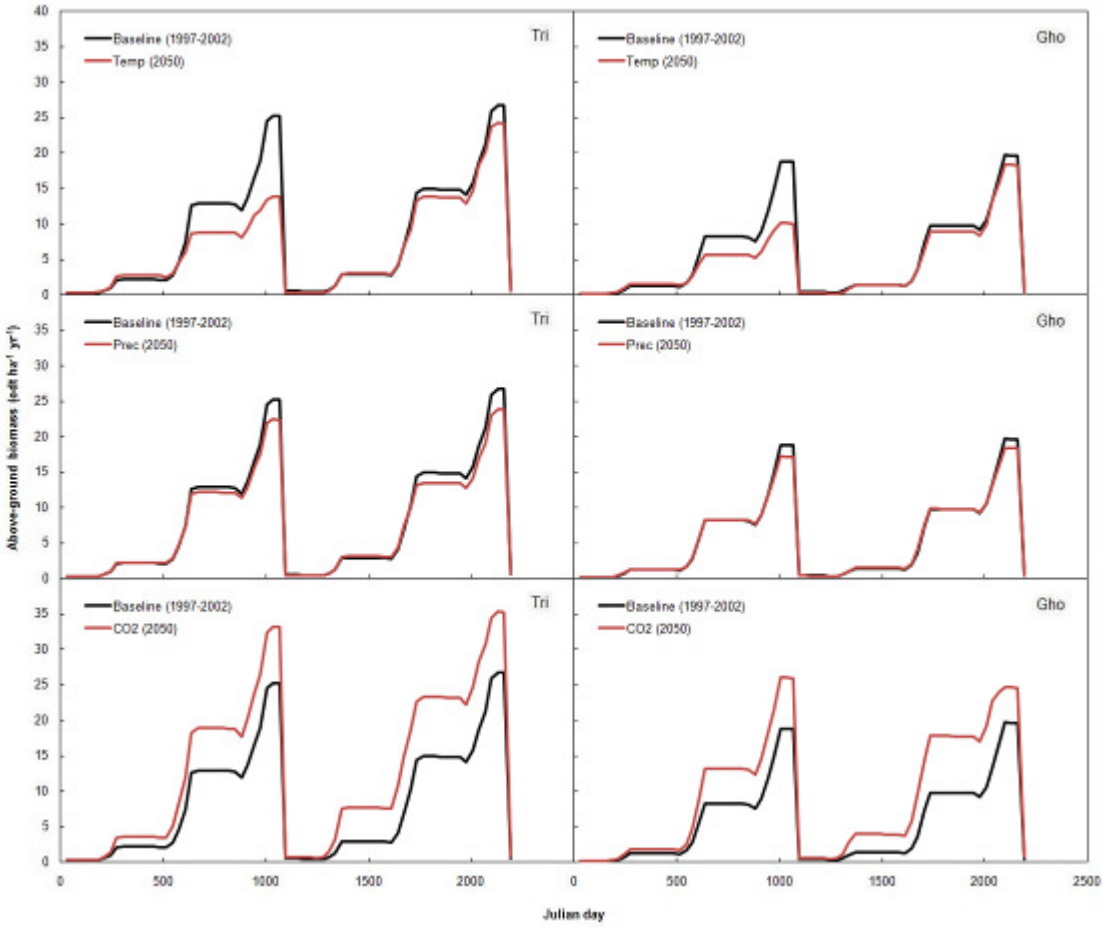

Figure 5.1. Interactions between above-ground biomass production and temperature, precipitation and CO_2 for poplar genotypes Trichobel (left) and Ghoy (right); baseline (1997-2002) vs. 2050 medium emissions scenarios.

5.3.2 Reduced precipitation

Poplar is a highly water dependant species and a decrease in precipitation can lead to a soil moisture deficit. At Alice Holt reduced precipitation in the summer resulted in a decline in above-ground biomass production. Yields (yr 6) of poplar genotype Ghoy decreased to 5.53 odt ha^{-1} yr^{-1} (-2 %, relative to the baseline) and for Trichobel decreased to 7.73 odt ha^{-1} yr^{-1} (-7 %) (Figure 5.1).

5.3.3 Elevated carbon dioxide

Elevated CO_2 had the biggest impact on plant growth of the three key factors considered here. By the end of the second coppice rotation elevated CO2 (527 ppm) increased above-ground biomass by 62 and 54 % compared to the baseline for genotypes Ghoy and Trichobel respectively (Figure 5.1); this equated to an additional 3.5 (Ghoy) and 4.5 odt $ha^{-1}yr^{-1}$ (Trichobel). Increased above-ground biomass accumulation was driven by higher rates of photosynthesis. Photosynthesis is increased as a result of greater leaf area expansion; *p*LAI = 8.43 vs. 7.10 (Trichobel) and 6.68 vs. 6.08 (Ghoy).

5.3.4 UK Climate Projections medium emissions scenario

In all scenarios above-ground biomass yields increased across the UK (Table 5.1). In general, yields by the end of the second rotation (yr 6) increase by 0.85 by 2020, 1.61 by 2050 and 2.02 odt ha^{-1} yr^{-1} by 2080, compared to the baseline (9.44 odt ha^{-1} yr^{-1}). Highest incremental increases were seen in years one and four (the first after coppicing). In general the greatest yield increases were on previously less productive sites (Figure 5.2), particularly in the colder northern areas of the UK.

Table 5.1. Percentage change in annual above-ground biomass in poplar genotype Trichobel, for 2020s, 2050s and 2080s medium emissions UK Climate Projections scenarios (compared to the baseline, 1997-2002).

	Above-ground biomass					
	Year 1	Year 2	Year 3	Year 4	Year 5	Year 6
2020s	+19	+11	+6	+34	+16	+9
2050s	+50	+25	+13	+71	+32	+17
2080s	+74	+37	+20	+97	+44	+21

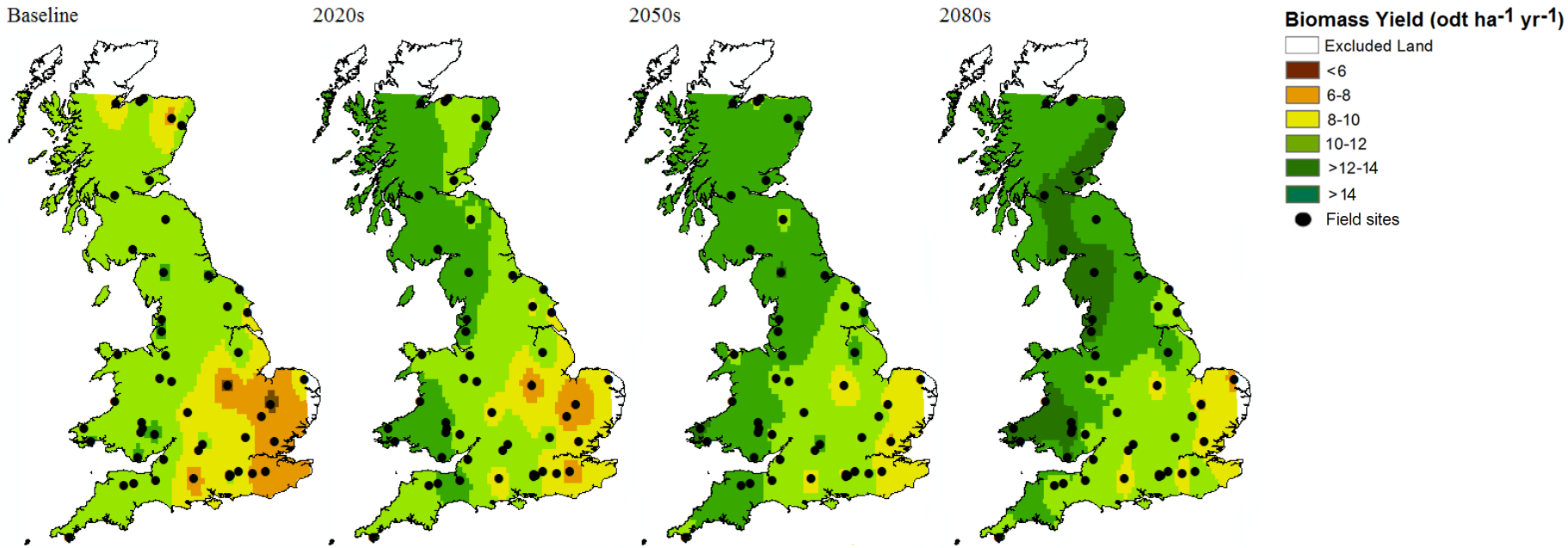

Figure 5.2. Estimated above-ground biomass yield for baseline (1997-2002), 2020s, 2050s and 2080s medium emissions climate scenarios (UK Climate Projections) for *P. trichocarpa* genotype Trichobel at Alice Holt. Black spots represent the distribution of sites used to construct the maps.

5.4. Discussion

Forests are highly sensitive to climate change and particularly to CO_2. A general increase in forest growth has been observed over the past 40 years (Cannell, 2002), which has been attributed to increased warmth, increased CO_2 concentrations and improved silviculture. In the future, changes to our climate are predicted to become more rapid (Hulme *et al.*, 2002). However, these predictions must be regarded with care as they are inherently uncertain (Murphy *et al.*, 2004; Stainforth *et al.*, 2005) and modelled plant responses to changing climates may accumulate compound errors in uncertainty. The net increase in biomass productivity predicted by ForestGrowth-SRC (+21 % in poplar genotype Trichobel by 2080) is in keeping with most process-based models that predict a net annual incremental increase in biomass growth (Sun *et al.*, 2000; Nabuurs *et al.*, 2002; Friend, 2010). Most of this stimulation relates to increased photosynthetic activity as a result of elevated CO_2.

Carbon dioxide

Poplar response to elevated CO_2 (excluding baseline changes to other variables) at the Alice Holt site was an estimated 54-62 % increase in above-ground biomass (yr 6), this is fairly high but within the range predicted by field trials (Kinney and Lindroth, 1997; Dickson *et al.*, 1998; Taylor *et al.*, 2001b). The effects of an increase in CO_2 on productivity and its implementation within the Farquhar *et al.* (1980) and Ball *et al.* (1987) models are fairly well understood, but its interactions with other factors are not (i.e. temperature and water-use efficiency). Furthermore, above to below-ground allocation ratios remain largely unchanged, as a result of the simple empirical allocation

relationships employed in the model. However, previous research has found more carbon allocation to below-ground pools under elevated CO_2 (Bosac *et al.*, 1995; Gielen *et al.*, 2005). Gielen *et al.* (2005) predicts below ground allocation could be up to 30 % higher in elevated CO_2.

Temperature

Temperature is known to have a significant role on photosynthetic activity and biomass productivity (Domingo and Gordon, 1974; Ciais *et al.*, 2005; Ow *et al.*, 2008), though has been described as a less significant determinant of photosynthesis than CO_2 (Tjoelker *et al.*, 1998). Poplar plants have been shown to thermally acclimate to higher temperatures within a given range (Turnbull *et al.*, 2002; Ow *et al.*, 2008), though this is not accounted for within the model. Increasing temperature increases respiration costs to the plant but conversely lengthens the growing season (predicted here to be between 3-5 days by 2050) in accordance with the findings of Menzel *et al.* (2006). ForestGrowth-SRC determines budburst using chilling and warming days. However, the threshold values for chilling and warming days and the mechanisms behind budburst are poorly understood.

Water

In parallel to the findings of the empirical model, water is again identified as a limiting factor to SRC poplar growth. The UK has a largely rain-fed agricultural system and its is unsurprising that low precipitation was identified as the principal limiting factor to crop yield and should be taken into account during site selection and for future breeding and improvement programmes. Poplar is known to have a particularly high uptake of

water (Souch and Stephens, 1998; Lindroth and Båth, 1999; Wikberg and Ogren, 2004). In the UK, water use from mature SRC during the summer months exceeds that of all other vegetation and on an annual basis is second only to coniferous forest – this is due to high transpiration and large interception losses as a result of large leaf areas (Hall, 2003b). In general, C_3 crops (e.g. poplar) are more sensitive to reduced water availability than C_4 crops (i.e. *Miscanthus* and switchgrass), due to their decreased water water-use efficiency compared (Finch *et al.*, 2004). ForestGrowth-SRC predicts that future reductions in water availability within the growing season are likely to decrease productivity and create a soil moisture deficit over the long term. This is a consequence of high evapotranspiration losses due to higher temperatures. However, the model does not account for adaptive plant responses (i.e. stomatal closure in *P. trichocarpa*). Furthermore, water use in ForestGrowth-SRC is not well described. Temporal integration is restricted to a daily time-step in order to use widely available meteorological data. The response of the evapotranspiration model is tightly coupled with the availability of water in the soil. The amount of water in the initial layer can be depleted by direct evaporation. If this layer is set too deep, then water-limitation problems may arise. In addition ForestGrowth has set rooting characteristics, which do not change with time or water availability. Future work on incorporating the results of the JULES model with ForestGrowth may help eliminate some of these issues.

Yield maps

Spatial interpolation is a means of converting point data into surface data. In this study we use inverse distance weighting interpolation to spatially estimate unknown yields from a series of known, modelled yields (Figure 5.2). Inverse distance weighting is

based on Tobler's first law of Geography, which states that "Everything is related to everything else, but near things are more related than distant things" (Tobler, 1970), i.e. we assume some degree of spatial autocorrelation between points.

Comparisons between different interpolation techniques suggest inverse distance weighting performs well when interpolating biological systems, particularly under conditions of high spatial autocorrelation (Gotway *et al.*, 1996; Dirks *et al.*, 1998; Lin *et al.*, 2002; Malhi *et al.*, 2006). Moran's I is a parametric test that can check data for autocorrelation in spatial data. Results from this study suggest the data has relatively high spatial autocorrelation (Table 5.2), which may make it suitable for inverse distance weighting interpolation.

Table 5.2. Moran I statistics calculated from annual above-ground biomass in poplar genotype Trichobel, second rotation, for baseline (2000s), and 2020s, 2050s and 2080s medium emissions UK Climate Projections scenarios.

	Moran I Index	z score (Standard Deviations)	p score (Probability)
2000s	0.43	8.41	0.01
2020s	0.41	8.02	0.01
2050s	0.38	7.63	0.01
2080s	0.35	6.85	0.01

However, the inverse distance weighting approach has a number of inherent disadvantages. For one, the estimated values are incapable of exceeding the value range of the sample data. As a result, inverse distance weighting may produce counter-intuitive results in areas of peaks and pits, and outside the area covered by the data points (Longley *et al.*, 2005). Consequently, we may fail to accurately calculate the full range of yields.

Such techniques are also sensitive to the positions of data points, particularly when the data points are very irregularly spaced, and spurious edge effects can be generated (Watson and Philip, 1985). This can lead to an insufficient representation of the desired surface. The best results from inverse distance weighting are obtained when sampling is sufficiently dense with regard to the local variation you are attempting to simulate (Watson and Philip, 1985; Dirks *et al.*, 1998; Chaplot *et al.*, 2006).

In addition, inverse distance weighting assumes that spatial autocorrelation changes uniformly in space (Lu and Wong, 2008). This is not always the case. Spatial autocorrelation is dependent on both the location and the variable being examined. For example, yields may change abruptly at the boundary of two soil types. The method also has no built-in method of testing for the quality of predictions so the map robustness can only be assessed by taking extra observations (Hutchinson, 1989).

Interpolation in this study uses 49 data points spread irregularly across the UK (Figure 5.2). As a result of this low density and sporadic coverage, caution is necessary when making conclusions based on these estimates and predictions should be seen as general trends rather than absolutes. Estimates will be less accurate the further away from the known data points. Furthermore, there is no masking of physical constraints (such as mountains). We can use polylines of physical constraints as barriers during interpolation. However, this requires careful consideration as a mountain may not necessarily be a significant barrier, for example, the size and scale of a mountain will influence its effect as a barrier.

Teegavarapu and Chandramouli (2005) suggest that in spite of the method's wide success and acceptability, inverse distance weighting suffers from major conceptual limitations compared to other methods. They suggest a modified distance-based method – coefficient of correlation weighting – which makes conceptual revisions to the inverse distance weighting approach to improve estimation of missing data (precipitation in their study), by defining better weighting parameters and surrogate measures for distances. The approach is particularly suitable if the spatial autocorrelation is strongly positive (Vasiliev, 1996), i.e. measured data points are strongly dependent on each other.

Another alternative is kriging; some studies have shown that the method offers superior weighting accuracy across a range of surfaces (Rouhani, 1996; Zimmerman *et al.*, 1999; Teegavarapu and Chandramouli, 2005; Palmer *et al.*, 2009; Zhang and Srinivasan, 2009), particularly at lower sampling densities. Kriging responds both to the proximity of sample points and to their directions, helping shield a point from influence if it lies beyond another point (Longley *et al.*, 2005).

Kriging is also not limited by the boundaries of the value range of the dataset. Thus, if a trend seems to be increasing towards the upper boundary of the value range, the trend will continue to rise. However, care is still needed to recognise areas of incorrect interpolation, including unrealistically high values and areas where no value should exist (such as yield on the top of a mountain).

Hu (1995) suggests kriging is an optimal interpolator in the sense that the estimates are unbiased and have known minimum variances. Since the estimation variances can be determined and mapped like the estimates, and assuming a particular distribution, we can calculate the confidence we can place in the estimates. This makes kriging uniquely different from other interpolation methods. The estimation variance can also be used to determine where more information is needed if future sampling is planned.

One weakness of kriging is that the original data points are seldom honoured (Longley *et al.*, 2005). Also kriging is the estimation of a semivariogram (a mathematical function used to quantify the dissimilarity between groups of points), and it is not always easy to ascertain whether a particular estimate of the semivariogram is in fact a true estimator of the spatial correlation in an area (Hu, 1995; Largueche, 2006). The reasons for choosing a particular semivariogram to fit the given data set are often difficult to explain in terms of physical processes, they can only be rationalized in terms of a least-squares on maximum likelihood fit to the data set (Hu, 1995; Largueche, 2006). Inverse distance weighting interpolation requires no semivariogram model-fitting, making it a simpler choice for users.

To determine the accuracy of the inverse distance weighting approach compared to an alternative interpolation method, we would need to compare a number of measured sites to those predicted by the interpolated values.

5.5 Conclusions

In the future temperate landscape, it is likely we will see an increase in value and production of these crops as feedstocks for heat, power and liquid transportation fuels. Early predictions using the ForestGrowth process model suggest C_3 bioenergy crop yields could increase by over 20 % in a future temperate UK landscape (2080 medium emissions scenario). Incremental annual increases in biomass production as a result of climate change decreased with age (Table 5.1). This suggests shorter rotations may be advantageous to some genotypes and in some areas in the future.

However, certain parameters are not accounted for within ForestGrowth-SRC, such as ozone. Rising tropospheric ozone may partially or fully offset increased future productivity (Isebrands *et al.*, 2001) and this should be incorporated in future model development. Furthermore, as plants grow and acclimate to new climates so too will pests and disease, potentially counteracting enhanced biomass production. Considering the limitations of the model caution is necessary in interpreting model predictions. However, in general ForestGrowth-SRC is a valuable tool for modelling climate change impacts and trends on the growth of SRC poplar in the UK. ForestGrowth-SRC could also be extended to other areas of the world, using existing climate change datasets (i.e. PRUDENCE for Europe and WORLDCLIM for the world).

Chapter 6 . General Discussion

6.1 Using SRC as a source of renewable energy

In 2008, total UK electricity supply was 400.7 TWh yr^{-1}, with nearly three quarters derived from non-renewable sources (46 % gas, 31 % coal and 1 % from oil) (DECC, 2009a). This figure of fossil fuel use is almost exactly what it was in 1990 (74.5 %), but in that year we were only producing 309.4 TWh of electricity. Furthermore, over 95 % of transport fuels are from non-renewable sources (RFA, 2008). Clearly we must do more if we are to reduce our reliance on fossil fuels and meet our GHG emissions targets. As part of a wider strategy to reduce emissions, dedicated energy crops have been identified as a valuable source of renewable energy for both electricity and transport fuel.

Both poplar and willow have a wide provenance, are fast growing and have significant potential to reduce our global dependence on non-renewable sources of energy for heat, power and transport fuel. However, their deployment is not devoid of conflict. Dedicated energy crops compete with food and ecosystem services for land and with other renewable energy sources for market share. An advantage of biomass energy crops over other renewables is that they can be stored for use when other renewables may suffer from intermittent supply. They also have been shown to perform well on marginal land, which could be exploited to minimise the conflict with food production and ecosystem services. Second-generation technology should also allow lignocellulosic plants, such as poplar and willow, to be used as liquid transportation fuels helping reduce conflicts with other land uses. However, the simplest and most efficient way to overcome these issues is to improve productivity.

The aim of this research was to identify the spatial and temporal variability in above-ground biomass production of poplar and willow varieties, grown in a short rotation coppice system. To achieve this, two different modelling approaches were employed to investigate the interactions between the environment and productivity, with a view to finding the key limiting factors to yield and the potential of these crops to fulfil UK renewable energy obligations, now and in the future. Results suggest poplar and willow can be grown across a wide range of climatic and soil conditions, and have the potential to become an important component of the UK government's renewable energy portfolio.

6.2 Modelling the potential supply of biomass from SRC

An empirical modelling technique, using partial least squares regression was developed to extrapolate actual field observations to a national scale. Genotype x age x environment interactions were studied to examine the key limiting factors to productivity. Modelled yields differed between genotypes, with mean annual above-ground biomass ranging from 4.9 to 10.7 oven dry tonnes (odt) per hectare for *Populus trichocarpa x P. deltoides* genotype 'Beaupré' and *Salix triandra* x *S. viminalis* genotype 'Q83', respectively. Variation in yield was primarily described by spring and summer precipitation, suggesting water availability is the key limiting factor to yield. Output from the model was up-scaled across the UK using a geographic information system (GIS) and scenarios were developed to better understand the role and impact of land use management and policy development on potential crop distribution. For

example, to meet UK biomass and biofuel targets without compromising food security or ecosystem services, would require 5 % of grade 3 land, 56 % grade 4 land and 47% of grade 5 land. This quantity of biomass would produce 7.5 M tonnes of biomass per annum and would theoretically generate 15.5 TWh yr^{-1} of electrical energy, displacing 3.3 M tonnes of oil – approximately 4% of current UK electricity demand. The South West and North West alone producing over a third of this figure (5.2 TWh yr^{-1}). These results suggest that SRC has the potential to become a significant component of a mixed portfolio of renewables. However, pests and disease were found to have a significant effect on SRC yields. Therefore, finding genotypes which are tolerant to pests and disease should be considered a vital component of future breeding programmes.

Furthermore in the future, genomic tools, such as Quantitative Trait Loci (QTL) mapping, should also enable the rapid deployment of plants with improved productivity (Taylor *et al.*, 2001a; Sims *et al.*, 2006). Rook (1991) suggested improved breeding could theoretically produce yields up to 30 odt ha^{-1} yr^{-1}. Production physiology has identified architectural traits associated with high poplar and willow biomass growth, including the production of large leaves, leaves with many small cells and late-season branching (Casella and Sinoquet, 2003; Rae *et al.*, 2004; Robinson *et al.*, 2004; Marron and Ceulemans, 2006). The availability of the full poplar DNA sequence should enable the identification of underlying genes that control these traits. Areas of the poplar genome determining yield have already been identified (Wullschleger *et al.*, 2005; Rae *et al.*, 2008), suggesting large-step improvements in yield are likely in the future.

Management regimes should also be considered, since increasing the plant spacing

within rows of coppice crops, such as poplar, is likely to increase their light interception efficiency, while increasing planting densities should benefit less productive ones because of their weak potential in canopy closure dynamic (Casella and Sinoquet, 2007). Planting genotypes with narrow leaves and small petioles may similarly increase productivity of high-density coppice poplar crop systems by improving light interception (Casella and Sinoquet, 2007).

6.3 Climate change impacts on the availability of SRC

Climate change is predicted to have far reaching consequences on crop growth and could further enhance yields. Elevated global CO_2 is predicted to lead to warmer conditions with less summer precipitation in the UK (Hulme *et al.*, 2002). Studies on climate change impacts on poplar productivity have suggested an atmosphere of elevated CO_2 could contribute to a rise in poplar yields of up to 27 % by 2050 (Calfapietra *et al.*, 2003). Temperature also plays a significant role on photosynthetic activity and biomass productivity (Domingo and Gordon, 1974; Ow *et al.*, 2008), though has been described as a less significant determinant of photosynthesis than CO_2 (Tjoelker *et al.*, 1998). Higher temperatures are expected to bring forward budburst and increase photosynthesis but may also increase autumnal frost damage, transpiration and respiration rates (Redfern and Hendry, 2002). Poplar and willow are also known to have a particularly high uptake of water (Souch and Stephens, 1998; Lindroth and Båth, 1999; Wikberg and Ogren, 2004). In the UK, water use from mature SRC during the summer months exceeds that of all other vegetation and on an annual basis is second only to coniferous forest – this is due to high transpiration and large interception losses

as a result of large leaf areas (Hall, 2003b). A predicted future reduction in water availability within the growing season is likely to decrease photosynthetic activity, although most species have developed adaptive responses (i.e. improved water use efficiency by stomatal closure in *P. trichocarpa*) (Cochard *et al.*, 1996).

Process-based models can help quantify these interactions and predict future productivity. We developed ForestGrowth, a process-based model designed for high-forest species and parameterise it for a coppice system. Climate change scenarios (UK Climate Projections) were run with the model to assess the impact of a changing climate on the availability and spatial distribution of SRC poplar. Results suggest ForestGrowth is capable of accurately simulating growth over a large spatial and temporal scale. In the absence of pests and disease, future productivity could be increased by 20 % (under a 2080 medium emissions scenario), suggesting we will see a future increase in the value and production of these crops as feedstocks for heat, power and liquid transportation fuels. However, certain parameters were not accounted for within ForestGrowth-SRC, such as ozone and pest and disease interactions with climate change. For example, rising tropospheric ozone may partially or fully offset increased future productivity (Isebrands *et al.*, 2001) and this should be incorporated in future model development. Future work could also see improved parameterisation of the budburst module, respiration relationships with crop age and within season carbon allocation mechanisms. Considering the limitations of the model caution is necessary in interpreting model predictions. However, in general ForestGrowth-SRC is a valuable tool for modelling climate change impacts and trends on the growth of SRC poplar in the UK. ForestGrowth-SRC could also be extended to other areas of the world, using existing

climate change datasets (i.e. PRUDENCE for Europe and WORLDCLIM for the world).

6.4 Empirical vs. Process modelling

Models are analytical tools for describing complex entities or processes, they are used to simulate the real world environment but are limited by the system boundaries they inhabit, and so may only serve as a best fit of reality. Models can be broadly split into two categories: empirical and process-based. Which approach is most appropriate for yield modelling remains a contentious issue (Korzukhin *et al.*, 1996; Doyle, 1998; Park *et al.*, 2005). Different models are designed for different purposes and caution is required in their implementation and when interpreting their results.

Therefore it is important to ask what are we trying to achieve and from results can we determine which method is most applicable in achieving this? In this study we use both empirical and process-based models to investigate the interactions between the physical environment and the productivity of poplar and willow short rotation coppice.

Empirical models offer a mathematical relationship between measured yield and abiotic factors. They can be undertaken without expert knowledge of plant-environment interactions and offer general trends or imply relationships. However, they have limited regard to an object's internal structure, rules or behaviour (Korzukhin *et al.*, 1996). They are neither intuitive nor likely to improve our understanding of the complex mechanisms underlying plant growth. Furthermore, empirical models should only be

extrapolated outside the range of the original measurements with caution, as linear or non-linear relationships may not be unilaterally replicated. Schwaber (2004) states that using a statistical sample (i.e. an empirical model) to summarise the operations of a complex process or series of complex processes will not yield a meaningful insight into their underlying structure, and attempts to create a sample can only be made by summarizing their operation to such a degree of coarseness that their effectiveness to understand or manage these processes is significantly reduced.

In comparison, process models are driven by plant processes, using our best understanding of the physiological basis to plant growth and development. They describe data using key mechanisms or processes that determine an object's internal structure, rules, and behaviour (Korzukhin *et al.*, 1996); allowing each variable to be controlled and cumulative responses to be assessed. However, process models are data intensive and require expert knowledge to use and parameterise.

Process-based models require knowledge-based calibrations which are often linked to allometric or empirical relationships. In fact, the majority of current process-based forest models used to predict the growth of poplar and willow, such as Sievanen (Sievanen, 1983) and ECOPHYS (Rauscher *et al.*, 1990) are based on empirical allometric relations and growth curves obtained from field experiments. Such relations do not necessarily hold when management practices change (Deckmyn *et al.*, 2004) and a more intuitive approach may be needed. This is an important aspect of what this study is trying to achieve.

Another aspect of this study is to find a general model that can be applied to a range of genotypes across the poplar and willow species, such is the speed at which new genotypes replace older varieties. Process-based models offer an immediate advantage in this respect. The mechanisms included in process-based models are often general enough that they can maintain some degree of relevance for new objects or conditions (mechanism constancy), while empirical models tend not to be tied to any specific mechanism, so that derived model parameters must remain constant (parameter constancy) for new objects or conditions (Korzukhin *et al.*, 1996).

Process-based models are often preferred over empirical ones in current modelling communities because they offer more complete and systematic approaches to identifying new management opportunities for improving production or quantifying responses to environmental change (Korzukhin *et al.*, 1996; Yaussy, 2000; Park *et al.*, 2005). Doyle (1998) suggests that when the underlying mechanisms by which a process operates are well understood then a process-based approach should be adopted. When the processes are too complex and poorly understood then the empirical approach is the appropriate choice. Similarly, Park *et al.* (2005) suggests that a well defined empirical model may offer a more reliable method of investigating crop response than a poorly calibrated process model. However, Park *et al.* goes further and suggests empirical crop growth models can play an important role in identifying the hidden structure of crop growth processes relating to a wide range of land management options.

Forest managers have been slow to adopt process-based models as a tool for decision making because they are seen as too complex and non-transferrable (Sands *et al.*, 2000;

Johnsen *et al.*, 2001). Empirical models use simpler and more readily available data and can provide more useful predictions to forest managers and it is suggested that this is a challenge process-based models must strive to address.

In this study we see the benefits and problems associated with both methodologies. The growth of poplar and willow are governed by complex interactions between plant and environment, making parameterisation challenging. For example, pests and disease are closely related to yield and while an empirical model will take account of this relationship statistically, a process model will require detailed information about how pests and disease affect the physiological growth processes within the leaf, stem and root. These relationships are complex and difficult to predict, particularly when considering attacks may be determined by the direction of the prevailing wind, small temperature fluctuations and proximity of crops to secondary hosts (Tabbush and Parfitt, 1999; Pei *et al.*, 1998, Tubby, 2005; Bayon *et al.*, 2009). There is also a wide spectrum of pests and disease affecting poplar and willow – each affecting growth in a different way. Currently there is little quantitative information available to accurately model these interactions.

It is valuable to compare the predictive ability of both approaches using the same sites and explore the reasons for any differences we may see between the different approaches. If we use the seven validation sites used in the process model and poplar genotype Trichobel as an example, we see that the empirical approach more accurately simulates yield (Table 6.1), a -2% percentage difference between he measured and the empirical model predictions compared to +18% for the process model.

Table 6.1. Comparison of measured yield (odt/ha/yr) vs. empirical and process model results for poplar genotype Trichobel, Alice Holt site. Results given at the end of the first and second rotation. The difference between the measured and modelled yield – expressed in odt/ha/yr and as a percentage – are given in the parenthesis.

Site	Year	Measured	Model	
			Empirical	Process
Alice Holt	1997-1999	6.51	7.70 (+1.19, +18%)	10.02 (+3.51, +54%)
	2000-2002	9.68	11.07 (+1.39, +14%)	10.18 (+0.50, +5%)
Balbirnie	1996-1998	12.36	10.66 (-1.70, -14%)	12.62 (+0.26, +2%)
	1999-2001	10.89	10.27 (-0.62, -6%)	10.37 (-0.52, -5%)
Loughall	1996-1998	5.91	5.04 (-0.87, -15%)	10.66 (+4.75, +80%)
	1999-2001	2.21	3.31 (+1.10, +50%)	11.90 (+9.69, +438%)
Loyton Bampton	1996-1998	8.06	8.21 (+0.15, +2%)	8.94 (+0.88, +11%)
	1999-2001	8.90	8.74 (-0.16, -2%)	9.83 (+0.93, +10%)
Thorpe Thewles	1996-1998	8.25	6.07 (-2.18, -26%)	7.92 (+0.33, +4%)
	1999-2001	9.58	9.47 (-0.11, -1%)	10.50 (+0.92, 10%)
Trefeinon	1996-1998	8.78	7.88 (-0.90, -10%)	9.02 (+0.24, +3%)
	1999-2001	9.60	10.22 (+0.62, +6%)	8.98 (-0.62, -6%)
Trumpington†	1996-1998	9.18	8.91 (-0.27, -3%)	8.66 (-0.52, -6%)
Total	-	8.45	8.27 (-0.18, -2%)	9.97 (+1.51, +18%)

† Results for Trumpington in the second rotation were not used because the empirical model yields were identified as outliers

Trichobel was affected by rust at all those sites considered here and particularly at Loughall. This may help explain the results we are seeing, as the process model takes no meaningful account of pest and disease damage. At Loughall the process model overestimated yield in the second rotation by 438% but at sites with less severe pests and disease damage, results were more comparable.

However, it is also important not to rule out other possible reasons for this difference, which could include microclimatic variation not accounted for by the coarser scale process-based approach, changes in carbon allocation not simulated by the process model, an artefact(s) picked up by the empirical model which does not represent a replicable effect or any of a number of more general calibration issues.

Further work is needed to compare the statistical accuracy of the models across a larger range of sites. This would require taking valid and complete soil profiles for a larger number of sites and running the process model for these. However, from this study we can conclude that both empirical and process-based models are important for a full and complete systems analysis of the complex plant-environment interactions in a short rotation coppice system. Empirical models may serve as useful tools for modelling and mapping current productivity, because they offer a simple, statistically valid approximation of reality. In addition, empirical functions continue to provide valuable information that drives process models. However, as we acquire more complete knowledge of how plants function and process models become simpler to use and understand the importance of empirical models may diminish in forest management. ForestGrowth-SRC offered a good fit of reality and proposes useful scenarios for future productivity changes in response to climate change. However, it failed to accurately simulate the effects of pest and disease.

6.5 Conclusions

Over the course of writing this thesis CO_2 levels in the atmosphere have risen by nearly 10ppm (NOAA, 2009) and it is important to adapt to the changes that will come in the future. Short rotation coppice poplar and willow have significant potential to help meet our renewable energy targets. Future breeding and improvement programmes, as well as climate change may increase this potential further.

We currently grow 15,500 ha of dedicated energy crops (i.e. SRC poplar, SRC willow

and *Miscanthus*) producing nearly 200,000 odt of biomass. However, dedicated energy crops account for less than 0. 1% of the UK's electricity production and most biofuels are derived from imported plant oils, with no second-generation lignocellulosic fuels. By 2020, 30 % of UK electricity must come from renewable sources and 10 % of UK fuel must be biofuel.

Results from this thesis suggest dedicated energy crops could be a valuable component of a mixed renewable energy portfolio. In the UK, 7.5 M t of biomass could potentially be available without compromising environmental, social or economic sustainability, which could be used to deliver up to 4 % of current electricity production. Climate change could expand this potential further, with yields up to 20 % higher under a 2050 medium emissions scenario. Therefore, climate change in combination with careful management, breeding and the development of advanced energy conversion technologies could deliver more bioenergy from the same area of land; reducing the conflict between food and fuel.

Chapter 7 . References

Abdi H. (2003) Partial Least Squares (PLS) Regression. In: Lewis-Beck M., Bryman A. and Futing T. (eds.) *Encyclopedia of Social Sciences Research Methods*. California, US: Thousand Oaks.

Aber J.D. and Federer C.A. (1992) A generalized, lumped-parameter model for photosynthesis, evapotranspiration and net primary production in temperate and boreal forest ecosystems. . *Oecologia* **92**: 463-474.

Acaroglu M. and Semi Aksoy A. (2005) The cultivation and energy balance of *Miscanthus* × *giganteus* production in Turkey. *Biomass and Bioenergy* **29**(1): 42-48.

Agriculture and Agri-Food Canada (2009) Considerations for Hybrid Poplar Production (Internet). Available from: http://www4.agr.gc.ca/AAFC-AAC/display-afficher.do?id=1192561823602&lang=eng. Accessed: 26 March 2009.

Ainsworth E.A. and Long S.P. (2005) What have we learned from 15 years of free-air CO_2 enrichment (FACE)? A meta-analytic review of the responses of photosynthesis, canopy properties and plant production to rising CO_2. *New Phytologist* **165**(2): 351-372.

Al Afas N., Pellis A., Niinemets Ü., *et al.* (2005) Growth and production of a short rotation coppice culture of poplar. II. Clonal and year-to-year differences in leaf and petiole characteristics and stand leaf area index. *Biomass and Bioenergy* **28**(6): 536-547.

Andersen R.S., Towers W. and Smith P. (2005) Assessing the potential for biomass energy to contribute to Scotland's renewable energy needs. *Biomass & Bioenergy* **29**: 73-82.

Armstrong A. (1997) *The United Kingdom network of experiments on site/yield relationships for short rotation coppice. Research Information Note 294.* Edinburgh, UK: Forestry Commission.

Armstrong A. (2003) *Research Information Note 294: The United Kingdom network of experiments on site/yield relationships for short rotation coppice.* Edinburgh, UK: Forest Research.

Armstrong A., Houston T., Matthews R., *et al.* (1998) Yield Models For Energy Coppice Of Poplar And Willow Phase II May 1996-April 1998. Edinburgh, UK: Forest Research.

Armstrong A.F., Logan D.C. and Atkin O.K. (2006) On the developmental dependence of leaf respiration: responses to short- and long-term changes in growth temperature. *American Journal of Botany* **93**: 1633-1639.

Aronsson P. and Perttu K. (2001) Willow vegetation filters for wastewater treatment and soil remediation combined with biomass production. *Forestry Chronicle* **77**(2): 293-299.

Atkin O.K., Holly C. and Ball M.C. (2000) Acclimation of snowgum (*Eucalyptus pauciflora*) leaf respiration to seasonal and diurnal variations in temperature, the importance of changes in the capacity and temperature sensitivity of respiration. *Plant, Cell & Environment* **23**: 15-26.

Avery B.W. (1980) *Soil Classification for England and Wales: Higher Categories,* Harpenden, UK: Rothamsted Research.

Aylott M.J., Casella E., Tubby I., *et al.* (2008) Yield and spatial supply of bioenergy poplar and willow short-rotation coppice in the UK. *New Phytologist* **178**(2): 358-370.

Ball J.T., Woodrow I.E. and Berry J.A. (1987) A model predicting stomatal conductance and its contribution to the control of photosynthesis under different environmental conditions. In: Biggins J. and Nijhoff M. (eds.) *Progress in photosynthesis research, vol.4.* Dordrecht, The Netherlands.

Barigah T., Saugier B., Mousseau M., *et al.* (1994) Photosynthesis, leaf area and productivity of five poplar clones during their establishment year. *Annales de*

Science Forestiere **51**: 613-25.

Bateman I.J. and Lovett A.A. (1998) Using geographical information systems (GIS) and large area databases to predict Yield Class: a study of Sitka spruce in Wales. *Forestry* **71**(2): 147-168.

Battaglia M. and Sands P.J. (1998) Process-based forest productivity models and their application in forest management. *Forest Ecology and Management* **102**(1): 13-32.

Bayon C., Pei M.H., Ruiz C., Hunter T., Karp A. and Tubby I. (2009). Genetic structure and population dynamics of a heteroecious plant pathogen *Melampsora larici-epitea* in Short Rotation Coppice. *Molecular Ecology* **18**(14): 3006-3019.

Beadle C., Ludlow M. and Honeysett J. (1993) Water Relations. In: Hall D., Scurlock J., Bolhar-Nordenkampf H., Leegood R. and Long S. (eds.) *Photosynthesis and Production in a Changing Environment: a field and labratory manual.* London: Chapman and Hall.

Beatty J. (1980) Optimality-Design and the Strategy of Model-Building in Evolutionary Biology. *Philosophy of Science* **47**.

Bell S. and McIntosh E. (2001) *Guideline Note 002: Short Rotation Coppice in the Landscape.* Edinburgh, UK: Forestry Commission.

Berndes G., Hoogwijk M. and Broek R.v.d. (2003) The contribution of biomass in the future global energy supply: a review of 17 studies. *Biomass and Bioenergy* **25**(1): 1-28.

BERR (2007) Meeting the Energy Challenge: A White Paper on Energy. London, UK: The Department for Business, Enterprise & Regulatory Reform.

BERR (2008) *The Digest of UK Energy Statistics 2008.* London, UK: The Department for Business, Enterprise & Regulatory Reform.

Berry J. and Bjorkman O. (1980) Photosynthetic Response and Adaptation to Temperature in Higher Plants. *Annual Review of Plant Physiology* **31**(1): 491-543.

Bortier K., De Temmerman L. and Ceulemans R. (2000) Effects of ozone exposure in open-top chambers on poplar (Populus nigra) and beech (Fagus sylvatica): a comparison. *Environmental Pollution* **109**(3): 509-516.

Bosac C., Gardner S., Taylor G.*, et al.* (1995) Elevated CO_2 and hybrid poplar: a detailed investigation of root and shoot growth and physiology of *Populus euramericana*, Primo. *Forest Ecology and Management* **74**(1-3): 103-116.

Bradbury N., Whitmore A., Hart P.*, et al.* (1993) Modelling the fate of nitrogen in crop and soil in the years following application of ^{15}N-labelled fertilizer to winter wheat. *Journal of Agricultural Science* **121**: 363-379.

Brewer C.A. (1994) Chapter 7: Colour Use Guidelines for Mapping and Visualisation. In: MacEachren A. and D.Taylor (eds.) *Visualisation in Modern Cartography.* Amsterdam, The Netherlands: Elsevier Science.

Britt C., Bullard M., Hickman G.*, et al.* (2002) Bioenergy Crops and Bioremediation - A Review (Final Report). In: Britt C. and Garstang J. (eds.). A Contract Report by ADAS for Defra.

BSI (1995) *Determination of pH. British Standard BS7755; ISO 10390 1994; Soil Quality, Part 3, Chemical methods, Section 3.2. ,* London, UK: British Standards Institution.

Bullard M. and Metcalfe P. (2001) Estimating the energy requirements and CO_2 emission from production of the perennial grasses Miscanthus, switchgrass and reed canary grass. ADAS Consulting Ltd.

Calfapietra C., Gielen B., Galema A.N.J.*, et al.* (2003) Free-air CO_2 enrichment (FACE) enhances biomass production in a short-rotation poplar plantation. *Tree Physiology* **23**: 805-814.

Cannell M.G.R. (2002) Impacts of climate change on forest growth. In: Broadmeadow M. (ed.) *Climate change: impacts on UK forests. Forestry Commission Bulletin 125.* Edinburgh, UK: Forestry Commission.

Cannell M.G.R. (2003) Carbon sequestration and biomass energy offset: theoretical, potential and achievable capacities globally, in Europe and the UK. *Biomass & Bioenergy* **24**(3): 97-116.

Cannell M.G.R., Sheppard L.J. and Milne R. (1988) Light Use Efficiency and Woody Biomass Production of Poplar and Willow. *Forestry* **61**(2): 125-136.

Casella E. and Ceulemans R. (2002) Spatial distribution of leaf morphological and physiological characteristics in relation to local radiation regime within the canopies of 3-year-old *Populus* clones in coppice culture. *Tree Physiology* **22**: 1277-1288.

Casella E. and Sinoquet H. (2003) A method for describing the canopy architecture of coppice poplar with allometric relationships. *Tree Physiology* **23**: 1153-1170.

Casella E. and Sinoquet H. (2007) Botanical determinants of foliage clumping and light interception in two-year-old coppice poplar canopies: assessment from 3-D plant mock-ups. *Annals of Forest Science* **64**: 395-404.

Ceulemans R. and Isebrands J.G. (1996) Chapter 15. Carbon acquisition and allocation. In: R. F. Stettler, H.D. Bradshaw Jr., P.E. Heilman and T.M. Hinckley (eds.) *Biology of Populus and its implications for management and conservation. Part II.* Ottawa, ON, Canada: National Research Council of Canada Research Press.

Ceulemans R., McDonald A.J.S. and Pereira J.S. (1996) A comparison among eucalypt, poplar and willow characteristics with particular reference to a coppice, growth-modelling approach. *Biomass and Bioenergy* **11**(2-3): 215-231.

Chaplot V., Darboux F., Bourennane H., *et al.* (2006) Accuracy of interpolation techniques for the derivation of digital elevation models in relation to landform types and data density. *Geomorphology* **77**(1-2): 126-141.

Christersson L. (2006) Biomass production of intensively grown poplars in the southernmost part of Sweden: Observations of characters, traits and growth

potential. *Biomass and Bioenergy* **30**(6): 497-508.

Ciais P., Reichstein M., Viovy N., *et al.* (2005) Europe-wide reduction in primary productivity caused by the heat and drought in 2003. *Nature* **437**(7058): 529-533.

Clifford P., Richardson S. and Hemon D. (1989) Assessing the significance of the correlation between two spatial processes. *Biometrics* **45**: 123-134.

Cochard H. (1992) Vulnerability of several conifers to air embolism. *Tree Physiology* **11**: 73-83.

Cochard H., Casella E. and Mencuccini M. (2007) Xylem vulnerability to cavitation varies among poplar and willow clones and correlates negatively with yield. *Tree Physiology* **27**: 1761-1767.

Cochard H., Ridolfi M. and Dreyer E. (1996) Responses to Water Stress in an ABA-Unresponsive Hybrid Poplar (*Populus koreana x trichocarpa* cv. Peace). II. Hydraulic Properties and Xylem Embolism. *New Phytologist* **134**(3): 455-461.

Coleman M., Dickson R. and Isebrands J. (2000) Contrasting fine-root production, survival and soil CO_2 efflux in pine and poplar plantations. *Plant and Soil* **225**(1): 129-139.

Coleman M.D., Dickson R.E., Isebrands J.G., *et al.* (1995a) Carbon allocation and partitioning in aspen clones varying in sensitivity to tropospheric ozone. *Tree Physiol* **15**(9): 593-604.

Coleman M.D., Isebrands J.G., Dickson R.E., *et al.* (1995b) Photosynthetic productivity of aspen clones varying in sensitivity to tropospheric ozone. *Tree Physiol* **15**(9): 585-592.

Constable J.V.H. and Retzlaff W.A. (2000) Asymmetric day/night temperature elevation: Growth implications for yellow-poplar and loblolly pine using simulation modelling. *Forest Science* **46**(2): 248-257.

Cranfield University (2006) NATMAPvector. National Soil Resources Institute.

Cunningham M.D., Bishop J.D., McKay H.V., *et al.* (2004) *ARBRE monitoring:*

Ecology of short rotation coppice

de Pury D.G.G. and Farquhar G.D. (1997) Simple scaling of photosynthesis from leaves to canopies without the errors of big-leaf models. *Plant, Cell and Environment* **20**: 537-557.

DECC (2009a) *The Digest of UK Energy Statistics 2009.* London, UK: The Department of Energy & Climate Change.

DECC (2009b) *The UK Renewable Energy Strategy 2009.* London, UK: The Department of Energy & Climate Change, HM Government.

Deckmyn G., Evans S.P. and Randle T.J. (2006) Refined pipe theory for mechanistic modeling of wood development. *Tree Physiology* **26**: 703-717.

Deckmyn G., Laureysens I., Garcia J., *et al.* (2004) Poplar growth and yield in short rotation coppice: model simulations using the process model SECRETS. *Biomass and Bioenergy* **26**(3): 221-227.

Defra (2004) *Growing Short Rotation Coppice: Best Practice Guidelines - For Applicants to Defra's Energy Crop Scheme,* London, UK: Department for Environment, Food and Rural Affairs.

Defra (2005) *Agriculture in the United Kingdom 2005.* London, UK: The Stationery Office.

Defra (2006) e-Digest Statistics - Land by agricultural and other uses: 2005, United Kingdom (Internet). Available from: http://www.defra.gov.uk/evidence/statistics/environment/land/download/xls/ldtb01.xls. Accessed: 1st July 2007.

Defra (2007a) *The Rural Development Programme for England 2007 – 2013.* London, UK: Department for Environment, Food and Rural Affairs.

Defra (2007b) *Securing a healthy natural environment: An action plan for embedding an ecosystems approach.* London, UK: Department for Environment, Food and Rural Affairs.

Defra (2008a) *Act on CO_2 Calculator: Data, Methodology and Assumption paper.* London, UK: Department for Environment, Food and Rural Affairs.

DEFRA (2008b) Opportunities and optimum sitings for for energy crops (Internet). Available from: http://www.defra.gov.uk/foodfarm/growing/crops/industrial/energy/opportunities/index.htm. Accessed: 01-10-2009.

Defra (2009) *Agriculture in the United Kingdom 2009.* London, UK: The Stationery Office.

DEFRA & DTI (2006) *The Government's Response to the Biomass Task Force Report.* London, UK: Department for Environment, Food and Rural Affairs.

Demirbaş A. (2004) Bioenergy, Global Warming, and Environmental Impacts. *Energy Sources* **26**(3): 225-236.

Desrochers A., Landhausser S.M. and Lieffers V.J. (2002) Coarse and fine root respiration in aspen (*Populus tremuloides*). **22**: 725-732.

Dickson R.E., Coleman M.D., Riemenschneider D.E., *et al.* (1998) Growth of five hybrid poplar genotypes exposed to interacting elevated CO_2 and O_3. *Canadian Journal of Forest Research* **28**: 1706-1716.

Dickson R.E., Lewin K.F., Isebrands J.G., *et al.* (2000) Forest atmosphere carbon transfer and storage (FACTS-II) the Aspen Free-air CO_2 and O_3 Enrichment (FACE) project: an overview. US Dept. of Agriculture, Forest Service.

Diniz-Filho J.A.F., Bini L.M. and Hawkins B.A. (2003) Spatial autocorrelation and red herrings in geographical ecology. *Global Ecology and Biogeography* **12**(1): 53-64.

Dirks K., Hay J., Stow C., *et al.* (1998) High-resolution studies of rainfall on Norfolk Island:: Part II: Interpolation of rainfall data. *Journal of Hydrology* **208**(3-4): 187-193.

Domac J., Richards K. and Risovic S. (2005) Socio-economic drivers in

implementing bioenergy projects. *Biomass and Bioenergy* **28**(2): 97-106.

Domingo I. and Gordon J. (1974) Physiological Responses of an Aspen-Poplar Hybrid to Air Temperature and Soil Moisture. *Botanical Gazette* **135**(3): 184-192.

Doncaster C.P. and Davey A.J.H. (2007) *Analysis of Variance and Covariance: How to Choose and Construct Models for the Life Sciences,* Cambridge, UK: Cambridge University Press.

Dormann C.F. (2007) Effects of incorporating spatial autocorrelation into the analysis of species distribution data. *Global Ecology and Biogeography* **16**(2): 129-138.

Doyle F.J. (1998) Process dynamics, modelling, and control. By B. A. Ogunnaike and W. H. Ray, Oxford University Press, New York, 1994, 1,260 pp. *AIChE Journal* **44**(5): 1232-1232.

Drax Power Limited (2008) Environmental Performance Review 2008.

DTI (2000) *Assessment of the Visual Impacts of SRC Plantations.* London, UK: Fawcett and Fawcett.

DTI (2003a) Carbon and energy balances for a range of biofuel options. In: Elsayed M., Matthews R. and Mortimer N. (eds.).

DTI (2003b) *Energy from Biofuels. DTI Sustainable Energy Technology Route Map.* London, UK.

DTI (2004) *Renewable Supply Chain Gap Analysis: Summary Report.* London, UK.

DTI (2007) *UK Biomass Strategy 2007: Working Paper 1 – Economic analysis of biomass energy.* London, UK: Department for Trade and Industry.

DTI and Carbon Trust (2004) *Renewables Innovation Review.* London, UK: Department for Trade and Industry.

DTI and Defra (2007) *UK Biomass Strategy.* London, UK: Department for Trade and Industry.

Eckersten H. (1991) *Simulation model for growth and nitrogen dynamics in short rotation forests. Report 163.,* Uppsala, Sweden: Swedish University of

Agricultural Sciences.

ECOTEC (1999) The impact of renewables on employment and economic growth. Brussels, Belgium: Directorate General for Energy, European Commission.

Edwards R., Larivé J.-F., Mahieu V.*, et al.* (2008) Well-to-wheels analysis of future automotive fuels and powertrains in the European context, version 3. Well-to-Wheels analysis of future automotive fuels and powertrains in the European context, WELL-TO-TANK Report Version 3.0. Appendix 2 v30. Description and detailed energy and GHG balance of individual pathways. Brussels, Belgium: EU Commission Joint Research Centre.

EEA (2006) How much bioenergy can Europe produce without harming the environment? Copenhagen, Denmark: European Environment Agency.

El Bassam N. (1998) *Energy Plant Species: their use and impact on environment and development,* London, UK: James and James.

Elobeid A. and Hart C. (2007) Ethanol Expansion in the Food versus Fuel Debate: How Will Developing Countries Fare? *Journal of Agricultural & Food Industrial Organization* **5**(2).

Erickson J., Stanosz G. and Kruger E. (2004) Photosynthetic consequences of *Massonina* leaf spot differ between two poplar hybrids. *New Phytologist* **161**: 577-583.

European Commission (2000) *Directive 2000/60/EC of the European Parliament and of the Council of 23 October 2000 establishing a framework for Community action in the field of water policy.* Brussels, Belgium: European Commission.

European Commission (2005) *Biomass Action Plan.* Brussels, Belgium: European Commission.

European Commission (2007) *Renewable Energy Road Map. Renewable energies in the 21st century: building a more sustainable future, COM(2006) 848 final {SEC(2006) 1719}, {SEC(2006) 1720}, {SEC(2007) 12}*. Brussels, Belgium:

European Commission.

European Commission (2008) *The European Union's Biodiversity Action Plan: Halting the loss of biodiversity by 2010 - and beyond - Sustaining ecosystem services for human well-being.* Brussels, Belgium: European Commission.

European Commission (2009) *Directive 2009/28/EC of the European Parliament and of the Council of 23 April 2009 on the promotion of the use of energy from renewable sources and amending and subsequently repealing Directives 2001/77/EC and 2003/30/EC.* Brussels, Belgium: European Commission.

Evans S.P., Mayr T.R., Hollis J.M., *et al.* (1999) SWBCM: a soil water balance capacity model for environmental applications in the UK. *Ecological Modelling* **121**: 17-49.

Evans S.P., Randle T., Henshall P., *et al.* (2004) Recent advances in mechanistic modelling of forest stands and catchments, Forest Research Annual Report 2003-2004. Edinburgh, UK: Forest Research.

Evans S.P., Tubby I., Straw N., *et al.* (2002) Yield Models for Short Rotation Coppice of Poplar and Willow. Edinburgh, UK: Forest Research.

Falge E., Graber W., Siegwolf R., *et al.* (1996) A model of the gas exchange response of *Picea abies* to habitat conditions. *Trees* **10**: 277-287.

Fang S., Xue J. and Tang L. (2007) Biomass production and carbon sequestration potential in poplar plantations with different management patterns. *Journal of Environmental Management* **85**(3): 672-679.

Fargione J., Hill J., Tilman D., *et al.* (2008) Land Clearing and the Biofuel Carbon Debt. *Science* **319**(5867): 1235-1238.

Farming Online Ltd. (2009) LIFFE Wheat Futures: May 2011 (Internet). Available from: http://www.liffe-commodities.com/. Accessed: 5 April 2009.

Farquhar G.D., Caemmerer S.v. and Berry J.A. (1980) A biochemical model of photosynthetic CO_2 assimilation in leaves of C3 species. *Planta* **149**: 78-90.

Felzer B.S., Reilly J.M., Melillo J.M., *et al.* (2004) Past and Future Effects of Ozone on Net Primary Production and Carbon Sequestration using a Global Biogeochemical Model. MIT Joint Program on the Science and Policy of Global Change.

Finch J.W., Hall R.L., Rosier P.T.W., *et al.* (2004) *The hydrological impacts of energy crop production in the UK*. London.

Forest Research (2003) Yield Models for Energy Coppice of Poplar and Willow: Field Trial Details (Internet). Available from: http://www.forestry.gov.uk/pdf/src_fieldtrialdetails.pdf/$FILE/src_fieldtrialdetails.pdf. Accessed: 5 April 2009.

Foulger A.N., Vimmerstedt J.P. and Eichar C. (1975) Stem Anatomy of 30-Year-Old Yellow-Poplar. *Forest Science* **21**: 23-33.

Friend A.D. (2010) Terrestrial plant production and climate change. *J. Exp. Bot.* **61**(5): 1293-1309.

Friend A.L., Scarascia-Mugnozza G., Isebrands J.G., *et al.* (1991) Quantification of two-year-old hybrid poplar root systems: morphology, biomass, and 14C distribution. **8**: 109-119.

Gallagher E. (2008) *The Gallagher Review of the indirect effects of biofuels production.* St Leonards-on-Sea, UK: Renewable Fuels Agency.

Gansert D. and Sprick W. (1998) Storage and mobilization of nonstructural carbohydrates and biomass development of beech seedlings (*Fagus sylvatica L*.) under different light regimes. *Trees - Structure and Function* **12**(5): 247-257.

Gash J.H.C., Lloyd C.R. and Lachaud G. (1995) Estimating sparse forest rainfall interception with an analytical model. *Journal of Hydrology* **170**: 79-86.

Gee G.W. and Bauder J.W. (1986) Particle-size analysis. In: Klute A. (ed.) *Methods of Soil Analysis, Part 1, Physical and Mineralogical Methods, 2nd edition.* Wisconsin, US: American Society of Agronomy.

Gielen B., Calfapietra C., Lukac M., *et al.* (2005) Net carbon storage in a poplar plantation (POPFACE) after three years of free-air CO_2 enrichment. **25**: 1399-1408.

Gielen B. and Ceulemans R. (2001) The likely impact of rising atmospheric CO_2 on natural and managed *Populus*: a literature review. *Environmental Pollution* **115**: 335-358.

Gielen B., Scarascia-Mugnozza G. and Ceulemans R. (2003) Stem respiration of Populus species in the third year of free-air CO_2 enrichment. *Physiologia Plantarum* **117**(4): 500-507.

Gigler J., Sims R. and Adams J. (2001) *Small scale biomass fired electricity production systems - present and future,* Palmerston North, New Zealand: Centre for Energy Research, Massey University.

Gong J.-R., Zhang X.-S., Huang Y.-M., *et al.* (2007) The effects of flooding on several hybrid poplar clones in Northern China. *Agroforestry Systems* **69**(1): 77-88.

Goodchild M.F. (1986) *Spatial Autocorrelation,* Norwich, UK: Geo Books.

Gotway C., Ferguson R., Hergert G., *et al.* (1996) Comparison of kriging and inverse-distance methods for mapping soil parameters. *Soil Science Society of America Journal* **60**(4): 1237-1247.

Gower S.T., McMurtrie R.E. and Murty D. (1996) Aboveground net primary production decline with stand age: potential causes. *Trends in Ecology & Evolution* **11**(9): 378-382.

Griffin K.L., Turnbull M. and Murthy R. (2002) Canopy position affects the temperature response of leaf respiration in Populus deltoides. *New Phytologist* **154**: 609-619.

Griffith D.A. and Layne L.J. (1999) *A casebook for spatial statistical analyses: a compilation of analyses of different thematic data sets.,* Oxford, UK: Oxford

University Press.

Guo L. and Gifford R. (2002) Soil carbon stocks and land use change: a meta analysis. *Global Change Biology* **8**: 345-360.

Guo X., Zhang X. and Huang Z. (2010) Drought tolerance in three hybrid poplar clones submitted to different watering regimes. *J Plant Ecol*: rtq007.

Hacke U. and Sauter J.J. (1996) Drought-Induced Xylem Dysfunction in Petioles, Branches, and Roots of Populus balsamifera L. and Alnus glutinosa (L.) Gaertn. *Plant Physiol.* **111**(2): 413-417.

Hall D., Reeve M., Thomasson A., *et al.* (1977) *Water retention, porosity and density of field soils. Soil Survey Technical Monograph 9.* Harpenden, UK: Rothamsted Research.

Hall R.L. (2003a) *Grasses for Energy Production: Hydrological Guidelines.* London, UK: Department for Trade and Industry.

Hall R.L. (2003b) *Short Rotation Coppice for Energy Production: Hydrological Guidelines.* London, UK: Department for Trade and Industry.

Hall R.L. and Allen S.J. (1997) Water use of poplar clones grown as short-rotation coppice at two sites in the United Kingdom. *Aspects of Applied Biology* **49**: 163-172.

Hall R.L., Allen S.J., Rosier P.T.W., *et al.* (1998) Transpiration from coppiced poplar and willow measured using sap-flow methods. *Agricultural and Forest Meteorology* **90**(4): 275-290.

Hansen E. (1991) Poplar woody biomass yields: a look to the future. *Biomass & Bioenergy* **1**: 1-7.

Hansen J.W. and Indeje M. (2004) Linking dynamic seasonal climate forecasts with crop simulation for maize yield prediction in semi-arid Kenya. *Agricultural and Forest Meteorology* **125**(1-2): 143-157.

Harvey H.P. and van den Driessche R. (1997) Nutrition, xylem cavitation and

drought resistance in hybrid poplar. *Tree Physiol* **17**(10): 647-654.

Haughton A.J., Bond A.J., Lovett A.A.*, et al.* (2009) A novel, integrated approach to assessing social, economic and environmental implications of changing rural land-use: a case study of perennial biomass crops. *Journal of Applied Ecology* **46**: 315-322.

Headey D. and Fan S. (2008) Anatomy of a crisis: the causes and consequences of surging food prices. *Agricultural Economics* **39**(s1): 375-391.

Hill J., Nelson E., Tilman D.*, et al.* (2006) Environmental, economic, and energetic costs and benefits of biodiesel and ethanol biofuels. *Proceedings of the National Academy of Science of the United States of America* **103**(30): 11206-11210

Hoosbeek M.R., Lukac M., Van Dam D.*, et al.* (2004) More new carbon in the mineral soil of a poplar plantation under Free Air Carbon Enrichment (POPFACE): cause of increased priming effect? *Global Biogeochemical Cycles* **18**(1): 1-7.

Houghton J. (2006) *Breaking the biological barriers for cellulosic: a joint research agenda.* Rockville, MD, USA: US Department of Energy.

Hu J. (1995) Methods of generating surfaces in environmental GIS applications. *Esri International User Conference.*

Hulme M., Jenkins G.J., Lu X.*, et al.* (2002) Climate Change Scenarios for the United Kingdom: The UKCIP02 Scientific Report. Norwich, UK: Tyndall Centre for Climate Change Research.

Hutchinson M.F. (1989) A new procedure for gridding elevation and stream line data with automatic removal of spurious pits. *Journal of Hydrology* **106**(3-4): 211-232.

Hutchinson M.F. (1991) *Climatic analysis in data sparse regions. Climatic risk in crop production: models and measurement for the semiarid tropics and arid subtropics,* Wallingford, UK: CAB International.

IEA (2007) *Good Practice Guidelines: Bioenergy Project Development & Biomass*

Supply. Paris, France: International Energy Agency.

IMF (2010) Indices of Primary Commodity Prices, 1998 - current (in terms of U.S. dollars). International Monetary Fund.

Inderwildi O. and King D. (2009) Quo vadis biofuels? *Energy & Environmental Science* **2**: 343-346.

Iqbal M. (1983) *An introduction to solar radiation,* Toronto, CA: Academic Press.

Isebrands J.G., McDonald E.P., Kruger E., *et al.* (2001) Growth responses of *Populus tremuloides* clones to interacting elevated carbon dioxide and tropospheric ozone. *Environmental Pollution* **115**(3): 359-371.

Jain A.K., Kheshgi H.S. and Wuebbles D.J. (1994) Integrated Science Model for Assessment of Climate Change. *Air and Waste Management Association's 87th Annual Meeting.* Cincinnati, Ohio: June 19-24

Jobling J. (1990) Poplars for Wood: Production and Amenity. Forestry Commission Bulletin 92. London, UK: Office of Public Sector Information.

Johnsen K., Samuelson L., Teskey R., *et al.* (2001) Process Models as Tools in Forestry Research and Management. *Forest Science* **47**: 2-8.

Jones M.B. (2007) *Verification of the calculations, methodology and costings used in determining proposed establishment grant payments under the Energy Crops Scheme.* London, UK: Department for Environment, Food and Rural Affairs.

Joos F., M. Bruno, R. Fink, *et al.* (1996) An efficient and accurate representation of complex oceanic and biospheric models fo anthropogenic carbon uptake. *Tellus* **48B**: 397-417.

Kalina J. and Ceulemans R. (1997) Clonal differences in the response of dark and light reactions of photosynthesis to elevated atmospheric CO_2 in poplar. *Photosynthetica* **33**: 51-61.

Kaufmann H., Nussbaumer T., Baxter L., *et al.* (2000) Deposit formation on a single cylinder during combustion of herbaceous biomass. *Fuel* **79**(2): 141-151.

Keitt T.H., Bjørnstad O.N., Dixon P.M., *et al.* (2002) Accounting for spatial pattern when modeling organism-environment interactions. *Ecography* **25**: 616-625.

Kilmer V.J. and Hanson A.A. (1982) *Handbook of Soils and Climate in Agriculture,* Florida, US: Cooperative Research Centre for Soil and Land Management.

Kilpatrick J. (2008) Addressing the land use issues for non-food crops, in response to increasing fuel and energy generation opportunities. York, UK: ADAS.

King J.S., Pregitzer K.S. and Zak D.R. (1999) Clonal variation in above- and below-ground growth responses of Populus tremuloides Michaux: Influence of soil warming and nutrient availability. *Plant and Soil* **217**: 119-130.

Kinney K.K. and Lindroth R.L. (1997) Responses of three deciduous tree species to atmospheric CO_2 and soil NO_3 availability. *Canadian Journal of Forest Research* **27**: 1-10.

Klein S.A. (1977) Calculation of monthly average insolation on tilted surfaces. *Solar Energy* **19**: 325-329.

Kline L.J., Davis D.D., Skelly J.M., *et al.* (2008) Ozone Sensitivity of 28 Plant Selections Exposed to Ozone Under Controlled Conditions. *Northeastern Naturalist* **15**(1): 57-66.

Koenig W.D. and Knops J.M.H. (1998) Testing for spatial autocorrelation in ecological studies. *Ecography* **21**(4): 423-429.

Kopp R.F., Abrahamson L.P., White E.H., *et al.* (1997) Cutting cycle and spacing effects on biomass production by a willow clone in New York. *Biomass and Bioenergy* **12**(5): 313-319.

Korzukhin M.D., Ter-Mikaelian M.T. and Wagner R.G. (1996) Process versus empirical models: which approach for forest ecosystem management? *Canadian Journal of Forest Research* **26**(5): 879-887.

Kreuzwieser J., Hauberg J., Howell K.A., *et al.* (2009) Differential Response of Gray Poplar Leaves and Roots Underpins Stress Adaptation during Hypoxia. *Plant*

Physiol. **149**(1): 461-473.

Kühn I. (2007) Incorporating spatial autocorrelation may invert observed patterns. *Diversity and Distributions* **13**(1): 66-69.

Kumar R., Singh S. and Singh O. (2008) Bioconversion of lignocellulosic biomass: biochemical and molecular perspectives. *Journal of Industrial Microbiology and Biotechnology* **35**(5): 377-391.

Labrecque M. and Teodorescu T.I. (2005) Field performance and biomass production of 12 willow and poplar clones in short-rotation coppice in southern Quebec (Canada). *Biomass & Bioenergy* **29**(1): 1-9.

Lambs L., Loubiat M., Girel J., *et al.* (2006) Survival and acclimatation of Populus nigra to drier conditions after damming of an alpine river, southeast France. *Ann. For. Sci.* **63**(4): 377-385.

Landau S., Mitchell R.A.C., Barnett V., *et al.* (2000) A parsimonious, multiple-regression model of wheat yield response to environment. *Agricultural and Forest Meteorology* **101**(2-3): 151-166.

Landhausser S.M. (2003) Effect of Soil Temperature on Rooting and Early Establishment of Balsam Poplar Cuttings. *Tree Planters Notes, US Department of Agriculture* **50**(1): 34-37.

Landhausser S.M. and Lieffers V.J. (2001) Photosynthesis and carbon allocation of six boreal tree species grown in understory and open conditions. *Tree Physiol* **21**(4): 243-250.

Largueche F. (2006) Estimating soil contamination with Kriging interpolation method. *American Journal of Applied Sciences* **3**(6): 1894-1898.

Laureysens I., Bogaert J., Blust R., *et al.* (2004) Biomass production of 17 poplar clones in a short rotation coppice culture on a waste disposal site and its relation to soil characteristics. *Forest Ecology & Management* **187**: 295-309.

Lawlor D.W. (1987) *Photosynthesis: Metabolism, control and physiology,* New York,

USA: Longman Scientific and technical.

Ledin S. and Willebrand E. (1995) Handbook on how to grow short-rotation coppice. IEA Bioenergy, Tasks VIII and XII.

Legendre P. (1993) Spatial autocorrelation: trouble or new paradigm? *Ecology* **74**(6): 1659-1673.

Legendre P., Dale M.R.T., Fortin M.-J., *et al.* (2002) The consequences of spatial structure for the design and analysis of ecological field surveys. *Ecography* **25**(5): 601-615.

Lennon J.J. (2000) Red-shifts and red herrings in geographical ecology. *Ecography* **23**(1): 101-113.

Lewandowski I., Kicherer A. and Vonier P. (1995) CO_2-balance for the cultivation and combustion of Miscanthus. *Biomass and Bioenergy* **8**(2): 81-90.

Li B., Hassel P.A., Morris A.J., *et al.* (2005) A non-linear nested partial least-squares algorithm. *Computational Statistics & Data Analysis* **48**(1): 87-101.

Liberloo M., Lukac M., Calfapietra C., *et al.* (2009) Coppicing shifts CO_2 stimulation of poplar productivity to above-ground pools: a synthesis of leaf to stand level results from the POP/EUROFACE experiment. *New Phytologist* **182**: 331-346.

Liberloo M., Tulva I., Raïm O., *et al.* (2007) Photosynthetic stimulation under long-term CO2 enrichment and fertilization is sustained across a closed Populus canopy profile (EUROFACE). *New Phytologist* **173**(3): 537-549.

Lin Z.H., Mo X.G. and Li H.X. (2002) Comparison of three spatial interpolation methods for climate variables in China. *Acta Geogr Sin* **57**(1): 47-56.

Linderson M.L., Iritz Z. and Lindroth A. (2007) The effect of water availability on stand-level productivity, transpiration, water use efficiency and radiation use efficiency of field-grown willow clones. *Biomass & Bioenergy* **31**(7): 460-468.

Lindroth A. and Båth A. (1999) Assessment of regional willow coppice yield in Sweden on basis of water availability. *Forest Ecology and Management* **121**: 57-

65.

Little Jr. E.L. (1971) *Atlas of United States trees, volume 1, conifers and important hardwoods*: U.S. Department of Agriculture.

Liu Z. and Dickmann D.I. (1996) Effects of water and nitrogen interaction on net photosynthesis, stomatal conductance, and water-use efficiency in two hybrid poplar clones. *Physiologia Plantarum* **97**(3): 507-512.

Llorente M.J.F. and Cuadrado R.E. (2007) Influence of the amount of bed material on the distribution of biomass inorganic elements in a bubbling fluidised bed combustion pilot plant. *Fuel* **86**(5-6): 867-876.

Lobell D.B. and Field C.B. (2007) Global scale climate-crop yield relationships and the impacts of recent warming. *Environmental Research Letters* (1): 014002.

Loewe A., Einig W., Shi L., *et al.* (2000) *Mycorrhiza* formation and elevated CO_2 both increase the capacity for sucrose synthesis in source leaves of spruce and aspen. *New Phytologist* **145**: 565-574.

Longley P., Goodchild M., Maguire D., *et al.* (2005) *Geographic Information Systems and Science*: John Wiley & Sons.

Lonsdale D. and Tabbush P. (2002) *Information Note 7(a): Poplar Rust and its Recent Impact in Great Britain.* Edinburgh, UK: Forestry Commission.

Lorenz D. and Morris D. (1995) How Much Energy Does It Take to Make a Gallon of Ethanol? Washington, US: Institute for Local-Self Reliance (ILSR).

Lovett A.A., Sünnenberg G.M., Richter G.M., *et al.* (2009) Land Use Implications of Increased Biomass Production Identified by GIS-Based Suitability and Yield Mapping for Miscanthus in England. *Bioenergy Research* **2**(1-2): 17-28.

Loveys B.R., Atkinson L.J., Sherlock D.J., *et al.* (2003) Thermal acclimation of leaf and root respiration: an investigation comparing inherently fast- and slow-growing plant species. *Global Change Biology* **9**(6): 895-910.

Lu G.Y. and Wong D.W. (2008) An adaptive inverse-distance weighting spatial

interpolation technique. *Computers & Geosciences* **34**(9): 1044-1055.

Lui B.H. and Jordan R.C. (1960) The interrelationship and characteristic distribution of direct, diffuse, and total solar radiation. *Solar Energy* **4**(3): 1-9.

Lukac M., Calfapietra C. and Godbold D.L. (2003) Production, turnover and mycorrhizal colonization of root systems of three Populus species grown under elevated CO2 (POPFACE). *Global Change Biology* **9**: 838-848.

Luo Z.-B., Calfapietra C., Liberloo M., *et al.* (2006) Carbon partitioning to mobile and structural fractions in poplar wood under elevated CO2 (EUROFACE) and N fertilization. *Global Change Biology* **12**(2): 272-283.

Lussenhop J., Treonis A., Curtis P.S., *et al.* (1998) Response of soil biota to elevated atmospheric CO_2 in poplar model systems. *Oecologia* **113**: 247-251.

MAFF (1988) *Agricultural Land Classification of England and Wales: Guidelines and criteria for grading the quality of agricultural land.* London.

MAGIC (2008) Dataset information and download facility (Internet). Available from: http://www.magic.gov.uk/DataDoc/datadoc.asp. Accessed: 05/09/09.

Magnusson M. (2002) Mineral Fertilizers and Green Mulch in Chinese Cabbage [Brassica pekinensis (Lour.) Rupr.]: Effect on Nutrient Uptake, Yield and Internal Tipburn. *Acta Agriculturae Scandinavica, Section B - Plant Soil Science* **52**(1): 25 - 35.

Mahoney J.M. and Rood S.B. (1991) A device for studying the influence of declining water table on poplar growth and survival. *Tree Physiology* **8**(3): 305-314.

Major I. and Constabel C. (2007) Insect Regurgitant and Wounding Elicit Similar Defense Responses In Poplar Leaves: Not Something to Spit At? *Plant Signal Behaviour* **2**(1): 1-3.

Mäkelä A. and Hari P. (1986) Stand growth model based on carbon uptake and allocation in individual trees. *Ecological modelling* **33**(2-4): 205-229.

Mäkelä A., Landsberg J., Ek A., *et al.* (2000) Process-based models for forest

ecosystem management: current state of the art and challenges for practical implementation. *Tree Physiology* **20**: 289-298.

Malaysian Palm Oil Council (2008) Fact sheet – Malaysian palm oil (Internet). Available from: http://www.malaysiapalmoil.org/pdf/20080908-factsheet.pdf. Accessed: 11 March 2009.

Malhi Y., Wood D., Baker T.R., *et al.* (2006) The regional variation of aboveground live biomass in old-growth Amazonian forests. *Global Change Biology* **12**(7): 1107-1138.

Mallows C.L. (1973) Some Comments on Cp. *Technometrics* **15**: 661-675.

Manzone M., Airoldi G. and Balsari P. (2009) Energetic and economic evaluation of a poplar cultivation for the biomass production in Italy. *Biomass and Bioenergy* **33**(9): 1258-1264.

Marron N. and Ceulemans R. (2006) Genetic variation of leaf traits related to productivity in a *Populus deltoides* × *Populus nigra* family. *Canadian Journal of Forest Research* **36**(2): 390-400(11).

Matthews R.W. (2001) Modelling of energy and carbon budgets of wood fuel coppice systems. *Biomass and Bioenergy* **21**: 1-19.

Matthews R.W., Henshall P. and Tubby I. (2003) Shoot Allometry and Biomass Productivity in Poplar and Willow Varieties Grown as Short Rotation Coppice. Edinburgh, UK: Forest Research.

McCarthy H., Oren R., Finzi A., *et al.* (2006) Canopy leaf area constrains CO_2-induced enhancement of productivity and partitioning among aboveground carbon pools. *Proceedings of the National Academy of Sciences, USA* **103**: 19356-19361.

McCracken A.R. and Dawson W.M. (1997) Growing clonal mixtures of willow to reduce effect of *Melampsora epitea var. epitea*. *European Journal of Forest Pathology* **27**(5): 319-329.

McCracken A.R. and Dawson W.M. (2003) Rust disease (*Melampsora epitea*) of

willow (*Salix* spp.) grown as short rotation coppice (SRC) in inter- and intra-species mixtures. *Annals of Applied Biology* **143**(3): 381-393.

McKendry P. (2002a) Energy production from biomass (part 1): overview of biomass. *Bioresource technology* **83**(1): 37-46.

McKendry P. (2002b) Energy production from biomass (Part 2): conversion technologies. *Bioresource technology* **83**(1): 47-54.

McMurtrie R.E., Leuning R., Thompson W.A., *et al.* (1992) A model of canopy photosynthesis and water use incorporating a mechanistic formulation of leaf CO_2 exchange. *Forest Ecology and Management* **52**: 261-278.

McNaughton S.J. (1981) Compensatory Plant Growth as a Response to Herbivory. *Herbivore-Plant Interactions at Northern Latitudes.* **40 (3)** 329-336 Kevo, Finland: 14-18 September

Medlyn B.E., Dreyer E., Ellsworth D., *et al.* (2002) Temperature response of parameters of a biochemically based model of photosynthesis. II. A review of experimental data. *Plant, Cell and Environment* **25**: 1167-1179.

Mencuccini M., Grace J. and Fioravanti M. (1997) Biomechanical and hydraulic determinants of tree structure in Scots pine: anatomical characteristics. *Tree Physiology* **17**: 105-113.

Menzel A., Sparks T.H., Estrella N., *et al.* (2006) European phenological response to climate change matches the warming pattern. *Global Change Biology* **12**(10): 1969-1976.

Millennium Ecosystem Assessment (2005) *Ecosystems and Human Well-being: General Synthesis.* Washington, DC: Island Press.

Mitchell C.P., Stevens E.A. and Watters M.P. (1999) Short-rotation forestry - operations, productivity and costs based on experience gained in the UK. *Forest Ecology and Management* **121**(1999): 123-136.

Mitchell D. (2008) A Note on Rising Food Prices: Policy Research Working Paper

4682. The World Bank, Development Prospects Group.

Mohren G.M.J. and Burkhart H.E. (1994) Contrasts between biologically-based proces models and management-oriented growth and yield models. *Forest Ecology and Management* **69**: 1-5.

Monsi M. and Saeki T. (1953) Über den Lichtfaktor in den Pflanzengesellenschaften und Seine Bedeutung für die Stoffproduktion. *Japanese Journal of Botany* **14**: 22-52.

Monteith J. (1965) Evaporation and environment. *Symposium of the Society for Experimental Biology, vol. 19.* 205-234

Montgomery D. (2008) *Design and analysis of experiments*: John Wiley & Sons Inc.

Moore G. (1971) A Mathematical Model for the Construction of Cladograms. Raleigh: North Carolina State University, US.

Morison J.I.L. and Morecroft M.D. (2006) Plant growth and climate change. In: Korner C. (ed.) *Significance of temperature in plant life.* USA: Blackwell Publishing.

Morrison M., Strickland M. and Block W. (2008) *Wildlife study design*: Springer Verlag.

Murphy J., Sexton D., Jenkins G., *et al.* (2009) *Climate Change Projections.* Met Office Hadley Centre.

Murphy J.M., Sexton D.M.H., Barnett D.N., *et al.* (2004) Quantification of modelling uncertainties in a large ensemble of climate change simulations. *Nature* **430**(7001): 768-772.

Nabuurs G.-J., Pussinen A., Karjalainen T., *et al.* (2002) Stemwood volume increment changes in European forests due to climate change; a simulation study with the EFISCEN model. *Global Change Biology* **8**(4): 304-316.

Nadelhoffer K.J., Emmett B.A., Gundersen P., *et al.* (1999) Nitrogen deposition makes a minor contribution to carbon sequestration in temperate forests. *Nature*

398(6723): 145-148.

Narodoslawsky M. and Obernberger I. (1996) From waste to raw material--the route from biomass to wood ash for cadmium and other heavy metals. *Journal of Hazardous Materials* **50**(2-3): 157-168.

Nash M., Chaloud D. and Lopez R. (2005) Multivariate analyses (canonical correlation analysis and partial least square, PLS) to model and assess the association of landscape metrics to surface water chemical and biological properties using Savannah River Basin Data.

Natural England (2008) *Rural Development Programme for England: Energy Crops Scheme, Establishment Grants Handbook.* London, UK: Department for Environment, Food and Rural Affairs.

Naylor R.L., Liska A., Burke M., *et al.* (2007) The Ripple Effect: Biofuels, Food Security, and the Environment. *Environment* **49**(9): 30-43.

Neenan M. (1990) *Short Rotation Forestry as a source of energy: Pests and Diseases*.

Newcombe G., Stirling B. and Bradshaw H.D. (2001) Abundant Pathogenic Variation in the New Hybrid Rust *Melampsora x columbiana* on Hybrid Poplar. *Phytopathology* **91**(10): 981-985.

Nguyen P.V., Dickmann D.I., Pregitzer K.S., *et al.* (1990) Late-season changes in allocation of starch and sugar to shoots, coarse roots, and fine roots in two hybrid poplar clones. *Tree Physiol* **7**(1-2-3-4): 95-105.

Nielsen H.P., Frandsen F.J., Dam-Johansen K., *et al.* (2000) The implications of chlorine-associated corrosion on the operation of biomass-fired boilers. *Progress in Energy and Combustion Science* **26**(3): 283-298.

Nikolov N.T. and Zeller K.F. (1992) A solar radiation algorithm for ecosystem dynamic models. *Ecological Modelling* **61**: 149-168.

Nixon D., Stephens W., Tyrrel S., *et al.* (2001) The potential for short rotation energy forestry on restored landfill caps. *Bioresource Technology* **77**: 237-245.

NNFCC (2009) Area Statistics for Non-Food Crops (Internet). Available from: http://www.nnfcc.co.uk/metadot/index.pl?id=2179;isa=Category;op=show. Accessed: 12/12/2009.

NOAA (2009) Mauna Loa CO_2 Annual Mean Data. US National Oceanic and Atmospheric Administration.

Norby R.J., DeLucia E.H., Gielen B., *et al.* (2005) Forest response to elevated CO_2 is conserved across a broad range of productivity. *Proceedings of the National Academy of Sciences, USA* **102**(50): 18052-18056.

Norby R.J., Wullschleger S.D., Gunderson C.A., *et al.* (1999) Tree responses to rising CO_2 in field experiments: implications for the future forest. *Plant, Cell and Environment* **22**: 683-714.

Nordh N.-E. and Verwijst T. (2004) Above-ground biomass assessments and first cutting cycle production in willow (Salix sp.) coppice--a comparison between destructive and non-destructive methods. *Biomass and Bioenergy* **27**(1): 1-8.

Norman J.M. (1980) *Interfacing leaf and canopy light interception models. In: Predicting photosynthate production and use for ecosystem models, vol. II.,* West Palm Beach (Florida), USA: Cooperative Research Centre for Soil and Land Management.

O'Connell A.A. and McCoach D.B. (2008) *Multilevel modeling of educational data,* Charlotte, NC, USA: Information Age.

OECD and UN Food and Agriculture Organisation (2009) *OECD-FAO Agricultural Outlook 2009-2018.* London.

Ofgem (2010) Renewables Obligation: Annual report 2008-2009. London, UK: Office of Gas and Electricity Markets.

Oliver R.J., Finch J.W. and Taylor G. (2009) Second generation bioenergy crops and climate change: a review of the effects of elevated atmospheric CO_2 and drought on water use and the implications for yield. *GCB Bioenergy* **1**(2): 97-114.

OPEC (2010) OPEC Basket Price (Internet). Available from: http://www.opec.org/opec_web/en/data_graphs/40.htm. Accessed: 12-04-2010.

OPSI (2002) The Renewables Obligation Order 2002. UK: Office of Public Sector Information.

OPSI (2009) The Renewables Obligation Order 2009. England and Wales: Office of Public Sector Information.

Ordnance Survey Land-Form Panorama DTM. UK.

Ow L.F., Griffin K.L., Whitehead D., *et al.* (2008) Thermal acclimation of leaf respiration but not photosynthesis in *Populus deltoides x nigra*. *New Phytologist* **178**(1): 123-134.

Palmer D.J., Höck B.K., Kimberley M.O., *et al.* (2009) Comparison of spatial prediction techniques for developing Pinus radiata productivity surfaces across New Zealand. *Forest Ecology and Management* **258**(9): 2046-2055.

Parcell J.L. and Westhoff P. (2006) Economic Effects of Biofuel Production on States and Rural Communities. *Journal of Agricultural and Applied Economics* **38**(2): 377-387.

Park S.J., Hwang C.S. and Vlek P.L.G. (2005) Comparison of adaptive techniques to predict crop yield response under varying soil and land management conditions. *Agricultural Systems* **85**(1): 59-81.

Parker S.R., Royle D.J. and Hunter T. (1993) Impact of Melampsora rust on yield of biomass willows. *6th International Congress of Plant Pathology.* 117 Montreal, Canada: 28 July-6 August

Parmesan C. and Yohe G. (2003) A globally coherent fingerprint of climate change impacts across natural systems. *Nature* **421**.

Pei M., Ruiz C., Bayon C., *et al.* (2004) Rust resistance in *Salix* to *Melampsora larici-epitea*. *Plant Pathology* **53**(6): 770-779.

Pei M.H., Hunter T., Ruiz C., *et al.* (2002) Quantitative inoculation of willow rust

Melampsora larici-epitea with the mycoparasite *Sphaerellopsis filum* (teleomorph *Eudarluca caricis*). *Mycological Research* **107**(1): 57-63.

Pei M.H., Royle D.J. and Hunter T. (1998) Population Dynamics of *Melampsora* rusts and disease control in renewable willow plantations: Monitoring rust variations for successful breeding and improvement of SRC energy willow. London, UK: Department for Trade and Industry.

Peñuelas J. and Filella I. (2001) Responses to a warming world. *Science* **294**.

Perry M. and Hollis D. (2005) The generation of monthly gridded datasets for a range of climatic variables over the UK. *International Journal of Climatology* **25**(8): 1041-1054.

Pettersson C.-G., Söderström M. and Eckersten H. (2006) Canopy reflectance, thermal stress, and apparent soil electrical conductivity as predictors of within-field variability in grain yield and grain protein of malting barley. *Precision Agriculture* **7**(5): 343-359.

Philippot S. (1996) Simulation Models of Short-rotation Forestry Production and Coppice Biology. *Biomass and Bioenergy* **II**(2/3): 85-93.

Phyllis (2003) Database for biomass and waste (Internet). Available from: http://www.ecn.nl/Phyllis. Accessed: 20th March 2009.

Piterou A., Shackley S. and Upham P. (2008) Project ARBRE: Lessons for bio-energy developers and policy-makers. *Energy Policy* **36**(6): 2044-2050.

Pockman W.T. and Sperry J.S. (2000) Vulnerability to xylem cavitation and the distribution of Sonoran Desert vegetation. *Am. J. Bot.* **87**(9): 1287-1299.

Post W.M., T.H. Peng, W. R. Emanuel*, et al.* (1990) The global carbon cycle. *American Scientist* **78**: 310-26.

Prasad A.K., Chai L., Singh R.P.*, et al.* (2006) Crop yield estimation model for Iowa using remote sensing and surface parameters. *International Journal of Applied Earth Observation and Geoinformation* **8**(1): 26-33.

Price L., Bullard M., Lyons H., *et al.* (2004) Identifying the yield potential of Miscanthus x Giganteus: an assessment of the spatial and temporal variability of M. x Giganteus biomass productivity across England and Wales. *Biomass & Bioenergy* **26**(2004): 3-13.

Proe M.F., Griffiths J.H. and Craig J. (2002) Effects of spacing, species and coppicing on leaf area, light interception and photosynthesis in short rotation forestry. *Biomass and Bioenergy* **23**(5): 315-326.

Pulford I., Riddell-Black D. and Stewart C. (2002) Heavy Metal Uptake by Willow Clones from Sewage Sludge-Treated Soil: The Potential for Phytoremediation. *International Journal of Phytoremediation* **4**(1): 59-72.

Pyatt D.G. and Suarez J.C. (1997) *An Ecological Site Classification for Forestry in Great Britain.* Edinburgh, UK: Forest Research.

Quinn G. and Keough M. (2002) *Experimental design and data analysis for biologists*: Cambridge Univ Pr.

Quinn Thomas R., Canham C.D., Weathers K.C., *et al.* (2010) Increased tree carbon storage in response to nitrogen deposition in the US. *Nature Geosci* **3**(1): 13-17.

Rabalais N.N., Turner R.E. and Wiseman W.J. (2002) Gulf of Mexico Hypoxia, aka. "The Dead Zone". *Annual Review of Ecology and Systematics* **33**(1): 235-263.

Rae A.M., Pinel M.C.P., Bastien C., *et al.* (2008) QTL for yield in bioenergy *Populus*: identifying GxE interactions from growth at three contrasting sites. *Tree Genetics & Genomes* **4**: 1614-2950.

Rae A.M., Robinson K.M., Street N.R., *et al.* (2004) Morphological and Physiological Traits Influencing Biomass Productivity in Short Rotation Coppice Poplar. *Canadian Journal of Forestry Research* **34**: 1488-1498.

Raudenbush S. and Bryk A. (2002) *Hierarchical linear models (2nd ed.),* Thousand Oaks, CA, USA: Sage.

Rauscher H.M., Isebrands I.G., Horst G.E., *et al.* (1990) ECOPHYS: an

ecophysiological growth process model for juvenile poplar. *Tree Physiology* **7**: 255-281.

Ray D. (2007) *Research Note 301: Impacts of climate change on forestry in Wales.* Edinburgh, UK: Forestry Commission.

Redfern D. and Hendry S. (2002) Climate change and damage to trees caused by extremes of temperature. In: Broadmeadow M. (ed.) *Climate change: impacts on UK forests. Bulletin 125*. Edinburgh, UK: Forestry Commission.

Reich P.B., Kloeppel B.D., Ellsworth D.S., *et al.* (1995) Different photosynthesis-nitrogen relations in deciduous hardwood and evergreen coniferous tree species. *Oecologia* **104**: 24-30.

Reichenbacker R.R., Schultz R.C. and Hart E.R. (1996) Artificial Defoliation Effect on *Populus* Growth, Biomass Production, and Total Nonstructural Carbohydrate Concentration. *Environmental Entomology* **25**: 632-642.

RFA (2008) Renewable Transport Fuel Obligation Quarterly report, 15 April - 14 July 2008. London, UK: Renewable Fuels Agency.

Richardson C.W. (1981) Stochastic simulation of daily precipitation, temperature and solar radiation. . *Water Resources Research* **17**: 182-190.

Richter G.M., Riche A.B., Dailey A.G., *et al.* (2008) Is UK biofuel supply from Miscanthus water-limited? *Soil Use and Management* **24**: 235-245.

Ridolfi M., Fauveau M.L., Label P., *et al.* (1996) Responses to water stress in an ABA - Unresponsive hybrid poplar (*Populus koreana* x *trichocarpa* cv. Peace) I. Stomatal function. *New Phytologist* **134**(3): 445-454.

Riehl Koch J., Scherzer A.J., Eshita S.M., *et al.* (1998) Ozone Sensitivity in Hybrid Poplar Is Correlated with a Lack of Defense-Gene Activation. *Plant Physiology* **118**(4): 1243-1252.

Ritchie J.T. (1972) A model for predicting evaporation from a row crop with incomplete cover. *Water Resources Research* **8**: 1204-1213.

Robinson B., Mills T., Petit D., *et al.* (2000) Natural and induced cadmium-accumulation in poplar and willow: Implications for phytoremediation. *Plant and Soil* **227**: 301-306.

Robinson K.M., Karp A. and Taylor G. (2004) Defining leaf traits linked to yield in short-rotation coppice *Salix*. *Biomass & Bioenergy* **26**: 417-431.

Rook D.A. (1991) Tree breeding and short rotation coppice. London, UK: ETSU Contractor Report for DTI.

Root T.L., Price J.T., Hall K.R., *et al.* (2003) Fingerprints of global warming on wild animals and plants. *Nature* **421**(6918): 57-60.

Rosenqvist H. and Dawson M. (2005) Economics of willow growing in Northern Ireland. *Biomass and Bioenergy* **28**(1): 7-14.

Ross S.M. (1983) *Stochastic processes,* New York, US: John Wiley and Sons.

Rouhani S. (1996) *Geostatistics for environmental and geotechnical applications*: ASTM International.

Rowe R.L., Street N.R. and Taylor G. (2009) Identifying potential environmental impacts of large-scale deployment of dedicated bioenergy crops in the UK. *Renewable Energy Reviews* **13**(1): 271-290.

Rutter A.J., Morton A.J. and Robins P.C. (1975) A predictive model of rainfall interception in forests. II. Generalisation of the model and comparison with observations in some coniferous and hardwood stands. *Journal of Applied Ecology* **12**: 367-380.

Ryan A., Cojocariu C., Possell M., *et al.* (2009) Defining hybrid poplar (*Populus deltoides x Populus trichocarpa*) tolerance to ozone: identifying key parameters. *Plant, Cell & Environment* **32**: 31-45.

Rytter R.-M. (2001) Biomass production and allocation, including fine-root turnover, and annual N uptake in lysimeter-grown basket willows. *Forest Ecology and Management* **140**(2-3): 177-192.

Sage R.B. (1994) A Review of the Status and Control Strategies of Known and Perceived Insect Pests on *Salix* and *Populus* in North West Europe. .

Sage R.F. and Kubien D.S. (2007) The temperature response of C_3 and C_4 photosynthesis. *Plant, Cell & Environment* **30**: 1086-1106.

Sands P.J., Battaglia M. and Mummery D. (2000) Application of process-based models to forest management: experience with PROMOD, a simple plantation productivity model. *Tree Physiology* **20**(5-6): 383-392.

Sauter J.J. and Cleve B. (1994) Storage, mobilization and interrelations of starch, sugars, protein and fat in the ray storage tissue of poplar trees. *Trees - Structure and Function* **8**(6): 297-304.

Scarasscia-Mugnozza G.E., Ceulemans R., Heilman P.E., *et al.* (1997) Production physiology and morphology of Populus species and their hybrids grown under short rotation. II. Biomass components and harvest index of hybrid and parental species clones. *Canadian Journal of Forestry Research* **27**(1997): 285-294.

Schmidhuber J. (2006) Impact of an increased biomass use on agricultural markets, prices and food security: A longer-term perspective. *International symposium of Notre Europe.* Paris: 27-29 November, 2006

Scholes H. (1998) Can Energy Crops Become A Realistic CO_2 Mitigation Option In South West England? *Biomass & Bioenergy* **15**(4/5): 333-344.

Scholz V. and Ellerbrock R. (2002) The growth productivity, and environmental impact of the cultivation of energy crops on sandy soil in Germany. *Biomass and Bioenergy* **23**(2): 81-92.

Schwaber K. (2004) *Agile project management with Scrum*: Microsoft Press.

Scottish Executive (2007) *Biomass Action Plan for Scotland.* Edinburgh, UK: Scottish Executive.

Searchinger T., Heimlich R., Houghton R.A., *et al.* (2008) Use of U.S. Croplands for Biofuels Increases Greenhouse Gases Through Emissions from Land-Use Change.

Science Express **319**: 1238-1240.

Sennerby-Forsse L., Ferm A. and Kauppi A. (1992) Coppicing ability and sustainability. In: Mitchell C.P., Ford-Robertson J.B., Hinckley T.M. and Sennerby-Forsse L. (eds.) *Ecophysiology of Short Rotation Forest Crops*. Oxford, UK: Elsevier Applied Science.

Shaw J.D., Packee(Sr.) E.C. and Pin C. (2001) Growth of balsam poplar and black cottonwood in Alaska in relation to landform and soil. *Canadian Journal of Forest Research* **31**(10): 1793-1804.

Sherrington C., Bartley J. and Moran D. (2008) Farm-level constraints on the domestic supply of perennial energy crops in the UK *Energy Policy* **36**(7): 2504-2512.

Shock C.C., Flock R., Feibert E., *et al.* (2005) *Sustainable Agriculture Techniques: Drip Irrigation Guide for Growers of Hybrid Poplar,* Oregon, US: Oregon State University

Sievanen R. (1983) *Growth model for mini-rotation plantations.,* Helsinki, Finland: Comm. Inst. Forestalis Fenniae.

Sigurdsson B.D., Thorgeirsson H. and Linder S. (2001) Growth and drymatter partitioning of young *Populus trichocarpa* in response to carbon dioxide concentration and mineral nutrient availability. *Tree Physiology* **21**(12-13): 941-50.

Sims R.E.H. (2003) Bioenergy to mitigate for climate change and meet the needs of society, the economy and the environment. *Mitigation and Adaptation Strategies for Global Change* **8**(4): 349-370.

Sims R.H., Hastings A., Schlamadinger B., *et al.* (2006) Energy crops: current status and future prospects. *Global Change Biology* (12): 2054-2076.

Sinclair W.A., Lyon H.H. and Johnson W.T. (1987) *Diseases of Trees and Shrubs*: Comstock Publishing.

Smith J., Bradbury N. and Addiscott T. (1996) SUNDIAL: a PC based system for simulating nitrogen dynamics in arable land. *Agronomy Journal* **88**: 38-43.

Smith J., Smith P., Watternbach M., *et al.* (2005) Projected changes in mineral soil carbon of European croplands and grasslands, 1990-2080. *Global Change Biology* **11**(12): 2141-2152.

Souch C. and Stephens W. (1998) Growth, productivity and water use in three hybrid poplar clones. *Tree Physiology* **18**(12): 829-835.

Sparks J.P. and Black R.A. (1999) Regulation of water loss in populations of Populus trichocarpa: the role of stomatal control in preventing xylem cavitation. *Tree Physiol* **19**(7): 453-459.

St. Clair S., Hillier J. and Smith P. (2008) Estimating the pre-harvest greenhouse gas costs of energy crop production. *Biomass and Bioenergy* **32**(5): 442-452.

Stainforth D.A., Aina T., Christensen C., *et al.* (2005) Uncertainty in predictions of the climate response to rising levels of greenhouse gases. *Nature* **433**(7024): 403-406.

Stern N. (2006) *The Economics of Climate Change: The Stern Review*. London, UK: Cabinet Office, HM Treasury.

Stettler R. (1996) *Biology of Populus and its implications for management and conservation*: Canadian Government Publishing.

Strawson J. (2003) Energy Crops and the Market for Biomass in the UK. Nuffield Farming Scholarships Trust.

Street N., Skogström O., Sjödin A., *et al.* (2006) The genetics and genomics of drought response in Populus. *The Plant Journal* **48**(3): 321-341.

Sun G., Amatya D.M., McNulty S.G., *et al.* (2000) Climate Change Impacts on the hydrology and productivity of a pine plantation. *Journal of the American Water Resources Association* **36**(2): 367-374.

SWS Forestry Services (2006) Billet harvesting, Drying and Processing of Willow

Short Rotation Coppice for the Wood Energy Market in the UK. County Cork, Ireland: SWS Forestry Services.

Tabachnick B.G. and Fidell L.S. (2007) *Using Multivariate Statistics (5th Edition),* Boston, US: Allyn & Bacon.

Tabbush P. and Parfitt R. (1999) *Information Note 17: Poplar and Willow Varieties for Short Rotation Coppice.* Edinburgh, UK: Forestry Commission.

Taylor G. (2008) Bioenergy for heat and electricity in the UK: A research atlas and roadmap. *Energy Policy* **36**: 4383-4389.

Taylor G., Beckett K., Robinson K., *et al.* (2001a) Identifying QTL for yield in UK biomass poplar. *Aspects of Applied Biology.* **65**: 173-182.

Taylor G., Ceulemans R., Ferris R., *et al.* (2001b) Increased leaf area expansion of hybrid poplar in elevated CO_2. From controlled environments to open-top chambers and to FACE. *Environmental Pollution* **115**: 463-472.

Teegavarapu R.S.V. and Chandramouli V. (2005) Improved weighting methods, deterministic and stochastic data-driven models for estimation of missing precipitation records. *Journal of Hydrology* **312**(1-4): 191-206.

Thomas C.D., Cameron A., Green R.E., *et al.* (2004) Extinction risk from climate change. *Nature* **427**(6970): 145-148.

Tjoelker M.G., Oleksyn J. and Reich P.B. (1998) Seedlings of five boreal tree species differ in acclimation of net photosynthesis to elevated CO_2 and temperature. *Tree Physiology* **18**: 715-726.

Tobler W. (1970) A computer movie simulating urban growth in the Detroit region. *Economic Geography* **46**(2): 234-240.

Tubby I. (2005) *Tree Death in poplar plantations, Summer 2005.* Edinburgh, UK: Forestry Commission.

Tubby I. and Armstrong A. (2002) *Establishment and Management of Short Rotation Coppice: Practice Note FCPN7 (REVISED).* Edinburgh, UK: Forestry

Commission.

Tuck G., Glendining M.J., Smith P., *et al.* (2006) The potential distribution of bioenergy crops in Europe under present and future climate. *Biomass & Bioenergy* **30**: 183-197.

Tucker K. and Sage R. (1998) Integrated Crop Management of SRC Plantations to Maximise Crop Value, Wildlife Benefits and Other Added Value Opportunities. Fordingbridge, UK: The Game Conservancy Trust.

Tucker K. and Sage R. (1999) Integrated pest management in short rotation coppice for energy – a grower's guide. Fordingbridge, UK: The Game Conservancy Trust.

Turley D.B., Boatman N.D., Ceddia G., *et al.* (2002) Liquid biofuels – prospects and potential impacts on UK agriculture, the farmed environment, landscape and rural economy. York: Central Science Laboratory.

Turnbull M.H., Murthy R. and Griffin K.L. (2002) The relative impacts of daytime and night-time warming on photosynthetic capacity in *Populus deltoides*. *Plant, Cell & Environment* **25**(12): 1729-1737.

UK Biomass Task Force (2005) Biomass Task Force: Report To Government. In: Gill B., MacLeod N., Clayton D., Cowburn R., Roberts J. and Hartley N. (eds.). London, UK: Department for Environment, Food and Rural Affairs.

UKERC (2006) Response to the Government's Energy Review consultation. In: Jim Skea (ed.).

Umetrics (2002) User Guide to Simca-P, Simca-P+; Version 10.

UN (2006) United Nations Millenium Development Goal Indicators: Carbon dioxide emissions (CO_2), thousand metric tons of CO_2 (CDIAC). United Nations.

UNFCC (2009) Kyoto Protocol (Internet). Available from: http://unfccc.int/kyoto_protocol/items/2830.php. Accessed: 25th March.

Urbanchuk J.M. (2008) Critique of the World Bank Working Paper "A Note on Rising Food Prices". Pennsylvania, USA: LECG LLC.

USDA (2002) *The Energy Balance of Corn Ethanol: An Update.* Washington DC, US.

Valente F., David J.S. and Gash J.H.C. (1997) Modelling interception loss for two sparse eucalypt and pine forests in central Portugal using reformulated Rutter and Gash analytical models. *Journal of Hydrology* **190**: 141-162.

van der Perk M., Burema J., Vandenhove H., *et al.* (2004) Spatial assessment of the economic feasibility of short rotation coppice on radioactively contaminated land in Belarus, Ukraine, and Russia. I. Model description and scenario analysis. *Journal of Environmental Management* **72**(2004): 217-232.

van Dijk A.I.J.M. and Bruijnzeel L.A. (2001) Modelling rainfall interception by vegetation of variable density using an adapted analytical model. Part 1. Model description. *Journal of Hydrology* **247**: 230-238.

Vandenhove H., Goor F., Timofeyev S., *et al.* (2004) Short rotation coppice as alternative land use for Chernobyl-contaminated areas of Belarus. *International Journal of Phytoremediation* **6**(2): 139-156.

Vasiliev I.R. (1996) Visualization of spatial dependence: an elementary view of spatial autocorrelation. *Practical Handbook of Spatial Statistics.* Boca Raton, Fla: CRC Press.

Venturi P. and Venturi G. (2003) Analysis of energy comparison for crops in European agricultural systems. *Biomass and Bioenergy* **25**(3): 235-255.

Ver Hoef J.M., Cressie N., Fisher R.N., *et al.* (2001) Uncertainty in spatial linear models for ecological data. In: Hunsaker C.T., Goodchild M.F., Friedl M.A. and Case T.J. (eds.) *Spatial uncertainty for ecology: implications for remote sensing and GIS applications.* New York, US: Springer-Verlag.

von Caemmerer S., Evans J., Hudson G., *et al.* (1994) The kinetics of ribulose-1,5-bisphosphate carboxylase/oxygenase in vivo inferred from measurements of photosynthesis in leaves of transgenic tobacco. *Planta* **195**: 88-97.

von Caemmerer S. and Farquhar G.D. (1981) Some relationships between the

biochemistry of photosynthesis and the gas exchange of leaves. *Planta* **153**: 376-387.

Wagner N.C., Maxwell B.D., Taper M.L.*, et al.* (2009) Developing an Empirical Yield-Prediction Model Based on Wheat and Wild Oat (*Avena fatua*) Density, Nitrogen and Herbicide Rate, and Growing-Season Precipitation. *Weed Science* **55**(6): 652-664.

Walsh M., de la Torre Ugarte D., Shapouri H., *et al.* (2003) Bioenergy Crop Production in the United States: Potential Quantities, Land Use Changes, and Economic Impacts on the Agricultural Sector. *Environmental and Resource Economics* **24**(4): 313-333.

Watson D.F. and Philip G.M. (1985) A refinement of inverse distance weighted interpolation. *Geo-proc.* **2**: 315-327.

Wermelinger B., Baumgartner J. and Gutierrez A.P. (1991) A demographic model of assimilation and allocation of carbon and nitrogen in grapevines. *Ecological modelling* **53**(1-2): 1-26.

Wheeler T.R., Craufurd P.Q., Ellis R.H., *et al.* (2000) Temperature variability and the yield of annual crops. *Agriculture, Ecosystems & Environment* **82**(1-3): 159-167.

Whelan M.J., HUNTER T., Parker S.R., *et al.* (1997) How effective is *Sphaerellopsis* as a biological control agent of *Melampsora* willow rust? *Aspects of Applied Biology* **48**: 143-148.

Wikberg J. and Ogren E. (2004) Inter-relationships between water use and growth traits in biomass-producing willows. *Trees* **18**: 70-76.

Wildlife and Countryside Link, Northern Ireland Environment Link, Wales Environment Link, *et al.* (2007) *Bioenergy in the UK: Turning Green Promises into Environmental Reality.* London, UK.

Williams A.G. and Whitham T.G. (1986) Premature Leaf Abscission: An Induced

Plant Defense Against Gall Aphids. *Ecology* **67**(6): 1619-1627.

Williams C.L., Liebman M., Edwards J.W., *et al.* (2008) Patterns of Regional Yield Stability in Association with Regional Environmental Characteristics. *Crop Sci.* **48**(4): 1545-1559.

Wullschleger S., Norby R., Love J., *et al.* (1997) Energetic Costs of Tissue Construction in Yellow-poplar and White Oak Trees Exposed to Long-term CO_2 Enrichment. *Annals of Botany* **80**: 289-297.

Wullschleger S.D., Yin T.M., DiFazio S.P., *et al.* (2005) Phenotypic variation in growth and biomass distribution for two advanced-generation pedigrees of hybrid poplar (*Populus* spp.). *Canadian Journal of Forest Research* **35**: 1779-1789.

Yamori W., Noguchi K. and Terashima I. (2005) Temperature acclimation of photosynthesis in spinach leaves: analyses of photosynthetic components and temperature dependencies of photosynthetic partial reactions. *Plant, Cell & Environment* **28**(4): 536-547.

Yaussy D.A. (2000) Comparison of an empirical forest growth and yield simulator and a forest gap simulator using actual 30-year growth from two even-aged forests in Kentucky. *Forest Ecology and Management* **126**(3): 385-398.

Zak D., Pregitzer K., Curtis P., *et al.* (2000) Atmospheric CO_2, Soil-N Availability, and Allocation of Biomass and Nitrogen by *Populus Tremuloides*. *Ecological Applications* **10**: 34-46.

Zhang X. and Srinivasan R. (2009) GIS-Based Spatial Precipitation Estimation: A Comparison of Geostatistical Approaches. *JAWRA Journal of the American Water Resources Association* **45**(4): 894-906.

Zhang Y., Reed D.D., Cattelino P.J., *et al.* (1994) A process-based growth model for young red pine. *Forest Ecology Management* **69**: 21-40.

Zimmerman D., Pavlik C., Ruggles A., *et al.* (1999) An Experimental Comparison of Ordinary and Universal Kriging and Inverse Distance Weighting. *Mathematical*

Geology **31**(4): 375-390.

Chapter 8 . Appendices

Appendix A: Empirical model yield Table

Name, sex, parentage, provenance, mean annual yield (odt ha^{-1} yr^{-1}) and rust score for the first and second rotation of all field trial genotypes.

Genus	Genotype	Sex	Parentage	Provenance	First rotation		Second rotation	
					Mean yield	Mean rust score	Mean yield	Mean rust score
Populus	71009/1 †	F	*P. deltoides* x *P. trichocarpa*	USA	**2.94** (1.98)	**1.89** (1.80)	**1.97** (1.84)	**3.37** (1.90)
Populus	71009/2 †	F	*P. deltoides* x *P. trichocarpa*	USA	**4.95** (3.45)	**1.67** (1.86)	**4.15** (3.86)	**3.03** (2.04)
Populus	71015/1 †	F	*P. deltoides* x *P. trichocarpa*	USA	**5.80** (2.67)	**1.61** (1.92)	**4.92** (3.39)	**2.96** (2.09)
Populus	Balsam Spire †	F	*P. trichocarpa* x *P. balsamifera*	USA	**7.24** (3.70)	**1.63** (1.73)	**7.03** (3.50)	**2.06** (1.72)
Populus	Beaupré*	F	*P. trichocarpa* x *P. deltoides*	USA	**7.34** (2.33) [bc]	**2.00** (1.91)	**4.87** (2.43) [a]	**2.87** (1.90)
Populus	Boelare	F	*P. trichocarpa* x *P. deltoides*	USA	**6.23** (3.02)	**1.98** (1.93)	**4.20** (3.57)	**2.93** (2.00)
Populus	Columbia River	M	*P. trichocarpa*	USA	**6.71** (3.33)	**1.49** (1.55)	**6.62** (3.04)	**1.77** (1.39)
Populus	Fritzi Pauley	F	*P. trichocarpa*	USA	**8.59** (2.11)	**0.72** (0.97)	**8.24** (2.95)	**1.37** (1.35)
Populus	Gaver	M	*P. deltoides* x *P. nigra*	USA x Belgium	**6.58** (2.72)	**0.92** (1.04)	**5.58** (3.18)	**1.73** (1.58)
Populus	Ghoy*	F	*P. deltoides* x *P. nigra*	USA/Canada x Belgium	**6.45** (2.47) [a]	**1.24** (1.47)	**5.77** (2.46) [ab]	**2.04** (1.75)
Populus	Gibecq	M	*P. deltoides* x *P. nigra*	USA x Belgium	**5.70** (2.39)	**1.21** (1.27)	**4.73** (3.28)	**2.16** (1.71)
Populus	Hazendans †	F	*P. trichocarpa* x *P. deltoides*	USA	**7.23** (2.29)	**0.34** (1.05)	**7.56** (2.94)	**0.76** (1.55)
Populus	Hoogvorst †	F	*P. trichocarpa* x *P. deltoides*	USA	**8.84** (2.42)	**0.39** (1.19)	**8.12** (3.81)	**0.62** (1.46)
Populus	Raspalje	F	*P. trichocarpa* x *P. deltoides*	USA	**6.69** (2.76)	**1.69** (2.02)	**4.66** (3.25)	**2.93** (1.91)
Populus	Trichobel*	M	*P. trichocarpa*	USA	**9.08** (2.67) [d]	**0.75** (0.92)	**9.59** (2.78) [d]	**1.11** (1.18)
Populus	Unal	M	*P. trichocarpa* x *P. deltoides*	USA	**7.55** (3.57)	**1.67** (1.87)	**5.25** (3.91)	**2.61** (1.96)
Salix	Bebbiana	M	*S. sitchensis*	USA	**8.08** (2.99)	**0.00** (0.01)	**12.16** (4.38)	**0.00** (0.00)
Salix	Bjorn	M	*S. viminalis* x *S. schwerinii*	Sweden	**7.59** (3.68)	**0.05** (0.16)	**11.21** (4.89)	**0.13** (0.44)
Salix	Dasyclados	F	*S. caprea* x *S. cinerea* x *S. viminalis*	Sweden	**7.17** (2.01)	**0.33** (0.78)	**8.21** (2.57)	**0.48** (0.90)
Salix	Delamere	F	*S. aurea* x *S. cinerea* x *S. viminalis*	England	**8.31** (1.10)	**0.33** (0.66)	**10.00** (3.13)	**0.61** (0.85)
Salix	Germany*	F	*S. burjatica*	Northern Ireland	**7.14** (2.94) [ab]	**1.55** (1.70)	**7.46** (4.00) [c]	**2.51** (1.75)
Salix	Jorr	M	*S. viminalis* x *S. viminalis*	Sweden	**10.50** (2.92)	**0.62** (0.90)	**11.01** (3.16)	**0.92** (1.38)
Salix	Jorunn*	F	*S. viminalis* x *S. viminalis*	Sweden	**9.09** (3.01) [d]	**0.31** (0.60)	**9.15** (2.70) [d]	**0.33** (0.74)
Salix	Orm	M	*S. viminalis* x *S. viminalis*	England	**8.33** (2.60)	**0.72** (0.91)	**8.47** (2.87)	**1.06** (1.32)
Salix	Q83*	F	*S. triandra* x *S. viminalis*	Northern Ireland	**8.03** (3.23) [c]	**1.59** (1.56)	**10.71** (3.74) [e]	**1.99** (1.64)
Salix	Spaethii	F	*S. spaethii*	Sweden	**7.30** (1.78)	**0.92** (1.24)	**9.44** (3.27)	**1.67** (1.73)
Salix	ST/2481/55	F	*S. triandra* x *S. viminalis*	Northern Ireland	**6.72** (2.39)	**1.40** (1.54)	**8.96** (3.29)	**1.95** (1.60)
Salix	Stott10 †	F	*S. burjatica* x *S. viminalis*	England	**10.35** (3.57)	**1.25** (1.51)	**9.12** (4.30)	**1.69** (1.87)
Salix	Stott11 †	F	*S. burjatica* x *S. viminalis*	England	**10.01** (3.49)	**1.11** (1.32)	**10.16** (4.51)	**1.56** (1.75)
Salix	Tora	F	*S. viminalis* x *S. schwerinii*	Sweden	**9.31** (3.52)	**0.02** (0.07)	**13.34** (4.43)	**0.05** (0.26)
Salix	Ulv	M	*S. viminalis* x *S. viminalis*	England	**10.12** (3.91)	**0.30** (0.55)	**10.86** (2.77)	**0.62** (1.17)
Salix	V789	-	*S. viminalis* x *S. caprea*	Finland	**4.12** (1.64)	**0.68** (1.35)	**5.07** (1.72)	**0.86** (1.51)

Footnote: Asterisks denote 'extensively' grown genotypes. Daggers denote new genotypes (at time of planting). Standard deviations are given in parentheses. Values with the same letter are not statistically different ($p > 0.05$) using t-test ('extensive' trials only).

Appendix B: Minitab linear regression outputs

P. trichocarpa, genotype Trichobel. First rotation.

The regression equation

RotationYield(odt) = - 10.2 + 0.000003 squAnnualRain + 4.84 logSlope - 0.0138 SeasonRain + 0.00431 GDDSummer_1 - 0.0206 Elevation_1 + 0.00772 AvailH2O + 0.213 Cloud Cover - 0.248 WindSpeed

138 cases used, 1 cases contain missing values

Predictor	Coef	SE Coef	T	P
Constant	-10.154	4.553	-2.23	0.027
squAnnualRain	0.00000304	0.00000078	3.87	0.000
logSlope	4.8427	0.5778	8.38	0.000
SeasonRain	-0.013824	0.003508	-3.94	0.000
GDDSummer_1	0.0043076	0.0008874	4.85	0.000
Elevation_1	-0.020588	0.003632	-5.67	0.000
AvailH2O	0.007718	0.002375	3.25	0.001
Cloud Cover	0.21298	0.05136	4.15	0.000
WindSpeed	-0.2483	0.1050	-2.37	0.020

S = 1.72144 R-Sq = 53.9 % R-Sq(adj) = 51.1 %

Analysis of Variance

Source	DF	SS	MS	F	P
Regression	8	447.276	55.909	18.87	0.000
Residual Error	129	382.274	2.963		
Total	137	829.549			

Source	DF	Seq SS
squAnnualRain	1	46.499
logSlope	1	74.664
SeasonRain	1	71.901
GDDSummer_1	1	60.735
Elevation_1	1	90.705
AvailH2O	1	34.669
Cloud Cover	1	51.525
WindSpeed	1	16.577

Unusual Observations

Obs	squAnnualRain	RotationYield(odt)	Fit	SE Fit	Residual	St Resid
43	450317	5.193	8.650	0.289	-3.457	-2.04R
49	521467	11.082	7.388	0.350	3.694	2.19R
91	1062789	8.160	4.512	0.446	3.648	2.19R
92	1062789	8.605	4.512	0.446	4.093	2.46R
93	1062789	8.623	4.512	0.446	4.111	2.47R
121	385405	2.255	5.779	0.419	-3.524	-2.11R
127	292486	10.097	8.990	0.787	1.106	0.72 X
128	237572	9.612	9.688	0.799	-0.076	-0.05 X
129	292486	8.028	8.990	0.787	-0.963	-0.63 X

R denotes an observation with a large standardized residual.
X denotes an observation whose X value gives it large leverage.

Appendix B: Minitab linear regression outputs

P. trichocarpa, genotype Trichobel. Second rotation.

The regression equation

RotationYield(odt) = 14.8 + 0.0396 Sand% - 21.4 logSeasonRain + 0.00807 AnnualRain + 4.09 logSlope + 23.8 logSunshineHours - 0.000003 squGDDSummer + 1.57 MMaxTemp + 0.000519 squClay% - 0.0217 Elevation

129 cases used, 2 cases contain missing values

Predictor	Coef	SE Coef	T	P
Constant	14.80	10.87	1.36	0.176
Sand%	0.03959	0.01073	3.69	0.000
logSeasonRain	-21.351	4.692	-4.55	0.000
AnnualRain	0.008073	0.001993	4.05	0.000
logSlope	4.0943	0.5919	6.92	0.000
logSunshineHours	23.814	7.660	3.11	0.002
squGDDSummer	-0.00000288	0.00000069	-4.19	0.000
MMaxTemp	1.5733	0.3073	5.12	0.000
squClay%	0.0005189	0.0002416	2.15	0.034
Elevation	-0.021673	0.004102	-5.28	0.000

S = 1.76236 R-Sq = 49.7 % R-Sq(adj) = 45.9 %

Analysis of Variance

Source	DF	SS	MS	F	P
Regression	9	365.835	40.648	13.09	0.000
Residual Error	119	369.603	3.106		
Total	128	735.437			

Source	DF	Seq SS
Sand%	1	10.687
logSeasonRain	1	72.526
AnnualRain	1	0.735
logSlope	1	79.230
logSunshineHours	1	41.715
squGDDSummer	1	3.685
MMaxTemp	1	37.534
squClay%	1	33.043
Elevation	1	86.680

Unusual Observations

Obs	Sand%	RotationYield(odt)	Fit	SE Fit	Residual	St Resid
5	62.2	10.819	7.381	0.397	3.438	2.00R
53	37.4	8.612	5.099	0.431	3.513	2.06R
54	37.4	8.831	5.099	0.431	3.731	2.18R
82	52.8	8.305	4.587	0.461	3.719	2.19R

R denotes an observation with a large standardized residual.

Appendix B: Minitab linear regression outputs

S. triandra x S. viminalis, genotype Jorunn. First rotation.

The regression equation

RotationYield(odt) = 54.8 + 0.00417 SeasonRain - 0.0219 Elevation + 4.17 logFrostDays - 0.587 OrgMatter - 23.8 logSilt% - 14.2 logClay% + 0.000029 squAvailH2O - 0.00348 squSand% + 0.667 squrtSlope + 1.49 SunshineHours - 0.00467 GDDSummer + 16.7 logpH

139 cases used, 8 cases contain missing values

Predictor	Coef	SE Coef	T	P
Constant	54.78	16.03	3.42	0.001
SeasonRain	0.004167	0.001474	2.83	0.005
Elevation	-0.021946	0.004828	-4.55	0.000
logFrostDays	4.167	1.148	3.63	0.000
OrgMatter	-0.58651	0.09503	-6.17	0.000
logSilt%	-23.756	5.362	-4.43	0.000
logClay%	-14.164	2.572	-5.51	0.000
squAvailH2O	0.00002859	0.00000671	4.26	0.000
squSand%	-0.0034843	0.0007513	-4.64	0.000
squrtSlope	0.6672	0.2539	2.63	0.010
SunshineHours	1.4936	0.6212	2.40	0.018
GDDSummer	-0.004672	0.001462	-3.20	0.002
logpH	16.710	5.104	3.27	0.001

S = 2.07915 R-Sq = 54.0 % R-Sq(adj) = 49.6 %

Analysis of Variance

Source	DF	SS	MS	F	P
Regression	12	638.230	53.186	12.30	0.000
Residual Error	126	544.680	4.323		
Total	138	1182.910			

Source	DF	Seq SS
SeasonRain	1	36.439
Elevation	1	65.111
logFrostDays	1	69.767
OrgMatter	1	106.740
logSilt%	1	3.663
logClay%	1	8.088
squAvailH2O	1	93.923
squSand%	1	140.464
squrtSlope	1	37.170
SunshineHours	1	0.394
GDDSummer	1	30.140
logpH	1	46.332

Unusual Observations

Obs	SeasonRain	RotationYield(odt)	Fit	SE Fit	Residual	St Resid
37	435	5.657	10.409	0.493	-4.752	-2.35R
38	435	5.924	10.409	0.493	-4.485	-2.22R
79	508	17.208	12.465	0.710	4.742	2.43R
88	605	12.504	8.389	0.495	4.115	2.04R
133	393	12.084	12.343	1.122	-0.259	-0.15 X
134	393	14.196	12.343	1.122	1.853	1.06 X
135	393	12.376	12.343	1.122	0.033	0.02 X

R denotes an observation with a large standardized residual.
X denotes an observation whose X value gives it large leverage.

Appendix B: Minitab linear regression outputs

S. triandra x S. viminalis, genotype Jorunn. Second rotation.

The regression equation

RotationYield(odt) = - 62.4 + 0.240 FrostDays - 0.885 MMaxTemp - 0.0114 squOrgMatter - 0.00360 squSand% - 24.0 logSilt% - 13.3 logClay% - 0.0237 Elevation + 1.74 RelativeHumidity - 0.150 Cloud Cover + 20.5 logSunshineHours - 0.369 WindSpeed

135 cases used, 6 cases contain missing values

Predictor	Coef	SE Coef	T	P
Constant	-62.38	21.01	-2.97	0.004
FrostDays	0.24024	0.05051	4.76	0.000
MMaxTemp	-0.8846	0.2273	-3.89	0.000
squOrgMatter	-0.011421	0.005102	-2.24	0.027
squSand%	-0.0036012	0.0006517	-5.53	0.000
logSilt%	-23.998	4.624	-5.19	0.000
logClay%	-13.348	2.285	-5.84	0.000
Elevation	-0.023701	0.003921	-6.04	0.000
RelativeHumidity	1.7369	0.2387	7.28	0.000
Cloud Cover	-0.14951	0.04873	-3.07	0.003
logSunshineHours	20.458	7.885	2.59	0.011
WindSpeed	-0.3685	0.1442	-2.56	0.012

S = 1.96606 R-Sq = 55.7 % R-Sq(adj) = 51.7 %

Analysis of Variance

Source	DF	SS	MS	F	P
Regression	11	598.001	54.364	14.06	0.000
Residual Error	123	475.445	3.865		
Total	134	1073.446			

Source	DF	Seq SS
FrostDays	1	83.134
MMaxTemp	1	21.285
squOrgMatter	1	3.009
squSand%	1	10.826
logSilt%	1	1.109
logClay%	1	49.758
Elevation	1	124.667
RelativeHumidity	1	226.323
Cloud Cover	1	43.140
logSunshineHours	1	9.514
WindSpeed	1	25.237

Unusual Observations

Obs	FrostDays	RotationYield(odt)	Fit	SE Fit	Residual	St Resid
5	12.8	11.275	6.175	0.470	5.100	2.67R
6	12.8	10.855	6.175	0.470	4.680	2.45R
36	18.0	8.330	12.228	0.756	-3.898	-2.15R
52	12.4	6.455	10.773	0.395	-4.318	-2.24R
60	9.3	12.796	8.771	0.659	4.025	2.17R
110	11.0	7.189	12.169	0.764	-4.981	-2.75R
120	7.3	11.559	7.727	0.645	3.832	2.06R

R denotes an observation with a large standardized residual.

Appendix B: Minitab linear regression outputs

S. viminalis x S. viminalis, genotype Q83. First rotation.

The regression equation

RotationYield(odt) = 33.5 - 0.0153 squOrgMatter - 0.504 RelativeHumidity_1 - 0.959 MMaxTemp_1 + 1.81 SunshineHours_1 + 7.95 logFrostDays + 0.000038 squAvailH2O + 2.92 logSlope + 20.0 logpH

138 cases used, 6 cases contain missing values

Predictor	Coef	SE Coef	T	P
Constant	33.50	13.57	2.47	0.015
squOrgMatter	-0.015348	0.006304	-2.43	0.016
RelativeHumidity_1	-0.5044	0.1635	-3.09	0.002
MMaxTemp_1	-0.9593	0.2202	-4.36	0.000
SunshineHours_1	1.8138	0.5792	3.13	0.002
logFrostDays	7.947	1.111	7.15	0.000
squAvailH2O	0.00003831	0.00000680	5.64	0.000
logSlope	2.9158	0.7832	3.72	0.000
logpH	20.037	5.281	3.79	0.000

S = 2.24094 R-Sq = 50.6 % R-Sq(adj) = 47.6 %

Analysis of Variance

Source	DF	SS	MS	F	P
Regression	8	664.773	83.097	16.55	0.000
Residual Error	129	647.813	5.022		
Total	137	1312.586			

Source	DF	Seq SS
squOrgMatter	1	11.061
RelativeHumidity_1	1	8.090
MMaxTemp_1	1	0.522
SunshineHours_1	1	9.950
logFrostDays	1	344.390
squAvailH2O	1	173.108
logSlope	1	45.349
logpH	1	72.302

Unusual Observations

Obs	squOrgMatter	RotationYield(odt)	Fit	SE Fit	Residual	St Resid
1	225	10.842	7.642	1.021	3.199	1.60 X
2	225	8.280	7.642	1.021	0.638	0.32 X
28	9	12.643	8.235	0.640	4.407	2.05R
90	49	11.055	6.528	0.289	4.526	2.04R
124	100	7.382	11.911	0.725	-4.529	-2.14R
127	49	11.267	6.846	0.578	4.421	2.04R
129	49	1.516	6.846	0.578	-5.330	-2.46R
133	100	12.505	12.589	1.230	-0.084	-0.04 X
134	100	12.673	12.589	1.230	0.084	0.04 X
135	100	11.160	12.589	1.230	-1.429	-0.76 X
144	42	0.663	5.633	0.487	-4.971	-2.27R

R denotes an observation with a large standardized residual.
X denotes an observation whose X value gives it large leverage.

Appendix B: Minitab linear regression outputs

S. viminalis x S. viminalis, genotype Q83. Second rotation.

The regression equation

RotationYield(odt) = - 160 + 1.69 RelativeHumidity - 0.000002 squGDDSummer + 0.0189 squOrgMatter + 5.78 logAvailH2O_1 + 4.57 logSlope + 3.82 SunshineHours

129 cases used, 7 cases contain missing values

Predictor	Coef	SE Coef	T	P
Constant	-160.16	29.07	-5.51	0.000
RelativeHumidity	1.6940	0.3432	4.94	0.000
squGDDSummer	-0.00000187	0.00000061	-3.09	0.003
squOrgMatter	0.018915	0.006758	2.80	0.006
logAvailH2O_1	5.784	2.042	2.83	0.005
logSlope	4.5657	0.9029	5.06	0.000
SunshineHours	3.820	1.021	3.74	0.000

S = 2.79244 R-Sq = 40.3 % R-Sq(adj) = 37.4 %

Analysis of Variance

Source	DF	SS	MS	F	P
Regression	6	643.13	107.19	13.75	0.000
Residual Error	122	951.32	7.80		
Total	128	1594.45			

Source	DF	Seq SS
RelativeHumidity	1	162.52
squGDDSummer	1	21.46
squOrgMatter	1	76.96
logAvailH2O_1	1	80.23
logSlope	1	192.91
SunshineHours	1	109.05

Unusual Observations

Obs	RelativeHumidity	RotationYield(odt)	Fit	SE Fit	Residual	St Resid
1	85.0	14.117	12.360	1.168	1.758	0.69 X
2	85.0	12.448	12.360	1.168	0.089	0.03 X
3	85.0	15.536	12.360	1.168	3.176	1.25 X
4	85.0	16.156	9.731	0.467	6.424	2.33R
7	85.0	5.939	11.581	0.475	-5.642	-2.05R
56	85.2	15.910	9.854	0.390	6.055	2.19R
87	86.1	16.313	10.149	0.479	6.165	2.24R
94	86.5	15.503	9.879	0.643	5.624	2.07R
130	86.0	7.205	12.762	0.964	-5.556	-2.12R

R denotes an observation with a large standardized residual.
X denotes an observation whose X value gives it large leverage.

Appendix C: PLS outputs

(1) Summary of PLS regression outputs for each intensively grown genotype from the SRC field trials network. Results refer to version 1.0 models, used in Chapter 2.

(2) PLS regression outputs for each of the three genotypes (Jorunn, Q83 and Trichobel) used in scenario development: (i) scaled PLS scatter plots for first vs. second components, (ii) scaled variable importance plots and (iii) scaled coefficient correlation plots. Results refer to version 1.0 models, used in Chapter 2.

(3) Unscaled PLS regression coefficient equations. Results refer to version 1.0 models, used in Chapter 2.

(4) Unscaled PLS regression coefficient equations. Results refer to version 2.0 models, used in Chapter 3.

(5) Residual analysis for unscaled PLS regression equations for Trichobel, first rotation. Results refer to version 1.0 models, used in Chapter 2: (i) residual list by site and (ii) residual normal probability plot

(1) Summary of observed vs. computed mean yields (odt ha^{-1} yr^{-1}), model r^2 scores and three highest ranking PLS VIP scores for poplar genotypes Beaupré, Ghoy and Trichobel and willow genotypes Germany, Jorunn and Q83. All VIP scores are significant to $p < 0.05$. Relative percentile contributions for variable importance plot (VIP) scores given in parentheses. Root mean standard errors (RMSE) for mean computed yields and standard deviations for mean observed yields given in parentheses. Values with the same letter are not statistically different ($p > 0.05$) using t-test.

Genus	Genotype	Rotation	Mean yield		r^2	VIP scores
			Observed	Computed		
Populus	Beaupré	First	**7.34** (2.33) [bc]	**7.42** (1.25) [bc]	0.70	*elevation (4.2), feb temp (3.5), oct ppt (3.1)*
Populus	Ghoy	First	**6.45** (2.47) [a]	**6.50** (1.38) [a]	0.69	*slope (4.1), elevation (3.3), feb temp (3.2)*
Populus	Trichobel	First	**9.08** (2.67) [d]	**9.31** (1.37) [d]	0.68	*feb temp (3.5), slope (3.4), jun ppt (3.3)*
Salix	Germany	First	**7.14** (2.94) [ab]	**7.05** (1.83) [ab]	0.55	*mar ppt (3.7), slope (3.6), feb ppt (3.6)*
Salix	Jorunn	First	**9.09** (3.01) [d]	**9.29** (2.09) [d]	0.51	*soil pH 25-50cm (4.6), soil pH 0-25cm (3.9), elevation (3.6)*
Salix	Q83	First	**8.03** (3.23) [c]	**8.21** (2.09) [c]	0.58	*mar ppt (3.5), slope (3.3), sep ppt (3.2)*
Populus	Beaupré	Second	**4.87** (2.43) [a]	**4.90** (1.38) [a]	0.69	*soil silt % (4.7), soil sand % (3.9) and jan temp (3.7)*
Populus	Ghoy	Second	**5.77** (2.46) [ab]	**5.85** (1.24) [a]	0.74	*elevation (4.1), soil pH 0-25cm (3.9) and annual ppt (3.7)*
Populus	Trichobel	Second	**9.59** (2.78) [d]	**9.70** (1.38) [b]	0.75	*jan temp(3.9), oct temp (3.8) and aug temp (3.2)*
Salix	Germany	Second	**7.46** (4.00) [c]	**7.49** (2.46) [c]	0.61	*feb temp (3.9), frost days (3.8) and jul ppt (3.8)*
Salix	Jorunn	Second	**9.15** (2.70) [d]	**9.30** (1.77) [d]	0.61	*elevation (4.8), avery class 8 (4.0) and jan temp (3.7)*
Salix	Q83	Second	**10.71** (3.74) [e]	**10.72** (1.38) [e]	0.58	*avery class 5 (4.7), dec temp (4.0) and avery class 8 (3.9)*

(2a) *S. triandra x S. viminalis*, genotype Jorunn. First rotation.

(i)

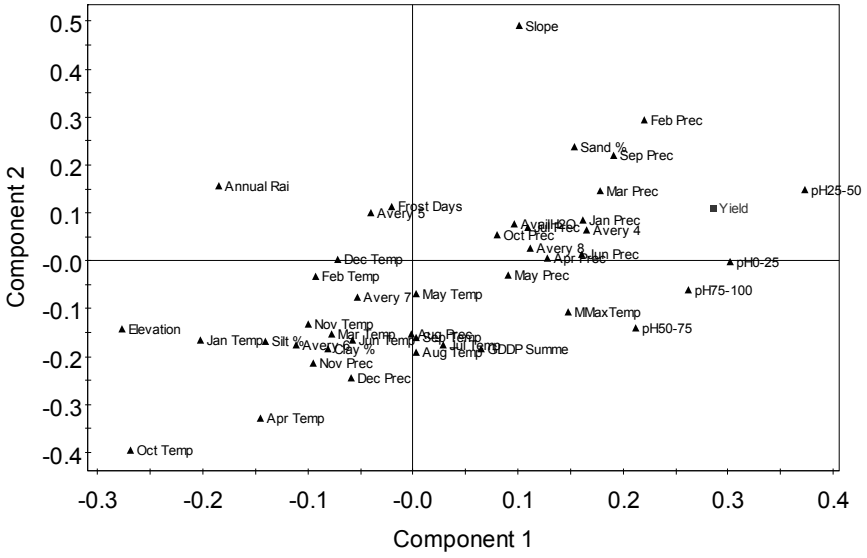

(ii)

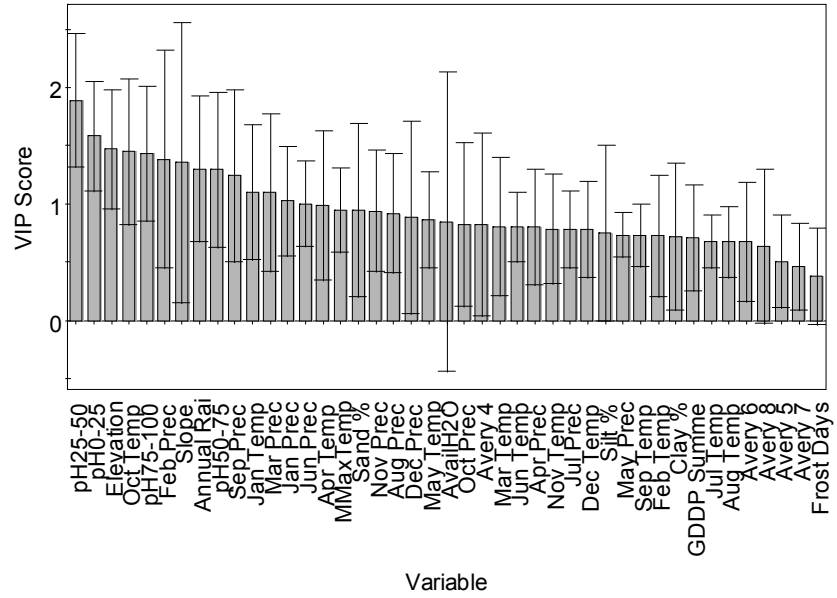

(iii)

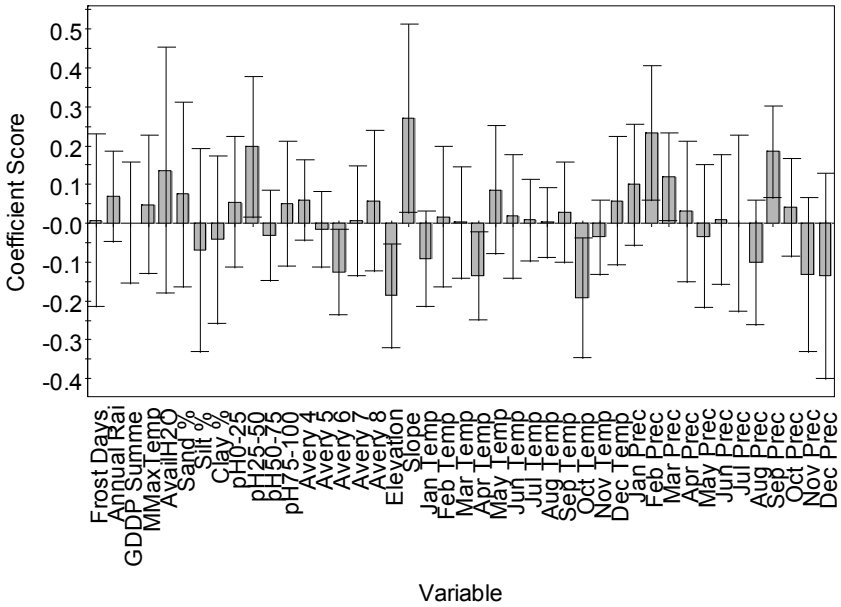

(2b) *S. triandra x S. viminalis,* genotype Jorunn. Second rotation.

(i)

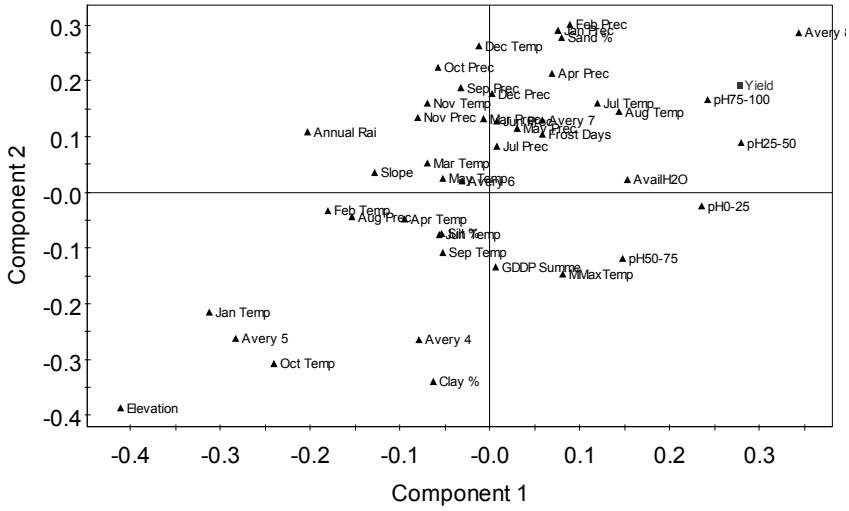

(ii)

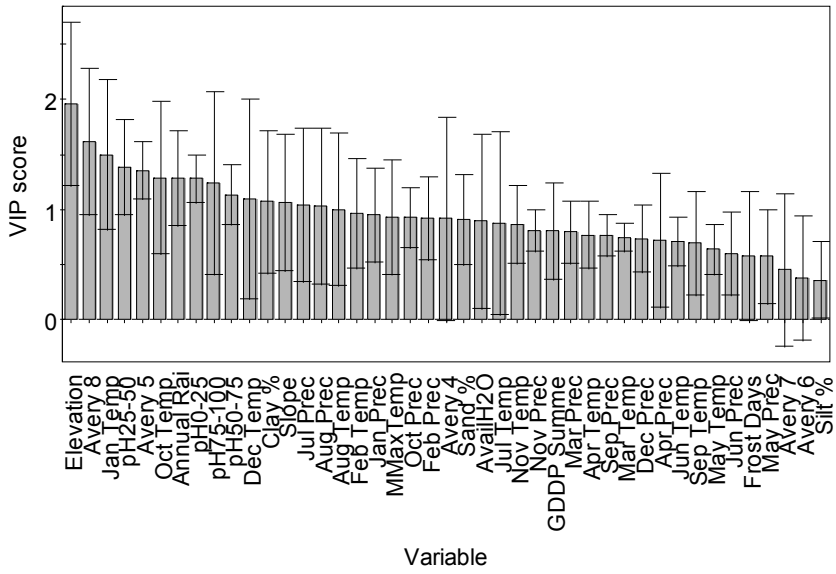

(iii)

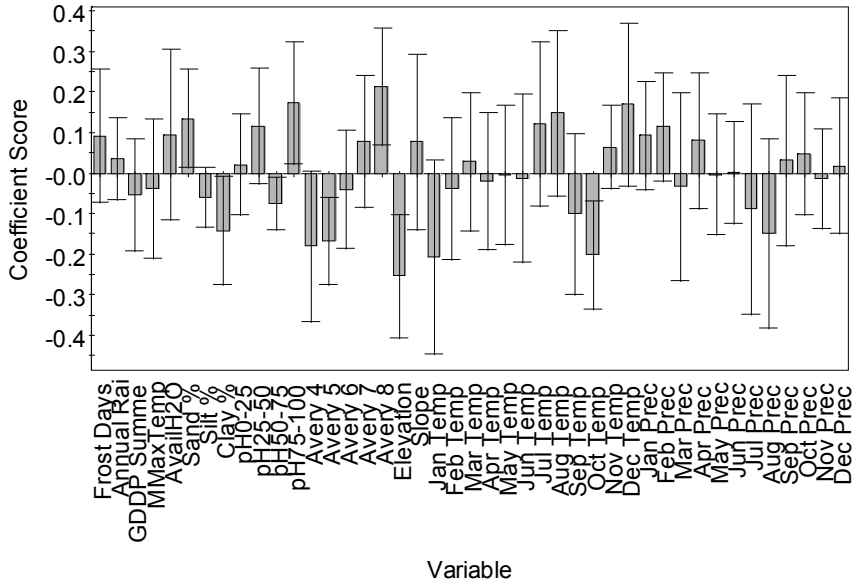

(2c) *S. viminalis x S. viminalis,* genotype Q83. First rotation.

(i)

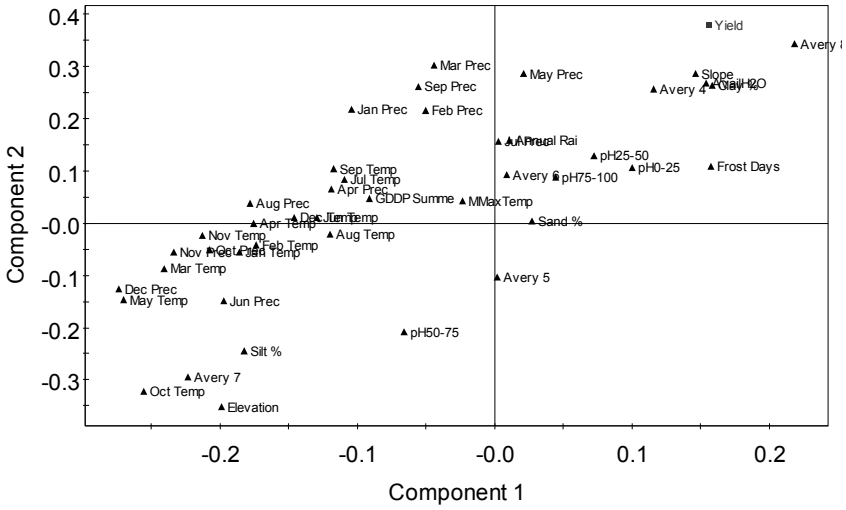

(ii)

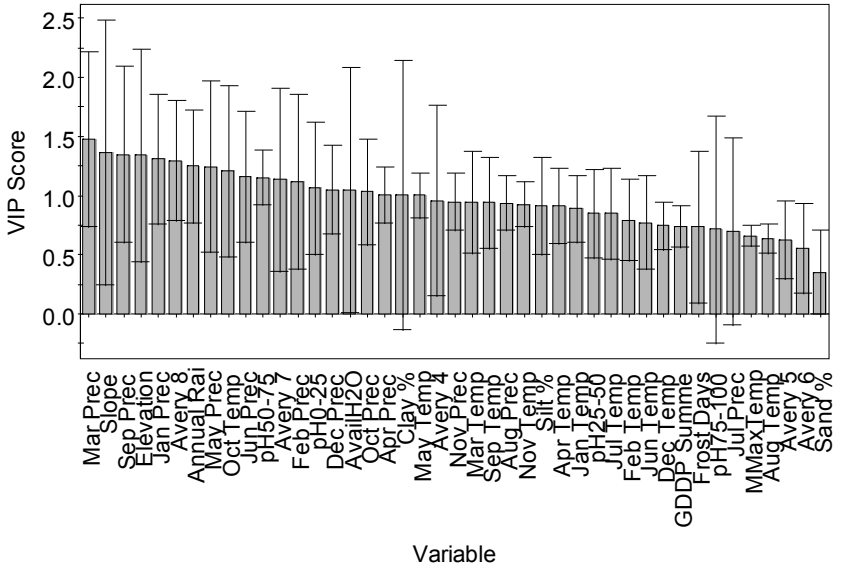

(iii)

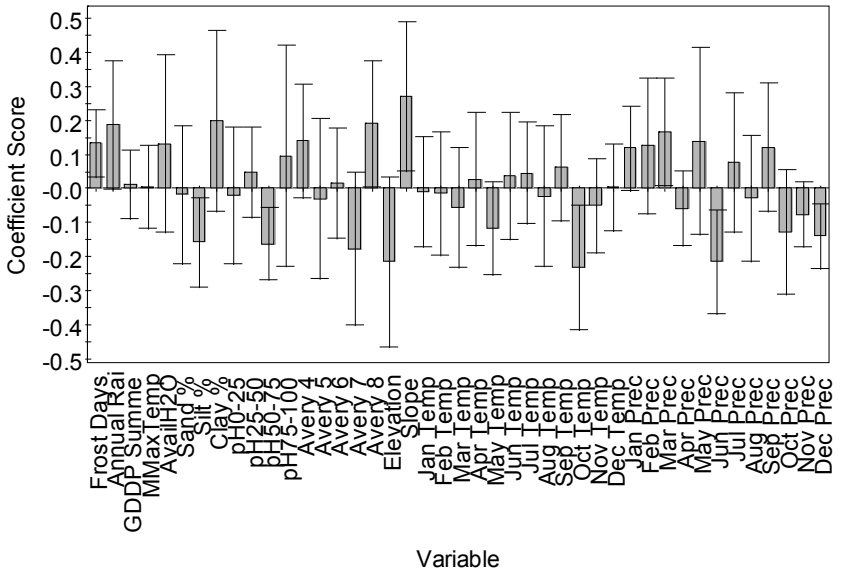

(2d) *S. viminalis x S. viminalis,* genotype Q83. Second rotation.

(i)

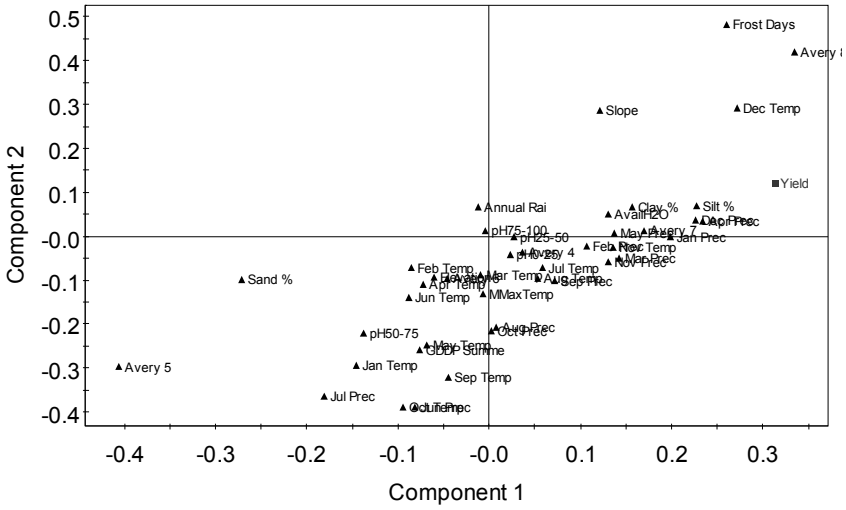

(ii)

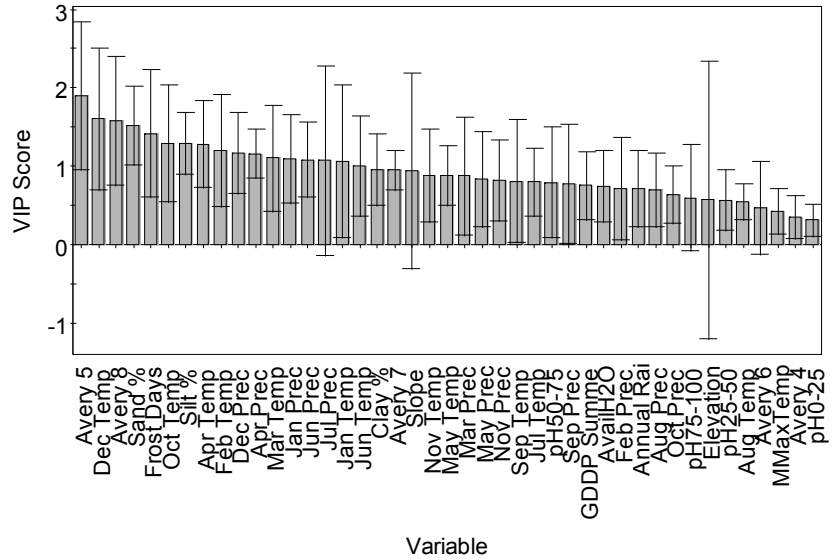

(iii)

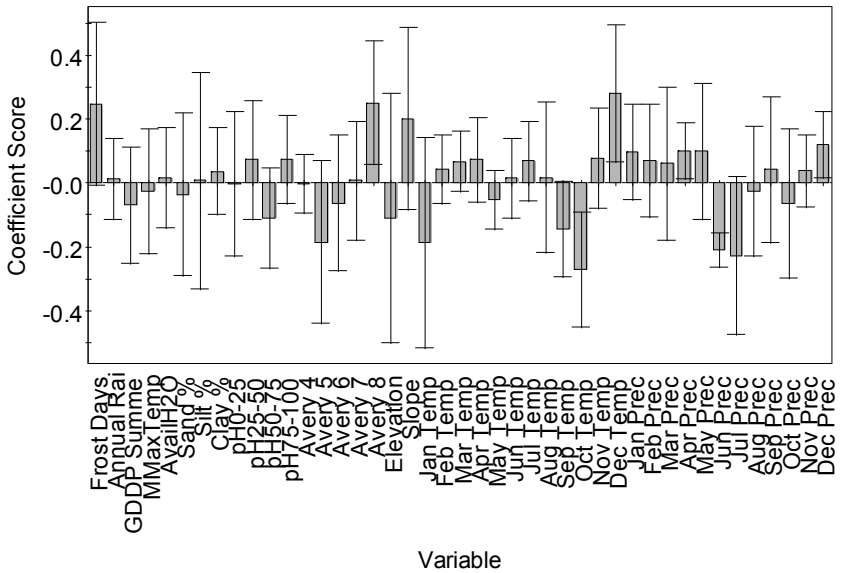

(2e) *P. trichocarpa,* genotype Trichobel. First rotation.

(i)

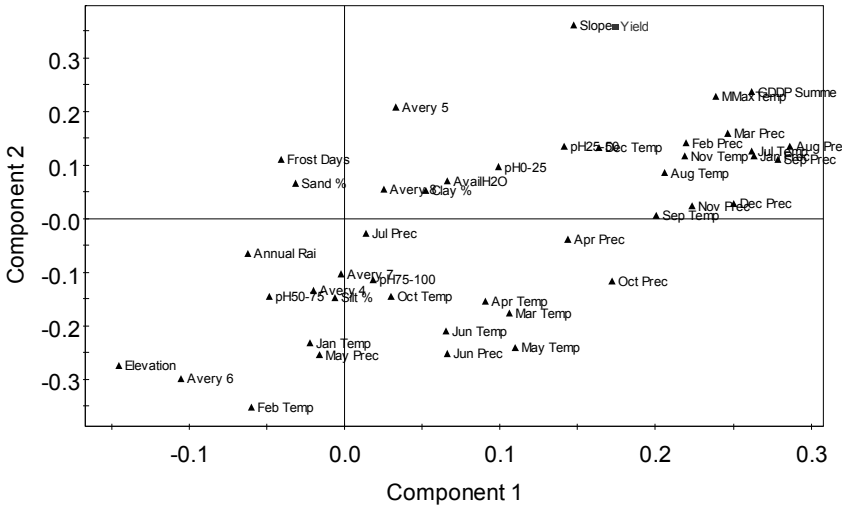

(ii)

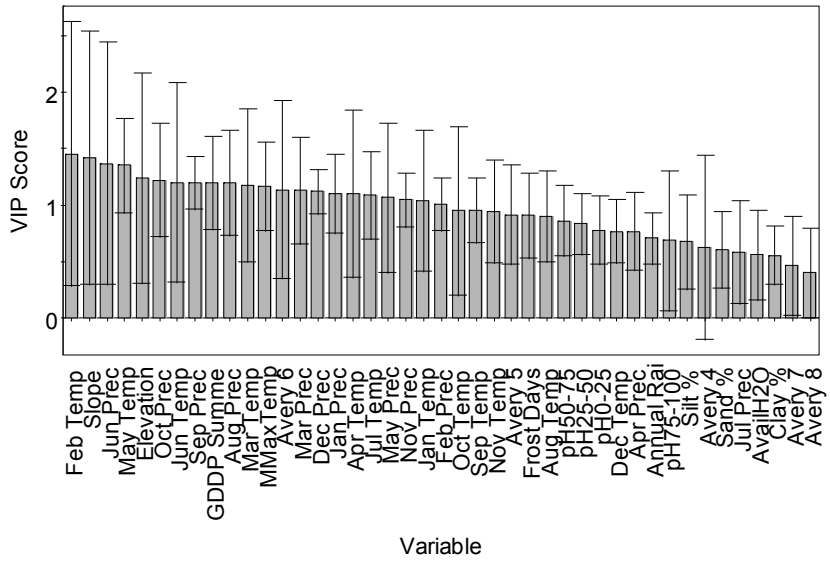

(iii)

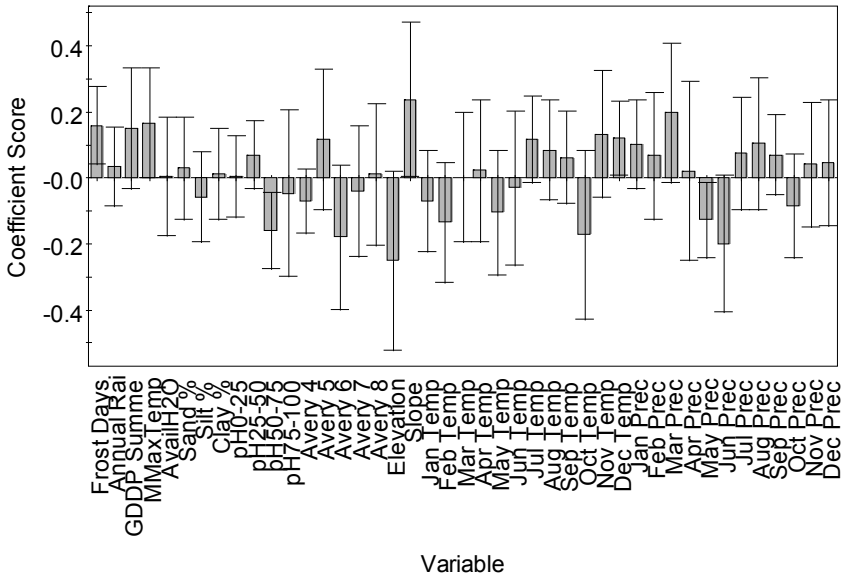

(2f) *P. trichocarpa,* genotype Trichobel. Second rotation.

(i)

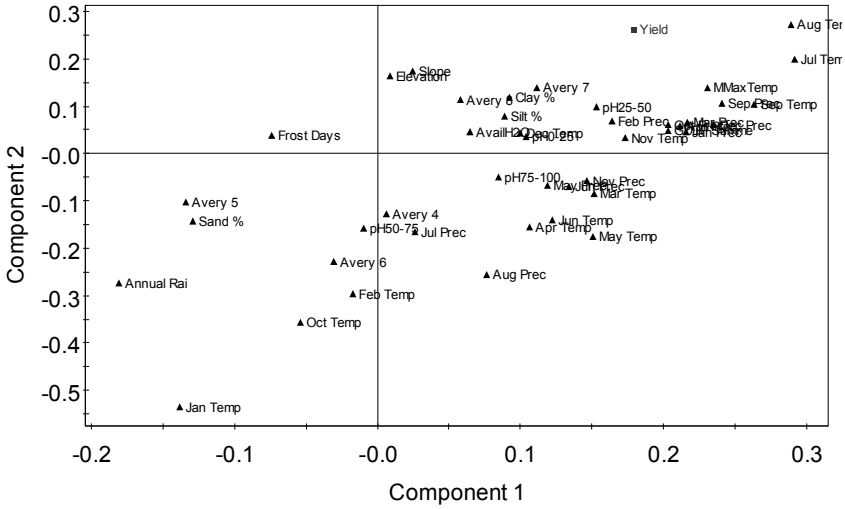

(ii)

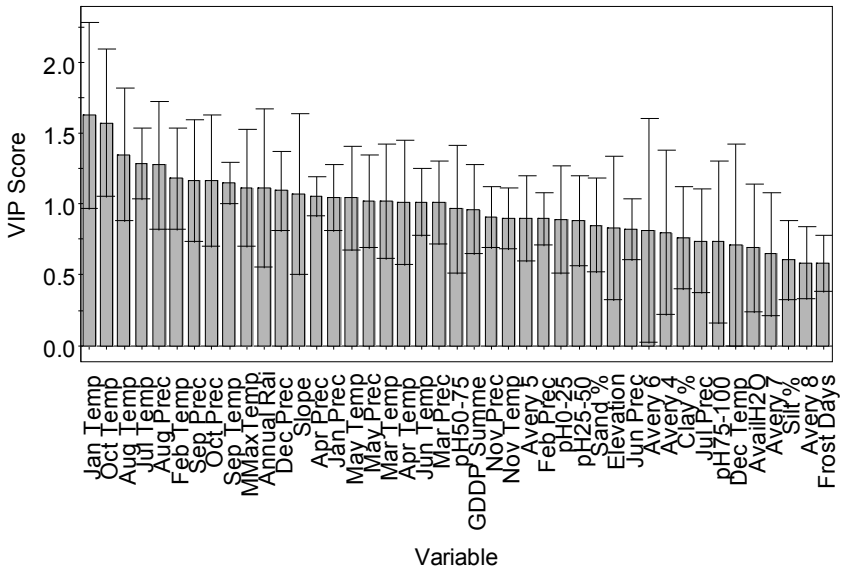

(iii)

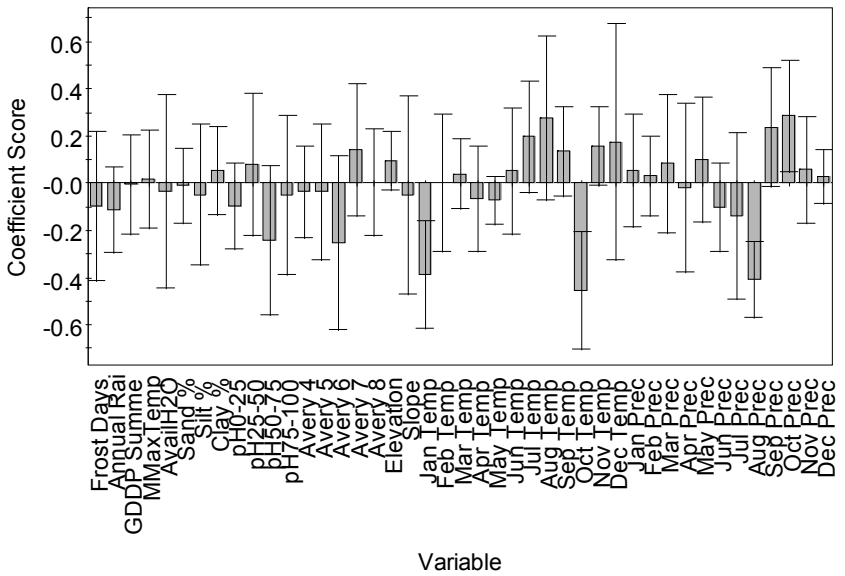

(3) PLS regression coefficient equations, version 1 (as used in Chapter 2).

S. viminalis x *S. viminalis*, genotype Jorunn. First Rotation.
r^2 = 0.48, RMSE = 2.15, Mean = 9.29, SD = 2.91
jorone = -4.05194 + ([frodays] * -0.0131306) + ([annrain] * 0.000808998) + ([gdd] * -8.88182e-005) + ([maxtemp] * 0.084389) + ([logsoilwater] * 2.17003) + ([logsoilsand] * -0.646827) + ([soilsilt] * -0.0195477) + ([logsoilclay] * -0.27235) + ([ph025] * 0.235176) + ([ph2550] * 0.723179) + ([ph5075] * -0.17232) + ([ph75100] * 0.0569613) + ([avery4] * 1.05837) + ([avery5] * -0.0255743) + ([avery6] * -1.8568) + ([avery7] * 0.0414784) + ([avery8] * 0.383394) + ([elevation] * -0.0111561) + ([slope] * 0.356265) + ([t_jan] * -0.318191) + ([t_feb] * 0.0206947) + ([t_mar] * -0.0246978) + ([t_apr] * -0.250124) + ([t_may] * 0.107518) + ([t_jun] * 0.0153818) + ([t_jul] * 0.0501574) + ([t_aug] * 0.0176812) + ([t_sep] * 0.0711848) + ([t_oct] * -0.46815) + ([t_nov] * -0.0440073) + ([t_dec] * 0.129035) + ([logp_jan] * 0.572347) + ([logp_feb] * 1.03665) + ([logp_mar] * 1.29307) + ([logp_apr] * -0.0639249) + ([logp_may] * -0.237712) + ([logp_jun] * -0.08438) + ([logp_jul] * -0.340816) + ([logp_aug] * -0.325371) + ([logp_sep] * 1.43638) + ([p_oct] * 0.000479506) + ([p_nov] * -0.00605406) + ([logp_dec] * 0.273783)

S. viminalis x *S. viminalis*, genotype Jorunn. Second Rotation.
r^2 = 0.60, RMSE = 1.79, Mean = 9.30, SD = 2.78
jortwo = 0.234032 + ([frodays] * 0.066503) + ([annrain] * 0.000458415) + ([gdd] * -0.000743154) + ([maxtemp] * -0.0826902) + ([logsoilwater] * 2.23324) + ([logsoilsand] * 0.790928) + ([soilsilt] * -0.0172298) + ([logsoilclay] * -1.93492) + ([ph025] * 0.0927317) + ([ph2550] * 0.400101) + ([ph5075] * -0.266207) + ([ph75100] * 0.634814) + ([avery4] * -3.25454) + ([avery5] * -0.959507) + ([avery6] * -0.653817) + ([avery7] * 0.604385) + ([avery8] * 1.42397) + ([elevation] * -0.0135553) + ([slope] * 0.115703) + ([t_jan] * -0.591079) + ([t_feb] * -0.0908008) + ([t_mar] * 0.0185792) + ([t_apr] * -0.0383059) + ([t_may] * -0.033695) + ([t_jun] * -0.0377853) + ([t_jul] * 0.280862) + ([t_aug] * 0.300089) + ([t_sep] * -0.223989) + ([t_oct] * -0.407867) + ([t_nov] * 0.211499) + ([t_dec] * 0.514164) + ([logp_jan] * -0.0108132) + ([logp_feb] * 0.406851) + ([logp_mar] * -0.0674893) + ([logp_apr] * 0.158021) + ([logp_may] * -0.436211) + ([logp_jun] * 0.148076) + ([logp_jul] * -0.140236) + ([logp_aug] * -0.422128) + ([logp_sep] * 0.299544) + ([p_oct] * 0.000929579) + ([p_nov] * -0.000683129) + ([logp_dec] * 0.533908)

S. burjatica, genotype Germany. First Rotation.
r^2 = 0.52, RMSE = 1.90, Mean = 7.05, SD = 2.68
gerone = 0.287507 + ([frodays] * 0.0332649) + ([annrain] * 0.00166492) + ([gdd] * -0.000365884) + ([maxtemp] * -0.0187126) + ([logsoilwater] * 1.7209) + ([logsoilsand] * 0.096187) + ([soilsilt] * -0.0180997) + ([logsoilclay] * 1.3308) + ([ph025] * -0.0330896) + ([ph2550] * 0.271026) + ([ph5075] * -0.452377) + ([ph75100] * 0.465977) + ([avery4] * 2.1372) + ([avery5] * 0.518727) + ([avery6] * -0.0154196) + ([avery7] * -0.644488) + ([avery8] * -0.386324) + ([elevation] * -0.0140035) + ([slope] * 0.323551) + ([t_jan] * -0.378277) + ([t_feb] * -0.0594207) + ([t_mar] * -0.00682021) + ([t_apr] * -0.378277) + ([t_may] * -0.114986) + ([t_jun] * -0.0010295) + ([t_jul] * 0.248878) + ([t_aug] * 0.0441509) + ([t_sep] * 0.179848) + ([t_oct] * -0.482727) + ([t_nov] * 0.273628) + ([t_dec] * -0.0248839) + ([logp_jan] * 0.483981) + ([logp_feb] * 0.642316) + ([logp_mar] * 2.08149) + ([logp_apr] * -0.0249154) + ([logp_may] * 1.5186) + ([logp_jun] * -1.02753) + ([logp_jul] * -1.32883) + ([logp_aug] * -1.25105) + ([logp_sep] * 0.576541) + ([p_oct] * -0.00397752) + ([p_nov] * -0.00471524) + ([logp_dec] * -0.422208)

S. burjatica, genotype Germany. Second Rotation.
r^2 = 0.61, RMSE = 2.49, Mean = 7.49, SD = 3.89
gertwo = -5.01814 + ([frodays] * 0.388644) + ([annrain] * -0.000794738) + ([gdd] * -0.00285205) + ([maxtemp] * -0.0232194) + ([logsoilwater] * 2.72482) + ([logsoilsand] * -1.18325) + ([soilsilt] * -0.00756348) + ([logsoilclay] * 0.100994) + ([ph025] * -0.0843541) + ([ph2550] * 0.870938) + ([ph5075] * -0.0259316) + ([ph75100] * 0.873907) + ([avery4] * -0.470577) + ([avery5] * 0.359745) + ([avery6] * 3.93244) + ([avery7] * -0.578406) + ([avery8] * -0.371936) + ([elevation] * -0.0162643) + ([slope] * 0.330522) + ([t_jan] * -0.287135) + ([t_feb] * -0.38163) + ([t_mar] * 0.225636) + ([t_apr] * -0.0534431) + ([t_may] * -0.3903) + ([t_jun] * -0.00311799) + ([t_jul] * 0.318617) + ([t_aug] * 0.539071) + ([t_sep] * -0.590522) + ([t_oct] * -1.25746) + ([t_nov] * 0.743119) + ([t_dec] * 1.61341) + ([logp_jan] * -

0.302987) + ([logp_feb] * 0.358059) + ([logp_mar] * 0.47524) + ([logp_apr] * 0.554866) + ([logp_may] * 1.68621) + ([logp_jun] * -1.99143) + ([logp_jul] * -3.40901) + ([logp_aug] * -1.43118) + ([logp_sep] * -0.535598) + ([p_oct] * -0.000214865) + ([p_nov] * 0.00532595) + ([logp_dec] * 4.06484)

S. triandra x *S. viminalis*, genotype Q83. First Rotation.
r^2 = 0.58, RMSE = 2.09, Mean = 8.21, SD = 3.18
q83one = 0.361422 + ([frodays] * 0.125191) + ([annrain] * 0.00251045) + ([gdd] * 0.000182944) + ([maxtemp] * 0.00359033) + ([logsoilwater] * 1.9771) + ([logsoilsand] * -0.293949) + ([soilsilt] * -0.0415838) + ([logsoilclay] * 3.06201) + ([ph025] * -0.0965463) + ([ph2550] * 0.188876) + ([ph5075] * -0.654809) + ([ph75100] * 0.367187) + ([avery4] * 2.76936) + ([avery5] * -0.0795706) + ([avery6] * 0.268027) + ([avery7] * -1.42276) + ([avery8] * 1.73321) + ([elevation] * -0.0138382) + ([slope] * 0.371522) + ([t_jan] * -0.029526) + ([t_feb] * -0.0207049) + ([t_mar] * -0.116428) + ([t_apr] * 0.047602) + ([t_may] * -0.192013) + ([t_jun] * 0.061877) + ([t_jul] * 0.147157) + ([t_aug] * -0.0537363) + ([t_sep] * 0.135155) + ([t_oct] * -0.604788) + ([t_nov] * -0.0992607) + ([t_dec] * -0.00935407) + ([logp_jan] * 0.704864) + ([logp_feb] * 0.262839) + ([logp_mar] * 1.64078) + ([logp_apr] * -0.276112) + ([logp_may] * 1.80661) + ([logp_jun] * -1.38689) + ([logp_jul] * 1.15862) + ([logp_aug] * -0.786841) + ([logp_sep] * 1.37027) + ([p_oct] * -0.00458692) + ([p_nov] * -0.00341369) + ([logp_dec] * -0.928352)

S. triandra x *S. viminalis*, genotype Q83. Second Rotation.
r^2 = 0.59, RMSE = 2.34, Mean = 10.72, SD = 3.60
q83two = 0.0532673 + ([frodays] * 0.291391) + ([annrain] * 0.000492852) + ([gdd] * -0.00171879) + ([maxtemp] * -0.129241) + ([soilwater] * 3.04594) + ([logsoilsand] * -0.150755) + ([soilsilt] * 0.00376958) + ([logsoilclay] * 0.657515) + ([ph025] * 0.0334221) + ([ph2550] * 0.359308) + ([ph5075] * -0.41001) + ([ph75100] * 0.506039) + ([avery4] * 0.191539) + ([avery5] * -1.33528) + ([avery6] * -0.649919) + ([avery7] * 0.00153764) + ([avery8] * 2.29719) + ([elevation] * -0.00622747) + ([slope] * 0.383562) + ([t_jan] * -0.630376) + ([t_feb] * 0.157522) + ([t_mar] * 0.156207) + ([t_apr] * 0.160798) + ([t_may] * -0.103917) + ([t_jun] * 0.00127778) + ([t_jul] * 0.206967) + ([t_aug] * 0.0454115) + ([t_sep] * -0.402579) + ([t_oct] * -0.783147) + ([t_nov] * 0.391544) + ([t_dec] * 1.2621) + ([logp_jan] * -0.328155) + ([logp_feb] * -0.280968) + ([logp_mar] * 0.348253) + ([logp_apr] * 0.933554) + ([logp_may] * 2.1215) + ([logp_jun] * -2.2024) + ([logp_jul] * -1.73835) + ([logp_aug] * 1.12065) + ([logp_sep] * -0.550731) + ([logp_oct] * -3.82083e-005) + ([p_nov] * 0.00359994) + ([p_dec] * 1.44642)

P. deltoides x *P. nigra*, genotype Ghoy. First Rotation.
r^2 = 0.69, RMSE = 1.36, Mean = 6.50, SD = 2.40
ghoone = 4.74776+ ([frodays] * 0.163357) + ([annrain] * 0.00117595) + ([gdd] * 0.00179694) + ([maxtemp] * 0.112003) + ([logsoilwater] * 2.14773) + ([soilsand] * 0.00365449) + ([soilsilt] * -0.0109322) + ([logsoilclay] * 0.973587 + ([ph025] * 0.0386439) + ([ph2550] * 0.389262) + ([ph5075] * -0.303649) + ([ph75100] * 0.104913) + ([avery4] * -0.104913) + ([avery5] * 0.797513) + ([avery6] * -0.117464) + ([avery7] * -1.24218) + ([avery8] * 0.246383) + ([elevation] * -0.0161496) + ([slope] * 0.368921) + ([t_jan] * -0.249646) + ([t_feb] * -0.284392) + ([t_mar] * -0.0411094) + ([t_apr] * -0.0376183) + ([t_may] * -0.195188) + ([t_jun] * 0.0440273) + ([t_jul] * 0.0140802) + ([t_aug] * 0.153956) + ([t_sep] * 0.0406565) + ([t_oct] * -0.1102534) + ([t_nov] * 0.0561654) + ([t_dec] * 0.627696) + ([logp_jan] * -0.303463) + ([logp_feb] * -0.298378) + ([logp_mar] * 0.234483) + ([logp_apr] * 0.16088) + ([logp_may] * 3.39797) + ([logp_jun] * -1.701) + ([logp_jul] * 1.01281) + ([logp_aug] * 0.208641) + ([logp_sep] * 0.316407) + ([p_oct] * -0.00523121) + ([p_nov] * -0.000363058) + ([p_dec] * 0.00394733)

P. deltoides x *P. nigra*, genotype Ghoy. Second Rotation.
r^2 = 0.75, RMSE = 1.22, Mean = 5.85, SD = 2.39
ghotwo = -2.20811 + ([frodays] * 0.21771) + ([annrain] * -0.001114) + ([gdd] * -0.000113424) + ([maxtemp] * -0.0278501) + ([soilwater] * 0.000826911) + ([logsoilsand] * 0.648701) + ([soilsilt] * -0.028436) + ([logsoilclay] * 0.845207) + ([ph025] * 0.262891) + ([ph2550] * 0.267746) + ([ph5075] * -0.197427) + ([ph75100] * -0.137369) + ([avery4] * 1.0585) + ([avery5] * 0.850516) + ([avery6] * -1.89521) + ([avery7] * -0.582295) + ([avery8] * -0.565644) + ([elevation] * -0.0170226) + ([slope] * 0.15233) + ([t_jan] * -0.434821) + ([t_feb] * -0.0854586) + ([t_mar] * 0.115347) + ([t_apr] * -0.0352185) + ([t_may] * -0.28249) + ([t_jun] * 0.0453417) + ([t_jul] * 0.0618093) + ([t_aug] * 0.43874)

+ ([t_sep] * 0.230519) + ([t_oct] * -0.413128) + ([t_nov] * -0.164894) + ([t_dec] * 0.677126) + ([logp_jan] * 0.00319195) + ([logp_feb] * -0.795256) + ([logp_mar] * 1.39053) + ([logp_apr] * 0.556393) + ([logp_may] * 1.5973) + ([logp_jun] * -0.231425) + ([p_jul] * -0.00556119) + ([logp_aug] * -2.15493) + ([logp_sep] * -0.157495) + ([p_oct] * -0.00266724) + ([p_nov] * 0.00189917) + ([p_dec] * 0.00640207)

P. trichocarpa x *P. deltoides*, genotype Beaupré. First Rotation.
r^2 = 0.71, RMSE = 1.25, Mean = 7.42, SD = 2.25
beaone = -9.62377 + ([frodays] * 0.248925) + ([annrain] * 0.00123089) + ([gdd] * 0.00126049) + ([maxtemp] * 0.0274979) + ([logsoilwater] * -1.15765) + ([soilsand] * 0.0117805) + ([soilsilt] * 0.002005) + ([logsoilclay] * 0.908237) + ([ph025] * 0.274846) + ([ph2550] * 0.396706) + ([ph5075] * -0.398795) + ([ph75100] * 0.325811) + ([avery4] * -0.658783) + ([avery5] * 0.813005) + ([avery6] * -0.291084) + ([avery7] * -0.547004) + ([avery8] * -0.554006) + ([elevation] * -0.0200557) + ([slope] * 0.378932) + ([t_jan] * -0.372438) + ([t_feb] * -0.391847) + ([t_mar] * 0.0425374) + ([t_apr] * 0.0326831) + ([t_may] * -0.256865) + ([t_jun] * 0.0660734) + ([t_jul] * 0.0354987) + ([t_aug] * 0.224225) + ([t_sep] * 0.138895) + ([t_oct] * -0.146489) + ([t_nov] * 0.346767) + ([t_dec] * 0.2374) + ([logp_jan] * -0.639789) + ([logp_feb] * -0.696145) + ([logp_mar] * -0.284812) + ([logp_apr] * -0.393977) + ([logp_may] * 4.012) + ([logp_jun] * -1.23083) + ([logp_jul] * 0.448805) + ([logp_aug] * 2.42967) + ([logp_sep] * -0.621988) + ([p_oct] * -0.00848675) + ([p_nov] * 0.0026017) + ([p_dec] * 0.00258867)

P. trichocarpa x *P. deltoides*, genotype Beaupré. Second Rotation.
r^2 = 0.69, RMSE = 1.39, Mean = 4.90, SD = 2.41
beatwo = 7.26347 + ([frodays] * 0.1206) + ([annrain] * -0.00148361) + ([gdd] * -4.29429e-005) + ([maxtemp] * -0.0842223) + ([soilwater] * -0.00590418) + ([soilsand] * 0.0175496) + ([soilsilt] * -0.047471) + ([logsoilclay] * 1.56642) + ([ph025] * 0.29524) + ([ph2550] * 0.469108) + ([ph5075] * -0.216415) + ([ph75100] * -0.32726) + ([avery4] * 0.0318274) + ([avery5] * 0.31443) + ([avery6] * 0.113787) + ([avery7] * -0.0373279) + ([avery8] * -0.4712) + ([elevation] * -0.00835733) + ([slope] * 0.0746656) + ([t_jan] * -0.740822) + ([t_feb] * -0.0205405) + ([t_mar] * 0.147258) + ([t_apr] * -0.0180718) + ([t_may] * -0.0412225) + ([t_jun] * -0.125804) + ([t_jul] * -0.0366318) + ([t_aug] * 0.259104) + ([t_sep] * 0.243117) + ([t_oct] * -0.493999) + ([t_nov] * -0.163474) + ([t_dec] * 0.231653) + ([logp_jan] * -0.0381214) + ([logp_feb] * 0.380049) + ([logp_mar] * 1.49955) + ([logp_apr] * -0.452736) + ([logp_may] * -0.482167) + ([logp_jun] * -0.229452) + ([p_jul] * -0.0030106) + ([logp_aug] * -0.0506) + ([logp_sep] * -0.760631) + ([p_oct] * -0.0065418) + ([p_nov] * 0.0100777) + ([p_dec] * 0.00449417)

Populus trichocarpa, genotype Trichobel. First Rotation.
r^2 = 0.69, RMSE = 1.40, Mean = 9.31, SD = 2.38
trione = -9.94495 + ([frodays] * 0.113366) + ([annrain] * 0.000481611) + ([gdd] * 0.00136893) + ([maxtemp] * 0.226002) + ([logsoilwater] * 1.16707) + ([soilsand] * 0.00704218) + ([soilsilt] * -0.0106876) + ([logsoilclay] * 0.661475) + ([ph025] * 0.0349708) + ([ph2550] * 0.230885) + ([ph5075] * -0.408876) + ([ph75100] * -0.138465) + ([avery4] * -1.50979) + ([avery5] * 0.767602) + ([avery6] * -2.02973) + ([avery7] * -0.346244) + ([avery8] * -0.0757151) + ([elevation] * -0.0110401) + ([slope] * 0.257038) + ([t_jan] * -0.159302) + ([t_feb] * -0.239877) + ([t_mar] * -0.0128013) + ([t_apr] * 0.0204007) + ([t_may] * -0.135762) + ([t_jun] * -0.0583814) + ([t_jul] * 0.2638) + ([t_aug] * 0.148952) + ([t_sep] * 0.118383) + ([t_oct] * -0.340918) + ([t_nov] * 0.388068) + ([t_dec] * 0.340579) + ([logp_jan] * 0.500554) + ([logp_feb] * 0.271663) + ([logp_mar] * 1.04388) + ([logp_apr] * 0.0941794) + ([logp_may] * -0.900058) + ([logp_jun] * -0.915966) + ([logp_jul] * 1.32218) + ([logp_aug] * 0.820308) + ([logp_sep] * 0.337234) + ([p_oct] * -0.00163432) + ([p_nov] * 0.00276976) + ([p_dec] * 0.00249386)

Populus trichocarpa, genotype Trichobel. Second Rotation.
r^2 = 0.75, RMSE = 1.39, Mean = 9.70, SD = 2.70
tritwo = 4.74776+ ([frodays] * -0.081672) + ([annrain] * -0.00121922) + ([gdd] * -0.000560637) + ([maxtemp] * -0.00530193) + ([soilwater] * -0.000840345) + ([logsoilsand] * -0.0426604) + ([soilsilt] * -0.00863078) + ([logsoilclay] * 0.744507) + ([ph025] * -0.355737) + ([ph2550] * 0.216917) + ([ph5075] * -0.730717) + ([ph75100] * -0.122473) + ([avery4] * -0.561884) + ([avery5] * 0.000843334) + ([avery6] * -4.66735) + ([avery7] * 0.736418) + ([avery8] * -0.0990643) + ([elevation] * 0.00401825) + ([slope] *

-0.0623873) + ([t_jan] * -1.28128) + ([t_feb] * 0.00768266) + ([t_mar] * 0.0249939) + ([t_apr] * -0.138697) + ([t_may] * -0.0609313) + ([t_jun] * 0.134431) + ([t_jul] * 0.51483) + ([t_aug] * 0.606907) + ([t_sep] * 0.317793) + ([t_oct] * -0.997493) + ([t_nov] * 0.613004) + ([t_dec] * 0.588937) + ([logp_jan] * 0.376723) + ([logp_feb] * 0.451384) + ([logp_mar] * 2.04644) + ([logp_apr] * -0.858813) + ([logp_may] * 1.98602) + ([logp_jun] * -0.693247) + ([logp_jul] * -2.04546) + ([logp_aug] * -4.22408) + ([logp_sep] * 0.555523) + ([logp_oct] * 1.12447) + ([p_nov] * 0.00438921) + ([p_dec] * 0.00452263)

(4) PLS regression coefficient equations, version 2 (as used in Chapter 3)

Poplar trichocarpa, genotype Trichobel. First Rotation.
r2 = 0.54, RMSE = 1.71, Mean = 9.32411, SD = 2.45652
trione = -13.6848 + ([log_fro] * -0.382603) + ([pop_rain] * -0.00240867) + ([annrain] * 0.000115209) + ([gdd] * 0.0000746704) + ([maxtemp] * 0.227953) + ([soilph] * -0.135838) + ([logorgmatter] * -2.52872) + ([logsoilwat_1] * 3.78158) + ([logsoilsand_1] * 1.56835) + ([soilsilt] * 0.0127502) + ([logsoilclay_1] * 1.39843) + ([elevation] * -0.00660766) + ([logslope05] * 3.55226) + ([t_jan] * -0.587214) + ([t_feb] * 0.196833) + ([t_mar] * -0.0183992) + ([t_apr] * 0.309413) + ([t_may] * 0.349667) + ([t_jun] * 0.2617) + ([t_jul] * 0.15922) + ([t_aug] * 0.277035) + ([t_sep] * 0.0057314) + ([t_oct] * -0.173291) + ([t_nov] * -0.276051) + ([t_dec] * -0.688328) + ([p_jan] * -0.0450687) + ([p_feb] * -0.00624746) + ([p_mar] * 0.0716349) + ([p_apr] * -0.0801342) + ([p_may] * 0.044831) + ([p_jun] * -0.00507821) + ([p_jul] * -0.00847487) + ([p_aug] * 0.00713153) + ([p_sep] * 0.0268828) + ([p_oct] * 0.0014137) + ([p_nov] * -0.000558828) + ([p_dec] * 0.0148261)

Poplar trichocarpa, genotype Trichobel. Second Rotation.
r2 = 0.65, RMSE = 1.78, Mean = 9.54579, SD = 2.93591
tritwo = -10.7652 + ([fro_days] * 0.0288345) + ([pop_rain] * -0.00778359) + ([annrain] * 0.000475346) + ([gdd] * -0.000635183) + ([maxtemp] * -0.021863) + ([soilph] * 0.316685) + ([logorgmatter] * -2.52263) + ([soilwater_1] * 0.0191659) + ([soilsand] * 0.00864972) + ([soilsilt] * 0.0273878) + ([soilclay] * -0.0775064) + ([elevation] * 0.0134009) + ([logslope05] * -0.581399) + ([t_jan] * -0.727624) + ([t_feb] * -1.25792) + ([t_mar] * -1.15539) + ([t_apr] * -0.142591) + ([t_may] * 0.273258) + ([t_jun] * 0.827032) + ([t_jul] * 0.322177) + ([t_aug] * 0.43467) + ([t_sep] * 0.894056) + ([t_oct] * -0.380154) + ([t_nov] * 0.810141) + ([t_dec] * -0.305292) + ([p_jan] * 0.0140265) + ([p_feb] * -0.028022) + ([p_mar] * 0.0106755) + ([p_apr] * -0.0243394) + ([p_may] * 0.0290793) + ([p_jun] * 0.0368982) + ([p_jul] * -0.0875102) + ([p_aug] * -0.0225844) + ([p_sep] * -0.0076352) + ([p_oct] * 0.0269025) + ([p_nov] * 0.018538) + ([p_dec] * 0.00239376)

(5) Spatial analysis of residuals for unscaled PLS regression equations for Trichobel, first rotation. Results refer to version 1.0 model, used in Chapter 2

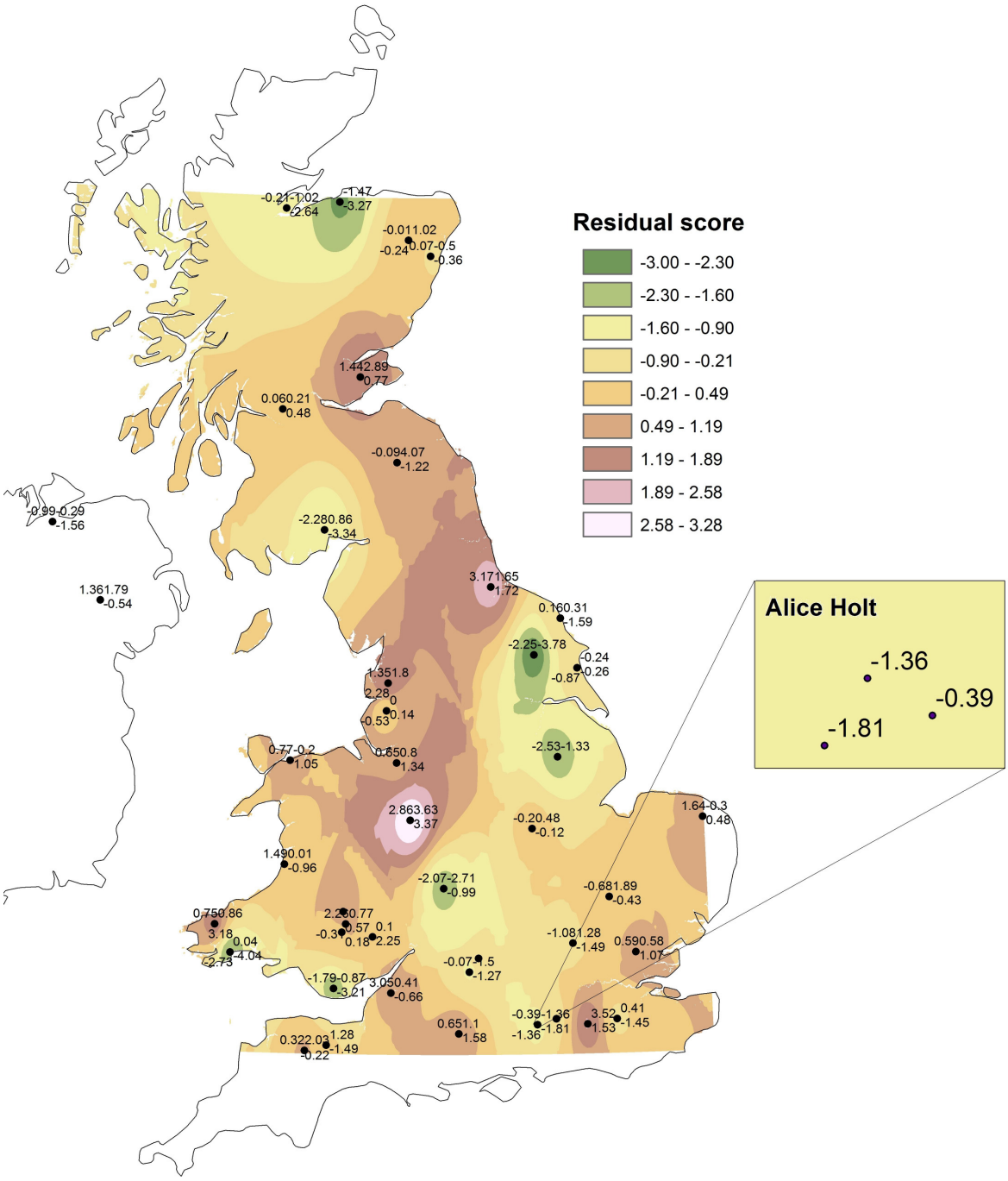

Appendix D: ForestGrowth inputs

Parameter	Units	Value	Reference
1. In situ			
Planting density	stools ha^{-1}	10000	assumed
Rotation length	years	3	assumed
Height of each layer	m	0.25	assumed
Storage used to replenish canopy	days	20	assumed
Day leaf fall	julian day	270 (tri); 250 (gho)	Forest Research (unpublished)
Leaf fall duration	days	40 (tri); 30 (gho)	
Albedo of beam radiation	-	0.25	assumed
Albedo of diffuse radiation	-	0.20	assumed
Maximum rooting depth	cm	110	Friend *et al.* (1991)
Wind height	m	30	assumed
Aero roughness	height ratio	0.123	assumed
Aero displacement	-	0.75	assumed
2. Carbon allocation			
Carbon content	% wet weight	46	Wullschleger *et al.* (1997), Luo *et al.* (2006)
Initial Carbon storage (by soil type)	kg (C)	0.01-0.08	assumed
Total below to above-ground carbon allocation ratio (non-limited)	-	0.07; 0.50 (yr one)	Rytter (2001); Gielen *et al.* (2005); King *et al.* (1999)
Maximum root to [non-storage] stem ratio	-	0.06; 0.15 (yr one)	Gielen *et al.* (2005); Casella (unpublished)
Carbon allocation ([non-storage] stem)	% ag	42; 51 (yr one)	
Carbon allocation (branch)	% ag	10; 4 (yr one)	
Carbon allocation (leaf)	% ag	48; 45 (yr one)	
Carbon allocation (fine root)	% bg	50; 27 (yr one)	
Carbon allocation (coarse root)	% bg	50; 73 (yr one)	
Leaf carbon relocation ratio	-	0.03	assumed
Storage capacity per unit DW parenchyma	-	0.6	Gansert & Sprick (1998); Sauter & Cleve (1994)
Coarse root storage ratio	-	0.675	Nguyen *et al.* (1990)
Fine root turnover rate	% yr^{-1}	115	Coleman *et al.*, (2000); Rytter (2001); Lukac *et al.* (2003)
Wood density	kg m^{-3}	380 (fibre); 500 (starch)	Cochard *et al.* (2007); assumed
Stem height to area increase ratio	-	1000	assumed
Width to height ratio of non-comp crown	-	0.2	assumed
3. Photosynthesis			
Photosynthetic capacity (V_{cmax}) activation energy	J mol^{-1}	68230	Casella (unpublished)
Electron transfer (J_{max}) activation energy	J mol^{-1}	74420	
J_{max} deactivation energy	J mol^{-1}	200000	
J_{max} temperature response	J K^{-1} mol^{-1}	653	
Nitrogen concentration (top of canopy)	mmol m^{-2}	205	
Leaf Nitrogen allocation coefficient	-	1.69	
Leaf Nitrogen (non-photosynthetic)	mmol m^{-2}	25	Reich *et al.* (1995)
Photosynthetic cap to leaf Nitrogen	-	1.16	de Pury & Farquhar (1997)
Stomatal conductance min. CO_2	mol m^{-2} s^{-1}	0.01	assumed
Stomatal conductance slope (Ball-Berry)	-	6.23	Falge *et al.* (1996)
CO_2 compensation at 25^{oC} (no respiration)	mmol mol^{-1}	3.69	de Pury & Farquhar(1997);

			Medlyn *et al.* (2002)
Light extinction coefficient	-	0.366	Casella & Sinoquet (2007)
Light compensation point for photosynthesis	μmol m^{-2} s^{-1}	25	Landhausser & Lieffers (2001)
Maximal transpiration	m^3 (H_2O) m^{-2} (leaf)	0.0008	Lambs *et al.* (2006)
Specific leaf area	m^2 kg^{-1} (C)	18.3	Casella & Ceulemans (2002); Al Afas *et al.* (2005)
Maximum leaf area density (LAD) per layer of the closed canopy	m^2 m^{-3}	2.19 (tri); 1.47 (gho)	Casella & Sinoquet (2007)
Solar constant	W m^{-2}	1366	-
4. Respiration			
Maintenance resp. at 15^{oC} (stem, branch)	kg (C) m^{-2}	0.00068	Gielen *et al.* (2003)
Maintenance resp. at 15^{oC} (coarse root)	kg (C) m^{-2}	0.00068	Desrochers *et al.* (2002)
Maintenance resp. at 15^{oC} (fine root)	kg (C) m^{-2}	0.0068	
Maintenance resp. at 15^{oC} (leaf)	kg (C) m^{-2}	0.0003	Landhausser & Lieffers (2001); Griffin *et al.* (2002)
Construction resp. at 15^{oC} (total plant)	kg (C) kg^{-1} (C)	0.15	Gielen *et al.* (2003)
Q10 (stem, branch)	-	2.1	Forest Research (unpub.); Gielen *et al.* (2003)
Q10 (leaf)	-	2.1	Gielen *et al.* (2003); Ow *et al.* (2008)
Q10 (coarse root)	-	2.1	Forest Research (unpub.); Desrochers *et al.* (2002)
Q10 (fine root)	-	2.5	
5. Pipe theory			
Pipe embolition chance	ratio of pipes/day	0.000001	assumed
Pipe efficiency	%	35	Deckymn *et al.* (2006)
Pipe volume	%	25 (stem); 35 (branch)	Hacke & Sauter (1996); Mencuccini *et al.* (1997)
Fibre volume	%	70 (stem); 60 (branch)	Foulger *et al.* (1975) ; Mencuccini *et al.* (1997)
Pipe radius	m	0.000068	Cochard *et al.* (2007)
Cell wall width	m	0.00000385	Cochard *et al.* (2007); Fang *et al.* (2007)
Pressure gradient	Pa	2500000	Cochard (1992)
Branch length efficiency	-	0.9	assumed
6. Pests and disease			
Start of defoliation	julian day	180	assumed
Defoliation duration	days	30	assumed
Daily defoliation	% of leaves	0.1	assumed

Appendix E: ForestGrowth equations

1. Climate

a. Number from a normal distribution

a1. A number from the normal equation (mean = 0, standard deviation = 1), given from a uniformly random number, is computed with:

$$rn_n = \frac{\left(rn_o^{0.135} - (1 - rn_0)^{0.135}\right)}{0.1975}$$

rn_0	uniformly random number [0,1]
rn_n	number from the normal equation [0,1]

b. Air temperature

b1. Mean daily air temperature (°C):

$$T_J^{est} = XT_{mT}^{obs} + \delta T_{mT}^{obs} \bullet (T_{J-1}^{est} - XT_{mT}^{obs}) + ST_{mT}^{obs} \bullet rn_{0J} \bullet (1 - (\delta T_{mT}^{obs})^2)^{0.5}$$

T_J^{est}	estimated mean daily air temperature (°C)
XT_{mT}^{obs}	mean observed daily air temperature (°C)
δT_{mT}^{obs}	observed first-order autocorrelation of mean observed daily air temperature for each month [correlation J J^{-1}] [default value = 0.65]
ST_{mT}^{obs}	standard deviation of the mean observed daily air temperature (°C)
rn_{0J}	random number [0,1]

b2. Air temperature amplitude (°C), modified from Bristow and Campbell (1984):

$$\Delta T_J^{est} = \left[\frac{n\log\left(1 - \frac{Tt_J^{est}}{\beta}\right)}{-A}\right]^{\left(\frac{1}{C_{sky}}\right)}$$

ΔT_J^{est}	air temperature amplitude (°C)
T_J^{est}	estimated mean daily air temperature (°C)
β	Ångström factor
C_{sky}	coefficient of maximum clear-sky transmittance with ΔT increase [2.4]
A	coefficient of maximum clear-sky transmittance characteristics [0.016]

b3. Maximum air temperature (°C):

$$Tmax_J^{est} = Tmean_J^{est} + \left(\frac{\Delta T_J^{est}}{2}\right)$$

$Tmax_J^{est}$	estimated maximum daily air temperature (°C)
$Tmean_J^{est}$	estimated mean daily air temperature (°C)
ΔT_J^{est}	air temperature amplitude (°C)

b4. Minimum air temperature (°C):

$$Tmin_J^{est} = Tmean_J^{est} - \left(\frac{\Delta T_J^{est}}{2}\right)$$

$Tmin_J^{est}$	estimated maximum daily air temperature (°C)
$Tmean_J^{est}$	estimated mean daily air temperature (°C)
ΔT_J^{est}	air temperature amplitude (°C)

c. Precipitation

c1. The fraction of wet days per month, after Geng *et al.* (1988):

$$FWD_{mT}^{obs} = \left(\frac{RJ_{mT}^{obs}}{MJ_{mT}^{obs}}\right)$$

FWD_{mT}^{obs}	fraction of wet days per month
RJ_{mT}^{obs}	number of rain days per month
MJ_{mT}^{obs}	number of days per month

Transitional probabilities for the first-order Markov chain

c2. Transitional probability of a wet day followed by a dry day per month, after Geng *et al.* (1988):

$$PWD_{mT}^{est} = 0.75 \bullet FWD_{mT}^{obs}$$

PWD_{mT}^{est}	transitional probability of a wet day followed by a dry day
FWD_{mT}^{obs}	fraction of wet days per month

c3. Transitional probability of a wet day followed by a wet day per month, after Geng *et al.* (1988):

$$PWW_{mT}^{est} = 0.25 + PWD_{mT}^{est}$$

PWW_{mT}^{est}	transitional probability of a wet day followed by a wet day
PWD_{mT}^{est}	transitional probability of a wet day followed by a dry day

Markov chain parameters

c4. Determining a wet/dry day, modified from Richardson and Wright (1984):

if IP_{J-1} = 1 then if $(rn_{1J} - PWW_J^{est})$	≤0	IP = 1 [wet day]
	>0	IP = 0 [dry day]
= 0 then if $(rn_{1J} - PWD_J^{est})$	≤0	IP = 1 [wet day]
	>0	IP = 0 [dry day]
P	wet/dry day [0 = dry day; 1 = wet day]		
rn_{1J}	random number [0,1]		
PWW_J^{est}	transitional probability of a wet day followed by a wet day		
PWD_J^{est}	transitional probability of a wet day followed by a dry day		

Amount of rainfall on a wet day

c5.1. Rainfall amount (mm) on a wet day is generated using a special case of the gamma probability distribution function (an exponential):

$$P_{IP_J=1}^{Est} = 0 - b \bullet \text{nlog}[rn(0,1)]$$

$P_{IP\ J=1}^{est}$	rainfall amount on a wet day (mm)
b	intermediate parameter

c5.2.

$$b = \frac{Pe_{mT}^{obs^2}}{1 + \frac{(rn(0,1) - 0.5)}{2}}$$

b	intermediate parameter
PE_{mT}^{obs}	mean observed precipitation for each rainfall event per month (mm)
rn	random number [0,1]

c6. Mean monthly duration per rainfall event (h^{-1}):

$$\overline{P}_{dur_{mT}}^{est} = \frac{\sum_{i=1}^{n} IP = 1_{mT}^{est}}{1.39 \bullet [(P_{range} + 0.1)^{-3.55}]}$$

$\overline{P}_{dur\ mT}^{est}$	mean rainfall duration (h^{-1})
ΣIP	sum of wet days in a given month with rainfall within a specified range
P_{range}	rainfall range [>5,10,15,20,25,50,75,100 mm converted to inches]

c7. Duration per rainfall event (min):

$$P_{dur_J}^{est} = \overline{P}_{dur_{mT}}^{est} \bullet \left(\frac{P_J^{est}}{P_{range}}\right) \bullet 60$$

P_{durJ}^{est}	duration per rainfall event (min)
$\overline{P}_{dur\ mT}^{est}$	mean rainfall duration (h^{-1})
P_J^{est}	rainfall amount on a wet day (mm)
P_{range}	rainfall range [>5,10,15,20,25,50,75,100 mm converted to inches]

c8. Rainfall intensity (mm h^{-1}):

$$P_{in_J}^{est} = \frac{\left(\frac{P_J^{est}}{est}\right)}{\frac{P_{dur_J}}{60}}$$

[A1.C7]

$P_{in\ J}^{est}$	rainfall intensity (mm h^{-1})
P_J^{est}	rainfall amount on a wet day (mm)
P_{durJ}^{est}	duration per rainfall event (min)

d. Solar radiation

Approximations of the total solar radiation reaching the earth are generated using spherical geometry.

d1. Solar declination (radians):

$$Ds_t = 23.45 \bullet \frac{\pi}{180} \bullet \sin\left(\frac{\pi}{180} \bullet \left[\frac{(360 \bullet J)}{TotJ^{-1} - 80}\right]\right)$$

Ds_t	solar declination (radians)
J	Julian day
TotJ	total number of days in the year [365/366]

d2. Sunrise [dawn] (h):

$$SR_J = 12 - \frac{Dayl_J}{2}$$

SR_J	time of sunrise (h)
$Dayl_J$	day length

d3. Solar time (h):

$$ST_J = GMT + EqT + \left[\frac{(180 \bullet Long)}{\pi \bullet 15}\right]$$

ST_J	solar time (h)
GMT	Greenwich Mean Time (h)
EqT	equation of time
Long	longitude (radians)

d4.1. Equation of time (h):

$$EqT = \frac{[(-107.7 \bullet \sin(C)) + 596.2 \bullet \sin(2 \bullet C) + 4.3 \bullet \sin(3 \bullet C) - 12.7 \bullet \sin(4 \bullet C) - 429.3 \bullet \cos(c) - 2 \bullet \cos(2 \bullet C) + 19.3 \bullet \cos(3 \bullet C)]}{3600}$$

EqT	equation of time
C	intermediate parameter (radians)

d4.2.

$$C = (279.575 + 0.986 \bullet J) \bullet \frac{\pi}{180}$$

C	intermediate parameter (radians)
J	Julian day

d5. Solar elevation (radians):

$$SE = \operatorname{asin}[\cos(L) \bullet \cos(Ds_J) \bullet \cos(H) + \sin(L) \bullet \sin(Ds_J)]$$

SE	solar elevation (radians)
L	latitude (radians)
Ds_J	solar declination (radians)
H	height of sun (radians)

d6. Height of the sun at a specified time of day (radians):

$$H = 15 \bullet (ST_J - 12) \bullet \frac{\pi}{180}$$

H	height of sun (radians)
ST_J	solar time (h)

d7. Day length (h):

$$Dayl_J = \left\{\operatorname{acos}\left[\frac{\sin(Lat) \bullet \sin(Ds_J) - \sin\left(0.833 \bullet \frac{\pi}{180}\right)}{\cos(L) \bullet \cos(Ds_J)}\right] \bullet \frac{180}{\pi}\right\} \bullet \frac{2}{15}$$

$Dayl_J$	day length
Lat	latitude (radians)
Ds_J	solar declination (radians)
L	latitude (radians)

d8. Sun-earth distance:

$$\left(\frac{\overline{d}}{d}\right)^2 = 1.00011 + 0.034221 * \cos\left(\frac{2 \bullet \pi \bullet (J-1)}{365}\right) + 0.00128 * \sin\left(\frac{2 \bullet \pi \bullet (J-1)}{365}\right) + 0.000719 * \cos\left(2 * \frac{2 \bullet \pi \bullet (J-1)}{365}\right) + 0.000077 * \sin\left(*2 * \frac{2 \bullet \pi \bullet (J-1)}{365}\right)$$

$(\frac{\overline{d}}{d})^2$	actual distance between sun and the earth
J	Julian day

d9. Extra-terrestrial radiation (W m^{-2} day^{-1}):

$$Rso_J^{est} = \frac{\left(\frac{\overline{d}}{d}\right)^2 \bullet S' \bullet \sin(SE) \bullet 2 \bullet Dayl_J}{\left[\pi \bullet \sin\left(\frac{\pi}{2}\right)\right] \bullet 3600}$$

$R_{so\,J}^{est}$	extra-terrestrial radiation (W m^{-2} day^{-1})
$(\frac{\overline{d}}{d})^2$	actual distance between sun and the earth
S’	solar constant [1367.0 W m^{-2}]
SE	solar elevation (radians)
$Dayl_J$	day length

Atmospheric characteristics relating to solar radiation

d10. Ångström turbidity factor [α] (W m^{-2}) is related to aerosol size and their optical characteristics influencing diffused transmission (modified from Nikolov and Zeller (1992)):

$$\alpha = 32.9835 - 64.884 \bullet [1 - 1.3614 \bullet \cos(L)] \bullet 4.1842 \bullet 100 \bullet 100$$

α	Ångström turbidity factor (W m^{-2})
L	latitude (radians)

d11. Ångström turbidity factor [β] is related to the maximum clear-sky atmospheric transmittance characteristics (modified from Nikolov and Zeller (1992)):

$$\beta = 0.715 - 0.3183 \bullet [1 - 1.3614 \bullet \cos(L)]$$

β	Ångström factor
L	latitude (radians)

d12. Ångström turbidity factor [σ] is related to the light absorption effects of cloud cover (Nikolov and Zeller, 1992):

$$\sigma = 0.03259$$

σ	Ångström turbidity factor

Cloudiness

The method approximates the formation of clouds on the basis of the atmosphere's saturated vapour pressure. Clouds are assumed to form every day, with rainfall occurring only on designated wet days.

d13. Cloudiness (tenths), after Nikolov and Zeller (1992):

$$C_J^{est} = 10 - 2.5 \bullet \left(\frac{ev_J^{est}}{P_J^{est}}\right)^{0.5}$$

C_J^{est}	cloudiness (tenths)
ev_J^{est}	saturated vapour pressure at a given air temperature (Pa)
P_J^{est}	rainfall amount on a wet day (mm)

d14. Mean saturation vapour pressure (Pa) at mean air temperature T, after Gueymard (1993):

$$ev_J^{est} = 6.1078 \bullet \exp\left[\frac{17.269 \bullet T_{mean_J}^{est}}{T_{mean_J}^{est} + 237.3}\right]$$

ev_J^{est}	saturated vapour pressure at a given air temperature (Pa)
$Tmean_J^{est}$	estimated mean daily air temperature (°C)

d15. Mean saturation vapour pressure (Pa) at mean air temperature T below 0 °C (over ice):

$$ev_J^{est} = \exp\frac{\left[\frac{[-6140.4]}{273 + Tmean_J^{est}} + 28.916\right]}{100}$$

ev_J^{est}	saturated vapour pressure at a given air temperature (Pa)
$Tmean_J^{est}$	estimated mean daily air temperature (°C)

Total solar radiation at the Earth's surface

d16. Total solar radiation at the earth's surface, after Nikolov and Zeller (1992):

$$R_J = Rso_J \bullet (\beta - \sigma \bullet C_J^{est}) - \alpha$$

R_J	terrestrial radiation on a horizontal surface at an elevation of 274 m above sea level (W m^{-2} day^{-1})
$R_{so\,J}^{est}$	extra-terrestrial radiation (W m^{-2} day^{-1})
β	Ångström factor
σ	Ångström turbidity factor
C_J^{est}	cloudiness (tenths)
α	Ångström turbidity factor (W m^{-2})

Direct and diffuse solar radiation at the Earth's surface

d17. Total transmission proportion, after Lui and Jordan (1960):

$$Tt_J = \frac{R_J}{Rso_J}$$

Tt_J	total transmission proportion (dimensionless)
R_J	terrestrial radiation on a horizontal surface at an elevation of 274 m above sea level (W m^{-2} day^{-1})
$R_{so\,J}^{est}$	extra-terrestrial radiation (W m^{-2} day^{-1})

d18. Diffuse transmission coefficient:

$Td_J =$ If $Tt_J < 0.07$ then $Td_J = 1$

If $Tt_J \geq 0.07 < 0.35$ then $Td_J = 1 - 2.3 \bullet (Tt_J - 0.07)^2$

If $Tt_J \geq 0.35 < 0.75$ then $Td_J = 1.33 - 1.46 \bullet Tt_J$

If $Tt_J \geq 0.75$ then $Td_J = 0.23$

Td_J	diffuse transmission coefficient (dimensionless)
Tt_J	total transmission proportion (dimensionless)

Solar radiation corrected for slope and aspect

After Duffie and Beckman (1991) correction of solar radiation for slope and aspect is as follows:

d19. The next hour after sunrise:

$$S_{r+1_J} = \text{int}(SR_J + 1)$$

$S_{r+1\,J}$ next hour after sunrise
SR_J time of sunrise (h)

d20. The sunrise hour fraction:

$$S_{mp_J} = SR_j + \frac{S_{r+1_J} - SR_j}{2}$$

$S_{mp\,J}$ sunrise hour fraction
SR_J time of sunrise (h)
$S_{r+1\,J}$ next hour after sunrise

d21. The sunrise hour angle (radians):

$$hs_J = \frac{15 \bullet (S_{mp_J} - 12) \bullet \pi}{180}$$

hs_J solar sunrise/sunset angle (radians)
$S_{mp\,J}$ sunrise hour fraction

d21.1. Intermediate parameters for approximating accumulated solar radiation on a tilted surface:

$$C1_0 = \sin(Ds_J) \bullet (\sin(L) \bullet \cos(Sl) - \cos(L) \bullet \sin(Sl) \bullet \cos(As))$$

$C1_0$ intermediate parameter to approximate solar radiation on tilted surface
Ds_J solar declination (radians)
L latitude (radians)
Sl slope (radians)
As aspect (radians)

d21.2.

$$Cts_0 = [C1_0 + (\cos(Ds_J) \bullet \cos(hs) \bullet \cos(L) \bullet \cos(Sl) + \sin(L) \bullet \sin(Sl) \bullet \sin(As)) + (\cos(Ds_J) \bullet \sin(Sl) \bullet \sin(As) \bullet \sin(hs))\ ] \bullet (S_{r+1} - SR_J)$$

Cts_0 intermediate parameter to approximate solar radiation on tilted surface
$C1_0$ intermediate parameter to approximate solar radiation on tilted surface
Ds_J solar declination (radians)
hs solar sunrise/sunset angle (radians)
L latitude (radians)
Sl slope (radians)

As	aspect (radians)
S_{r+1}	next hour after sunrise
SR_J	time of sunrise (h)

d22. Intermediate parameter for approximating accumulated solar radiation on flat surface:

$$Ctz_0 = (\cos(L) \bullet \cos(Ds_J) \bullet \cos(hs) + \sin(L) \bullet \sin(Ds_J)) \bullet (S_{r+1} - SR_J)$$

Ctz_0	intermediate parameter to approximate solar radiation on a flat surface
L	latitude (radians)
Ds_J	solar declination (radians)
hs	solar sunrise/sunset angle (radians)
S_{r+1}	next hour after sunrise
SR_J	time of sunrise (h)

d22.1. Daily ratio of beam sun on a tilted/flat surface:

$$Tfr_J = \left(Cts_o + \sum_{i=1}^{11} Cts_i\right) \Big/ \left(Ctz_o + \sum_{i=1}^{11} Ctz_i\right)$$

Tfr_J	daily tilted/flat ratio of beam sun
Cts_0	intermediate parameter to approximate solar radiation on tilted surface
Cts_i	intermediate parameter to approximate daily tilted:flat ratio of beam sun
Ctz_0	intermediate parameter to approximate solar radiation on a flat surface
Ctz_i	intermediate parameter to approximate daily tilted:flat ratio of beam sun

d22.2.

$$Cts_i = C1_0 + (\cos(Ds_j) \bullet \cos(hs_i) \bullet \cos(L) \bullet \cos(Sl) + \sin(L) \bullet \sin(Sl) \bullet \cos(As)) + (\cos(Ds_j) \bullet \sin(Sl) \bullet \sin(As) \bullet \sin(hs_i))$$

Cts_i	intermediate parameter to approximate daily tilted:flat ratio of beam sun
$C1_0$	intermediate parameter to approximate solar radiation on tilted surface
Ds_J	solar declination (radians)
hs_i	solar sunrise/sunset angle (radians)
L	latitude (radians)
Sl	slope (radians)
As	aspect (radians)

d22.3.

$$Ctz_i = \cos(L) \bullet \cos(Ds_J) \bullet \cos(hs_i) + \sin(L) \bullet \sin(Ds_J)$$

Ctz_i	intermediate parameter to approximate daily tilted:flat ratio of beam sun
L	latitude (radians)
Ds_J	solar declination (radians)
hs_i	solar sunrise/sunset angle (radians)

d22.4.

$$hs_i = 15 \bullet (t - 12) \bullet \frac{\pi}{180}$$

hs_i	solar sunrise/sunset angle (radians)
t	0.5, 1.5, 2.5...11.5 as *i* = 1,2,3...11

d23. Direct (beam) radiation (W m^{-2} day^{-1}):

$$Rdir_j = Tfr_J \bullet R_j \bullet (1 - Tt_j)$$

$R_{dir\,J}$	direct (beam) radiation (W m^{-2} day^{-1})
Tfr_J	daily tilted/flat ratio of beam sun
R_J	terrestrial radiation on a horizontal surface at an elevation of 274 m above sea level (W m^{-2} day^{-1})
Tt_J	total transmission proportion (dimensionless)

d24. Diffuse radiation (W m^{-2} day^{-1}):

$$Rdif_J = \cos^2\left(\frac{Sl}{2}\right) \bullet (R_J \bullet Tt_J)$$

$R_{dif\,j}$	diffuse radiation (W m^{-2} day^{-1})
Sl	slope (radians)
R_J	terrestrial radiation on a horizontal surface at an elevation of 274 m above sea level (W m^{-2} day^{-1})
Tt_J	total transmission proportion (dimensionless)

e. Wind speed

e1. Mean wind speed (m s^{-1}):

$$u(z)_J^{est} = XW_{mT}^{obs} + \delta W_{mT}^{obs} \bullet (W_{J-1}^{est} - XW_{mT}^{obs}) + SW_{mT}^{obs} \bullet rn_{1_J} \bullet (1 - (\delta W_{mT}^{obs})^2)^{0.5}$$

$u[z]_J^{est}$	wind speed (m s^{-1})
XW_{mT}^{obs}	mean daily wind speed for each month (m s^{-1})
δW_{mT}^{obs}	first-order autocorrelation of mean daily wind speed for each month
W_{J-1}^{est}	estimated wind speed of the previous day (m s^{-1})
SW_{mT}^{obs}	standard deviation of mean daily wind speed (m s^{-1})

rn_{1J}	random number [0,1]

f. Relative humidity

f1. Relative humidity (%):

$$Rh_J^{est} = \left(\frac{E_J^{est}}{ev_J^{est}} \right) \bullet 100$$

Rh_J^{est}	relative humidity (%)
E_J^{est}	intermediate parameter
ev_J^{est}	saturated vapour pressure at a given air temperature (Pa)

f2.

$$E_J^{est} = \min(1, ev_J^{est} - 0.66 \bullet (Tdb_J^{est} - Twb_J^{est})$$

E_J^{est}	intermediate parameter
ev_J^{est}	saturated vapour pressure at a given air temperature (Pa)
Tdb_J^{est}	intermediate parameter
Twb_J^{est}	intermediate parameter

f3.

$$Tdb_J^{est} = \left(Twb_J^{est} + \partial T_J^{est} \right)$$

Tdb_J^{est}	intermediate parameter
Twb_J^{est}	intermediate parameter
∂T_J^{est}	intermediate parameter

f4.

$$\partial T_J^{est} = \max(0, rn_o \bullet Tsd_J^{est} + Tampwd_J^{est}$$

∂T_J^{est}	intermediate parameter
rn_0	random number [0,1]
Tsd_J^{est}	intermediate parameter
$Tampwd_J^{est}$	intermediate parameter

f5.

$$Tsd_J^{est} = abs\left(\frac{Twb_J^{est}}{5} \right)$$

Tsd_J^{est}	intermediate parameter
Twb_J^{est}	intermediate parameter

f6. For winter months (December – January) in the UK the following apply:

$$Tampwd_J^{est} = 0.0587 \bullet Twb_J^{est} + 0.3845$$

$Tampwd_J^{est}$	intermediate parameter
Twb_J^{est}	intermediate parameter

f7.

$$Twb_J^{est} = 1.0695 \bullet Tmean_J^{est} - 1.2073$$

Twb_J^{est}	intermediate parameter
$Tmean_J^{est}$	estimated mean daily air temperature (°C)

f8. For the remaining months (March – November) in the UK the following apply:

$$Tampwd_J^{est} = 0.1351 \bullet Twb_J^{est} + 0.2891$$

$Tampwd_J^{est}$	intermediate parameter
Twb_J^{est}	intermediate parameter

f9.

$$Twb_J^{est} = 0.9513 \bullet Tmean_J^{est} - 0.5788$$

Twb_J^{est}	intermediate parameter
$Tmean_J^{est}$	estimated mean daily air temperature (°C)

f10. UK site correction factor for relative humidity:

$$Rh_J^{est} = \min(100, \frac{Rh_J^{est}}{Rh_{corr}})$$

Rh_J^{est}	relative humidity (%)
Rh_{corr}	correction factor

f11. UK site correction factor for daily air temperature:

$$Rh_{corr} = \max(0.9172 - 0.0031 \bullet Tmean_J^{est^2} + 1.0.0377 + Tmean_J^{est} + 0.9172)$$

Rh_{corr}	correction factor
$Tmean_J^{est}$	estimated mean daily air temperature (°C)

g. Atmospheric pressure

g1. Atmospheric pressure (mbar) uses the US Standard Atmospheric method:

$$P_J^{est} = P_0 \left(\frac{\left[T_0' - \delta(alt - alt_0) \right]^{\frac{g}{\delta R_{gas}}}}{T_0'} \right)$$

P_J^{est}	atmospheric pressure (mbar)
P_0	standard sea level atmospheric pressure (1013 mbar)
T'_0	standard sea level temperature (288 K)
δ	standard lapse rate (6.5 K 100m^{-1})
alt	elevation of site (m)
alt_0	base elevation (m)
g	acceleration due to gravity (9.81m s^{-1})
R_{gas}	universal gas constant for air (287 J kg^{-1} K^{-1})

2. Plant water

h. Canopy rainfall interception

All equations follow Gash *et al.* (1995).

h1. Calculates the precipitation necessary to saturate the canopy, i.e. holding capacity and evaporation while its raining:

$$P_G' = MAX\{S_c, \frac{R * S_c}{E_{wet}} \ln(1 - \frac{E_c}{R})\}$$

P_G'	rainfall needed to saturate the canopy (mm)
S_c	holding capacity of the canopy (mm rain/projected area)
R	average rate of rainfall in the day (mm hr^{-1})
E_{wet}	average evaporation during rain (mm hr^{-1}) (stand basis not projected area, typical Penman-Monteith = 0.17 mm hr^{-1})

h2. Rainfall interception by a stand canopy:

$$\text{If } PPT <= P_G' \quad I_{can,unsat} = PPT * p_{Cover}$$

$$\text{If } PPT > P_G' \quad I_{can,unsat} = 0.0$$

$I_{can,unsat}$	interception by canopy of samm rainfall incidents (mm)
PPT	rainfall (mm.day^{-1})
P_G'	rainfall needed to saturate the canopy (mm)
p_{cover}	projected crown cover of stand (m^2 m^{-2})

h3. Evaporation from a canopy during its process of saturation ie raining and will saturate canopy:

If $PPT = 0.0$ and $P_G' > PPT$ $\quad I_{can,wet} = 0.0$

Else $I_{can,wet} = (P_G' - S_c) * p_{cover}$

$I_{can,wet}$ interception of rain for evaporation during the period of wetting (mm)
PPT rainfall (mm day^{-1})
P_G' rainfall needed to saturate the canopy (mm)
S_c holding capacity of the canopy (mm rain/projected area)
p_{cover} projected crown cover of stand (m^2 m^{-2})

h4. Interception/evaporation from saturation to end of rain:

if $PPT <= P_G'$ $\quad I_{can,rain} = 0.0$

if $PPT > P_G'$ $\quad I_{can,rain} = Cover * E_c \frac{(PPT - P_G')}{R * Cover}$

$I_{can,rain}$ intercepted rain for evaporation during rain (mm)
PPT rainfall (mm day^{-1})
P_G' rainfall needed to saturate the canopy (mm)
E_c average evaporation during rain (mm hr^{-1}) (stand basis not projected area, typical Penman-Monteith = 0.17 mm hr^{-1})
Cover projected crown cover of stand (m^2 m^{-2})
R rate of rainfall (mm hr^{-1})

h5. Loss of water from canopy storage:

If $I_{can,rain} <= 0$ $\quad I_{can,post} = 0.0$

if $I_{can,rain} > 0$ $\quad I_{can,post} = S_c * p_{cover}$

$I_{can,post}$ intercepted rain evaporated after saturation (mm)
$I_{can,rain}$ intercepted rain for evaporation during rain (mm)
S_c holding capacity of the canopy (mm rain/projected area)
p_{cover} projected crown cover of stand (m^2 m^{-2})

h6. Interception and loss of water via the stem - assumed that small instances of rain are intercepted by the canopy:

$$\text{If } PPT >= \frac{S_t}{P_t} \qquad I_{stem} = S_t$$

$$\text{If } PPT < \frac{S_t}{P_t} \text{ and } I_{can,rain} > 0 \qquad I_{stem} = PPT * P_t$$

I_{stem}	intercepted rain evaporated from stem (mm)
$I_{can,\ rain}$	intercepted rain for evaporation during rain (mm)
S_t	holding capacity of the stem (trunk) (mm)
P_t	proportion of rainfall diverted to stemflow (dimensionless)
PPT	precipitation (mm)

i. Evaporation equations for the system and canopy

i1. Rate of change of saturated vapour pressure with temperature:

$$\Delta V = \frac{4098.25 e_s}{(\overline{T} + 237.3)^2}$$

ΔV	rate of change of saturated vapour pressure with temperature (mbar K^{-1})
e_s	saturated vapour pressure (mbar)
T	mean daily temperature ($^{\circ}C$)

i2. Heat-sink ground function:

$$G = 0.033 R_{net}$$

G	ground heat-sink (J m^{-2} day^{-1})
R_{net}	net radiation (J m^{-2} day^{-1})

i3. Latent heat of vapourisation:

$$\lambda = 2500.78 - 2.3601T$$

λ	latent heat of vapourisation (Kj kg^{-1})
T	air temperature ($^{\circ}C$)

i4. Canopy aerodynamic resistance:

$$r_a = \frac{\ln\left(\frac{z_m - d}{z_{om}}\right)\ln\left(\frac{z_h - d}{z_{oh}}\right)}{k^2 u_z}$$

r_a	aerodynamic resistance (s m^{-1})
z_m	height of wind measurements (m)
z_h	height of humidity measurements (m), assume = z_m
d	zero plane displacement height (m), assume = 0.75 h
h	crop height (m)
z_{om}	roughness length governing momentum transfer (m), assume = 0.123 h
z_{oh}	roughness length governing transfer of heat and vapour (m), assume = 0.1 z_{om}
k	Von Karman's constant (dimensionless = 0.41)
u_z	windspeed at height z_m (m s^{-1})

i5. Psychrometric constant (relationship between vapour pressure deficit and wet bulb depression) function:

$$\gamma_p = \frac{1.0035 P_{atm}}{0.62198 \lambda}$$

γ_p	psychometric constant (mbar K^{-1})
P_{atm}	barometric atmospheric pressure (mbar)
λ	latent heat of vapourisation (Kj kg^{-1})

i6. Emissivity of a clear sky:

$$\varepsilon_{atm} = -0.02 + 0.261 * e^{-0.000777 T^2}$$

ε_{atm}	emissivity of the clear sky atmosphere (W $^{\circ}C^{-1}$ day^{-1})
T	air temperature (°C)

i7. Emissivity of the total sky atmosphere, including below cloud:

$$\varepsilon_{sky} = \varepsilon_{atm} + C(1 - \varepsilon_{atm})\left(1 - \frac{4 * \Delta T_C}{T + 273.15}\right)$$

ε_{sky}	emissivity of the total sky atmosphere, including below cloud (W $^{\circ}C^{-1}$ day^{-1})
ε_{atm}	emissivity of the clear sky atmosphere (W $^{\circ}C^{-1}$ day^{-1})
C	cloud cover ratio (dimensionless)
ΔT_C	difference in cloud base temperature and air temperature (K), assume = 2
T	air temperature ($^{\circ}C$)

i8. Net longwave radiation:

$$R_{lw,net} = \varepsilon_{surf} \sigma (273.13 + T)^4 \times 1.28 \left[\left(\frac{e_a}{273.13 + T} \right)^{\frac{1}{7}} - 1 \right]$$

$R_{lw,net}$	net longwave radiation (W m^{-2})
E_{surf}	surface emissivity (dimensionless, assume = 0.97)
Σ	Steffan-Boltzmann constant (W m^{-2} K^{-4}, assume = 5.67e^{-8})
T	air temperature ($^{\circ C}$)
e_a	actual (unsaturated) vapour pressure (mbar)

i9. Net radiation:

$$R_{net} = R_{lw,net,day}(1-C) + (R_{sw,abs} + R_{sw,tran})$$

R_{net}	net daily radiation (J m^{-2} day^{-1})
$R_{lw,net}$	net longwave radiation (W m^{-2})
C	cloud cover ratio (dimensionless)
$R_{sw,abs}$	shortwave radiation absorbed by the crop (J m^{-2} day^{-1})
$R_{sw,tran}$	shortwave radiation transmitted by the crop (J m^{-2} day^{-1})

i10. Air density function

$$\rho_a = \frac{101.325 - 0.01055A}{0.27\left[\frac{273.13+T}{1-0.378\left(\frac{e_a}{101.325-0.01055A}\right)}\right]}$$

ρ_a	air density (kg m^{-3})
A	altitude (m)
T	air temperature (°C)

i11. Evaporation from a wet canopy:

$$E_{wet} = 3600 D_{hr} \frac{\Delta V\left(\frac{R_n}{3600 D_{hr}} - \frac{G}{3600 D_{hr}}\right) * f_{abs} + \rho_a c_p \left(\frac{e_s - e_a}{r_a}\right)}{\lambda \times 10^3 (\Delta V + \gamma_p)}$$

E_{wet}	evaporation from a wet canopy (mm day^{-1})
D_{hr}	daylit time for the day (h)
ΔV	rate of change of saturated vapour pressure with temperature (mbar K^{-1})
R_n	net daily radiation (J m^{-2} day^{-1})
G	ground heat-sink (J m^{-2} day^{-1})
f_{abs}	fraction of incoming radiation absorbed by the canopy (dimensionless)
ρ_a	air density (kg m^{-3})
c_p	specific heat capacity of air (J kg^{-1} K^{-1}), assume = 1005.01
e_s	saturated vapour pressure (mbar)

e_a	actual vapour pressure (mbar)
r_a	aerodynamic (boundary layer) resistance of the canopy to water diffusion (s m^{-1})
λ	latent heat of vapourisation (kj kg^{-1})
γ_p	psychometric constant (mbar K^{-1})

i12. Total evapotranspiration:

$$E_{total} = (1 - p_{dry}) \cdot E_{wet} \cdot p_{cover} + p_{dry} \cdot E_{transp} \cdot p_{cover} + E_{shade} \cdot p_{cover} + E_{bare} \cdot (1 - p_{cover})$$

E_{tot}	total evapotranspiration
p_{dry}	proportion of the daylight time that is dry (dimensionless)
E_{wet}	evaporation from a wet canopy (mm day^{-1})
p_{cover}	projected canopy cover (dimensionless)
E_{transp}	transpiration from a dry canopy (mm day^{-1})
E_{shade}	evaporation from soil shaded by the canopy (mm ay^{-1})
E_{bare}	evaporation from the bare soil (mm day^{-1})

i13. Evaporation during rain:

$$E_{rain} = \frac{E_{wet}}{D_{hr}}$$

E_{rain}	rate of evaporation from the canopy during rain (mm h^{-1})
E_{wet}	potential wet canopy evaporation (mm day^{-1})
D_{hr}	daylit time for the day (h)

i14. Proportion of the day that is dry:

$$p_{dry} = 1 - \frac{I_{ppt,canopy}}{E_{wet}}$$

p_{dry}	proportion of the daylight time that is dry (dimensionless)
$I_{ppt,canopy}$	precipitation intercepted by the canopy (mm day^{-1})
E_{wet}	potential wet canopy evaporation (mm day^{-1})

i15. Quantity of precipitation that reaches the soil:

$$I_{ppt,soil} = (1 - p_{cover}) P_{IP} + p_{cover} (P_{IP} - I_{ppt,canopy})$$

$I_{ppt,soil}$	rain that reaches the soil (mm day^{-1})
p_{cover}	projected canopy cover (dimensionless)
P_{IP}	precipitation for the day (mm day^{-1})
$I_{ppt,canopy}$	precipitation intercepted by the canopy (mm day^{-1})

i16. Projected cover:

$$p_{cover} = \min(L_c, C_{max})$$

p_{cover} projected cover of the canopy (dimensionless)
L_c canopy leaf area index ($m^2\ m^{-2}$)
C_{max} maximum canopy cover (dimensionless)

3. Soil hydrology

j. Volumetric water content for each horizon

j1. Volumetric water content at total porosity:

$$OTP^n = T_p^n \bullet LD^n$$

OTP^n volumetric water content at total porosity
T_p^n total porosity

j2. Volumetric water content at field capacity:

$$OFC^n = PFC^n \bullet LD^n$$

OFC^n volumetric water content at field capacity
PFC^n field capacity

j3. Volumetric water content at wilting point:

$$OWP^n = PWP^n \bullet LD^n$$

OWP^n volumetric water content at wilting point
PWP^n wilting point

j4. Volumetric water content at 30 % wilting point:

$$Oair^n = PWP^n \bullet LD^n \bullet 0.3$$

$Oair^n$ volumetric water content at 30 % wilting point
PWP^n wilting point
LD^n

j5. Volumetric air capacity at 0.05 bar suction is given by:

$$C_a^n = (T^n - PFC^n) \bullet 100$$

C_a^n	volumetric air capacity at 0.05 bar suction
PFC^n	field capacity

j6. Total water content at total porosity:

$$WQS^n = PWQS^n \bullet LD^n$$

WQS^n	total water content at total porosity

k. Pedo-transfer functions for calculating saturated sub-vertical and sub-lateral hydraulic conductivity

k1. Retained volume of soil water:

$$\theta_m(x) = \frac{\left(\frac{\theta_v(x)}{100}\right)}{D_{bt}}$$

$\theta_m(x)$	retained volume of soil water
x	suction pressure at 0, 0.1, 0.4, 2 and 15 bar, respectively

k2. Volumetric total pore space, corrected for organic matter and stoniness:

$$T = \left[\left(1 - \left(\frac{D_{bt}}{D_p}\right)\right) \bullet (1 - S) \bullet [(1 - OM) + OM]\right] \bullet 100$$

T	volumetric total pore space
D_p	assume = 2.65
S	stoniness
OM	organic matter

k3. Sub-vertical saturated conductivity:

$if\ C < 16\ and\ [(Z + 2 \bullet C) < 31]$	$if\ C_a$	< 7.5	$Ks_v = \left(0.4535 \bullet T^{1.03423}\right)$
		> 7.5	$Ks_v = \left[8.03578 - (6.7707 \bullet T) + \left(0.833 \bullet T^2\right)\right]$
$if\ C > 16\ and\ [(Z + 2 \bullet C) > 31]$	$if\ C_a$	< 4	$Ks_v = \left[0.14143 \bullet e^{(T \bullet 0.46944)}\right]$
		> 4	$Ks_v = \left[5.8521 - (5.4125 \bullet T) + \left(1.05138 \bullet T^2\right)\right]$

C_a	air capacity
Ks_v	sub-vertical saturated conductivity
T	volumetric total pore space

k4. Sub-lateral conductivity:

if $C < 16$ *and* $[(Z + 2 \bullet C) < 31]$	*if* $C_a < 7.5$	$Ks_L = (0.4535 \bullet T^{1.03423})$
	> 7.5	$Ks_L = [8.03578 - (6.7707 \bullet T) + (0.833 \bullet T^2)]$
if $C > 16$ *and* $[(Z + 2 \bullet C) > 31]$	*if* $C_a < 5.5$	$Ks_L = [0.14143 \bullet e^{(T \bullet 0.46944)}]$
	if $C_a > 5.5$	$Ks_L = [3.155 - (4.639 \bullet T) + (0.8143 \bullet T^2)]$

C_a air capacity
Ks_L sub-lateral saturated conductivity
T volumetric total pore space

k5. Air capacity:

$C_a = T - \theta_V^{0.05}$
C_a air capacity
T volumetric total pore space

l. Unsaturated hydraulic conductivity

l1. Soil water retention at different pressure heads in the soil matrix is described using the simplified version of the Brooks-Corey expression (1964) introduced by Campbell (1974), in which the residual water content is assumed zero, and given by:

$$\frac{K(\theta)}{K_S} = \left(\frac{h_b}{h}\right)^{-\lambda}$$

Values of (*b*) and (□) can be derived from PTFs or from non-linear interpolation of measured data, as carried out for this simulation experiment.

m. Drainage

m1. When $FC > \theta < T$, excess volumetric water (*Ex*) is available for drainage (*D*):

$Ex_t = \theta_t - PFC_n$
Ex_t excess volumetric water
PFC^n field capacity

m2. Drainage occurs at the sub-vertical hydraulic conductivity rate (Ks_v):

$\min\{Ks_V^z, Ks_V^{z+1}\}$
Ks_v sub-vertical saturated conductivity

Drainage (*D*), both sub-vertical (D_V) and sub-lateral (D_L) occurring at the sub-vertical (K_{SV}) and sub-lateral saturated (K_{SL}) hydraulic conductivity rates, adjusted to the water content at the previous integration respectively, develops under a range of boundary conditions:

m3.1. *Condition A*: free drainage both within the profile and at the lower boundary:

$$if\ Ex_t < Ks_V \qquad D_{V_t} = Ex_t \ and\ D_{L_t} = 0$$

$$if\ Ex_t - Ks_V < Ks_L \ D_{V_t} = Ks_V \ and\ D_{L_t} = Ex_t - Ks_L$$

$$if\ Ex_t - Ks_V > Ks_L \ D_{V_t} = Ks_V \ and\ D_{L_t} = Ks_L$$

Ex_t	excess volumetric water
Ks_V	sub-vertical saturated conductivity
D_V	sub-vertical drainage
D_L	sub-vertical drainage

Under this condition a temporary perched water table is formed and carries over into the next day.

m3.2.1 *Condition B*: temporary restricted drainage from one horizon (*z*), due to the formation of a perched water Table in a lower horizon (*z+1*) restricts the potential drainable volume (DP):

$$if\ PFC^{z+1} > \theta_t^{z+1} < T^{z+1} \qquad DP_t^{z+1} = T^{z+1} - \theta_t^{z+1}$$

$$if\ DP_t^{z+1} < D_{V_t}^z \qquad and\ if\ \left(Ex_t^z - DP_t^{z+1}\right) < Ks_L^z \quad D_{V_t}^z = DP_t^{z+1}$$

$$D_{L_t}^z = Ex_t^z - DP_t^{z+1}$$

PFC	field capacity
T	volumetric total pore space
DP	potential drainable volume
D_V	sub-vertical drainage
Ex_t	excess volumetric water
Ks_L	sub-lateral saturated conductivity
D_L	sub-lateral drainage

m3.2.2. Under this condition a temporary perched water Table can be formed, which drains both vertically and laterally in the same day.

$$\left(Ex_t^z - DP_t^{z+1}\right) > Ks_L^z$$

$$D_{L_t}^z = Ks_L^z$$

Ex_t	excess volumetric water
DP	potential drainable volume
Ks_L	sub-lateral saturated conductivity
D_V	sub-vertical drainage
D_L	sub-lateral drainage

Under this condition a temporary perched water Table can be formed which drains both vertically and laterally, and is carries over into the next day.

m3.3. *Condition C*: restrictions in drainage from one horizon (*z*) due to a lower saturated layer (*z+1*):

if $\theta_t^{z+1} > T^{z+1}$ $DP_t^{z+1} = 0$

if $DP_t^{z+1} < x$ *and if* $Ex_t^z < Ks_L^z$ $D_{V_t}^z = 0$

$D_{L_t}^z = Ex_t^z$

θ_t	
T	volumetric total pore space
DP	potential drainable volume
x	suction pressure at 0, 0.1, 0.4, 2 and 15 bar, respectively
Ex_t	excess volumetric water
Ks_L	sub-lateral saturated conductivity
D_V	sub-vertical drainage
D_L	sub-lateral drainage

m3.4. Under this condition a temporary perched water Table can be formed which only drains laterally in the same day.

$Ex_t^z > Ks_L^z$ $D_{V_t}^z = 0$

$D_{L_t}^z = Ks_L^z$

Ex_t	excess volumetric water
Ks_L	sub-lateral saturated conductivity
D_V	sub-vertical drainage
D_L	sub-lateral drainage

Under this condition a temporary perched water Table can be formed which only drains laterally and is carried over into the next iteration.

m3.5. *Condition D*: restrictions to drainage from one horizon as a function of the water content of an adjacent downstream horizon:

$$if\ (\theta_{t-1}^{z+1} - D_{V_t}^{z}) < T^{z+1}\ D_{L_t}^{z} = T^{z} - \theta_{t-1}^{z}$$

$$if\ (\theta_{t-1}^{z+1} - D_{V_t}^{z}) > T^{z+1}\ D_{L_t}^{z} = 0$$

θ_t

D_V sub-vertical drainage

T volumetric total pore space

D_L sub-lateral drainage

n. Soil water balance

n1. Volumetric soil water content of the topsoil:

$$\theta_t^z = \left[\left(\theta_{t-1}^z - D_{V_{t-1}}^z - D_{L_{t-1}}^z\right) + P_t - \left(E_t + Tp_t\right)\right]$$

D_V sub-vertical drainage

D_L sub-lateral drainage

n2. Volumetric soil water content of all lower horizons:

$$\theta_t^{z+1} = \left[\left(\theta_{t-1}^{z+1} - D_{V_{t-1}}^{z+1} - D_{L_{t-1}}^{z+1}\right) + D_{V_t}^{z}\right] - \left(E_t + Tp_t\right)$$

D_V sub-vertical drainage

D_L sub-lateral drainage

n3. Minimum air-dry soil water content:

$$if\ \theta_t < \theta_{air}\ then\ \theta_t = \theta_{air}$$

θ_{air} minimum air dry soil water content

o. Surface runoff

o1. Surface runoff (*R*) from topsoil:

$$\text{if } (\theta_t^z > T^z) \qquad R_t = \theta_t^z - T^z$$

$$\text{if } (P_t > Ks_V^z) \qquad R_t = \theta_t^z - P^z$$

θ_t

T volumetric total pore space

R_t surface runoff

Ks_V	sub-vertical saturated conductivity

p. Soil matric potential

p1. Soil matric potential:

$$Mpot_t^z = \frac{\left(\frac{\theta_t^z}{WQS^z}\right)^{(1/\lambda)}}{h_b}$$

M_{pot}	soil matric potential
WQS	total water content at total porosity

q. Evaporation from the soil

q1. Evaporation from the bare soil:

$$E_{bare} = 3600 D_{hr} \frac{\Delta V\left(\frac{R_n}{3600 D_{hr}} - \frac{G}{3600 D_{hr}}\right) + \rho_a c_p \left(\frac{e_s - e_a}{r_{a,s}}\right)}{\lambda \times 10^3 \left[\Delta V + \gamma_p * \left(1 + \frac{r_{s,s}}{r_{a,s}}\right)\right]}$$

E_{bare}	evaporation from a bare soil (mm day^{-1})
D_{hr}	daylit time for the day (h)
ΔV	rate of change of saturated vapour pressure with temperature (mbar K^{-1})
R_n	net daily radiation (J m^{-2} day^{-1})
G	ground heat-sink (J m^{-2} day^{-1})
ρ_a	air density (kg m^{-3})
c_p	specific heat capacity of air (J kg^{-1} K^{-1}), assume = 1005.01
e_s	saturated vapour pressure (mbar)
e_a	actual vapour pressure (mbar)
$r_{a,s}$	aerodynamic (boundary layer) resistance of the soil to water diffusion (s m^{-1}), assume = 2
$r_{s,s}$	resistance of the soil surface to water diffusion (s m^{-1}), assume = 100
λ	latent heat of vapourisation (Kj kg^{-1})
γ_p	psychometric constant (mbar K^{-1})

q2. Evaporation from the shaded soil:

$$E_{shade} = 3600 D_{hr} \frac{\Delta V(1 - f_{abs})\left(\frac{R_n}{3600 D_{hr}} - \frac{G}{3600 D_{hr}}\right) + \rho_a c_p \left(\frac{e_s - e_a}{r_2 + r_a}\right)}{\lambda \times 10^3 (\Delta V + \gamma_p)}$$

E_{shade}	evaporation from the shaded soil (mm day^{-1})
D_{hr}	daylit time for the day (h)
ΔV	rate of change of saturated vapour pressure with temperature (mbar K^{-1})
f_{abs}	fraction of incoming radiation absorbed by the canopy (dimensionless)
R_n	net daily radiation (J m^{-2} day^{-1})
G	ground heat-sink (J m^{-2} day^{-1})
ρ_a	air density (kg m^{-3})
c_p	specific heat capacity of air (J kg^{-1} K^{-1}), assume = 1005.01
e_s	saturated vapour pressure (mbar)
e_a	actual vapour pressure (mbar)
r_2	aerodynamic resistance between the soil surface and the sink for momentum in the canopy (s m^{-1})
r_a	aerodynamic (boundary layer) resistance of the canopy to water diffusion (s m^{-1})
λ	latent heat of vapourisation (kJ kg^{-1})
γ_p	psychometric constant (mbar K^{-1})

q3. Exchange coefficient:

$$K(h) = \frac{k^2 (h-d) u_z}{\ln\left(\frac{z_m - d}{z_{om}}\right)}$$

K(h)	exchange coefficient at height h (m^2 s^{-1})
k	Von Karman's constant (dimensionless)
h	crop height (m)
d	zero plane displacement height (m), assume = 0.75 h
u_z	windspeed at height z_m (m s^{-1})
r_a	aerodynamic resistance (s m^{-1})
z_m	height of wind measurements (m)
z_{om}	roughness length governing momentum transfer (m), assume = 0.123 h

q4. Aerodynamic resistance between the soil surface and the canopy:

$$r_2 = \frac{h \cdot e^{\alpha_f}}{\alpha_f K(h)} \left(e^{\frac{-\alpha_f z'_{om}}{h}} - e^{\frac{-\alpha (d + z_{om})}{h}} \right)$$

r_2	aerodynamic resistance between the soil surface and canopy (s m^{-1})
h	crop height (m)
α_f	attenuation factor (dimensionless, assume = 2)
K(h)	exchange coefficient at height h (m^2 s^{-1})
z'_{om}	roughness length of the soil surface (m), assume = 0.003
d	zero plane displacement height (m), assume = 0.75 h

z_{om}	roughness length governing momentum transfer (m), assume = 0.123 h

r. Soil geometry

r1. Soil geometry (node depths):

$$D_i = 0 \qquad ;0 \le i \le 1$$

$$D_{i+1} = D_i + D_z * i^2 \qquad ;1 < i \le N_{nodes}$$

$$D_z = \frac{LD}{S_c}$$

$$S_c = \sum_{i=0}^{i=N_{node}} S_{c,i}$$

$$S_{c,i} = 0 \qquad ;i = 0$$

$$S_{c,i} = S_{c,i-1} + i^2 \qquad ;0 < i \le N_{nodes}$$

D_i	depth of node i (m)
N_{nodes}	number of soil nodes
D_z	intermediate calculation (m)
LD	soil depth (m)
S_c	intermediate calculation (dimensionless)
i	node (dimensionless)

r2. Node liquid flux:

$$F_{L,i} = \frac{(\phi_{l,i} - \phi_{u,i})}{D_{i+1} - D_i} - g \bullet \bar{k}_i$$

(A5.2)

$F_{L,i}$	node liquid water flux
$\Phi_{l,i}$	lower node value of intermediate Φ
$\Phi_{u,i}$	upper node value of intermediate Φ
D_i	node depth (m)
g	gravitational acceleration (m s^{-1}), assume = 9.81
k_i	intermediate value
i	node number

r3.

$$\frac{dj}{dp}_{l,i} = \frac{k_l}{D_{i+1} - D_i} + g\frac{dk}{dp}_{l,i}$$

$\frac{dj}{dp_{l,i}}$	derivative of vapour flux at the lowest node point
$k_{u,i}$	intermediate value for upper node
D_i	node depth (m)
g	gravitational acceleration (m s^{-1}), assume = 9.81
$\frac{dk}{dp_{l,i}}$	intermediate derivative
i	node number

r4.

$$\frac{dj}{dp_{u,i}} = \frac{k_{u,i}}{D_{i+1} - D_i} + g\frac{dk}{dp_{u,i}}$$

$\frac{dj}{dp_{u,i}}$	derivative of vapour flux at the highest node point
$k_{u,i}$	intermediate value for upper node
D_i	node depth (m)
g	gravitational acceleration (m s^{-1}), assume = 9.81
$\frac{dk}{dp_{u,i}}$	intermediate derivative
i	node number

r5.

IF($p_{w,i+1} < p_{ae,i}$)

$$k_{l,i} = k_{s,i}\left(\frac{p_{ae,i}}{p_{w,i+1}}\right)^{b_{uc,i}}$$

$$\phi_{l,i} = k_{l,i}\left(\frac{p_{w,i+1}}{1 - b_{uc,i}}\right)$$

ELSE

$$k_{l,i} = k_{s,i}$$

$$\phi_{l,i} = k_{s,i}\left(\frac{p_{ae,i}b_{uc,i}}{1 - b_{uc,i}} + p_{w,i+1}\right)$$

$p_{w,i}$	node water potential
$p_{ae,i}$	node air entry water potential
$b_{uc,i}$	node slope of unsaturated conductivity
$\Phi_{l,i}$	lower node value of intermediate Φ

r6.

IF($p_{w,i} < p_{ae,i}$)

$$k_{u,i} = k_{s,i}\left(\frac{p_{ae,i}}{p_{w,i}}\right)^{b_{uc,i}}$$

$$\phi_{u,i} = k_{u,i}\left(\frac{p_{w,i}}{1 - b_{uc,i}}\right)$$

ELSE

$$k_{u,i} = k_{s,i}$$

$$\phi_{u,i} = k_{s,i}\left(\frac{p_{ae,i} b_{uc,i}}{1 - b_{uc,i}} + p_{w,i}\right)$$

$p_{w,i}$	node water potential
$p_{ae,i}$	node air entry water potential
$k_{u,i}$	intermediate value for upper node
$b_{uc,i}$	node slope of unsaturated conductivity
$\Phi_{u,i}$	upper node value of intermediate Φ

r7.

IF($|p_i - p_{i+1}| < 0.1$)

$$\bar{k}_i = \frac{(k_{u,i} + k_{l,i})}{2}$$

$$\frac{dk}{dp}_{u,i} = -b_{uc,i}\frac{k_{u,i}}{p_{w,i}}$$

$$\frac{dk}{dp}_{,il} = -b_{uc,i}\frac{k_{l,i}}{p_{w,i+1}}$$

ELSE

$$\bar{k}_i = \frac{\phi_{u,i} - \phi_{l,i}}{p_{w,i} - p_{w,i+1}}$$

$$\frac{dk}{dp}_{u,i} = \frac{\bar{k}_i - k_{u,i}}{p_{w,i+1} - p_{w,i}}$$

$$\frac{dk}{dp}_{l,i} = \frac{k_{l,i} - \bar{k}_i}{p_{w,i+1} - p_{w,i}}$$

p_i	node porosity
$k_{u,i}$	intermediate value for upper node

$\frac{dk}{dp_{u,i}}$	intermediate derivative
$b_{uc,i}$	node slope of unsaturated conductivity
$p_{w,i}$	node water potential
$\frac{dk}{dp_{l,i}}$	intermediate derivative
$\Phi_{u,i}$	upper node value of intermediate Φ
$\Phi_{l,i}$	lower node value of intermediate Φ

r8. Node vapour flux:

$$F_{V,i} = k_{v,i}(h_{i+1} - h_i)$$

$$k_{v,i} = 0.66 V_{diff} V_{conc} P_i$$

$$P_i = \theta_{sat,i} - \frac{\theta_{su,i} - \theta_{sl,i}}{2}$$

h_i	node humidity
V_{diff}	vapour diffusivity, assume = 0.000024
V_{conc}	vapour concentration (kg m^{-3}), assume = 0.017
p_i	node porosity
$\theta_{sat,i}$	saturated water content for the node
$\theta_{su,i}$	upper node water content at start of time step
$\theta_{lu,i}$	lower node water content at start of time step

r9. Derivative of vapour flux for upper node:

$$\frac{djv}{dp_{u,i}} = \frac{k_{v,i} M_w h_i}{R_m T_i}$$

$\frac{djv}{dp_{u,i}}$	vapour flux derivative for upper node
h_i	node humidity
M_w	molecular mass of water (kg mol^{-1}), = 0.018
R_m	universal gas constant (J mol^{-1} K^{-1}), assume = 8.314
T_i	temperature of the node (K)
i	node number

r10. Derivative of vapour flux for lower node:

$$\frac{djv}{dp_{l,i}} = \frac{k_{v,i} M_w h_i}{R_m T_i}$$

$\frac{djv}{dp}_{l,i}$	vapour flux derivative for lower node
h_i	node humidity
M_w	molecular mass of water (kg mol^{-1}), = 0.018
R_m	universal gas constant (J mol^{-1} K^{-1}), assume = 8.314
T_i	temperature of the node (K)
i	node number

r11. Node humidity:

$$h_i = e^{\frac{M_w p_{w,i}}{R_m \cdot T_i}}$$

h_i	node humidity
M_w	molecular mass of water (kg mol^{-1}), = 0.018
$p_{w,j}$	node water potential
R_m	universal gas constant (J mol^{-1} K^{-1}), assume = 8.314
T_i	temperature of the node (K)
i	node number

r12. Node water content:

IF($p_{w,i} < p_{ae,i}$)

$$\theta_{u,i} = \theta_{sat,i} + \left(\frac{p_{ae,i}}{p_{w,i}} \right)^{b_{1,i}}$$

$$b_{1,i} = \frac{1}{b_i}$$

$$\frac{dw}{dp}_{u,i} = \frac{-\theta_i b_{1,i}}{p_{w,i}}$$

ELSE

$$\theta_{u,i} = \theta_{sat,u,i}$$

$$\frac{dw}{dp}_{u,i} = 0.0001$$

i	node number
$b_{1,i}$	reciprocal of soil b value
$\frac{dw}{dp}_{u,i}$	upper water content derivative
$\theta_{u,i}$	upper node water content at end of time step
$p_{ae,i}$	node air entry water potential

$p_{w,j}$	node water potential

r13.

IF($p_{w,i+1} < p_{ae,i+1}$)

$$\theta_{l,i} = \theta_{sat,i+1} + \left(\frac{p_{ae,i+1}}{p_{w,i+1}} \right)^{b_{l,i+1}}$$

$$b_{l,i+1} = \frac{1}{b_{i+1}}$$

$$\frac{dw}{dp}_{l,i} = \frac{-\theta_i b_{l,i+1}}{p_{w,i+1}}$$

ELSE

$$\theta_{l,i} = \theta_{sat,i+1}$$

$$\frac{dw}{dp}_{l,i} = 0.0001$$

i	node number
$b_{l,i}$	reciprocal of soil b value
$\frac{dw}{dp}_{l,i}$	lower water content derivative
$\theta_{l,i}$	lower node water content at end of time step
$p_{ae,i}$	node air entry water potential
$p_{w,j}$	node water potential

To find evaporation, solve the following, such that the mass balance error (E_s) < a maximum allowable value (0.000001):

Calculate humidity for the first node

r14. Calculate the node vapour flux for node 0:

$$k_{v,i=0} = \frac{E_0}{1 - h_f}$$

$k_{v,i=0}$	node vapour flux for node 0
E_0	potential (Penman) evaporation (mm), per time step
h_f	fractional relative humidity (dimensionless)

r15.

$$F_{v,i=0} = k_{v,i=0}(h_{i=1}, -h_f)$$

$k_{v,i=0}$ node vapour flux for node 0
$h_{i=1}$ node 1 humidity
h_f fractional relative humidity (dimensionless)

r16.

$$\frac{djv}{dp}_{u,i=0} = 0$$

$\frac{djv}{dp}_{u,i=0}$ vapour flux derivative for upper node 0

r17.

$$\frac{djv}{dp}_{l,i=0} = \frac{k_{v,i=0} M_w h_{i=1}}{R_m T_{i=1}}$$

$\frac{djv}{dp}_{l,i=0}$ vapour flux derivative for lower node 0
$k_{v,i=0}$ node vapour flux for node 0
M_w molecular mass of water (kg mol^{-1}), = 0.018
$h_{i=1}$ node 1 humidity
R_m universal gas constant (J mol^{-1} K^{-1}), assume = 8.314
$T_{i=1}$ temperature of node 1 (K)

r18.

$$\frac{dj}{dp}_{l,i=0} = 0$$

$$\frac{dj}{dp}_{u,i=0} = 0$$

For each node i, where i > 0 and i <= number of nodes

Calculate the node humidity for the next node

r20. Calculate the vapour and liquid fluxes and their derivatives for node i.e. Calculate the upper and lower node soil water-contents:

$$C_{wl,i} = \frac{V_{soil,i} \frac{dw}{dp}_{l,i}}{2t_s}$$

$C_{ul,i}$ upper node water capacity
$V_{soil,i}$ volume of soil at the node
t_s model time-step (s)

r21.

$$C_{wl,i} = \frac{V_{soil,i} \frac{dw}{dp}_{u,i}}{2t_s}$$

$C_{wl,i}$ lower node water capacity
$V_{soil,i}$ volume of soil at the node
t_s model time-step (s)

r22.

$$a_i = -\frac{dj}{du}_{u,i-1} - \frac{djv}{du}_{u,i-1}$$

r23.

$$c_i = -\frac{dj}{dp}_{l,i} - \frac{djv}{dp}_{l,i}$$

r24.

$$b_{x,i} = \frac{dj}{dp}_{l,i-1} + \frac{dj}{dp}_{u,i} + \frac{djv}{dp}_{l,i-1} + \frac{djv}{dp}_{u,i} + C_{ul,i} + C_{wl,i-l}$$

$C_{ul,i}$ upper node water capacity
$C_{wl,i}$ lower node water capacity

r25.

$$f_i = F_{L,i-1} + F_{V,i-1} - F_{L,i} = F_{V,i} + \frac{V_{soil,i}(\theta_{u,i} - \theta_{su,i} + \theta_{l,i-1} - \theta_{sl,i-1})}{2t_s}$$

$V_{soil,i}$ volume of soil at the node

$\theta_{u,i}$	upper node water content at end of time step
$\theta_{l,i}$	lower node water content at end of time step
t_s	model time-step (s)

r26. If ($p_{surface} < 0$), $p_{surface}$ – water potential at the upper boundary, INPUT

$$f_{i=1} = 0$$
$$c_{i=1} = 0$$

r27.

$$E_s = \sum |f_i|$$

Prepare values for next iteration

r28. For all nodes from i = 1 to i = $N_{nodes} - 1$:

$$c_i = \frac{c_i}{b_{x,i}}$$

r29.

$$f_i = \frac{f_i}{b_{x,i}}$$

r30.

$$b_{x,i+1} = b_{x,i+1} - a_{i+1} c_i$$

r31.

$$f_{i+1} = f_{i+1} - a_{i+1} f_i$$

r32. Calculate new node water potentials:

$$dp_{i=N_{nodes}} = \frac{f_{i=N_{nodes}}}{b_{x,i=N_{nodes}}}$$

dp_i	change in node water potential or node i

Appendix E: ForestGrowth equations

r33.

$$p_{w,i=N_{nodes}} = p_{w,i=N_{nodes}} - dp_{i=M_{nodes}}$$

dp_i change in node water potential or node i

r34. For all nodes from i = N_{nodes} – 1 down to i = 1:

$$dp_i = f_i - c_i dp_{i+1}$$

$$I_{t,i} = 0.8\left|p_{w,i}\right|$$

$$a_{bv,i} = \left|dp_i\right|$$

$$\text{IF}\,(a_{bv,i} > I_{t,i})$$

$$dp_i = I_{t,i}\frac{dp_i}{a_{bv,i}}$$

$$p_{w,i} = p_{w,i} - dp_i$$

dp_i change in node water potential or node i

r35.

$$E_{soil} = F_{v,i=0}$$

E_{soil} soil evaporation for the time step

$F_{v,i=0}$ change in node water potential or node i

When iteration is complete (i.e. $E_s < 0.00001$), set the start upper water content to the end upper water content, for the upper and lower nodes.

4. Photosynthesis

s. Canopy radiative transfer

Irradiance equations follow de Pury and Farquhar (1997).

s1. Irradiance absorbed by a canopy per unit ground area:

$$I_c = (1-\rho_{cb})I_b(0).(1-e^{-k_b L_c}).(1-\rho_{cd})I_d(0).(1-e^{-k_d L_c})$$

I_c irradiance absorbed by canopy per unit ground area (μmol m^{-2} s^{-1})

ρ_{cb} canopy reflection coefficient for beam radiation

$I_c(0)$ diffuse PAR per unit ground area at top of canopy (μmol m^{-2} s^{-1})

k_d radiation extinction coefficient of canopy for diffuse irradiance, adjusted for

	scatter (dimensionless)
L_c	canopy leaf area index (m^2 m^{-2})
ρ_{cd}	canopy reflection coefficient for diffuse radiation

s2. Calculates sunlit leaf area index:

$$L_{sun} = \frac{(1 - e^{k_b' l_c})}{k_b'}$$

L_{sun}	sunlit leaf area index (m^2 m^{-2})
k_b'	radiation extinction coefficient of canopy for beam irradiance, adjusted for scatter (dimensionless)
L_c	canopy leaf area index. (m^2 m^{-2})

s3. Irradiance absorbed by the sunlit canopy per unit ground area:

$$I_{cSun} = I_{clbSun} + I_{cldSun} + I_{clbsSun}$$

I_{cSun}	irradiance absorbed by sunlit fraction of canopy (μmol m^{-2} s^{-1})
I_{clbSun}	direct beam irradiance absorbed by sunlit leaves (μmol m^{-2} s^{-1})
I_{cldSun}	diffuse irradiance absorbed by sunlit leaves (μmol m^{-2} s^{-1})
$I_{clbsSun}$	scattered beam irradiance absorbed by sunlit leaves (μmol m^{-2} s^{-1})

s4. Direct beam irradiance absorbed by sunlit leaves:

$$I_{clbSun} = I_b(0)(1-\sigma)(1-e^{-k_b L_c})$$

I_{clbSun}	direct beam irradiance absorbed by sunlit leaves (μmol m^{-2} s^{-1})
$I_b(0)$	beam PAR per unit ground area at top of canopy (μmol m^{-2} s^{-1})
σ	leaf scattering coefficient of PAR
k_b	radiation extinction coefficient of canopy for beam irradiance
L_c	canopy leaf area index (m^2 m^{-2})

s5. Direct beam irradiance absorbed by sunlit leaves:

$$I_{clbSun} = I_b(0)(1-\sigma)(1-e^{-k_b L_c})$$

I_{clbSun}	direct beam irradiance absorbed by sunlit leaves (μmol m^{-2} s^{-1})
$I_b(0)$	beam PAR per unit ground area at top of canopy (μmol m^{-2} s^{-1})
σ	leaf scattering coefficient of PAR
k_b	radiation extinction coefficient of canopy for beam irradiance
L_c	canopy leaf area index (m^2 m^{-2})

s6. Diffuse irradiance absorbed by sunlit canopy per unit ground area:

$$I_{cldSun} = \frac{I_d(0).(1-\rho_{cd})(1-e^{-(k_d'+k_b)*L_c}).k_d'}{(k_d'+k_b)}$$

I_{cldSun}	diffuse irradiance absorbed by sunlit leaves (μmol m^{-2} s^{-1})
$I_b(0)$	beam PAR per unit ground area at top of canopy (μmol m^{-2} s^{-1})
ρ_{cd}	canopy reflection coefficient for diffuse radiation (dimensionless)
k_d'	radiation extinction coefficient of canopy for diffuse irradiance, adjusted for scatter (dimensionless)
k_b	radiation extinction coefficient of canopy for beam irradiance
L_c	canopy leaf area index (m^2 m^{-2})

s7. Scattered beam irradiance absorbed by a canopy per unit ground area:

$$I_{lbs} = \frac{I_b(0)(1-\rho_{cb})(1-e^{-(k_b'+k_b)*L_c})*k_b'}{(k_b'+k_b)} - \frac{(1-\sigma)(1-e^{-2k_b L_c})}{2}$$

I_{lbs}	irradiance - photosynthetically active radiation (PAR) per unit ground area - scattered beam (μmol m^{-2} s^{-1})
$I_b(0)$	beam PAR per unit ground area at top of canopy (μmol m^{-2} s^{-1})
ρ_{cb}	canopy reflection coefficient for beam radiation
k_b'	radiation extinction coefficient of canopy for beam irradiance, adjusted for scatter (dimensionless)
k_b	radiation extinction coefficient of canopy for beam irradiance
L_c	canopy leaf area index. (m^2 m^{-2})
σ	leaf scattering coefficient of PAR

s8. Calculate the irradiance absorbed by the shaded canopy fraction:

$$I_{cSh} = I_c - I_{cSun}$$

I_{cSh}	PAR absorbed by the shaded canopy fraction (μmol m^{-2} s^{-1})
I_c	PAR absorbed by the canopy (μmol m^{-2} s^{-1})
I_{cSun}	PAR absorbed by the sunlit canopy fraction (μmol m^{-2} s^{-1})

s9. Calculates sunfleck penetration:

$$f_{sun}(L) = e^{-k_b L}$$

$f_{sun}(L)$	sunfleck penetration
k_b	radiation extinction coefficient of canopy for beam irradiance
L	cumulative leaf area index from top of canopy (L = 0 at top) (m^2 m^{-2})

s10. Calculates irradiance, either beam, beam with scatter, or diffuse:

$$I_{lr} = (1 - \rho_c) k_{ec} I_b(0) e^{-k_{ec} L}$$

I_{lr}	irradiance (PAR) -per unit ground area - either beam, beam-with-scatter, or diffuse
ρ_{ec}	canopy reflection coefficient for beam radiation (different for beam, ρ_{cb} and diffuse, ρ_{cd}, radiation)
k_{ec}	radiation extinction coefficient of canopy - either for beam, beam adjusted for scatter, or diffuse adjusted for scatter i.e. either k_b, k_b', or k_d'
$I_b(0)$	beam PAR per unit ground area at top of canopy (μmol m^{-2} s^{-1})
L	cumulative leaf area index from top of canopy (L = 0 at top) (m^2 m^{-2})

s11. Takes an extinction co-efficient, and modifies it for scatter:

$$k_{ec}' = k_{ec} \sqrt{(1 - \sigma)}$$

k_{ec}'	radiation extinction coefficient of canopy adjusted for scatter
k_{ec}	radiation extinction coefficient of canopy
σ	leaf scattering coefficient of PAR

s12. Calculate the leaf scattering co-efficient of PAR:

$$\sigma = \rho + \tau$$

σ	leaf scattering coefficient of PAR
ρ	leaf reflection coefficient for PAR
τ	leaf transmissivity to PAR

s13. Calculates the irradiance absorbed by shaded leaves:

$$I_{lSh} = I_{ld}(L) + I_{bs}(L)$$

I_{lSh}	irradiance PAR absorbed by shaded leaves (μmol m^{-2} s^{-1})
I_{ld}	irradiance PAR per unit ground area - diffuse (μmol m^{-2} s^{-1})
L	cumulative leaf area index from top of canopy (L = 0 at top) (m^2 m^{-2})
I_{lbs}	irradiance (PAR) per unit ground area - scattered beam (μmol m^{-2} s^{-1})

s14. Calculates scattered beam irradiance:

$$I_{lbs} = I_b(0)((1 - \rho_{cb}) k_b' e^{-k_b' L} - (1 - \sigma) k_b e^{-k_b L}$$

I_{lbs}	irradiance (PAR) per unit ground area - scattered beam (μmol m^{-2} s^{-1})
$I_b(0)$	beam PAR per unit ground area at top of canopy (μmol m^{-2} s^{-1})

ρ_{cb}	canopy reflection coefficient for beam radiation
k_b'	radiation extinction coefficient of canopy for beam irradiance, adjusted for scatter (dimensionless)
L	cumulative leaf area index from top of canopy (L = 0 at top) (m^2 m^{-2})
σ	leaf scattering coefficient of PAR
k_b	radiation extinction coefficient of canopy for beam irradiance

s15. Calculates the fraction of leaves in each leaf-angle class:

$$f_{l1,2} = \cos \alpha_{1_1} - \cos \alpha_{1_2}$$

f_l1,2	fraction of leaves in this leaf-angle class
$\alpha 1_1$	upper leaf angle for this angle class
$\alpha 1_2$	lower leaf angle for this angle class

s16. Calculates the mean cosine of leaf angle for each class:

$$\overline{\cos} \alpha_{1_{1,2}} = 0.5 (\cos \alpha_{1_1} + \cos \alpha_{1_2})$$

$\overline{\cos} \alpha_{1_{1,2}}$	mean of the cosine of leaf angle for this class
α11	upper leaf angle for this angle class
α12	lower leaf angle for this angle class

s17. Calculates beam irradiance absorbed by sunlit leaves:

$$I_{lbSun} = (1 - \sigma) I_b(0) \frac{\overline{\cos} \alpha}{\sin \beta}$$

I_{lbSun}	beam irradiance absorbed by sunlit leaves (μmol m^{-2} s^{-1})
σ	leaf scattering coefficient of PAR
$I_b(0)$	beam PAR per unit ground area at top of canopy (μmol m^{-2} s^{-1})
α	angle of beam irradiance to leaf normal
β	solar angle of elevation

s18. Calculates total irradiance absorbed by sunlit leaves:

$$I_{lSun} = I_{lbSun} + I_{lSh}$$

I_{lSun}	total irradiance absorbed by sunlit leaves (μmol m^{-2} s^{-1})
I_{lbSun}	beam irradiance absorbed by sunlit leaves (μmol m^{-2} s^{-1})
I_{lSh}	irradiance absorbed by shaded leaves (μmol m^{-2} s^{-1})

s19. Calculates total irradiance:

$I_I = I_{Ib} + I_{Id}$

I_I total irradiance (μmol m^{-2} s^{-1})

I_{Ib} beam irradiance (μmol m^{-2} s^{-1})

I_{Id} diffuse irradiance (μmol m^{-2} s^{-1})

s20. Beam irradiance, uniform leaf angle distribution, canopy reflection coefficient:

$$CanopyReflectionBeam = 1 - e^{(\frac{2\rho_h k_b}{1+k_b})}$$

CanopyReflectionBeam Beam irradiance, uniform leaf angle distribution, canopy reflection coefficient

ρ_h canopy reflection coefficient

k_b radiation extinction coefficient of canopy for beam irradiance

s21. Beam irradiance, horizontal leaves, canopy reflection coefficient:

$$CanopyReflectionBeamHorizontal = \frac{1 - \sqrt{1-\sigma}}{1 + \sqrt{1-\sigma}}$$

CanopyReflectionBeamHorizontal Beam irradiance, horizontal leaves, canopy reflection coefficient

σ leaf scattering coefficient of PAR

Diffuse irradiance canopy reflection coefficient = 0.36

s22. Fraction of incoming radiation absorbed:

$$f_{abs} = \frac{I_c}{I_b(0) + I_d(0)}$$

f_{abs} fraction of incoming radiation absorbed by the canopy (dimensionless)

I_c radiation absorbed by the canopy (J m^{-2} day^{-1})

$I_b(0)$ beam radiation at the top of the canopy (J m^{-2} day^{-1})

$I_d(0)$ diffuse radiation at the top of the canopy (J m^{-2} day^{-1})

s23. Canopy beam extinction co-efficient:

$$k_b = \frac{k_{b,0}}{\sin(\beta)}$$

k_b canopy extinction coefficient for beam irradiance (dimensionless)

$k_b,0$	reference canopy extinction coefficient for beam irradiance (dimensionless)
β	solar elevation

s24. Scaling radiation absorbed at midday to a daily radiation value:

$$R = R_{12} \int_{t=0}^{t=D} \sin\left(\frac{\pi t}{D}\right) dt = \frac{2DR_{12}}{\pi}$$

R	daily radiation (J m^{-2} day^{-1})
R_{12}	radiation at solar noon (W m^{-2})
D	daylit time for the day (s)

t. Gas exchange and carbon productivity

t1. Convert radiation from total radiation to photosynthetically active radiation:

$$R_{PAR} = \frac{R_{tot} p_{PAR}}{100}$$

R_{PAR}	photosynthetically active radiation (W m^{-2})
R_{tot}	total solar radiation (W m^{-2})
p_{PAR}	percentage of incoming radiation that is in the photosynthetically active range (%), assume = 45 %

t2. Convert photosynthetically active radiation (W m^{-2}) to photosynthetic photon flux density (umol m^{-2}):

$$R_{PPFD} = R_{PAR} p_{PPFD}$$

R_{PPFD}	radiation as a photosynthetic photon flux density (μmol m^{-2})
R_{PAR}	photosynthetically active radiation (W m^{-2})
p_{PPFD}	conversion factor for W to μmol PAR (μmol W^{-1}), assume = 4.5

t3. Canopy leaf nitrogen (per m^2 leaf):

$$N_c = (N_0 - N_b)\frac{(1 - e^{-k_n})}{k_n} + N_b$$

N_c	canopy nitrogen content per m^2 leaf area (mmol m^{-2})
N_0	leaf nitrogen content at the top of the canopy (mmol m^{-2})
N_b	leaf nitrogen content not associated with photosynthesis (mmol m^{-2})
k_n	leaf nitrogen allocation coefficient

t4. Mitochondrial (dark) respiration (R_d):

$$R_d = 1.658 \times 10^6 e^{\frac{-54836}{8.3144(T_{leaf}+273.15)}} N_{leaf} \times 10^6$$

R_d	mitochondrial (dark) respiration (μmol m^{-2} s^{-1})
T_{leaf}	leaf temperature (°C)
N_{leaf}	leaf nitrogen content per m^2 of leaf (kg m^{-2})

t5. Intercellular oxygen concentration von Caemmerer *et al.* (1994):

$$O_i = 210\left(\frac{0.047 - 0.0013087T_{leaf} + 0.000025603T_{leaf}^2 - 0.00000021441T_{leaf}^3}{0.026934}\right)$$

O_i	intercellular oxygen concentration (mmol.mol^{-1})
T_{leaf}	leaf temperature (°C)

nb. there is an approximate equivalence that 1 bar is equal to 1 mol mol^{-1} at 1atm.

t6. Rubisco to oxygen:

$$k_o = 248e^{\frac{36000(T_{leaf}+273-298)}{298R_m(T_{leaf}+273)}}$$

k_o	Rubisco to O_2 coefficient (mmol mol^{-1})
T_{leaf}	leaf temperature (°C)

t7. Rubisco to carbon dioxide:

$$k_c = 404e^{\frac{59400(T_{leaf}+273-298)}{298R_m(T_{leaf}+273)}}$$

k_c	Rubisco to CO_2 coefficient (μmol mol^{-1})
T_{leaf}	leaf temperature (°C)

t8. Effective Michaelis-Menten constant of Rubisco:

$$k_m = k_c\left(1 + \frac{O_i}{k_o}\right)$$

k_m	effective Michaelis-Menten constant of Rubisco (μmol m^{-2} mol^{-1})
k_c	Michaelis-Menten constant of Rubisco for CO_2 (μmol m^{-2} mol^{-1})
O_i	intercellular oxygen concentration (mmol m^{-2} s^{-1})
k_o	Michaelis-Menten constant of Rubisco to O_2 (mmol m^{-2} s^{-1})

t9. Leaf Rubisco catalytic site content:

$$e_t = \frac{8 \bullet 6.25 \bullet 0.22 N_{leaf}}{550} \times 10^6$$

e_i leaf Rubisco catalytic site content (μmol m^{-2} s^{-1})

N_{leaf} leaf nitrogen content (kg m^{-2})

t10. Maximum rate of carboxylation by Rubisco (V_{cmax}) at 25 °C:

$$V_{cmax,25} = 1.584 e_t$$

$V_{cmax,25}$ maximum rate of carboxylation by Rubisco at 25 °C (μmol m^{-2} s^{-1})

e_i leaf Rubisco catalytic site content (μmol m^{-2} s^{-1})

t11. Maximum rate of carboxylation by Rubisco (V_{cmax}):

$$V_{cmax} = V_{cmax,25}(1 + 0.0505(T_{leaf} - 25) - 0.000284(T_{leaf} - 25)^2 - 0.000309(T_{leaf} - 25)^3)$$

V_{cmax} maximum rate of carboxylation by Rubisco (μmol m^{-2} s^{-1})

$V_{cmax,25}$ maximum rate of carboxylation by Rubisco at 25 °C (μmol m^{-2} s^{-1})

T_{leaf} leaf temperature (°C)

t12. Fraction of the canopy that is sunlit:

$$f_{sun} = \frac{1 - e^{-k'_b L_c}}{k'_b L_c}$$

f_{sun} fraction of leaves that are sunlit

L_c leaf area index of the canopy (m^2 m^{-2})

k'_b beam radiation canopy extinction coefficient (dimensionless)

t13. Sunlit canopy carboxylation by Rubisco (V_{cmax}) per unit leaf area:

$$V_{cmax,sun} = f_{sun} V_{cmax}$$

$V_{cmax,sun}$ sunlit canopy carboxylation by Rubisco (μmol m^{-2} s^{-1})

f_{sun} fraction of leaves that are sunlit

V_{cmax} maximum rate of carboxylation by Rubisco (μmol m^{-2} s^{-1})

t14. Shaded canopy carboxylation by Rubisco (V_{cmax}) per unit leaf area:

$$V_{cmax,shade} = (1 - f_{sun}) V_{cmax}$$

$V_{cmax,shade}$	shaded canopy carboxylation by Rubisco (μmol m^{-2} s^{-1})
f_{sun}	fraction of leaves that are sunlit
V_{cmax}	maximum rate of carboxylation by Rubisco (μmol m^{-2} s^{-1})

t15. Maximum rate of potential electron transport (J_{max}) per unit leaf area at 25 ˚C:

$$J_{max,25} = 2.1 \cdot V_{cmax,25}$$

$J_{max,25}$	maximum rate of electron transport rate at 25 °C (μmol m^{-2} s^{-1})
$V_{cmax,25}$	maximum rate of carboxylation by Rubisco at 25 °C (μmol m^{-2} s^{-1})

t16. Maximum rate of potential electron transport (J_{max}) per unit leaf area:

$$J_{max} = J_{max,25} \cdot e^{\frac{(T_K - 298)E_a}{298 R_m \cdot T_k}} \left(\frac{1 + e^{\frac{298S - H}{298R}}}{1 + e^{\frac{S \cdot T_K - H}{R_m T_K}}} \right)$$

J_{max}	maximum rate of electron transport rate (μmol m^{-2} s^{-1})
$J_{max,25}$	maximum rate of electron transport rate at 25 °C (μmol m^{-2} s^{-1})
T_K	leaf temperature (K)
E_a	activation energy of electron transport (J mol^{-1})
R_m	universal gas constant (J mol^{-1} K^{-1})
S	electron transport temperature response parameter (J K^{-1} mol^{-1})
H	curvature parameter of J_{max} (J mol^{-1})

t17. Irradiance dependence of electron transport:

$$\theta_l J^2 - (I_{le} + J_{max})J + I_{le} J_{max} = 0$$

θ_l	curvature of leaf response of electron transport to irradiance (dimensionless)
J	rate of electron transport rate per unit leaf area (μmol m^{-2} s^{-1})
I_{le}	PAR effectively absorbed by PSII per unit leaf area (μmol m^{-2} s^{-1})
J_{max}	maximum rate of electron transport rate (μmol m^{-2} s^{-1})

t18. Photosynthetically Active Radiation (PAR) effectively absorbed by PSII:

$$I_{le} = \frac{I_l}{2}(1 - f)$$

I_{le}	PAR effectively absorbed by PSII per unit leaf area (μmol m^{-2} s^{-1})
I_l	total absorbed PAR per unit leaf area (μmol m^{-2} s^{-1})
f	spectral correction factor (dimensionless, assume = 0.15)

t19. CO_2 compensation point of photosynthesis in the absence of respiration:

$$\Gamma^* = \Gamma^*_{25} + 1.88(T_l - 25) + 0.036(T_l - 25)^2$$

Γ*	CO_2 compensation point in the absence of respiration (μmol mol^{-1})
Γ^*_{25}	CO_2 compensation point in the absence of respiration at 25 °C (μmol mol^{-1})
T_l	leaf temperature ($^{\circ C}$)

Numerically solve the following equations to give a value for photosynthetic rate and stomatal conductance, by altering the value for stomatal conductance

t20. Rearranged Ball-Berry equation (Ball *et al.*, 1987):

$$A_n = \frac{(g_c - g_0)Ca}{g_1 h_f}$$

A_n	net photosynthesis calculated by the Ball-Berry-Woodrow method (μmol m^{-2} s^{-1})
g_c	stomatal conductance of CO_2, value changed to find solution (mol m^{-2} s^{-1})
C_a	atmospheric carbon concentration (μmol mol^{-1}), baseline = 370ppm
g_0	minimum stomatal conductance (mol m^{-2} s^{-1})
h_f	fractional relative humidity (dimensionless)

t21. RubP limited photosynthesis:

$$\frac{4}{g_c} A_{j,n}{}^2 + \left(\frac{(4 * R_d - J)}{g_c} - 8\Gamma^* - 4C_a \right) A_{j,n} + \left[J(C_a - \Gamma^*) - 4R_d(C_a + 2\Gamma^*) \right] = 0$$

$A_{j,n}$	RubP limited value of net photosynthesis (μmol mol^{-1} s^{-1})
R_d	mitochondrial (dark) respiration (μmol m^{-2} s^{-1})
J	rate of electron transport rate per unit leaf area (μmol m^{-2} s^{-1})
g_c	stomatal conductance for CO_2 (mol m^{-2} s^{-1})
Γ*	CO_2 compensation point in the absence of respiration (μmol mol^{-1})
C_a	atmospheric carbon concentration (μmol mol^{-1}), baseline = 370ppm

t22. Rubisco limited photosynthesis:

$$\frac{1}{g_c} A_{c,n}{}^2 + \left(\frac{R_d - V_{cmax}}{g_c} - C_a - k_m \right) A_{c,n} + \left[V_{cmax}(C_a - \Gamma^*) - R_d(C_a + k_m) \right] = 0$$

$A_{c,n}$	Rubisco limited value of net photosynthesis (μmol mol^{-1} s^{-1})
R_d	mitochondrial (dark) respiration (μmol m^{-2} s^{-1})
V_{cmax}	maximum rate of carboxylation by Rubisco (μmol m^{-2} s^{-1})
g_c	stomatal conductance for CO_2 (mol m^{-2} s^{-1})
Γ*	CO_2 compensation point in the absence of respiration (μmol mol^{-1})

C_a	atmospheric carbon concentration (μmol mol^{-1}), baseline = 370ppm
k_m	effective Michaelis-Menten constant (mol m^{-2} s^{-1})

t23. Net photosynthesis, by Farquhar method:

$$A_n = \min(A_{c,n}, A_{j,n})$$

A_n	Net photosynthesis (μmol mol^{-1} s^{-1})
$A_{c,n}$	Rubisco limited value of net photosynthesis (μmol mol^{-1} s^{-1})
$A_{j,n}$	RubP limited value of net photosynthesis (μmol mol^{-1} s^{-1})

t24. Transpiration:

$$E_{transp} = 3600 D_{hr} \frac{\Delta V\left(\frac{R_n}{3600 D_{hr}} - \frac{G}{3600 D_{hr}}\right) + \rho_a c_p \left(\frac{e_s - e_a}{r_a}\right)}{\lambda \times 10^3 \left[\Delta V + \gamma_p * \left(1 + \frac{r_s}{r_a}\right)\right]}$$

E_{transp}	transpiration from the plants (mm day^{-1})
D_{hr}	daylit time for the day (hr)
ΔV	rate of change of saturated vapour pressure with temperature (mbar K^{-1})
R_n	net daily radiation (J m^{-2} day^{-1})
G	ground heat-sink (J m^{-2} day^{-1})
ρ_a	air density (kg m^{-3})
c_p	specific heat capacity of air (J kg^{-1} K^{-1}), assume = 1005.01
e_s	saturated vapour pressure (mbar)
e_a	actual vapour pressure (mbar)
r_a	aerodynamic (boundary layer) resistance of the canopy to water diffusion (s m^{-1})
r_s	resistance of the canopy surface to water diffusion (s m^{-1})
λ	latent heat of vapourisation (kj kg^{-1})
γ_p	psychometric constant (mbar K^{-1})

5. Allocation and growth rules

u. Refined pipe theory

All equations in this module follow Deckmyn *et al.* (2006).

u1.

$$E = k_l(\psi_r - \psi_l - \psi_g)$$

E	transpiration per unit leaf area at steady state ($m^3H_2O\ m^{-2}\ s^{-1}$)
k_l	stem conductance per unit leaf area ($s\ m^{-1}$)
ψ_r	root water potential (Pa or $kg\ m^{-1}\ s^{-2}$)
ψ_l	leaf water potential (Pa or $kg\ m^{-1}\ s^{-2}$)
ψ_g	potential due to gravity (Pa or $kg\ m^{-1}\ s^{-2}$)

u2.

$$\psi_g = \rho g h$$

ψ_g	potential due to gravity (Pa or $kg\ m^{-1}\ s^{-2}$)
ρ	water density ($10^3\ kg\ m^{-3}$)
g	acceleration due to gravity ($9.8\ m\ s^{-2}$)
h	stem height (m)

u3.

$$f = \frac{-\pi r_i^4 \Delta P}{8\eta \Delta X}$$

f	flow in a capillary tube ($m^3\ s^{-1}$)
r_I	tube radius (m)
ΔP	pressure difference (Pa)
η	viscosity of water ($0.001\ kg\ m^{-1}\ s^{-1}$)
ΔX	path length (m)

u4.

$$f_p = \frac{\pi(\psi_r - \psi_l - \rho g h) r_i^4 P_e}{8\eta h}$$

f_p	flow through a pipe ($m^3\ s^{-1}$)
ψ_r	root water potential (Pa or $kg\ m^{-1}\ s^{-2}$)
ψ_l	leaf water potential (Pa or $kg\ m^{-1}\ s^{-2}$)
ρ	water density ($10^3\ kg\ m^{-3}$)
g	acceleration due to gravity ($9.8\ m\ s^{-2}$)
h	stem height (m)
r_I	pipe radius (m)
P_e	species-specific parameter included to describe the conductive efficiency of a pipe (0 or 1)
η	viscosity of water ($0.001\ kg\ m^{-1}\ s^{-1}$)

u5.

$P_c = \pi\left((W_t + r_i)^2 - r_i^2\right)W_d$ or $P_c = \pi\left(Wt^2 + 2r_iW_t\right)W_d$

P_c	carbon required to build a unit length of pipe (kgC m^{-1})
W_t	cell wall thickness (m)
r_i	pipe radius (m)
W_d	cell wall density (kgC m^{-3})

Assumption: pipe radius is a function of pipe growth rate (increase in pipe biomass dB_p), where dB_p is derived from simulated photosynthesis and allocation of the previous day.

Assumption: based on observational data, we assumed that r_i is never below 0.9 times mean latewood diameter (r_a), and never above 6.9 r_a.

u6.

$r_i = r_a\left(0.9 + 6\tanh\left(dB_p\alpha\right)\right)$

r_i	pipe radius (m)
r_a	mean latewood diameter (m)
dB_p	increase in pipe biomass
α	radius plasticity

Assumption: the radius plasticity α is proportional to the rate of mobilization of stored NSC in spring, and is related to the rate of leaf transpiration.

u7.

$f_c = \frac{f_p}{P_c h}$

f_c	flow per unit pipe mass (m^3 H_2O $kg^{-1}C$ s^{-1})
f_p	flow through a pipe (m^3 s^{-1})
P_c	carbon required to build a unit length of pipe (kgC m^{-1})
h	stem height (m)

Assumption: we know (or calculate) a maximum transpiration rate on a leaf carbon basis (T_{max}) and the ratio of leaf mass (C_l) to pipe mass (C_p) is approximated so that flow equals transpiration.

u8.

$$C_l T_{\max} = f_c C_p$$

C_l	leaf mass (kgC)
T_{max}	maximum transpiration rate on a leaf carbon basis ($m^3 H_2O\ kg^{-1}C\ s^{-1}$)
f_c	flow per unit pipe mass ($m^3 H_2O\ kg^{-1}C\ s^{-1}$)
C_p	pipe mass (kgC)

u9.

$$C_l T_{\max} = \frac{C_p f_p}{P_c h}$$

C_l	leaf mass (kgC)
T_{max}	maximum transpiration rate on a leaf carbon basis ($m^3 H_2O\ kg^{-1}C\ s^{-1}$)
C_p	pipe mass (kgC)
f_p	flow through a pipe ($m^3\ s^{-1}$)
P_c	carbon required to build a unit length of pipe ($kgC\ m^{-1}$)
h	stem height (m)

u10.

$$\frac{C_l}{C_p} = \frac{f_p}{T_{\max} P_c h}$$

C_l	leaf mass (kgC)
C_p	pipe mass (kgC)
f_p	flow through a pipe ($m^3\ s^{-1}$)
T_{max}	maximum transpiration rate on a leaf carbon basis ($m^3 H_2O\ kg^{-1}C\ s^{-1}$)
P_c	carbon required to build a unit length of pipe ($kgC\ m^{-1}$)
h	stem height (m)

u11.

$$T_{\max} = \frac{E_{\max}}{L_{wr}}$$

T_{max}	maximum transpiration rate on a leaf carbon basis ($m^3 H_2O\ kg^{-1}C\ s^{-1}$)
E_{max}	maximum transpiration per unit leaf area at steady state ($m^3 H_2O\ m^{-2}\ s^{-1}$);
L_{wr}	ratio of leaf mass to leaf area ($kgC\ m^{-2}$)

u12.

$$\frac{C_l}{C_p} = \frac{\pi(\psi_r - \psi_l - \rho g h) r_i^4 P_e L_{wr}}{8\eta h^2 E_{\max} P_c}$$

C_l	leaf mass (kgC)
C_p	pipe mass (kgC)
ψ_r	root water potential (Pa or kg m^{-1} s^{-2})
ψ_l	leaf water potential (Pa or kg m^{-1} s^{-2})
ρ	water density (10^3 kg m^{-3})
g	acceleration due to gravity (9.8 m s^{-2})
h	stem height (m)
r_i	pipe radius (m)
P_e	species-specific parameter included to describe the conductive efficiency of a pipe (0 or 1)
L_{wr}	ratio of leaf mass to leaf area (kgC m^{-2})
η	viscosity of water (0.001 kg m^{-1} s^{-1})
E_{max}	maximum transpiration per unit leaf area at steady state (m^3 H_2O m^{-2} s^{-1});
P_c	carbon required to build a unit length of pipe (kgC m^{-1})

Assumption: The sapwood plasticity term (S_p) describes changes in k_l as a result of the increase in number of pipes (the total sapwood area per unit leaf area) occurring with tree development.

u13.

$$k_l \propto \frac{1 + S_p(h-1))}{h}$$

k_l	stem conductance per unit leaf area (s m^{-1})
S_p	sapwood plasticity
h	stem height (m)

u14.

$$\frac{C_l}{C_p} = \frac{\pi(\psi_r - \psi_l - \rho g h) r_i^4 P_e L_{wr}}{8\eta h(1 + S_p(h-1)) E_{\max} P_c}$$

C_l	leaf mass (kgC)
C_p	pipe mass (kgC)
ψ_r	root water potential (Pa or kg m^{-1} s^{-2})
ψ_l	leaf water potential (Pa or kg m^{-1} s^{-2})
ρ	water density (10^3 kg m^{-3})
g	acceleration due to gravity (9.8 m s^{-2})

h	stem height (m)
r_i	pipe radius (m)
P_e	species-specific parameter included to describe the conductive efficiency of a pipe (0 or 1)
L_{wr}	ratio of leaf mass to leaf area (kgC m^{-2})
η	viscosity of water (0.001 kg m^{-1} s^{-1})
S_p	sapwood plasticity
E_{max}	maximum transpiration per unit leaf area at steady state (m^3 H_2O m^{-2} s^{-1});
P_c	carbon required to build a unit length of pipe (kgC m^{-1})

6. Appendix E references

Ball J.T., Woodrow I.E. and Berry J.A. (1987) A model predicting stomatal conductance and its contribution to the control of photosynthesis under different environmental conditions. In: Biggins J. and Nijhoff M. (eds.) *Progress in photosynthesis research, vol.4.* Dordrecht, The Netherlands.

Bristow R.L. and Campbell G.S. (1984) On the relationship between incoming solar radiation and daily maximum and minimum temperature. *Agriculture and Forestry Meteorology* **31**: 159-166.

de Pury D.G.G. and Farquhar G.D. (1997) Simple scaling of photosynthesis from leaves to canopies without the errors of big-leaf models. *Plant, Cell and Environment* **20**: 537-557.

Deckmyn G., Evans S.P. and Randle T.J. (2006) Refined pipe theory for mechanistic modeling of wood development. *Tree Physiology* **26**: 703-717.

Duffie J.A. and Beckman W.A. (1991) *Solar Engineering of Thermal Processes (second ed.),* New York, US: Wiley Interscience.

Farquhar G.D., von Caemmerer S. and Berry J.A. (1980) A biochemical model of photosynthetic CO_2 assimilation in leaves of C3 species. *Planta* **149**: 78-90.

Gash J.H.C., Lloyd C.R. and Lachaud G. (1995) Estimating sparse forest rainfall interception with an analytical model. *Journal of Hydrology* **170**: 79-86.

Geng S., Auburn J., Brandstetter E. and Baoquan L. (1988) *A program to simulate meteorological variables: documentation for SIMMETEO,* California, US: Department of Agronomy and Range Science.

Gueymard C. (1993) Mathematically integrable parameterization of clear-sky beam and global irradiances and its use in daily irradiation applications. *Solar Energy* **50**(5): 385-397.

Lui B.H. and Jordan R.C. (1960) The interrelationship and characteristic distribution of direct, diffuse, and total solar radiation. *Solar Energy* **4**(3): 1-9.

Nikolov N.T. and Zeller K.F. (1992) A solar radiation algorithm for ecosystem dynamic models. *Ecological Modelling* **61**: 149-168.

Richardson C. and Wright D. (1984) WGEN: a model for generating daily weather variables, Washington DC, US: US Government Printing Office.

von Caemmerer S., Evans J., Hudson G. and Andrews T. (1994) The kinetics of ribulose-1,5-bisphosphate carboxylase/oxygenase in vivo inferred from measurements of photosynthesis in leaves of transgenic tobacco. *Planta* **195**: 88-97.

Appendix F: Publications arising from this work

Appendix F: Publications arising from this work

1. **Aylott M.J., Casella E., Tubby I., Street N.R., Smith P. & Taylor G.** (2008) Yield and spatial supply of bioenergy poplar and willow short-rotation coppice in the UK. *New Phytologist,* 178: 358-370.
2. **Aylott M.J., Taylor G. & Casella E.** (2008) Productivity of C3 bioenergy crops grown as short rotation coppice under current and future climates. *Comparative Biochemistry and Physiology - Part A: Molecular & Integrative Physiology* 150 (3):180-181. Abstracts of the Annual Main Meeting of the Society of Experimental Biology, 6th - 10th July 2008, Marseille, France.
3. **Aylott M.J., Taylor G. & Casella E.** (2009) Growing poplar and willow for fuel – How coppicing may help us meet our bioenergy targets. *British Bioenergy Newsletter* 8.
4. **Aylott M.J., Casella E., Farrall K. & Taylor G.** (2010) Social, economic and environmental impacts on the supply of biomass from short rotation coppice in England. *Biofuels* 1 (5): 719-727.
5. **Bauen A.W., Richter G.M., Dunett A., Riche A.B., Dailey A.G., Casella E., Aylott M. & Taylor G.** (2009) Modelling demand and supply of bioenergy from short rotation coppice and *Miscanthus* in the UK. *Bioresource Technology* 101 (21): 8132-8143.
6. **Casella E., E. Dreyer, M. Vandame, R. Ceulemans, M.J. Aylott, G. Taylor & H. Sinoquet.** Temperature response of photosynthesis in poplar as inferred from changes in the N-photosynthesis relationship within a growing season. In preparation.
7. **Hillier J., Whittaker C., Dailey G., Aylott M.J., Casella E., Richter G.M., Riche A., Murphy R., Taylor G. & Smith P.** (2009) Greenhouse gas emissions from bioenergy crops in England and Wales: Integrating spatial estimates of yield and soil carbon balance in life cycle analyses. *Global Change Biology Bioenergy*, 1 (4): 267-281.